Molecular Analysis of the Unconventional Export Machinery of Galectin-1, a β-Galactoside-specific Lectin of the Extracellular Matrix

Dissertation submitted to the
Combined Faculties for the Natural Sciences and for Mathematics
of the Ruperto Carola University of Heidelberg, Germany

for the degree of
Doctor of Natural Sciences

presented by

Diplom-Biologin Claudia Seelenmeyer
born in Karlsruhe

DISSERTATION

submitted to the
Combined Faculties for the Natural Sciences and for Mathematics
of the Ruperto Carola University of Heidelberg, Germany

for the degree of
Doctor of Natural Sciences

presented by

Diplom-Biologin Claudia Seelenmeyer
born in Karlsruhe

Oral examination:

Molecular Analysis of the Unconventional Export Machinery of Galectin-1, a β-Galactoside-specific Lectin of the Extracellular Matrix

Referees:

Prof. Dr. rer. nat Walter Nickel

Prof. Dr. rer. nat Michael Brunner

List of Publications

Engling, A., Backhaus, R., Stegmayer, C., Zehe, C., Seelenmeyer, C., Kehlenbach, A., Schwappach, B., Wegehingel, S., and Nickel, W. (2002). Biosynthetic FGF-2 is targeted to non-lipid raft microdomains following translocation to the extracellular surface of CHO cells. J Cell Sci *115*, 3619-3631.

Seelenmeyer, C., Wegehingel, S., Lechner, J., and Nickel, W. (2003). The cancer antigen CA125 represents a novel counter receptor for galectin-1. J Cell Sci *116*, 1305-1318.

Seelenmeyer, C., Wegehingel, S., Tews, I., Kunzler, M., Aebi, M., and Nickel, W. (2005). Cell surface counter receptors are essential components of the unconventional export machinery of galectin-1. J Cell Biol *171*, 373-381.

Wohin auch immer wir reisen,
wir suchen, wovon wir träumten,
und finden doch stets nur uns selbst.

*Günter Kunert (*1929)*

Contents

Abbreviation

Abbreviation	
ABC	ATP binding cassette
APC	allophycocyanin
Ac	Acetate
APS	ammonium peroxo disulphate
ARF	ADP-ribosylation factor 1
ATP	adenosin triphosphate
BFA	brefeldin A
bp	basepairs
cDNA	Complementary DNA
CDB	cell dissociation buffer
CHO	Chinese hamster ovary (cells)
CRD	carbohydrate recognition domain
COP	Coat proteine
C-terminal	carboxy terminal
DMSO	dimethyl sulphoxide
DNA	desoxyribonucleic acid
E.coli	Escherichia coli
e.g.	exempli gratia
ECL	enhanced chemoluminescence
ECM	Extracellular matrix
EDTA	ethylenediaminetetraacetic acid
En2	engrailed 2
ER	endoplasmatic reticulum
et al.	et altera
FACS	fluorescence activated cell sorting
FCS	fetal calf serum
FGF2	fibroblast growth factor 2
FGFR	fibroblast growth factor receptor

g_{av}	Average gravitation
GAG	glycosaminoglycans
Gal-1	galectin-1
GalNAc	N-acetylgalactosamine
GFP	green fluorescence protein
Glc	Glucose
GlcNAc	N-acetylglycosamine
GM1	Ganglioside GM1
GTP	guanosine triphosphate
h	hour
HASPB	hydrophilic acylated surface protein B
HCl	hydrochlorid acid
HEK 293T	Human endothelial kidney cells
HIV	human immunodeficiency virus
HMGB	high mobility group protein
HRP	horse raddish peroxidase
HS	heparan sulfate
HSPG	heparan sulfate proteoglycans
HUT78	T-cell lymphoma cell line HUT78
i.e.	id est
IgG	Immunoglobulin G
IL	interleukin
kDa	kilo Dalton
L1-CAM	L1 cell adhesion molecule
LTR	long terminal repeat
Man	Mannose
MCAT/mt	Mouse cationic amino acid transporter
MES	2-(N-morpholino) ethane sufonacid
MIF	migration inhibtory factor
NAD	Nicotinaminde adenine dinucleotide, oxidized
NLS	nuclear localization signal
nm	nanometer (wavelength)

NSF	N-ethylmaleimide sensitive factor
N-terminal	Amino terminal
ORF	open reading frame
PAGE	polyacrylamide gel electrophoresis
PBS	phosphate buffered saline
PCR	polymerase chain reaction
PE	phycoerythrin
POD	peroxidase
PVDF	polyvinyliden fluoride
RNA	ribonucleic acid
RT	Room temperature
SDS	sodium dodecyl sulfate
SNAP	Soluble NSF attachment protein
SNARE	SNAP receptors
SRP	signal recognition particle
Tat	HIV transactivator protein
TEMED	N,N;N´,N´-tetramethylethylenediamine
Tris	Tris[hydroxymethyl]aminoethane
Tween 20	polyoxethylene sorbitane monolaureate
U	units (enzyme activity)
UDP	Uridine diphosphate
v/v	volume/volume relationship
w/v	weight/volume relationship
α-MEM	α-modification of Minimal Essential Medium

Amino Acids

Abbreviation	Abbreviation	Animo acid
A	Ala	alanine
C	Cys	cysteine
D	Asp	aspartic acid
E	Glu	glutamic acid
F	Phe	phenylalanine
G	Gly	glycine
H	His	histidine
I	Ile	isoleucin
K	Lys	lysine
L	Leu	leucine
M	Met	methionine
N	Asn	asparagine
P	Pro	proline
Q	Gln	glutamine
R	Arg	arginine
S	Ser	serine
T	Thr	threonine
V	Val	valine
W	Trp	tryptophan
Y	Tyr	tyrosine

Zusammenfassung

Galectin-1 ist ein β-Galaktosid-spezifisches Lektin der extrazellulären Matrix, das an der Regulation verschiedener zellulärer Prozesse wie Zellproliferation, Differenzierung und Apoptose beteiligt ist. Das extrazelluläre Auftreten von Galectin-1 war zunächst eine überraschende Entdeckung, da das Protein kein Signalpeptid enthält und somit nicht über ER/Golgi-vermittelten Transport sezerniert werden kann. Darüber hinaus ist die Sekretion von Galectin-1 in Gegenwart von Brefeldin A nicht gehemmt, so dass ein unkonventioneller Sekretionsweg postuliert wurde.

In der vorliegenden Dissertation wurde ein robustes *in vivo* Modell zur funktionellen Rekonstitution der Galectin-1 Sekretion etabliert. Es wurden mittels retroviraler Transduktion stabile Zelllinien generiert, die verschiedene Galectin-1 Reportermoleküle als GFP Fusionsproteine in Abhängigkeit von der exogenen Zugabe von Doxicyclin exprimieren. Da die exportierte Population über β-Galaktosid-haltige Rezeptoren an Zelloberflächen bindet, konnte die Galectin-1 Sekretionsrate über verschiedene Methoden wie Durchflusszytometrie, konfokale Laserscan-mikroskopie sowie biochemische Zelloberflächenbiotinylierung unter verschiedenen experimentellen Bedingungen quantifiziert werden.

Die etablierten Modellsysteme wurden einerseits zur funktionellen Charakterisierung eines in dieser Arbeit identifizierten Galectin-1 Rezeptors genutzt und andererseits zur Analyse der molekularen Sortierungsdeterminanten verwendet, die Galectin-1 zur entsprechenden Exportmaschinerie dirigieren. Eine systematische Mutagenese des offenen Leserasters von Galectin-1 ergab hierbei, dass Mutationen, die zu einer Bindungsdefizienz führen, letztlich auch einen Exportdefekt verursachen. Komplementär hierzu konnte gezeigt werden, dass Galectin-1 von Zelllinien, die nicht zur Expression von β-Galaktosid-haltigen Rezeptoren befähigt sind, nicht exportiert wird. Hieraus wurde der Schluss gezogen, dass β-Galaktosid-haltige Zelloberflächenrezeptoren für den Gesamtprozess der Galectin-1 Sekretion essentiell sind. Dieser Befund konnte durch die Expression des mit Galectin-1 entfernt verwandten

Proteins CGL-2 aus dem multizellulären Pilz *Coprinopsis cinerea* bestätigt werden. CGL-2 wird von Säugetierzellen unkonventionell exportiert, wobei dieser Prozess von der Bindung an β-Galaktosid-haltige Zelloberflächenrezeptoren abhängt. Die beschriebenen Arbeiten haben somit gezeigt, dass das primäre Sortierungssignal für die unkonventionelle Sekretion von Galectin-1 durch die β-Galaktosid-Bindungsstelle definiert ist und haben weitreichende Implikationen für die weitere Analyse der Galectin-1 Exportmaschinerie.

Abstract

Galectin-1 is a β-galactoside-specific lectin of the extracellular matrix that has been implicated in a number of important cellular processes such as the regulation of cell proliferation, differentiation and apoptosis. Even though galectin-1 occurs outside cells, it does not contain a signal peptide for ER/Golgi-mediated secretion and, therefore, unconventional mechanisms of galectin-1 export have been postulated.

In the current thesis, a robust experimental model system has been established that allows for a precise quantitation of galectin-1 export from mammalian cells. Based on a retroviral transduction system, stable cell lines have been generated expressing various galectin reporter molecules as GFP fusion proteins using a doxicycline-dependent transactivator. As read out systems, flow cytometry, confocal microscopy and a biochemical cell surface biotinylation assay were used since exported galectins bind to cell surfaces via β-galactoside-containing counter receptors.

This novel experimental system was used for two main purposes, one being the functional characterization of a novel galectin-1 counter receptor, the tumor-specific antigen CA125 that was identified in this study. A second aspect of the current thesis was to define molecular sorting determinants in galectin-1 that direct the protein to its unconventional export machinery. A systematic mutational analysis of the galectin-1 open reading frame was conducted. Additionally, surface residues as well as amino acids in galectin-1 conserved across species were exchanged by targeted mutation. A major outcome of these studies was that mutations causing a defect in galectin-1 binding to β-galactosides resulted in a loss of export competence. Intriguingly, when expressing the wild-type form of galectin-1 in mutant cells lacking β-galactoside-containing counter receptors, the protein also failed to get access to its export machinery. These findings were taken to mean that a functional interaction between galectin-1 and cell surface counter receptors is an obligatory step in the overall process of galectin-1 export. Consistently, despite being unrelated with regard to

primary structure, a distant galectin relative from the fungus *Coprinopsis cinerea*, CGL-2, was shown to be exported from mammalian cells depending on its ability to bind to β-galactosides. Therefore, the work presented in this thesis demonstrates that the β-galactoside binding site represents the primary targeting motif for non-classical export of galectins defining a galectin export machinery that makes use of β-galactoside-containing surface molecules as export receptors for intracellular galectin-1. These results have a number of functional implications such as aspects of galectin folding during membrane translocation and with regard to the analysis of the subcellular site of membrane translocation that is now being investigated based on the results described above.

1 Introduction

Protein secretion occurs in prokaryotic and eukaryotic cells and involves the delivery of secretory products packaged into membrane-bound vesicles to the cell exterior. Cells specialized for neurotransmission, enzyme secretion or hormone release utilize a highly regulated secretory process. All eukaryotic cells possess an endomembrane system that makes up the secretory pathway and endocytic pathway (Lee et al., 2004; Rothman and Wieland, 1996). This network consists of a number of independent organelles that function sequentially to effect protein secretion to the extracellular environment (Keller and Simons, 1997). Each compartment provides a specialized surrounding that facilitates various stages in protein biogenesis, modification, sorting and secretion (Palade, 1975). Secretory vesicles are transported to plasma membrane, where they dock and fuse to release their contents (Bonifacino and Glick, 2004). Membrane fusion and secretion are fundamental cellular processes regulating ER-Golgi transport, plasma membrane recycling, cell division, acid secretion and the release of enzymes, hormones and neurotransmitters (Lee et al., 2004; Sudhof, 2004). Therefore it is not surprising that defects in secretion and membrane fusion give rise to a number of diseases like diabetes, Alzheimer's, Parkinson's and acute gastroduodenal diseases (Amara et al., 1992; Nagy, 2005; Orci et al., 1997).

1.1 ER/Golgi-mediated protein secretion

After synthesis of secretory proteins begins on free ribosomes in the cytosol, a 16- to 30- residue ER signal sequence in the nascent protein directs the ribosome to the ER membrane and initiates translocation of the growing polypeptide across the ER membrane (Blobel and Dobberstein, 1975a; Blobel and Dobberstein, 1975b; Walter et al., 1984). An ER signal sequence typically is located at the N-terminus of the protein (Rapoport et al., 1992; Walter, 1992). For most secretory proteins, the signal peptide is cleaved off the protein (Blobel and Dobberstein, 1975a; Blobel and

Dobberstein, 1975b; Dalbey and Von Heijne, 1992). Since secretory proteins are synthesized in association with the ER membrane, a signal-sequence recognition mechanism targets them to the ER membrane (Meyer et al., 1982). The two key components of this targeting process are the **s**ignal-**r**ecognition **p**article (SRP) and its receptor located in the ER membrane. SRP is a cytosolic ribonucleoprotein particle that transiently binds simultaneously to the ER signal sequence in a nascent protein, to the large ribosomal unit, and to the SRP receptor. The SRP receptor is an integral membrane protein made up of two subunits: an α subunit and a smaller β subunit (Tajima et al., 1986). Once SRP and its receptor have targeted a ribosome synthesizing a secretory protein to the ER membrane, the ribosome and the nascent chain are rapidly transferred to the translocon, a protein-lined channel within the membrane (Rapoport, 1991). During the translation process, the elongating chain passes directly from the large ribosomal subunit into the central pore of the translocon (High et al., 1991; Powers and Walter, 1996; Rapoport, 1991). The 60S ribosomal subunit is aligned with the pore of the translocon preventing the growing chain from being exposed to the cytoplasm and therefore inhibits folding until it reaches the ER lumen. Three proteins collectively termed the *Sec61 complex* were found to form the mammalian translocon: Sec61α, an integral membrane protein with 10 membrane spanning α helices, and two smaller proteins, *Sec61*β and *Sec61*γ (High et al., 1993; Rapoport, 1992). As the growing polypeptide chain enters the lumen of the ER, the signal sequence is cleaved by a signal peptidase, which is a transmembrane protein of the ER associated with the translocon (Dalbey and Von Heijne, 1992). After the signal sequence has been cleaved, the growing polypeptide translocates through the translocon into the ER lumen.

Soluble and membrane proteins synthesized at the rough ER and translocated into the ER are now ready to follow to their final destination via the secretory pathway. A single unifying principle governs all protein trafficking in the secretory pathway as transport of membrane and soluble proteins from one membrane-bounded compartment to another is mediated by transport vesicles. Most of the newly synthesized proteins in the ER lumen or membrane are incorporated into small, 50 nm-diameter transport vesicles. These vesicles either fuse with the *cis*-Golgi or with each other to form the membrane stacks known as the *cis*-Golgi

reticulum (network). From the *cis*-Golgi some proteins, mainly ER localized proteins, are retrieved to the ER via a different set of retrograde transport vesicles (Lee et al., 2004). Importantly, as transport vesicles bud from one membrane and fuse with the next, the membrane topology is maintained.

Two different models of intra-Golgi transport have been discussed in the literature (Mironov et al., 2005; Warren and Malhotra, 1998). In the synthesis of collagen by fibroblasts, large aggregates of the procollagen precursor often form in the lumen of the *cis*-Golgi. These aggregates are too large to be incorporated into small transport vesicles. Newly synthesized procollagen peptides get folded and form aggregates in the *cis*-Golgi where they could subsequently be seen to move as a 'wave' from the *cis*- through the *medial*-Golgi cisternae to the *trans*-Golgi, followed by secretion and incorporation into the extracellular matrix. Procollagen aggregates could never be detected in small transport vesicles (Mironov et al., 2005). In this process called cisternal migration or cisternal progression, a new cis-Golgi stack containing its cargo of luminal proteins physically moves from the *cis* position (nearest the ER) to the *trans* position, successively becoming first a *medial*-Golgi cisterna and finally a *trans*-Golgi cisterna (Graham and Emr, 1991; Mellman and Simons, 1992; Mironov et al., 2005; Rothman and Orci, 1990). In contrast to this cisternal progression model a second model exists proposing that transport within the Golgi is mediated by vesicles. According to this vesicular transport model, the Golgi is a relatively static structure, with its enzymes held in place, while the molecules in transit are moved through the cisternae in sequence, carried by transport vesicles (Warren and Malhotra, 1998).

At the molecular level three kinds of transport vesicles have been functionally characterized and can be defined by both membrane origin and coat proteins (Kirchhausen, 2000; Robinson, 1987). Clathrin-coated vesicles are formed from both the plasma membrane and the *trans*-Golgi network and mediate vesicular trafficking within the endosomal membrane system (Schmid, 1997). COPI-coated vesicles and COPII-coated vesicles are transport intermediates of the early secretory pathway (Barlowe, 1998; Nickel et al., 2002; Rothman and Wieland, 1996; Schekman and Orci, 1996). COPII vesicles emerge from the ER in order to export newly synthesized secretory proteins towards the Golgi (Barlowe, 1998; Schekman and Orci, 1996). In

contrast, COPI-coated vesicles appear to be involved in both biosynthetic (anterograde) and retrograde transport within the Golgi complex (Orci et al., 1997), as well as mediating the recycling of proteins from the Golgi to the ER (Cosson and Letourneur, 1994; Letourneur et al., 1994; Sonnichsen et al., 1996). All types of coated vesicles are formed by polymerization of coat proteins on the cytosolic surface of the corresponding donor membrane to form vesicle buds that eventually pinch off from the membrane to release a complete vesicle. Shortly after vesicle release, the coat is shed exposing proteins required for fusion with the target membrane (Lee et al., 2004).

Small GTP-binding proteins (ARF for COPI and clathrin coated vesicles, respectively; SAR1 for COPII-vesicles) belonging to the ras GTPase superfamily control polymerization of coat proteins, the initial step in vesicle budding. Both ARF and Sar1 are monomeric proteins with an overall structure similar to that of ras (Orci et al., 1993; Serafini et al., 1991). After vesicles are released from the donor membrane, hydrolysis of GTP-bound to ARF or SAR1 triggers disassembly of the vesicle coat (Serafini et al., 1991). The primary mechanism by which the vesicle coat selects cargo molecules is by directly binding to specific sequences termed sorting signals that typically lie in the cytosolic domain of membrane cargo proteins (Goldberg, 2000; Kirchhausen et al., 1997; Lee et al., 2004; Mossessova et al., 2003). The polymerized coat thus acts as an affinity matrix to cluster selected membrane cargo proteins into forming vesicle buds. Soluble proteins within the lumen of the parental organelles can in turn be selected by binding to the luminal domains of certain membrane cargo proteins (e.g. KDEL signal sequence and KDEL receptor) (Lewis and Pelham, 1992a).

Vesicle budding requires protein coats (Bonifacino and Glick, 2004) and small GTPases of the ARF family (Nie et al., 2003), while vesicle targeting and fusion depend on SNARE proteins (soluble N-ethylmaleimide-sensitive factor attachment protein receptor) (Ungar and Hughson, 2003; Weber et al., 1998), small GTPases of the Rab family (Pfeffer, 2001b) and a diverse group of tethering factors (Lee et al., 2004; Lupashin and Sztul, 2005; Pfeffer, 2001a). The Rab proteins regulate docking of vesicles with the correct target membrane. Each Rab appears to bind to a specific

Rab effector, typically a long coiled-coil protein associated with the target membrane (Goud, 1992; Zerial and Stenmark, 1993).

The term “tethering factors” describes a group of proteins believed to mediate initial, loose ‘tethering’ of vesicles with their targets. This loose interaction is followed by a tighter, more stable ‘docking’ interaction involving SNAREs (Pfeffer, 2001a). The tethering factors form physical links between the vesicles and the acceptor membrane before the engagement of SNAREs. Tethering may provide the initial level of recognition that is then amplified by SNARE pairing. Tethering factors can be generally divided into a group of coiled-coil proteins and a group of multi-subunits complexes (Lupashin and Sztul, 2005; Pfeffer, 2001a).

Disassembly of the vesicle coat uncovers a vesicle-specific v-SNARE. Likewise, each type of target membrane in a cell contains a specific t-SNARE membrane protein. After Rab mediated docking of a vesicle on its target membrane, the interaction of cognate SNAREs brings the two membranes in close proximity resulting in membrane fusion. In this process the v-SNAREs and t-SNAREs on the two opposing membranes mediate the short-range docking of the vesicle with the target compartment by the formation of the so called *trans*-SNARE complex (Chen and Scheller, 2001; Jahn and Grubmuller, 2002; Jahn and Sudhof, 1999; Rothman, 2002; Sudhof, 2004). The SNARE motifs are believed to be unstructured before complex assembly and become highly organized into a four-helical bundle during formation of the *trans*-SNARE-complex. The *trans*-SNARE complex directly catalyzes the fusion of the two opposing membranes. Therefore, following fusion, the complex becomes a *cis*-SNARE complex in the target compartment (Lee et al., 2004).

Finally, to be ready for subsequent rounds of transport, the *cis*-SNARE complex needs to be disassembled. This is catalyzed by the combined action of α-SNAP (soluble N-ethylmaleimide-sensitive factor attachment protein) and the ATPase NSF (N-ethylmaleimide-sensitive factor). Interaction of NSF in a form of a hexamer and three α-SNAPs with the *cis*-SNARE complex leads to the transient formation of a 20 S complex (Furst et al., 2003; Hohl et al., 1998; Wimmer et al., 2001). ATP hydrolysis catalyzed by NSF leads to the disassembly of the 20 S complex as well as the *cis*-SNARE complex. The free v-SNARE can then be recycled to the donor compartment

by retrograde transport, while the t-SNARE subunits can be re-organized into functional t-SNARE for the next round of docking and fusion events.

1.2 Unconventional secretion

As already discussed soluble secretory proteins typically contain N-terminal signal peptides that direct them to the translocation apparatus of the endoplasmic reticulum (ER) (Rapoport et al., 1996; Walter et al., 1984). Following vesicular transport from the ER via the Golgi to the cell surface, luminal proteins are released into the extracellular space by fusion of Golgi-derived secretory vesicles with the plasma membrane (Mellman and Warren, 2000; Palade, 1975; Rothman and Wieland, 1996; Schekman and Orci, 1996). This pathway of protein export from eukaryotic cells is known as the classical or ER/Golgi-dependent secretory pathway (see 1.1).

However, about 15 years ago, it was reported that interleukin 1β (IL-1β) and Galectin-1 (Gal-1) can be exported from cells in the absence of a functional ER/Golgi system (Cooper and Barondes, 1990; Rubartelli et al., 1990). Since then, the list of proteins demonstrated to be secreted by unconventional means is steadily growing (Nickel, 2003). Fig. 1 gives an overview of cellular, viral proteins and proteins derived from parasites that have been shown to be exported by mechanisms independent of the classical secretory pathway. Current members of this group of proteins are, for example: angiogenic growth factors FGF-1 and -2 (1.2.2) (Florkiewicz et al., 1995; Jackson et al., 1992; Mignatti et al., 1992), cytokines such as interleukin 1β and thioredoxin (1.2.4) (Rubartelli et al., 1992; Rubartelli et al., 1990; Rubartelli and Sitia, 1991), lectins of the extracellular matrix such as Gal-1 (1.2.1) (Cho and Cummings, 1995a; Cho and Cummings, 1995b; Cooper and Barondes, 1990; Mehul and Hughes, 1997), viral proteins such as Herpes simplex tegument protein VP22 (Elliott and O'Hare, 1997) as well as cell surface proteins such as **h**ydrophilic **a**cylated **s**urface **p**rotein **B** (HASPB; 1.2.3) (Denny et al., 2000).

The basic observations (Cleves, 1997; Hughes, 1999) that led to the proposal of alternative pathways of eukaryotic protein secretion are (i) the lack of conventional signal peptides, (ii) the exclusion of these proteins from classical secretory organelles such as the ER and the Golgi, (iii) the lack of ER/Golgi-dependent post-translational modifications such as N-glycosylation and (iv) resistance of these export processes to brefeldin A and monensin, both classical inhibitors of ER/Golgi-dependent protein secretion (Lippincott-Schwartz et al., 1989; Misumi et al., 1986; Orci et al., 1991).

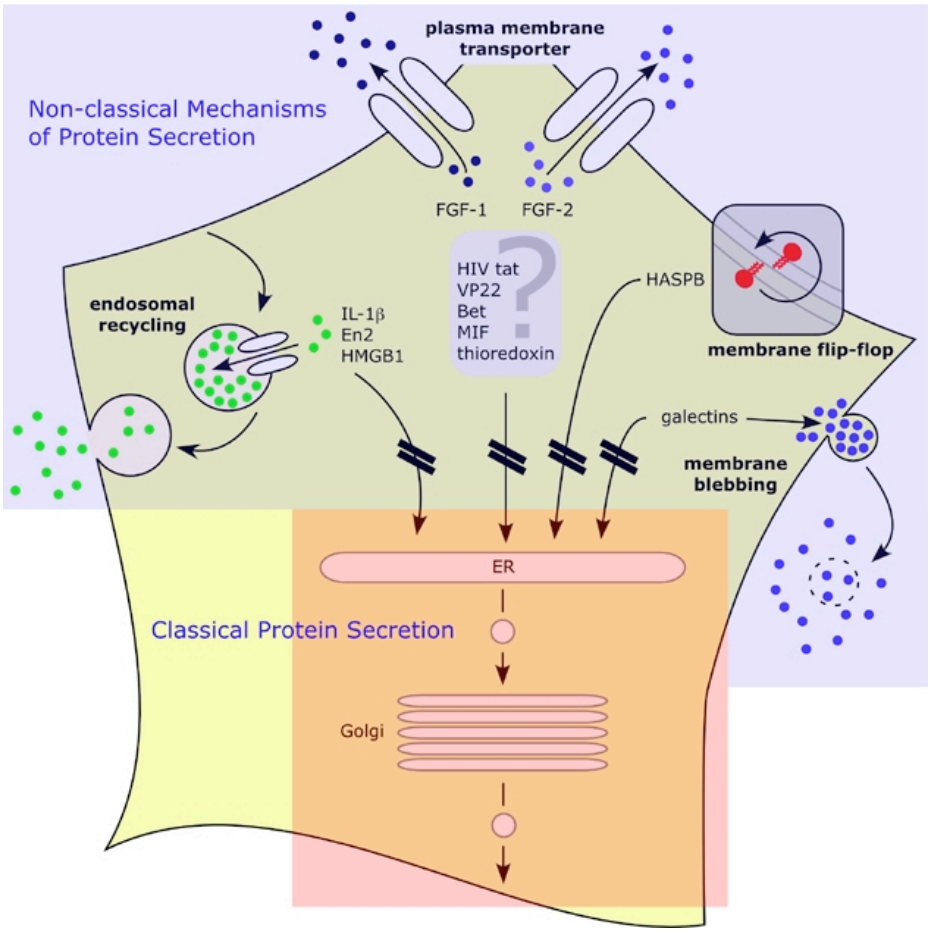

Fig. 1 Cargo proteins and potential export routes of unconventional protein secretion.

Because unconventional secretory proteins are soluble factors synthesized on free ribosomes in the cytoplasm, various experimental strategies have been pursued in order to exclude unspecific release based on cell death under the experimental conditions applied. These experiments included quantitative measurements of the

appearance of unrelated cytoplasmic proteins in cellular supernatants (Cleves, 1997; Engling et al., 2002; Hughes, 1999) as well as the identification of a CHO mutant cell line expressing the unconventional secretory protein HASPB that is deficient in non-classical export of this protein (Stegmayer et al., 2005).

Moreover, non-conventional protein secretion of FGF-2 was shown to be dependent on both energy (Florkiewicz et al., 1995) and temperature (Schäfer et al., 2004) and is stimulated or inhibited by various treatments (Cleves, 1997; Hughes, 1999). Furthermore, Gal-1 secretion was shown to be regulated for example by cell differentiation (Cooper and Barondes, 1990; Lutomski et al., 1997). Finally, it was described that FGF-2 export is regulated by NF-κB-dependent signaling pathways (Wakisaka et al., 2002).

Based on these observations, it can be concluded that unconventional secretory proteins exit eukaryotic cells in a controlled manner mediated by proteinaceous machineries.

Four potential mechanisms of unconventional protein export have been discussed so far in the literature to mediate translocation of cytosolic factors into the extracellular space (Hughes, 1999; Nickel, 2005). Two of these (Fig. 2; mechanism 1 and 3) involve intracellular vesicles of the endocytic membrane system such as secretory lysosomes (Clark and Griffiths, 2003; Stinchcombe et al., 2004) and exosomes (Stoorvogel et al., 2002), the latter ones being internal vesicles of multivesicular bodies (Stahl and Barbieri, 2002). Under suitable conditions, lysosomal contents gain access to the exterior of cells when specialized endocytic structures such as secretory lysosomes of T lymphocytes or melanosomes of melanocytes fuse with the plasma membrane (Stinchcombe et al., 2004). Similarly, luminal contents of endocytic structures can be released into the extracellular space when multivesicular bodies fuse with the plasma membrane, a process that results in the release of exosomal vesicles along with their cargo molecules (Stoorvogel et al., 2002).

Two alternative unconventional secretory mechanisms are characterized by a direct translocation of cytosolic factors across the plasma membrane using either protein conducting channels such as adenosine triphosphate-binding cassette (ABC) transporters proposed for FGF-2 secretion (Cleves and Kelly, 1996) (Fig. 2;

mechanism 2) or a process called membrane blebbing (Fig. 2; mechanism 4), the latter one being characterized by shedding of plasma membrane derived microvesicles that are released into the extracellular space (Freyssinet, 2003; Hugel et al., 2005; Martinez et al., 2005).

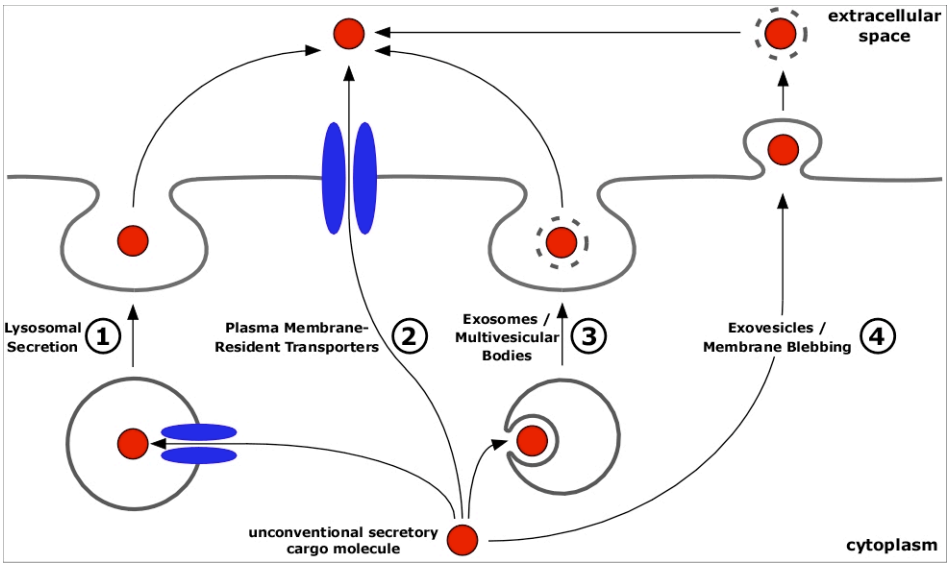

Fig. 2 Vesicular and non-vesicular pathways potentially involved in unconventional processes. 1, export by secretory lysosomes; 2, export mediated by plasma membrane-resident transporters; 3, export through the release of exosomes derived from multivesicular bodies; 4, export mediated by plasma membrane shedding of microvesicles

1.2.1 Galectins

All 15 members of the galectin protein family are abundant β-galactoside-specific lectins of the extracellular matrix (Chiariotti et al., 2004; Gray et al., 2004; Gray et al., 2005; Perillo et al., 1998). Lectins are defined as carbohydrate-binding proteins. They were first discovered more than 100 years ago in plants; they are now known to be present throughout nature. For a while after their discovery, animal lectins were classified according to the carbohydrate sequence to which they bound best. With the advent of molecular cloning a more consistent classification emerged, based on amino acid sequence homology and conservation of these lectins.

Until the 1990s, all of the animal lectins discovered were found to be naturally multivalent, either because of their defined multisubunit structure or by virtue of having multiple carbohydrate-binding sites within a single polypeptide (Sharon, 1993). Indeed, high avidity generated by multivalent binding of low-affinity single sites appears to be a common mechanism for optimizing lectin function in nature (Rini, 1995a), and a traditional definition for a lectin was “a multivalent carbohydrate-binding protein that is not an antibody”. The first exception to this general rule appeared to be the selectins (Crocker and Feizi, 1996; Rosen and Bertozzi, 1994), which have only a single CRD site within their extracellular polypeptide domains. The same situation applies to the Siglecs (for sialic acid/immunoglobulin superfamily/lectins) (Crocker, 2002). However, evidence is emerging that these molecules become functionally multimeric by clustering on cell surfaces (Crocker, 2002; Varki, 1992).

The galectins are β-galactoside-specific lectins and have been implicated in many cellular processes such as regulation of cell growth, cell proliferation, differentiation and apoptosis (see 1.4). Galectins can act either extracellularly or intracellularly to exert effects on cell growth and apoptosis (Pace et al., 1999; Perillo et al., 1998; Perillo et al., 1995; Rabinovich et al., 2002a). The best-characterized members of this family are Gal-1 and Gal-3 which are expressed in a wide range of vertebrate cell lines and tissues (Cerra et al., 1984; Cho and Cummings, 1995b; Cooper and Barondes, 1990; Lutomski et al., 1997; Mehul and Hughes, 1997; Sato et al., 1993b; Seelenmeyer et al., 2003).

1.2.1.1 Structure and classification

Members of the galectin family are composed of one or two **c**arbohydrate-**r**ecognition **d**omains (CRD) of approximately 130 amino acids. So far 15 members could be identified (Gal-1 to Gal-15). The structures of galectins can be generally classified into three categories:

1) The prototype galectin (Gal-1, -2, -5, -7, -10, -11, -13, -14, -15), which may exist as monomers or homodimers consisting of one carbohydrate recognition domain (CRD) per subunit
2) The chimera type (Gal-3), which contains a non-lectin N-terminal short sequence segment followed by 8-12 collagen-like repeats of 9 amino acids connected to the C-terminal CRD domain
3) The tandem-repeat type (galectin-4, -6, -8, -9, -12), composed of two CRD domains in a single polypeptide chain connected by a linker peptide (Ahmed et al., 1996; Yang et al., 2001).

Gal-1 is a homodimer of two 14-kDa polypeptides. Each subunit consists almost exclusively of a carbohydrate recognition domain (CRD) (Barondes et al., 1994). The crystal structure of Gal-1 was the first to be determined among galectins (Fig. 3). The overall folding of human Gal-1 involves a β-sandwich consisting of two antiparallel β-sheets of five (F1-F5) and six (S1-S6a/b) strands (Lobsanov et al., 1993), respectively. The N- and C-termini of each monomer are positioned at the dimer interface and the CRDs are located at the far ends of the same face of the surface, which presents a long negatively charged cleft in the cavity. The presence of this cleft deserves attention as a site for ionic interactions. The distance between the two CRDs is approximately 44 Å (Lopez-Lucendo et al., 2004).

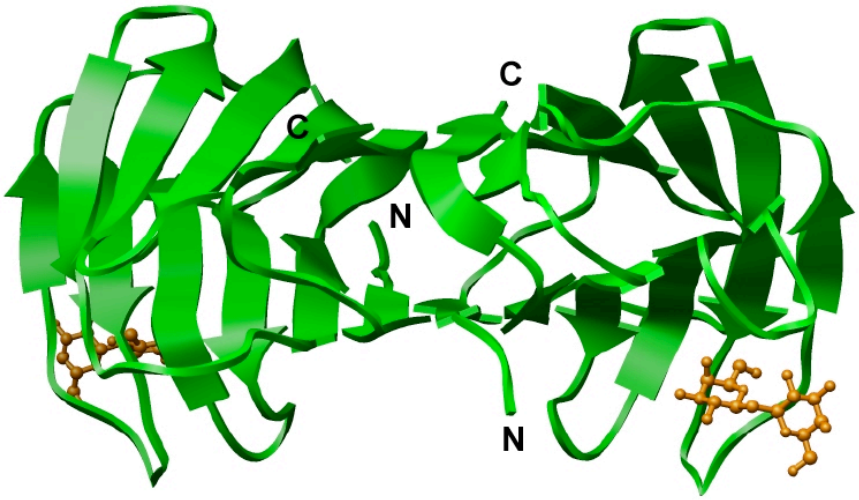

Fig. 3 Crystal structure of human Gal-1 (Lopez-Lucendo et al., 2004).

Similar to interleukin 1β, FGF-1, FGF-2 and HASPB, galectins apparently do not contain signal peptides in their primary structure suitable for ER/Golgi-mediated secretion (Couraud et al., 1989). Consistently, galectins are synthesized on free ribosomes in the cytoplasm (Wilson et al., 1994) and galectin secretion has been shown not to be blocked by inhibitors of the ER/Golgi-dependent pathway such as brefeldin A and monensin (Hughes, 1999; Lindstedt et al., 1993; Sato et al., 1993b). Unlike interkeukin 1β, Gal-1 and Gal-3 do not appear to be packaged into intracellular vesicles prior to export (Cooper and Barondes, 1990; Hughes, 1999; Mehul and Hughes, 1997; Sato et al., 1993a). Rather, Gal-1 and Gal-3 have been shown to accumulate directly underneath the plasma membrane, followed by an export mechanism that appears to involve so far the formation of membrane bound vesicles that pinch off before being released into the extracellular space (Cooper and Barondes, 1990; Hughes, 1999; Mehul and Hughes, 1997; Sato et al., 1993a). This potential mechanism also distinguishes galectin export from FGF-1 and FGF-2 export, as there is no evidence that these proteins are packaged into membrane-bound vesicles.

Extracellular galectins are found either bound to the extracellular surface of the plasma membrane or as abundant components of the extracellular matrix (Cerra et al., 1984; Cho and Cummings, 1995b; Cooper and Barondes, 1990; Lutomski et al., 1997; Mehul and Hughes, 1997; Sato et al., 1993a; Seelenmeyer et al., 2003). Cell surface association of galectins is mediated by both *N*- and O-linked oligosaccharide side chains of glycoproteins bearing terminal β-galactosides (Hughes, 1999; Perillo et al., 1998) as well as by β-galactoside-containing glycolipids such as GM1 (Kopitz et al., 1998; Perillo et al., 1998). As Gal-1 and Gal-3 can form homodimers (Cho and Cummings, 1995b; Giudicelli et al., 1997; Hughes, 1999), it has been proposed that extracellular galectins affect their glycosylated cell surface counter receptors by inducing conformational changes of their extracellular domains and/or by clustering galectin counter receptors based on non-covalent crosslinking of oligosaccharide moieties (Perillo et al., 1998). In this way, secreted galectins are thought to affect processes such as cell differentiation by cell surface counter receptor-mediated signaling (Perillo et al., 1998; Sacchettini et al., 2001). While classical counter receptors of, e.g., Gal-1 include laminin (Zhou and Cummings, 1990), fibronectin

(Ozeki et al., 1995) and cell-type specific receptors such as T-cell CD43 and CD45 (Pace et al., 1999), it has been shown that tumor-specific cell surface antigen CA125 also represents a galectin counter receptor that preferentially binds Gal-1 (Seelenmeyer et al., 2003). This latter example is of particular interest as it provides a potential molecular mechanism for how tumor cells can differentially interact with the extracellular matrix, a process crucial for tumor progression (Liu and Rabinovich, 2005).

1.2.1.2 Gal-1-mediated signaling and biosynthesis of Gal-1 counter receptors

Galectins represent a group of proteins that bind β-galactosyl-containing glyco-conjugates. Galectins are widely distributed throughout the animal kingdom. Certain members of the galectin family promote cell-cell adhesion such as Gal-1 (Perillo et al., 1998; van den Brule et al., 1995), whereas some have potent biological activities, such as the ability to induce apoptosis (Lanteri et al., 2003; Perillo et al., 1995), and to induce metabolic changes, such as cellular activation and mitosis (Liu et al., 2002). Galectins are soluble proteins that are secreted by a nonclassical pathway and require reducing conditions to maintain activity in the absence of ligands (de Waard et al., 1976). To fulfill their extracellular function, galectins need d

To bind to β-galactoside-containing counter receptors. Functional counter receptors with regard to galactosylation are obligatory components in order to promote cell-cell adhesion, cell-matrix adhesion and to effect cell growth and viability.

Asparagine-linked glycosylation (N-glycosylation) begins with the assembly of the complete dolichol-linked oligosaccharide donor (initial composition $Glc_3Man_9GlcNAc_2$) (Hebert et al., 2005). This process begins on the cytosplasmic face of the ER and is finished within the lumen, where the glycan chain is transferred *en bloc* by oligosaccharyltransferase to an Asn residue in the consensus sequence Asn-X-Ser/Thr. Following translocation into the ER lumen and glycosylation, proteins encounter chaperones that facilitate the maturation process (Hebert et al., 2005). The initial branched carbohydrate structure is modified and trimmed in the ER, but 5 of

the 14 residues are maintained in the structure of all N-linked oligosaccharides on secretory and membrane proteins (Kornfeld and Kornfeld, 1985). Further modifications and additions of sugar residues occur in the Golgi apparatus, depending on the protein (Farquhar, 1981). For example, UDP-galactose is specifically transferred by Golgi-resident galactosyltransferases to N-linked glycoproteins, which are potential counter receptors for Gal-1.

The first glycosylation enzyme to be biochemically localized to Golgi membranes is galactosyltransferase (GalNAcT) (Fleischer et al., 1969; Morre et al., 1969). Nearly all eukaryotic GalNAcT (Hennet, 2002) have been shown to be membrane-bound proteins (type II transmembrane proteins) with their active sites being exposed to the lumen of the Golgi (Carey and Hirschberg, 1981; Creek and Morre, 1981; Fleischer, 1981; Schachter et al., 1970). These terminal glycosyltransferases are biochemically localized to regions of the Golgi distinct from early oligosaccharides trimming enzymes (Deutscher et al., 1983; Dunphy et al., 1981; Goldberg and Toole, 1983).

The modification of serine or threonine residues on proteins by addition of a GalNAc residue results in an O-linked oligosaccharide or O-glycan. O-glycan biosynthesis is simpler than oligosaccharide transfer to asparagines in that a lipid-linked oligosaccharide precursor used to transfer sugars to target proteins is not required (Hebert et al., 2005). The initiating event is the addition of the monosaccharide GalNAc (from UDP-GalNAc) to serine and threonine residues catalyzed by a polypeptide GalNAc transferase (GalNAcT) (Hirschberg and Snider, 1987).

Galactose can be activated to UDP-Gal in several ways (Holton, 1996). The first is by direct phosphorylation at the C1-position (Gal-1-P), which can react with UTP to form UDP-Gal (Gahl, 1997; Holton, 1996). Alternatively, Gal-1-P can be converted to UDP-Gal via the uridyl transferase-catalyzed exchange reaction with UDP-Glc. Finally, UDP-Gal can be formed from UDP-Glc by the NAD-dependent reaction catalyzed by UDP-Gal-4-epimerase (Gahl, 1997). Cytosolic UDP-galactose is translocated into the lumen of the Golgi apparatus by a specific UDP-galactose transporter localized in the Golgi membrane (Deutscher and Hirschberg, 1986).

In contrast to N-glycosylation, a consensus sequence for GalNAc addition to polypeptides has not been identified (Hebert et al., 2005; Hennet, 2002). Many O-glycans are extended into long chains with variable termini that may be similar to the termini of N-glycans. However, O-glycans are less branched than most N-glycans and are commonly biantennary structures. O-glycosylation can result in the formation of mucin-type molecules. Mucins are defined as soluble or membrane-bound glycoproteins with a large number of clustered O-glycans. The clustering of O-glycans on mucins is in part due to the presence of a large number of serine and threonine residues in an uncharged and often proline-rich peptide context.

1.2.2 Pro-angiogenic Growth Factors: FGF-1 and FGF-2

Fibroblast growth factors 1 and 2 (FGF-1 and FGF-2) belong to a large family of heparin-binding growth factors that, apart from their mitogenic activity (Burgess and Maciag, 1989; Schweigerer et al., 1987), are key activators of tumor-induced angiogenesis. In vertebrates, the 22 members of the FGF family range in molecular mass from 17 to 34 kDa and are highly conserved in both gene structure and amino acid sequence (Ornitz and Itoh, 2001). Most of the different FGF family members share 28 highly conserved and six identical amino acid residues. Structural studies on FGF-1 and FGF-2 identified 12 antiparallel β-strands in the conserved core region of the protein. Two β-strands include several basic amino acid residues that form the primary heparin-binding site of FGF-2, which is responsible for the affinity for heparan sulfate proteoglycans (Raman et al., 2003).

Most FGFs (FGF 3-8, 10, 15, 17-19, and 21-23) have amino-terminal signal peptides and are secreted from cells by a classical mechanism. A second group, mainly FGF 11-14 lack a signal sequence and are thought to remain intracellularly (Ornitz and Itoh, 2001). Their function is presently unknown.

The other growth factors lack a classical sequence, but are nevertheless secreted. FGF-9 and FGF-16, which share 73% homology, contain a new N-terminal, non-cleaved signal peptide. As FGF-9 and FGF-16 are glycosylated, it is consistent that they are secreted via the classical vesicular pathway (Revest et al., 2000).

The remaining FGFs (FGF-1, the 18 kDa isoform of FGF-2, and FGF-20), which lack a known signal sequence, are exported in an unconventional manner. As FGF-20 was discovered only recently, its function and secretion mechanism is largely unknown (Hajihosseini and Heath, 2002; Jeffers et al., 2001; Kirikoshi et al., 2000).

As illustrated in Fig. 2 it has been proposed for FGF-2 that membrane translocation is mediated by plasma membrane-resident transporters. While it was first assumed that angiogenic growth factors might be released from mechanically injured tissue to promote wound healing (McNeil et al., 1989), a process that requires angiogenesis, various lines of evidence suggest that FGF-1 and FGF-2 are exported from cultured cells in the absence of appreciable amounts of cell death (Engling et al., 2002; Florkiewicz et al., 1995; Jackson et al., 1992; Mignatti et al., 1992; Trudel et al., 2000). Like IL-1β (Rubartelli et al., 1990), FGF-1 is increasingly secreted under stress conditions such as heat shock treatment (Jackson et al., 1992; Shin et al., 1996). In contrast, FGF-2 export is not affected under these conditions (Mignatti and Rifkin, 1991). While serum starvation has been reported to inhibit export of FGF-2 (Mignatti et al., 1992), it was found to induce secretion of FGF-1 (Shin et al., 1996).

Recently it was shown that direct translocation of FGF-2 across the plasma membrane does not require protein unfolding (Backhaus et al., 2004). In case of classical secretory transport, quality control occurs at the level of the ER in that secretory proteins not being folded properly do not have access to transport vesicle-mediated exit from this compartment but rather are targeted for degradation (Sayeed and Ng, 2005; Sitia and Braakman, 2003; Trombetta and Parodi, 2003). Thus, it appears quite reasonable that translocation of FGF-2 is in some way coupled to a mechanism that ensures secretion only of functional, properly folded FGF-2 (Backhaus et al., 2004). These considerations imply that FGF-2 might not be released in an unfolded state but rather is exported from cells in a functional form that has passed quality control measures (Nickel, 2005).

1.2.3 Leishmania hydrophilic acylated surface protein B (HASPB)

Another quite remarkable example of nonclassical protein export from eukaryotic cells is the mechanism of cell surface expression of Leishmania HASPB which is found associated with the outer leaflet of the plasma membrane only in infectious stages of the parasite lifecycle (Alce et al., 1999; Flinn et al., 1994; McKean et al., 2001; Pimenta et al., 1994). The protein is synthesized on free ribosomes in the cytoplasm. HASPB biogenesis starts with cotranslational myristoylation of its N-terminus. A second acylation step involves palmitoylation at cysteine 5 of the SH4 domain of HASPB (Denny et al., 2000). The HASPB primary structure differs from all other unconventional secretory proteins known to date, as it contains an N-terminal SH4 domain commonly found in src kinases that is a substrate for N-terminal protein acylation (Resh, 2004).

Mutational analysis revealed that a HASPB construct lacking its 18 N-terminal amino acids is localized to the cytoplasm (Denny et al., 2000). The same is true for a mutant that retains the N-terminus but lacks the myristoylation site (Denny et al., 2000). Interestingly, a mutant that lacks the palmitoylation site (C5A), but continues to be myristoylated, has been found associated with the cytoplasmic surface of the Golgi apparatus (Denny et al., 2000) suggesting that the putative palmitoylacyltransferase is a resident enzyme of the Golgi apparatus (Denny et al., 2000; Stegmayer et al., 2005). Dual acylation of the SH4 domain of HASPB mediates stable membrane association of the molecule. Following transient association with the Golgi, HASPB is transported to the inner leaflet of the plasma membrane. Based on these observations, there are in principle three options how this transport step is mediated: (i) HASPB might be transported to the plasma membrane associated with the cytoplasmic leaflet of secretory vesicles, (ii) HASPB might be targeted first to endosomal structures followed by translocation to the plasma membrane or (iii) HASPB transport from the Golgi to the plasma membrane might not rely on transport vesicles. Intriguingly, heterologous expression of various HASPB fusion proteins in mammalian cells revealed the existence of a machinery that is capable of translocating the protein across the plasma membrane (Denny et al., 2000), demonstra-

ting a conserved pathway among lower and higher eukaryotes. No endogenous mammalian cargo proteins that make use of this type of export system have been identified so far. In any case, palmitoylation of HASPB is strictly required for plasma membrane targeting as palmitoylation deficient mutants of HASPB are efficiently retained at the level of the Golgi (Denny et al., 2000; Stegmayer et al., 2005). The final localization of HASPB is characterized by its stable association with the outer leaflet of the plasma membrane with the protein moiety being exposed to the extracellular space. Therefore, HASPB must translocate across at least one membrane during its biogenesis pathway. Recently, it was shown that the HASPB membrane translocation is likely to be mediated by a plasma membrane-resident transporter (Stegmayer et al., 2005).

1.2.4 Cytokines: Interleukin-1β, Thioredoxin and Macrophage Migration Inhibitory Factor

A classical example of an unconventional secretory protein whose export mechanism involves intracellular vesicles is IL-1β (Rubartelli et al., 1990). In 1987, Dinarello and colleague demonstrated that interleukin 1, a cytokine (Dinarello, 1991; Dinarello, 1997) lacking a classical signal peptide for ER/Golgi-mediated protein secretion, is exported from activated human monocytes (Auron et al., 1984). Two isoforms of interleukin 1 termed 1α and 1β have been described which represent proteolytically processed forms derived from two related but distinct precursors (Dinarello, 1997). The processing of IL-1α involves myristoylation and, following insertion into the plasma membrane, calpain-dependent cleavage that is thought to cause release of the mature form of IL-1α into the extracellular space (Kobayashi et al., 1990; Watanabe and Kobayashi, 1994). In the case of IL-1β, interleukin converting enzyme produces mature IL-1β (Black et al., 1988; Wilson et al., 1994), which is then exported (Dinarello, 1991). When homogenates of activated monocytes were analyzed by gradient centrifugation and protease protection experiments, an IL-1β subpopulation could be detected in the lumen of intracellular vesicles (Andrei et al., 1999). On the basis of immunolocalization studies employing electron

microscopy, these subcellular vesicles have been identified as an endolysosomal subcompartment because IL-1β-positive vesicles display the typical morphology of endocytic organelles and are positive for cathepsin D and Lamp-1, classical markers of late endosomes and lysosomes. However, only a fraction of the total population of cathepsin D- and Lamp-1-positive vesicles was also labeled by anti-IL-1β antibodies suggesting that this population represent a specialized subspecies of endolysosomes (Andrei et al., 1999). Following appropriate stimulation during the onset of inflammatory processes, IL-1β-containing vesicles undergo fusion with the plasma membrane resulting in the release of IL-1β into the extracellular space (Andrei et al., 1999; Andrei et al., 2004). Uptake of IL-1β into secretory lysosomes might be mediated by a protein-conducting ABC transporter as the overall process of IL-1β secretion is sensitive to glyburide, a drug targeted against the ABC1 family of membrane transporters (Hamon et al., 1997; Zhou et al., 2002). Other unconventional secretory protein such as high mobility group 1 protein (HMGB1) and possibly MIF (migration inhibiting factor), an inflammatory cytokine mediating a number of immune and inflammatory diseases, e.g. bacterial septic shock, are released by secretory lysosomes as well (Bonaldi et al., 2003; Gardella et al., 2002) and glyburide also appears to inhibit nonclassical secretion of MIF (Flieger et al., 2003).

Another example for unconventionally secreted proteins are thioredoxins, ubiquitous intracellular enzymes that catalyze thiol disulfide exchange reactions (Holmgren, 1989). Additionally, extracellular populations of thioredoxin have been detected that, similar to IL-1β and MIF, follow an ER/Golgi-independent route of secretion (Rubartelli et al., 1992; Rubartelli et al., 1995; Rubartelli and Sitia, 1991; Sahaf and Rosen, 2000). This observation is consistent with additional physiological roles of thioredoxin such as its function as a mitogenic cytokine that requires extracellular localization (Pekkari et al., 2001; Pekkari et al., 2000). Secretion of thioredoxin appears to be mediated by a pathway distinct from IL-1β as it could neither be detected in intracellular vesicles, nor was the secretion process reported to be inhibited by reagents that interfere with the function of ABC transporters. However, as with IL-1β (Rubartelli et al., 1990), secretion of thioredoxin is inhibited my methylamine and stimulated by brefeldin A (Rubartelli et al., 1992).

1.3 Gal-1 receptors in different cell types

As already described galectins are a family of animal lectins defined by two properties: shared amino acid sequences in their carbohydrate recognition domain, and affinity to β-galactosides. A wide variety of biological phenomena are related to galectins, i.e. development, differentiation, morphogenesis, tumor metastasis, apoptosis, RNA splicing, and immunoregulatory functions. Several Gal-1 receptors are discussed such as CD45, CD7, CD43, CD2, CD3, CD4, CD107, CEA, extracellular matrix proteins such as laminin and fibronectin, glycosaminoglycans, integrins, a β-lactosamine glycolipid, GM1 ganglioside, Polypeptide HBGp82, glycoprotein 90 K/ Mac-2BP and pre-B-cell receptor.

1.3.1 Biological functions of Gal-1 in different cell types

A wide variety of biological phenomena have been shown to be related to Gal-1, i.e. cell adhesion, proliferation, apoptosis, T-cell receptor counter-stimulation, immunomodulatory effects, cell cycle arrest, pre-B cell signaling, RNA splicing and promotion of H-Ras membrane anchorage (Kuwabara et al., 2003; Liu et al., 2002) (Rabinovich et al., 2002a; Rabinovich et al., 2002b). Gal-1 is involved in cell-cell and cell-matrix adhesion, in processes such as tumor invasion and metastasis, inflammation, and organ development. Gal-1 binds to poly-N-acetyl-lactosamine chains from extracellular cell matrix proteins such as laminin and fibronectin, thereby modulating cell adhesion both positively and negatively (Moiseeva et al., 2000; Ozeki et al., 1995; van den Brule et al., 1995; Zhou and Cummings, 1990; Zhou and Cummings, 1993). Gal-1 also affects the interaction of tumor cells with endothelia cells, which is critical in invasion and metastasis. Accumulation of Gal-1 is observed at the contact sites between breast tumor cells and the endothelium: Gal-1 localizes on tumor cells and Gal-3 preferentially localizes on endothelial cells, suggesting different roles of these lectins in adhesion. Increased Gal-1 expression has been reported in many types of human cancer such as those arising from the thyroid,

endometrium, head and neck, thymus, bladder, pancreas, and colon, and in cholangiocarcinoma, and glioma (Danguy et al., 2002; Lahm et al., 2004).

In the immune system, Gal-1 is expressed in the thymus, spleen, lymph nodes, bone marrow, liver, and immune-privileged sites (Perillo et al., 1998). Gal-1 from human thymic epithelial cells binds to core 2-O-glycans on immature cortical thymocytes and induces cell apoptosis during thymocyte maturation. Immature cortical thymocytes bind more Gal-1 than mature medullar thymocytes do (Perillo et al., 1997). The apoptotic effect is dose dependent, carbohydrate-specific, and Fas-, steroid- and CD3- independent. In addition, Gal-1 expressed on endothelial cells can trigger apoptosis of adherent T cells in a carbohydrate-dependent manner (Nguyen et al., 2001; Perillo et al., 1995).

In inflammation, activated macrophages, antigen-stimulated T cells, activated B cells, and alloreactive T cells produce high levels of Gal-1 to kill effector T cells after immune response. Immune privileged tissues such as the retina, placenta, testis, and the ovary overexpress Gal-1, which might ensure the rapid elimination of inflammatory T cells by the Gal-1 apoptotic pathway to protect the integrity and function of these vulnerable tissues (Rabinovich et al., 2002a; Rabinovich et al., 2002b).

Gal-1 also modulates proliferation of normal and malignant cells, depending on the cell type: growth inhibition may be observed at high Gal-1 concentrations whereas lower concentrations enhance cell proliferation (Adams et al., 1996). In human ovary carcinoma cells, low concentration of Gal-1 do not show any effect, but higher concentration decreases cell proliferation (van den Brule et al., 2003). Gal-1 increases serum-induced DNA synthesis in human SMC cultured cells (Moiseeva et al., 2000). In rat pulmonary arterial endothelial cells, Gal-1 also promotes proliferation (Sanford and Harris-Hooker, 1990).

1.3.2 Galectin-1 receptors

1.3.2.1 Extracellular matrix receptors

Laminin, fibronectin, thrombospondin, vitronectin, and glycoaminoglycans Gal-1 can modulate cell-ECM interactions in different biological systems. Laminin and fibronectin are two ECM receptors proposed as the main receptors for Gal-1 (van den Brule et al., 1995; Zhou and Cummings, 1993).

Laminin is a large glycoprotein and a major component of the basement membrane in all types of tissues. Many biological phenomena such as cellular adhesion, spreading, proliferation, and differentiation involve interaction between cells and laminin. It is composed by three chains, the A chain (400 kDa), B1 chain (210 kDa), and B2 chain (200 kDa). It shows ASN-linked oligosaccharides containing the repeating disaccharide or poly-N-acetyl-lactosamine sequence (Zhou and Cummings, 1990). Gal-1 also modulates human melanoma cell adhesion to laminin. Local increases or decreases of Gal-1 expression may play a critical role during attachment and detachment of cancer cells throughout the cancer progression process (van den Brule et al., 1995).

Tissue fibronectin has also been proposed as an endogenous receptor for Gal-1 (Ozeki et al., 1995). Fibronectin, laminin, and Gal-1 colocalize in the extracellular matrix of placental tissue.

Other ECM proteins such as thrombospondin and vitronectin, and, to a lower extent, osteopontin can also bind to Gal-1 (Moiseeva et al., 2000). It binds to several ECM in a dose-dependent and β-galactoside dependent manner; moreover, Gal-1 interacts with GAG chains from ECM. For example, heparan sulfate and chondroitin sulfate reduce the binding of Gal-1 to ECM proteins (Moiseeva et al., 2003). Interactions between Gal-1 and chondroitin sulfate proteoglycans have also been described (Seelenmeyer et al., 2003). Chondroitin sulfate B contains galactose-like residues and shows significant β-galactoside-dependent binding to Gal-1 in the solid

phase, compared to chondroitin sulfate A and C and heparan sulfate, which do not bind to Gal-1.

Interaction between Gal-1 and vitronectin seem to depend on the vitronectin conformation. Vitronectin exist either as folded inactive monomer or as an unfolded multimer able to interact with ECM components. It shows a significant binding to Gal-1 in the presence of lactose, probably because lactose induces unfolding of vitronectin. Moreover, Gal-1 bound to the ECM reduces the incorporation of vitronectin and chondroitin sulfate B to the ECM in a β-galactoside dependent manner. Thus, ECM bound Gal-1 can decrease incorporation of its receptors into the ECM, which suggests a role for Gal-1 in ECM assembly and tissue matrix remodeling (Moiseeva et al., 2003).

1.3.2.2 Cell surface receptors

1.3.2.2.1 Integrins

The α7β1 integrin is the predominant laminin-binding integrin on differentiating skeletal muscle cells (Song et al., 1993). The expression of the α7 is developmentally regulated during skeletal muscle differentiation and has been used to identify cells at distinct stages of the myogenic lineage. The addition of purified recombinant Gal-1 to myogenic cells plated on laminin inhibits myoblast spreading and fusion suggesting that Gal-1 regulates muscle cell interactions with the extracellular matrix (Cooper et al., 1991).

1.3.2.2.2 CD45

CD45 is a family of integral membrane tyrosine phosphatases expressed on cells of hemopoietic origin. Human CD45 molecules described vary in molecular weight from 180 to 220 kDa, accounted for by alternative splicing of a single precursor mRNA (Streuli et al., 1987). Additional heterogeneity is accounted for by differences in glycosylation of the protein backbone (Sato et al., 1993b).

The role of CD45 in T cell apoptosis mediated by Gal-1 is controversial (Fajka-Boja et al., 2002), because CD45 expression is not absolutely required for Gal-1 induced T cell death. Gal-1-induced T cell apoptosis is regulated by expression of specific glycosyltransferase enzymes such as core 2 β-1,6-N-acetylglucoseaminyl-transferase, which creates a core 2 branch on O-glycans allowing the addition of lactosamine sequences (Hernandez and Baum, 2002).

1.3.2.2.3 CD43

CD43 has also been identified as a Gal-1 ligand in T cells. Confocal microscopy studies have demonstrated that Gal-1 treatment promotes CD45 segregation, virtually excluding CD43. To verify apoptosis of cells undergoing receptor redistribution, annexin V binding was evaluated. Annexin V only localized in large patches of CD45 on the surface of apoptotic cells treated with Gal-1. Indeed, before galectin induction, CD7 colocalized with CD43, and after addition of Gal-1, CD43 and CD7 were still associated and moved into larger aggregation. These observations indicate that CD43 and CD7 may act as a complex during delivery of Gal-1 apoptotic signals (Pace et al., 1999; Perillo et al., 1995).

Altered glycosylation of CD43 and CD45 has been observed in HIV-1-infected of T cells: decreased sialylation and increased expression of core 2 O-glycans have been demonstrated. Therefore, HIV-1 infection results in accumulation of exposed lactosamine residues, oligosaccharides recognized by Gal-1 on CD43 and CD45,

promoting Gal-1 binding, receptor cross linking, and segregation, critical steps in triggering apoptosis (Lanteri et al., 2003).

1.3.2.2.4 CD7

CD7 appears to have immunomodulatory activity, although ligands for CD7 have been difficult to find (Lanteri et al., 2003). To determine whether CD7 is necessary for Gal-1-induced T cell apoptosis, human CD7 has been expressed in a CD7- HUT78 T cell line, which is not susceptible to Gal-1-induced apoptosis. CD7 expression renders HUT78 cells susceptible to Gal-1. Indeed, CD7 is necessary for Gal-1-induced T cell apoptosis via a Ca2+-independent pathway. CD7 is present on human immature thymocytes and is up-regulated on activated T cells. Therefore, CD7+ T cells may bind Gal-1 expressed by stromal or dendritic cells in tissues where T cells die, such as the thymus during T cell development or peripheral lymphoid organs following an immune response (Pace et al., 2000).

1.3.2.2.5 GM1 Ganglioside

Gal-1 is a major receptor for the carbohydrate portion of ganglioside GM1 exposed on the surface of cultured human SK-N-MC neuroblastomas cells. When cells were exposed to a ganglioside sialidase inhibitor, which prevents the generation of GM1 ganglioside, a significant decrease of Gal-1 binding was detected (Kopitz et al., 1998). The pentasaccharide of GM1 presents two building blocks, the disaccharide Galβ1-3GalNAC and the central trisaccharide Neu5Acα2-3Galβ1-4Glc: these two galactose moieties in central and terminal position are potential binding sites for Gal-1. Laser photo-chemically-induced dynamic polarization shows that GM1 binding to Gal-1 involves interaction between Trp69 and a galactose residue (Siebert et al., 2003).

1.4 Galectins and apoptosis

Programmed cell death or apoptosis is indispensable for proper development of multicellular organisms. Cell death shapes the proliferating mass of cells into tissues and shapes tissues into organs (Meyer and Rustin, 2000). In the mature organism, cell death plays a critical role in regulating tissue homeostasis. Dysregulation of cell death can cause diseases; excess cell death is associated with immunodeficiency and neurodegenerative disorder; and diminished cell death is associated with autoimmunity and cancer (Thompson, 1995). To maintain the critical balance between cell proliferation and cell death, distinct families of proteins that regulate cell death have evolved. These include death-inducing ligands, death receptors, and intracellular regulators of death pathways. To date, only two families of proteins have been described as death-inducing ligands: the tumor necrosis factor (TNF) family and the galectin family (Rabinovich et al., 2002a; Zimmermann et al., 2001). TNF ligands bind to cognate TNF receptor polypeptides to initiate cell death.

The intracellular machinery responsible for apoptosis seems to be similar in all animal cells. This machinery depends on a family of proteases that have a cysteine at their active site and cleave their target proteins at specific aspartic acids, therefore called caspases, which are synthesized as inactive precursors. Procaspase activation can be triggered from outside the cell by the activation of death receptors on the cell surface. Lymphocytes can induce apoptosis by producing Fas ligand, which binds the receptor Fas on the surface of the target cells. The Bcl-2 family of intracellular proteins regulates the activation of procaspases.

In contrast, pro-apoptotic galectins bind to specific saccharide ligands on cell surface glycoprotein to initiate cell death. Similar to the Bcl family, galectins also function intracellularly to promote cell survival or cell death (Kuwabara et al., 2003; Yang et al., 1996). Galectins are unique among molecules regulating cell viability because they act both outside the cell to initiate death signal and inside the cell to regulate susceptibility to death.

Thymocyte maturation in the thymus is accompanied by changes in the sialylation of cells (i.e. immature cells are less sialylated than mature cells). These observations led to studies regarding the possibility that maturing thymocytes interact with endogenous thymic lectins. Gal-1 can bind to both activated and resting thymocytes and that its binding to activated T cells and T cell leukemic cell lines induces apoptosis (Baum et al., 1995a) that is controlled by specific surface receptors capable of oligomerization an intracellular caspase cascade. Resting T cells also bind Gal-1, but do not undergo apoptosis. The mechanism of Gal-1 induced apoptosis appears to be distinct from that triggered by Fas (Baum et al., 1995a). The thymocytes receptors for Gal-1 appear to be CD45 and CD43, both of which are highly glycosylated membrane glycoproteins. CD45, CD43 and CD7 are the three major glycoproteins on the T cell surface that bind galectin (Walzel et al., 1999), and Gal-1 regulates CD45-induced signaling in burkitt lymohoma B cells. Although initial experiments identified CD7 (Pace et al., 2000) and CD45 (Baum et al., 1995b; Nguyen et al., 2001) as the major mediator of Gal-1-induced apoptosis in T cells, recent work showed that CD45-deficient Jurkat cells exhibits susceptibility to Gal-1 (Fajka-Boja et al., 2002). There is also one report showing the involvement of the transcription factor AP-1 and Bcl-2 in Gal-1 induced apoptosis (Rabinovich et al., 2000). When mature T cells were cultured in the presence of Gal-1, AP-1 was activated. Treatment of cells before Gal-1 exposure with curcumin, an inhibitor of AP-1 activation, suppresses apoptosis, suggesting that AP-1 activation is required for Gal-1-induced apoptosis. Gal-1 also inhibits the induction of Bcl-2 by the plant lectin concanavalin A (Con A).

1.5 Aim of this work

Aim of this work was to elucidate the molecular machinery mediating the export of Gal-1. Therefore, a novel experimental system was planned to be established in order to facilitate studies on the molecular machinery of Gal-1 secretion. A key aspect was to reconstitute Gal-1 secretion in living cells based on a read-out method that provides a precise and quantitative analysis of this process. A Gal-1-GFP-based system was designed to measure total protein expression (GFP-derived fluorescence) and secreted Gal-1-GFP (APC-derived cell surface staining) can be measured simultaneously.

Employing a biochemical approach, a search for Gal-1-interacting proteins potentially involved in the unconventional secretion process of Gal-1 was conducted. Therefore, a GST-Gal-1 affinity matrix was used to identify human proteins that interact with Gal-1. A major aim of this thesis was to characterize such factors in terms of function and impact on Gal-1 secretion employing the system described above.

In the third part of this thesis the issue of how Gal-1 is recognized by its transport machinery was studied. A targeting motif, directing the protein to its translocation apparatus has so far not been described. Therefore, a major aim was to generate a large collection of Gal-1 mutants carrying single amino acid substitutions. Using the experimental systems to be established in the first part of this thesis, it was planned to elucidate the molecular determinants directing Gal-1 to its unconventional export machinery.

2 Material and Methods

2.1 Material

2.1.1 Chemicals

Chemicals	Manufacturer
Agar	Becton Dickinson, Le Pont de Claix, France
Agarose electrophoresis grade	Invitrogen Ltd., Paisley, UK
αMEM	Biochrom AG, Berlin
Ammonium chloride	Carl Roth GmbH, Karlsruhe
Ampicillin sodium salt	Gerbu Biotechnik GmbH, Gaiberg
APS (Ammonium peroxo disulfate)	Carl Roth GmbH, Karlsruhe
β-Mercaptoethanol	Merck, Darmstadt
EZ-Link Sulfo-NHS-SS-Biotin	Pierce, Perbio Sciences, Bonn
Bromphenol Blue Na-salt	Serva Electrophoresis GmbH, Heidelberg
BSA (Bovine serum albumine, Albumin fraction V)	Carl Roth GmbH, Karlsruhe
Calcium chloride dihydrate	Applichem, Darmstadt
Cell dissociation buffer (CDB)	Invitrogen, Paisley, UK
Chloroquine	Sigma-Aldrich Chemie GmbH, Steinheim
CL-4B Sepharose (Beads)	Amersham Biosciences Pharmacia, Uppsala, Sweden
Clear Nail Protector	Wet'n Wild USA, North Arlington, USA
Complete Mini (Protease Inhibitor Cocktail Tablets)	Roche Diagnostics, Mannheim

Deoxycholic acid sodium salt	Sigma-Aldrich Chemie GmbH, Steinheim
DMEM	Biochrom AG, Berlin
DMSO (Dimethyl sulfoxide)	J.T. Baker, Deventer, USA
DNA ladder (1 kb and 100 bp)	New England Biolabs, Frankfurt
dNTP-Mix	Peqlab, Erlangen
Doxicycline	Clontech, Palo Alto, USA
ECL Western Blotting Detection Reagent	Amersham Biosciences Pharmacia, Uppsala, Sweden
EDTA (Ethylene diamine tetraacetic acid)	Merck, Darmstadt
Ethanol pro analysi	Riedel-de Haën, Seelze
FCS (Fetal Calf Serum)	PAA Laboratories GmbH, Linz, Austria
Fluoromount G	Southern Biotechnologies Association Inc., Birmingham, USA
Glycerol	Carl Roth GmbH, Karlsruhe
Glycine	Applichem, Darmstadt
Hepes	Carl Roth GmbH, Karlsruhe
Isopropanol	Merck, Darmstadt
Kanamycin sulfate	Gerbu Biotechnik GmbH, Gaiberg
L-Glutamine	Biochrom AG, Berlin
Magnesium chloride hexahydrate	Applichem, Darmstadt
Methanol pro analysi	Merck, Darmstadt
Milk Powder	Carl Roth GmbH, Karlsruhe
Nonidet P40 (NP-40)	Roche, Mannheim
Paraformaldehyde	Electron Microscope Sciences, Hatfield, UK
Penicillin/Streptomycin for cell culture	Biochrom AG, Berlin
Ponceau S	Serva Electrophoresis GmbH, Heidelberg
Potassium dihydrogen carbonate	Carl Roth GmbH, Karlsruhe

Potassium hydroxide	J.T.Baker, Deventer, USA
Protein A-Sepharose (Beads)	Amersham Biosciences Pharmacia, Uppsala, Sweden
PVDF Membrane Immobilon P	Millipore Corporation, Bedford
PVDF Membrane Immobilon FL	Millipore Corporation, Bedford
QuikChange®Site-Directed Mutagenesis Kit	Stratagene, La Jolla, USA
Rotiphorese Gel 30 (37.5:1)	Carl Roth GmbH, Karlsruhe
Sodium chloride	J.T. Baker, Deventer, USA
Sodium dodecyl sulfate	Serva Electrophoreis GmbH, Heidelberg
Sodium hydrogen carbonate	J.T. Baker, Deventer, USA
Sodium hydroxide	J.T. Baker, Deventer, USA
TEMED (N,N,N',N'-tetramethylethylenediamine)	Bio-Rad, München
Trichloroacetic acid	Carl Roth GmbH, Karlsruhe
Tris	Carl Roth GmbH, Karlsruhe
Trition X-100	Roche, Mannheim
Trypsin / EDTA for cell culture	Biochrom AG, Berlin
Trypsin	Sigma-Aldrich Chemie GmbH, Steinheim
Tryptone	Becton Dickinson, Le Pont de Claix, France
Tween 20 (Polyoxyethylenesorbitan monolaurate)	Carl Roth GmbH, Karlsruhe
UltraLink immobilized streptavidin (Beads)	Pierce, Perbio Sciences, Bonn
Whatman MM	Whatman AG, Würzburg
Xylencyanol FF	Serva Electrophoresis GmbH, Heidelberg
Yeast Extract	Beckton Dickinson, Le Pont de Claix, France

2.1.2 Technical devices

Technical devices	Manufacturer
Anthos 2001 Microplate Photometer	Anthos, Hombrechtikon, Switzerland
Bacterial Incubator Infors HT ITE	Infors AG, Einsbach
Bacterial Shaker Centromat R	Braun, Melsungen
Centrifuge 5415 R	Eppendorf, Hamburg
Centrifuge 5417 R	Eppendorf, Hamburg
Centrifuge Avanti J-25	Beckman Coulter, Krefeld
Centrifuge Megafuge 1.0 R	Kendro, Langenselbold
Centrifuge Optima TLX Ultracentrifuge	Beckman Coulter, Krefeld
Centrifuge Rotor Sorvall SS-34	Kendro, Langenselbold
Centrifuge Sorvall Evolution RC	Kendro, Langenselbold
Centrifuge Sorvall RC 6	Kendro, Langenselbold
Ultracentrifuge Rotor TLA-45	Beckman Coulter, Krefeld
EmulsiFlex-C5	Avestin Europe GmbH Mannheim, Germany
FACSAria	Becton Dickinson, Heidelberg
FACSVantage	Becton Dickinson, Heidelberg
FACSCalibur	Becton Dickinson, Heidelberg
Gel Doc 2000	Bio-Rad, München
Incubator Heraeus CO_2-Auto-Zero	Kendro, Langenselbold
LKB Ultraspec III	Amersham Biosciences, Freiburg
Microscope Axiovert 40 C	Zeiss, Göttingen
Microscope LSM 510 Meta Confocal	Zeiss, Göttingen
Mini Trans-Blot Cell	Bio-Rad, München
Mini-PROTEAN 3 Electrophoresis System	Bio-Rad, München
Nanodrop ND-1000 Spectrophotometer	Peqlab, Erlangen
Odyssey Infrared Imaging System	LI-COR Biosciences, Bad Homburg

PCR Primus Advanced 25 and 96	Peqlab, Erlangen
pH-Meter 766 Calimatic	Knick, Egelsbach
Power Pack 200 and 300	Bio-Rad, München
Roto-Shake Genie	Scientific Industries, Bohemia, USA
Sonifier Cell Disruptor B 30	Heinemann, Schwäbisch Gmünd
Sonorex Super RK 103 h	Bandelin, Berlin
SpectraMax Gemini XPS Microplate Spectrofluorometer	Molecular Devices Corporation, Orleans, U.S
Thermomixer compact and comfort	Eppendorf, Hamburg
Tricorn 5/150 Column	Amersham Biosciences, Freiburg

2.1.3 Plasmids

Name	**Origin**
peGFP-C1	Clontech, Mountain View, USA
pET-15b-eGFP	AG Nickel, BZH, Heidelberg
pGEX-2T-Gal-1	AG Nickel, BZH, Heidelberg
pGEX-2T-Gal-3	AG Nickel, BZH, Heidelberg
pFB-CA125-C-TERM	AG Nickel, BZH, Heidelberg
pIVEX 2.4b Nde CA125-C-TERM	AG Nickel, BZH, Heidelberg
pGEM-T	Promega, Madison, USA
pGEM-T-Gal-1	AG Nickel, BZH, Heidelberg
pSilencer™ 1.0-U6	Ambion
pLNCD4	AG Schwappach, ZMBH, Heidelberg
pRevTRE2	Clontech, Mountain View, USA
pRevTRE2-GFP	AG Nickel, BZH, Heidelberg
pFB-hrGFP	Stratagene, La Jolla, USA
pVPack-Eco	Stratagene, La Jolla, USA
pVPack-GP	Stratagene, La Jolla, USA

2.1.4 DNA modifying enzymes

Enzyme	Manufacturer
AmpliTaq Polymerase	Perkin Elmer (Roche), Branchburg, USA
PfuTurbo Polymerase	Stratagene, La Jolla, USA
Age I	New England Biolabs, Frankfurt
Apa I	New England Biolabs, Frankfurt
BamH I	New England Biolabs, Frankfurt
Dpn I	New England Biolabs, Frankfurt
EcoR I	New England Biolabs, Frankfurt
Nde I	New England Biolabs, Frankfurt
Not I	New England Biolabs, Frankfurt
Sma I	New England Biolabs, Frankfurt
Calf Intestinal Phosphatase (CIP)	New England Biolabs, Frankfurt

2.1.5 Primers and oligonucleotides

Primers and oligonucleotides were purchased from Thermo Electron Company.

PCR primers for Gal-1, Gal-3 and eGFP:

5'-primer for His_6-eGFP (pET-15b/eGFP), NdeI-restriction-site:
5‘ - CGTTCATATGGTGAGCAAGGGCGAGGAG - 3‘
3'-primer for His_6-eGFP (pET-15b/eGFP), BamHI-restriction-site:
5‘ - CGGGATCCTTACTTGTACAGCTCGTCCAT - 3‘

5'-primer for GST-Gal-3(pGEX-2T-Gal-3), BamHI-restriction-site:
5‘ - GGAATTCAGCTCTTAGCAGACATTGG - 3‘
3'-primer for GST-Gal-3 (pGEX-2T-Gal-3), EcoRI-restriction-site:
5‘ - GGAATTCTTATATCATGGTATATGAAGC - 3‘

5'-primer for GST-Gal-1 (pGEX-2T-Gal-1), BamHI-restriction-site:
5‘ - CGGGATCCATGGCTTGTGGTCTGGTCGCC - 3‘
3'-primer for GST-Gal-1 (pGEX-2T-Gal-1), SmaI-restriction-site:
5‘ - TCCCCCGGGTCAGTCAAAGGCCACACATTTG - 3‘

PCR primers for pFB/CA125-C-TERM:

5'-primer for CA125-C-TERM, BamHI-restriction-site:
5’-CGGGATCCCGCCACCATGGGGCTGGACATACAGCAGCTT-3’
3'-primer for CA125-C-TERM, NotI-restriction-site:
5’-GACCTGGAGGATCTGCAATGAGCGGCCGCTTTTTTCCTT-3’

PCR primers for CA125 in vitro translation pIVEX 2.4b Nde CA125-C-TERM

5’-primer for CA125-C-TERM, NotI-restriction-site:
5’-AAGGAAAAAAGCGGCCGCATGGGGCTGGACATACAGCAGCTT-3’
3’-primer for CA125-C-TERM, BamHI-restriction-site:
5’-CGGGATCCTCATTGCAGATCCTCCAGGTC-3’

siRNA oligonucleotides directed against CA125-cytoplasmic tail:

Sense:
5’-GAAGGAAGGAGAATACAACTTCAAGAGAGTTGTATTCTCCTTCCTTCTTTTTT-3’

Antisense:
5’-AATTAAAAAAGAAGGAAGGAGAATACAACTCTCTTGAAGTTGTATTCTC-CTTCCTTCGGCC-3’

Site-directed mutagenesis primers:

Primer	Sequence	T_m
Gal-1-GFP		
C3A	5'-TGGCGACCAGACCAGCAGCCATGGTGGCG-3'	79.3°C
	5'-CGCCACCATGGCTGCTGGTCTGGTCGCCA-3'	
V6A	5'-GCTTGTGGTCTGGCCGCCAGCAACC-3'	71.4°C
	5'-GGTTGCTGGCGGCCAGACCACAAGC-3'	
A7I	5'-TGGCTTGTGGTCTGGTCATCAGCAACCTGAATCTCAAAC-3'	75.7°C
	5'-GTTTGAGATTCAGGTTGCTGATGACCAGACCACAAGCCA-3'	
N9A	5'-GTCTGGTCGCCAGCGCCCTGAATCTCAAACCTG-3'	76.4°C
	5'-CAGGTTTGAGATTCAGGGCGCTGGCGACCAGAC-3'	
K13A	5'-CCAGCAACCTGAATCTCGCGCCTGGAGAGTGCCTT-3'	78.1°C
	5'-AAGGCACTCTCCAGGCGCGAGATTCAGGTTGCTGG-3'	
P14A	5'-CAACCTGAATCTCAAAGCTGGAGAGTGCCTTCG-3'	70.6°C
	5'-CGAAGGCACTCTCCAGCTTTGAGATTCAGGTTG-3'	
E16A	5'-TCTCAAACCTGGAGCGTGCCTTCGAGTGC-3'	71.6°C
	5'-GCACTCGAAGGCACGCTCCAGGTTTGAGA-3'	
V20A	5'-GTGCCTTCGAGCGCGAGGCGAGG-3'	71.1°C
	5'-CCTCGCCTCGCGCTCGAAGGCAC-3'	
R21A	5'-AGTGCCTTCGAGTGGCAGGCGAGGTGGCT-3'	74.8°C
	5'-AGCCACCTCGCCTGCCACTCGAAGGCACT-3'	
V32A	5'-GCTAAGAGCTTCGCGCTGAACCTGGGC-3'	69.7°C
	5'-GCCCAGGTTCAGCGCGAAGCTCTTAGC-3'	
V32G	5'-GCTAAGAGCTTCGGGCTGAACCTGGGC-3'	68.9°C
	5'-GCCCAGGTTCAGCCCGAAGCTCTTAGC-3'	
V32E	5'-ACGCTAAGAGCTTCGAGCTGAACCTGGGC-3'	69.3°C
	5'-GCCCAGGTTCAGCTCGAAGCTCTTAGCGT-3'	
V32S	5'-TGACGCTAAGAGCTTCTCGCTGAACCTGGGCAAAG-3'	74.4°C
	5'-CTTTGCCCAGGTTCAGCGAGAAGCTCTTAGCGTCA-3'	
V32W	5'-TGACGCTAAGAGCTTCTGGCTGAACCTGGGCAAAG-3'	74.3°C
	5'-CTTTGCCCAGGTTCAGCCAGAAGCTCTTAGCGTCA-3'	
N34A	5'-AGAGCTTCGTGCTGGCCCTGGGCAAAGACAG-3'	74.6°C
	5'-CTGTCTTTGCCCAGGGCCAGCACGAAGCTCT-3'	
L35A	5'-AGCTTCGTGCTGAACGCGGGCAAAGACAGCAAC-3'	76.6°C
	5'-GTTGCTGTCTTTGCCCGCGTTCAGCACGAAGCT-3'	
K37A	5'-GCTGAACCTGGGCGCAGACAGCAACAACCTG-3'	75.0°C
	5'-CAGGTTGTTGCTGTCTGCGCCCAGGTTCAGC-3'	
K37E	5'-GCTGAACCTGGGCGAAGACAGCAACAACC-3'	70.9°C
	5'-GGTTGTTGCTGTCTTCGCCCAGGTTCAGC-3'	
D38E	5'- GTGCTGAACCTGGGCAAAGAGAGCAACAACCTGTGCCTG-3'	78.4°C
	5'-CAGGCACAGGTTGTTGCTCTCTTTGCCCAGGTTCAGCAC-3'	
D38K	5'-GTGCTGAACCTGGGCAAAAAAAGCAACAACCTGTGCCTG-3'	78.0°C
	5'-CAGGCACAGGTTGTTGCTTTTTTTGCCCAGGTTCAGCAC-3'	
N40A	5'-CTGGGCAAAGACAGCGCCAACCTGTGCCTGCAC-3'	78.9°C
	5'-GTGCAGGCACAGGTTGGCGCTGTCTTTGCCCAG-3'	

N41A	5’-GGCAAAGACAGCAACGCCCTGTGCCTGCACT-3’	75.9°C
	5’-AGTGCAGGCACAGGGCGTTGCTGTCTTTGCC-3’	
L44A	5’-CAGCAACAACCTGTGCGCGCACTTCAACCCTCGC-3’	79.8°C
	5’-GCGAGGGTTGAAGTGCGCGCACAGGTTGTTGCTG-3’	
L44D	5’-GACAGCAACAACCTGTGCGATCACTTCAACCCTCGCTTC-3’	77.6°C
	5’-GAAGCGAGGGTTGAAGTGATCGCACAGGTTGTTGCTGTC-3’	
L44F	5’-CAGCAACAACCTGTGCTTCCACTTCAACCCTCGCT-3’	75.1°C
	5’-AGCGAGGGTTGAAGTGGAAGCACAGGTTGTTGCTG-3’	
L44S	5’-GACAGCAACAACCTGTGCAGTCACTTCAACCCTCGCTTC-3’	76.7°C
	5’-GAAGCGAGGGTTGAAGTGACTGCACAGGTTGTTGCTGTC-3’	
H45A	5’-CAACAACCTGTGCCTGGCCTTCAACCCTCGCTTCAAC-3’	78.2°C
	5’-GTTGAAGCGAGGGTTGAAGGCCAGGCACAGGTTGTTG-3’	
F46A	5’-CAACCTGTGCCTGCACGCAAACCCTCGCTTCAACG-3’	79.9°C
	5’-CGTTGAAGCGAGGGTTTGCGTGCAGGCACAGGTTG-3’	
R49A	5’-CCTGCACTTCAACCCTGCATTCAACGCCCACGGCG-3’	81.9°C
	5’-CGCCGTGGGCGTTGAATGCAGGGTTGAAGTGCAGG-3’	
N51A	5’-CAACCCTCGCTTCGCCGCCCACGGCGA-3’	80.4°C
	5’-TCGCCGTGGGCGGCGAAGCGAGGGTTG-3’	
A52I	5’-CAACCCTCGCTTCAACATCCACGGCGACGCC-3’	78.0°C
	5’-GGCGTCGCCGTGGATGTTGAAGCGAGGGTTG-3’	
H53A	5’-CGCTTCAACGCCGCCGGCGACGCCAAC-3’	80.5°C
	5’-CGCTTCAACGCCGGCGGCGACGCCAAC-3’	
H53E	5’-TCGCTTCAACGCCGAGGGCGACGCCAACA-3’	79.7°C
	5’-TGTTGGCGTCGCCCTCGGCGTTGAAGCGA-3’	
H53G	5’-CGCTTCAACGCCGGCGGCGACGCCAAC-3’	80.5°C
	5’-GTTGGCGTCGCCGCCGGCGTTGAAGCG-3’	
G54A	5’-TCAACGCCCACGCCGACGCCAACAC-3’	74.8°C
	5’-GTGTTGGCGTCGGCGTGGGCGTTGA-3’	
D55A	5’-CGCCCACGGCGCCGCCAACACCA-3’	78.2°C
	5’-TGGTGTTGGCGGCGCCGTGGGCG-3’	
N57A	5’-CACGGCGACGCCGCCACCATCGTGTGCAA-3’	81.7°C
	5’-TTGCACACGATGGTGGCGGCGTCGCCGTG-3’	
V60A	5’-CGCCAACACCATCGCGTGCAACAGCAAGG-3’	76.4°C
	5’-CCTTGCTGTTGCACGCGATGGTGTTGGCG-3’	
C61A	5’-CGCCAACACCATCGTGGCTAACAGCAAGGACGGCG-3’	80.7°C
	5’-CGCCGTCCTTGCTGTTAGCCACGATGGTGTTGGCG-3’	
D65A	5’-CAACAGCAAGGCCGGCGGGGCCT-3’	73.3°C
	5’-AGGCCCCGCCGGCCTTGCTGTTG-3’	
D65K	5’-TGTGCAACAGCAAGAAGGGCGGGGCCTGG-3’	77.3°C
	5’-CCAGGCCCCGCCCTTCTTGCTGTTGCACA-3’	
G66A	5’-GCTTGTGGTCTGGCCGCCAGCAACC-3’	73.8°C
	5’-CCCAGGCCCCGGCGTCCTTGCTG-3’	
G67A	5’-CAAGGACGGCGCGGCCTGGGGGA-3’	75.8°C
	5’-TCCCCCAGGCCGCGCCGTCCTTG-3’	
A68I	5’-AGCAAGGACGGCGGGATTTGGGGGACCGAGCAG-3’	80.7°C
	5’-CTGCTCGGTCCCCCAAATCCCGCCGTCCTTGCT-3’	
W69G	5’-CGGCGGGGCCGGGGGGACCGAGC-3’	80.2°C
	5’-GCTCGGTCCCCCCGGCCCCGCCG-3’	

G70A	5’-CGGGGCCTGGGCGACCGAGCAGC-3’	75.7°C
	5’-GCTGCTCGGTCGCCCAGGCCCCG-3’	
E72A	5’-CTGGGGGACCGCGCAGCGGGAGG-3’	75.6°C
	5’-CCTCCCGCTGCGCGGTCCCCCAG-3’	
R74A	5’-GGGACCGAGCAGGCGGAGGCTGTCTTTCC-3’	75.2°C
	5’-GGAAAGACAGCCTCCGCCTGCTCGGTCCC-3’	
E75A	5’-CGGGACCGAGCAGCGGGCCGCTGTCTTTCCCTTC-3’	82.6°C
	5’-GAAGGGAAAGACAGCGGCCCGCTGCTCGGTCCCG-3’	
F80A	5’-GGGAGGCTGTCTTTCCCGCCCAGCCTGGAAGTGTTGCAG-3’	82.4°C
	5’-CTGCAACACTTCCAGGCTGGGCGGGAAAGACAGCCTCCC-3’	
F80K	5’-GGGAGGCTGTCTTTCCCAAGCAGCCTGGAAGTGTTGC-3’	78.3°C
	5’-GCAACACTTCCAGGCTGCTTGGGAAAGACAGCCTCCC-3’	
F80S	5’-GAGGCTGTCTTTCCCAGCCAGCCTGGAAGTGTT-3’	73.6°C
	5’-AACACTTCCAGGCTGGCTGGGAAAGACAGCCTC-3’	
P82A	5’-GTCTTTCCCTTCCAGGCTGGAAGTGTTGCAGAG-3’	71.3°C
	5’-CTCTGCAACACTTCCAGCCTGGAAGGGAAAGAC-3’	
S84A	5’-CCTTCCAGCCTGGAGCTGTTGCAGAGGTGTG-3’	73.2°C
	5’-ACACATTTGATCTTGAAGGCACCGTCAGCTGCC-3’	
E87A	5’-CTGGAAGTGTTGCAGCGGTGTGCATCACCTT-3’	72.5°C
	5’-AAGGTGATGCACACCGCTGCAACACTTCCAG-3’	
I90A	5’-AAGTGTTGCAGAGGTGTGCGCCACCTTCGACCAGGCC-3’	81.0°C
	5’-GGCCTGGTCGAAGGTGGCGCACACCTCTGCAACACTT-3’	
F92A	5’-GGTGTGCATCACCGCCGACCAGGCCAACC-3’	77.9°C
	5’-GGTTGGCCTGGTCGGCGGTGATGCACACC-3’	
A95I	5’-CATCACCTTCGACCAGATCAACCTGACCGTCAAGC-3’	74.3°C
	5’-GCTTGACGGTCAGGTTGATCTGGTCGAAGGTGATG-3’	
D103A	5’-CCGTCAAGCTGCCAGCTGGATACGAATTCAAGT-3’	71.9°C
	5’-ACTTGAATTCGTATCCAGCTGGCAGCTTGACGG-3’	
G104A	5’-CTGACCGTCAAGCTGCCAGATGCCTACGAATTCAAGTTCC-3’	77.0°C
	5’-GGAACTTGAATTCGTAGGCATCTGGCAGCTTGACGGTCAG-3’	
E106A	5’-CTGCCAGATGGATACGCATTCAAGTTCCCCAAC-3’	71.9°C
	5’-GTTGGGGAACTTGAATGCGTATCCATCTGGCAG-3’	
F109A	5’-ATGGATACGAATTCAAGGCCCCCAACCGCCTCAAC-3’	76.3°C
	5’-GTTGAGGCGGTTGGGGGCCTTGAATTCGTATCCAT-3’	
R112A	5’-ATTCAAGTTCCCCAACGCCCTCAACCTGGAGGCCATC-3’	79.0°C
	5’-GATGGCCTCCAGGTTGAGGGCGTTGGGGAACTTGAAT-3’	
R112H	5’-CAAGTTCCCCAACCACCTCAACCTGGAGG-3’	69.9°C
	5’-CCTCCAGGTTGAGGTGGTTGGGGAACTTG-3’	
N114A	5’-CCCAACCGCCTCGCCCTGGAGGCCATC-3’	77.3°C
	5’-GATGGCCTCCAGGGCGAGGCGGTTGGG-3’	
E116A	5’-CGCCTCAACCTGGCGGCCATCAACTACAT-3’	66.7°C
	5’-ATGTAGTTGATGGCCGCCAGGTTGAGGCG-3’	
A117I	5’-CAACCTGGAGATAATCAACTACATGGCAGCTGAC-3’	67.4°C
	5’-GTCAGCTGCCATGTAGTTGATTATCTCCAGGTTG-3’	
I118A	5’-CAACCTGGAGGCCGCCAACTACATGGCAGCT-3’	74.8°C
	5’-AGCTGCCATGTAGTTGGCGGCCTCCAGGTTG-3’	
N119E	5’-CCTGGAGGCCATCGAGTACATGGCAGCTGAC-3’	72.9°C
	5’-GTCAGCTGCCATGTACTCGATGGCCTCCAGG-3’	

N119K	5'-CCTGGAGGCCATCAAGTACATGGCAGCTG-3'	70.0°C
	5'-CAGCTGCCATGTACTTGATGGCCTCCAGG-3'	
N119W	5'-CAACCTGGAGGCCATCTGGTACATGGCAGCTGACG-3'	77.1°C
	5'-CGTCAGCTGCCATGTACCAGATGGCCTCCAGGTTG-3'	
Y120A	5'-CCTGGAGGCCATCAACGCAATGGCAGCTGACGGTG-3'	81.2°C
	5'-CACCGTCAGCTGCCATTGCGTTGATGGCCTCCAGG-3'	
Y120D	5'-CTGGAGGCCATCAACGATATGGCAGCTGACGGT-3'	75.2°C
	5'-ACCGTCAGCTGCCATATCGTTGATGGCCTCCAG-3'	
M121A	5'-GAGGCCATCAACTACGCGGCAGCTGACGGTG-3'	76.1°C
	5'-CACCGTCAGCTGCCGCGTAGTTGATGGCCTC-3'	
A122I	5'-GAGGCCATCAACTACATGATAGCTGACGGTGACTTCAAG-3'	72.2°C
	5'-CTTGAAGTCACCGTCAGCTATCATGTAGTTGATGGCCTC-3'	
D126A	5'-GGCAGCTGACGGTGCCTTCAAGATCAAATGTGT-3'	72.8°C
	5'-ACACATTTGATCTTGAAGGCACCGTCAGCTGCC-3'	
F127A	5'-GCAGCTGACGGTGACGCCAAGATCAAATGTGTGGC-3'	77.9°C
	5'-GCCACACATTTGATCTTGGCGTCACCGTCAGCTGC-3'	
F127D	5'-GCAGCTGACGGTGACGACAAGATCAAATGTGTGGC-3'	75.6°C
	5'-GCCACACATTTGATCTTGTCGTCACCGTCAGCTGC-3'	
I129R	5'-GCTGACGGTGACTTCAAGAGGAAATGTGTGGCCTTTGAC-3'	74.6°C
	5'-GTCAAAGGCCACACATTTCCTCTTGAAGTCACCGTCAGC-3'	
K130A	5'-ACGGTGACTTCAAGATCGCATGTGTGGCCTTTGACTG-3'	76.0°C
	5'-CAGTCAAAGGCCACACATGCGATCTTGAAGTCACCGT-3'	
V132A	5'-CTTCAAGATCAAATGTGCGGCCTTTGACTCACCG-3'	73.3°C
	5'-CGGTGAGTCAAAGGCCGCACATTTGATCTTGAAG-3'	
V132E	5'-ACTTCAAGATCAAATGTGAGGCCTTTGACTCACCG-3'	70.5°C
	5'-CGGTGAGTCAAAGGCCTCACATTTGATCTTGAAGT-3'	
V132R	5'-GTGACTTCAAGATCAAATGTAGGGCCTTTGACTCACCGG-3'	73.7°C
	5'-CCGGTGAGTCAAAGGCCCTACATTTGATCTTGAAGTCAC-3'	
F134E	5'-AGATCAAATGTGTGGCCGAGGACTCACCGGTCGGC-3'	78.6°C
	5'-GCCGACCGGTGAGTCCTCGGCCACACATTTGATCT-3'	
F134R	5'-GATCAAATGTGTGGCCCGTGACTCACCGGTCGG-3'	77.5°C
	5'-CCGACCGGTGAGTCACGGGCCACACATTTGATC-3'	
GFP-CGL-2		
W72G	5'-GACGGCGGGGCCGGTGGGACCGAGCAGC-3'	80.2°C
	5'-GCTGCTCGGTCCCACCGGCCCCGCCGTC-3'	
Control Primers		
primer Gal-1 forw.	5'-CGGGATCCCGCCACCATGGCTTGTGGTCTGGTCGCC-3'	84.9°C
primer Gal-1 revers.	5'-GCCGACCGGTGAGTCAAAGGCCACACATTTGATCTTG-3'	77.6°C

Table 1 Site-directed mutagenesis primers

Truncations primer:

Primer	Sequence
Gal-1-GFP	
ΔN5	5'-CGGGATCCCGCCACCATGGTCGCCAGCAACCTGAATCTCAAA-3'
ΔN10	5'-CGGGATCCCGCCACCATGGAGAATCTCAAACCTGGAGAGTGCCTTCG-3'
ΔN20	5'-CGGGATCCCGCCACCATGGGACGAGGCGAGGTGGCTCCTGACG-3'
ΔC4	5'-TTTTCCTTTTGCGGCCGCCTAACATTTGATCTTGAAGTCACCGTCAG-3
ΔC9	5'-TTTTCCTTTTGCGGCCGCCTAGTCACCGTCAGCTGCCATGTAGT-3
ΔC20	5'-TTTTCCTTTTGCGGCCGCCTACAGGTTGAGGCGGTTGGGGAAC-3
ΔC30	5'-TTTTCCTTTTGCGGCCGCCTAGTATCCATCTGGCAGCTTGACGG-3
ΔC40	5'-TTTTCCTTTTGCGGCCGCCTAGGCCTGGTCGAAGGTGATGCAC-3
ΔC50	5'-TTTTCCTTTTGCGGCCGCCTAAACACTTCCAGGCTGGAAGGGAAAG-3
Reverse primer for ΔN truncations	5'-GCCGACCGGTGAGTCAAAGGCCACACATTTGATCTTG-3'
Forward primer for ΔC truncations	5'-GACTGGTGTACAAGATGGCTTGTGGTCTGGTCGCCAG-3

Table 2 Truncation primers

2.1.6 Bacteria and bacterial media

For transformation and plasmid amplification competent DH5α cells (Invitrogen) or XL1-Blue supercompetent cells (Stratagene) were used. For transformation and protein expression BL21 pLysS (DE3) cells were used. They were grown in LB medium (Luria Bertani medium) or on LB agar plates supplied with ampicillin or kanamycin in a final concentration of 100 µg/ml to select for successfully transformed cells carrying plasmids containing a resistance gene.

Bacteria: subcloning efficiency DH5α competent cells, Genotype:
F$^-$ ϕ80d*lac*ZΔM15 Δ(*lac*ZYA-*arg*F) U169 *rec*A1 *end*A1 *hsd*R17 (r_k^-, m_k^+) *pho*A *sup*E44 λ$^-$ *thi*-1 *gyr*A96 *rel*A1

XL1-Blue supercompetent cells, Genotype:
recA1 endA1 gyrA96 thi-1 hsdR17 supE44 relA1 lac [F´ proAB lacIqZΔM15 Tn10 (Tetr)].

BL21 pLysS (DE3) competent cells, Genotype:
F^- *omp*T *hsd*S_B($r_B^-m_B^-$) *gal dcm* (DE3)

LB medium:	0.5% (v/w)	NaCl
	1% (w/v)	Tryptone
	0.5% (w/v)	Yeast extract
LB agar plates:	0.5% (w/v)	NaCl
	1% (w/v)	Tryptone
	0.5% (w/v)	Yeast extract
	1.6% (w/v)	Agar
SOC-Medium:	10 mM	NaCl
	2% (w/v)	Tryptone
	0.5% (w/v)	Yeast extract
	2.5 mM	KCl
	10 mM	$MgCl_2$
	20 mM	$MgSO_4$
	20 mM	Glucose

2.1.7 Eukaryotic cell lines

The cell line HEK 293T (Human Embryonic Kidney cells) was used as a host to produce retroviral particles carrying the various reporter constructs.
S-HeLa cells were used as a source for human proteins applied to interaction studies with human Gal-1.

HeLa and CHO cells (Chinese Hamster Ovary cells) were target cell lines for retroviral transduction. They were stably transduced with cDNA constructs and used for the expression of reporter molecules to function as a eukaryotic *in vivo* system to investigate proteins in a living cell environment.

Eukaryotic cell lines: HEK 293Tcells (ATCC CRL-11268)
S-HeLa cells (ATCC CCL-2.2)
HeLa cells (ATCC CCL-2.1)
CHO cells (ECACC 85050302)

2.1.8 Eukaryotic cell culture media

α Modification of the Minimal Essential Medium (αMEM)

The α-modification of the Minimal Essential Medium (Biochrom AG) was used to cultivate CHO cells. Dry medium was dissolved in 5 l ddH_2O, and 10 g of sodium hydrogencarbonate were added to adjust the pH to 7.4, which was checked continuously. The prepared medium was sterile filtered into autoclaved bottles and stored at 4°C. Before addition to cells the medium was supplemented with 10% (v/v) fetal calf serum (FCS), 100 µg/ml Streptomycin/Penicillin and, if stored longer than 6 weeks, 2 mM L-Glutamine.

Dulbecco's Modified Eagle Medium (DMEM)

Dulbecco's Modified Eagle Medium (Biochrom AG) was used to cultivate HEK 293T and HeLa cells. Dry medium was dissolved in 5 l ddH_2O and 10 g of sodium hydrogencarbonate were added to adjust the pH to 7.4. The prepared medium was sterile filtered into autoclaved bottles and stored at 4°C. Before addition to cells 10% (v/v) FCS, 100 µg/ml Streptomycin/Penicillin and, if stored longer than 6 weeks, 2 mM L-Glutamine were supplemented.

2.1.9 Primary antibodies

Anti-GFP or anti-Gal-1 antibodies were affinity-purified by incubation of the corresponding serum with His_6-eGFP or GST-Gal-1 coupled Epoxy-Sepharose beads (Amershan).

Anti-Gal-1 antibodies and anti-GFP antibodies were eluted from the corresponding affinity matrix under acidic and basic conditions according to standard procedures.

To detect endogenous Gal-1 affintiy-purified anti-Gal-1 antibodies (Pineda Antibodies, acidic elution) were used. They were applied in a 1:100 dilution for Western blot and FACS analysis and in a 1:50 dilution for confocal microscopy.

To detect GFP-containing reporter constructs affinity-purified anti-GFP antibodies (Pineda Antibodies, acidic elution) were used (Engling et al., 2002). They were applied in a 1:200 dilution for Western blot and FACS analysis and in a 1:50 dilution for confocal microscopy.

When performing immunoprecipitation experiments 20 µl of affinity-purified anti-GFP antibodies (Pineda Antibodies, basic elution, (Engling et al., 2002)) were coupled to 20 µl Protein A sepharose: CL4B beads pro reaction.

The mAb anti-CA125 antibody OC125 was purchased from Zymed and was applied in a 1:200 dilution for Western blot analysis (Lloyd and Yin, 2001).

The polyclonal anti-CA125-C-$TERM_{1-356}$ antiserum was applied in a 1:200 dilution for Western blot analysis (Seelenmeyer et al., 2003).

2.1.10 Secondary antibodies

Secondary antibodies for Western blot analysis were goat anti-rabbit IgG HRP-coupled antibodies (Bio-Rad; 1:5,000), goat anti-mouse IgG HRP-coupled antibodies (Bio-Rad; 1:5,000), monoclonal mouse anti-rabbit IgG clone RG-16 HRP-coupled (Sigma-Aldrich; 1:3,000), goat anti-rabbit IgG Alexa 680-coupled antibodies (Molecular Probes; 1:10,000) and goat anti-mouse IgG Alexa 680-coupled antibodies (Molecular Probes; 1:10,000).

Secondary antibodies for FACS analysis were goat anti-rabbit IgG and goat anti-mouse IgG antibodies, both conjugated with Allophycocyanin (APC) (Molecular Probes). They were used in a 1:750 dilution.

Secondary antibodies for confocal microscopy were goat anti-rabbit or goat anti-mouse IgG Alexa 546-coupled antibodies (Molecular Probes). They were applied in a 1:750 dilution.

2.2 Molecular biological methods

2.2.1 Bacterial transformation

To transform DH5α cells, 1 µl of plasmid DNA (1-10 ng DNA) or 3 µl of a ligation reaction were added to 30 µl bacteria suspension and incubated on ice for 30 min followed by a heat shock of 20 s at 37°C and an additional incubation period of 2 min on ice. After that 1 ml LB medium without ampicillin was added followed by incubation at 37°C for 1 h under constant shaking (300 rpm).

To transform XL1-Blue cells, 1 µl of plasmid DNA (1-10 ng DNA) or 5 µl of a ligation reaction were added to 50 µl bacteria suspension and incubated on ice for 30 min followed by a heat shock of 45 s at 42°C and an additional incubation period of 2 min on ice. After that 1 ml LB medium without ampicillin was added followed by incubation at 37°C for 1 h under constant shaking (300 rpm).

To transform BL21 pLysS (DE3) cells 1 µl of plasmid DNA (1-10 ng) was added to 20 µl bacteria suspension and incubated on ice for 5 min followed by heat shock of 30 s at 42°C and an additional incubation period of 2 min on ice. After that 80 µl SOC medium without antibiotics were added followed by incubation at 37°C for 1 h under constant shaking (300 rpm).

After transformation bacteria were spread on LB plates supplemented with 100 µg/ml ampicillin or kanamycin and incubated at 37°C for 12 to 16 h or used to inoculate liquid cultures of LB medium supplemented with the respective antibiotics, which were grown at 37°C under constant shaking (180 rpm) for 12 to 16 h.

2.2.2 Selection and amplification of plasmids

If bacteria were grown on agar plates in correct density they form colonies each originating from a single bacterium. To obtain genetically identical plasmids, bacteria from one colony were transferred to 5-10 ml LB medium culture using a 20 µl pipet tip. The liquid cultures containing the respective antibiotic to select for bacteria carrying plasmids containing a resistance gene were incubated at 37°C overnight under constant shaking (180 rpm).

2.2.3 Plasmid preparation

Plasmids were prepared from overnight LB medium cultures of transformed bacteria by the application of Qiagen or Macherey Nagel DNA purification kits. The kit used was dependent on the volume of the overnight culture.

Volume of bacterial culture	Qiagen Kit	Macherey Nagel Kit
5 - 10 ml	QIAprep Spin Miniprep Kit	Nucleospin Plasmid
20 – 150 ml	QIAGEN Plasmid Midi Kit	Nucleobond-PC 100
More than 150 ml	QIAGEN Plasmid Maxi Kit	Nucleobond-PC 500

Purification was performed following the manufacturer's manual employing alkaline lysis and binding of DNA to silica membranes or anion-exchange resins, respectively. Elution of the DNA was performed using appropriate volumes of ddH_2O.

2.2.4 Determination of DNA concentration

The concentration of a DNA solution was determined photometrically by measuring the absorption at 260 nm wavelength. The measurement was either performed in a photometer with a diluted DNA solution using a quarz cuvette with a thickness of 10 mm or by directly measuring 1 µl of the DNA solution in a Nanodrop photometer. The concentration of double stranded DNA was calculated based on the fact that an optical density (OD) of 1 corresponds to a concentration of 50 µg/ml.

To determine contamination the OD at 280 nm was measured additionally. The ratio OD_{260}/OD_{280} represents the grade of purity since pure DNA shows a value between 1.8 and 2.0. Values above 2.0 show contaminations with RNA, values below 1.8 contaminations with protein.

2.2.5 Agarose gel electrophoresis

To separate mixtures of DNA molecules by size agarose gel electrophoresis was used. Separation is achieved by loading the negatively charged DNA molecules on a gel matrix with a defined pore size and subjecting them to an electric field where they migrate to the anode. The migration speed depends on the size of the DNA molecules and is limited by the pore size of the gel, which is defined by the amount of agarose used.

Agarose gels were prepared by heating 1% agarose (w/v) in TAE buffer. After the agarose was dissolved ethidiumbromide in a final concentration of 0.5 µg/ml was added. The gel was poured into an agarose gel-casting chamber and a plastic comb was inserted which forms the loading wells. After hardening the gel can be stored at 4°C until use.

To perform electrophoresis the gel was transferred into an agarose gel running chamber and TAE was added until the gel was completely covered with liquid. Samples containing DNA sample buffer in a 1:5 dilution were loaded on the gel and electrophoresis was performed at 100 V until sufficient separation was reached

visualized by the migration behaviour of the blue bromphenol marker front. Agarose gels were documented using the Gel Doc 2000 imaging system (Bio-Rad).

TAE buffer (50x):	242 g	Tris
	57.1 ml	Glacial acidic acid
	100 ml	0.5 M EDTA, pH 8
	ad 1 l	ddH_2O
DNA sample buffer (5x):	0.25% (w/v)	Bromphenol Blue
	0.25% (w/v)	Xylencyanol FF
	30% (w/v)	Glycerol

2.2.6 DNA marker

As a size standard two premixed DNA ladders were used, the 1 kb DNA ladder and the 100 bp DNA ladder (New England Biolabs). They contain DNA fragments of defined sizes ranging from 100 to 1,500 bp (100 bp ladder) to analyze smaller DNA fragments or from 500 to 10,000 bp (1 kb ladder) to analyze large inserts and vectors. The markers were applied by loading 10 µl of a stock solution containing 0.05 µg/µl DNA in DNA sample buffer. Since each band of the marker contains a defined amount of DNA, the marker can be used to approximate the mass of DNA of an unknown sample by comparing band intensities visually.

2.2.7 Site-directed mutagenesis

The QuikChange site-directed mutagenesis kit (stratagene) was used to insert point mutations, switch amino acids, and delete or insert single or multiple amino acids. The site-directed mutagenesis method was performed using *PfuTurbo* DNA polymerase and a temperature cycler. *PfuTurbo* DNA polymerase replicates both plasmid strands with high fidelity and without displacing the mutant oligonucleotide primers. The basic procedure utilizes a supercoiled double-stranded DNA (dsDNA) vector with the insert of interest (pGEM-T/Gal-1 or CGL-2; 3500 bp) and two synthetic oligonucleotide primers (see Table 1) containing the desired mutation. Stratagene has developed a web-based software program to design optimal mutagenic primers for use with the QuikChange site directed mutagenesis kit:

http://labtools.stratagene.com/QC

The control and sample reaction was prepared as indicated below. The oligonucleotide primers were extended during temperature cycling (see below) by *PfuTurbo* DNA polymerase. Following temperature cycling, the product was treated with 1 µl Dpn I (10 U/µl) for 1 h at 37°C. The Dpn I endonuclease (target sequence: 5'-Gm^{6}ATC-3') is specific for methylated DNA and was used to digest the parental DNA template derived from methylase positive E.coli strainds and to select for mutation containing newly synthesized DNA. The vector DNA containing the desired mutations was then transformed into DH5α or XL1-Blue competent cells according to standard procedure (2.2.1). The isolated DNA was sequenced and the correctly mutagenized insert was digested with BamH I and Age I, purified and ligated with a retroviral Vector (pRevTRE2/GFP).

Control reaction:

5 µl of 10x reaction buffer
2 µl (10 ng) dsDNA template pGEM-T/gal-1 or CGL-2
1 µl (125 ng) oligonucleotide primer Gal-1 forw.
1 µl (125 ng) oligonucleotide primer Gal-1 revers.
1 µl dNTP mix
40 µl ddH_2O
1 µl *PfuTurbo* DNA Polymerase (2.5 U/µl)

Sample reaction:

5 µl 10x reaction buffer
2 µl (10 ng) dsDNA template pGEM-T/gal-1 or CGL-2
1 µl (125 ng) oligonucleotide primer # 1 (sense)
1 µl (125 ng) oligonucleotide primer # 2 (antisense)
1 µl dNTP mix
40 µl ddH_2O
1 µl *PfuTurbo* DNA Polymerase (2.5 U/µl)

Cycling parameters:

Denaturation	30 s, 95°C	
Amplification	30 sec, 95°C	Denaturation
(16 cycles)	1 min, 55°C	Hybridization
	4 min, 68°C	Elongation

2.2.8 Polymerase chain reaction

To amplify a gene or DNA fragment the polymerase chain reaction (PCR) was used (Lawyer et al., 1989; Saiki et al., 1988). During PCR a DNA template defined by a forward and reverse primer is amplified in high amounts and can be used for further cloning to generate desired reporter constructs. PCRs were performed with the enzyme *Ampli*Taq polymerase (Perkin Elmer) which generate adenosine overhangs at the 3' ends. This was important regarding the use of the pGEM-T vector system for further cloning since this vector contains thymidine overhangs at its 3' ends for simplified ligation of PCR products. The following reaction mix was used for PCRs.

Sample reaction:

10 µl 10x reaction buffer
2 µl (10 ng) dsDNA template
1 µl (25 pmol) oligonucleotide forward primer
1 µl (25 pmol) oligonucleotide reverse primer
10 µl (10 mM) dNTP mix
5.9 µl (25 mM) $MgCl_2$
69.1 µl ddH_2O
1 µl of A*mpliTaq* DNA Polymerase (2.5 U/µl)

The reaction was performed employing a Primus Advance Thermocycler (PeqLab). The following program was used to amplify DNA.

Cycling parameters:

Denaturation	2 min, 95°C	
Amplification	45 sec, 94°C	Denaturation
(30 cycles)	1 min, T<T_m of primers	Hybridization
	1 min, 72°C	Elongation
Elongation	10 min, 72°C	
Store	∞, 4°C	

The annealing temperature was chosen depending on the melting temperatures (T_m) of the used primers after subtracting 5°C from the lower one ($T = T_m - 5°C$). The melting temperature for each individual primer was calculated according to the following equation.

$$T_m = 81.5 + 16.6 \times \log\left[Na^+\right] + 41 \times \%\ GC - \frac{675}{N}$$

$\left[Na^+\right] = 0.05\ M$

$\%\ GC =$ GC content of annealing sequence

$N =$ number of annealing bases

When problematic primers were used which resulted in very low yields or no amplification, up to 10% DMSO (dimethyl sulfoxide) were added to the reaction mix. DMSO reduces secondary structures like loops or hairpins and the primers can anneal more easily at the template. A disadvantage of DMSO is that mutations and mispairing of bases occur more frequently. When using DMSO it was of great

importance to verify obtained PCR products by sequencing before using them for further cloning.

2.2.9 PCR purification

To purify PCR products and remove primers and reaction mix components PCR samples were processed using a PCR purification kit (QiaQuick PCR purification kit, Qiagen). The DNA was bound to a silica membrane under high salt conditions and eluted after washing with an appropriate volume of ddH_2O.

2.2.10 Gel extraction of DNA fragments

To purify desired DNA fragments from a restriction digest the reaction mix was separated on a 1% agarose gel. The bands were transiently visualized with a UV lamp (366 nm) and cut out of the gel with a sharp blade. To purify the DNA from the agarose gel the samples were processed using a gel extraction kit (Qiagen). The agarose was melted in a specific buffer and DNA was bound to a silica membrane under high salt conditions. Elution was performed after a washing step in an appropriate volume of ddH_2O.

2.2.11 Restriction digests

Restriction enzymes were purchased from New England Biolab. Restriction digests were performed according to the manufacturer's manual. An optimized buffer system consisting of buffer 1 to 4 from which one is optimal for a specific enzyme was used. Additionally unique buffers for certain enzymes are available. In the case of a double digest a buffer was chosen which provides the highest cleavage efficiency for both enzymes or the digest was performed sequentially with a DNA purification step in between (2.2.9). Depending on the enzyme and the quality of the DNA 1 to 5 U/µg DNA were used in a restriction digest incubated 2 to 4 h at 37°C.

2.2.12 DNA dephosphorylation

To dephosphorylate linearized vectors at the 5'-end after restriction digests in order to prevent self-ligation, *Calf Intestinal Phosphatase* (CIP, New England Biolabs) was added to the reaction mix in a concentration of 1 U/µg DNA for 30 min at 37°C. The enzyme was heat inactivated by incubation at 70°C for 10 min.

2.2.13 Ligation of DNA fragments

In order to ligate PCR products or other DNA fragments to each other or into linearized vectors a ligation kit was used (Takara Bio Inc.). The ligation partners were digested with the same restriction enzymes to provide compatible ends. Following the manual, 50 ng of vector (or the longer DNA fragment) were used. The amount of insert (or the shorter DNA fragment) was calculated according to the following equation.

$$\frac{\text{amount vector}\,[\text{ng}] \times \text{number of basepairs insert}\,[\text{bp}]}{\text{number of basepairs vector}\,[\text{bp}]} = \text{amount insert}\,[\text{ng}]$$

The DNA solutions and 5 µl of Takara Solution 1, which contains the T4 DNA ligase and an optimized buffer in a 2-fold concentration, were mixed and ddH_2O was added to a total volume of 10 µl. The reaction was incubated for 3 h at 37°C or for at least 16 h at 4°C. After the incubation period the enzyme was heat inactivated by incubation at 70°C for 10 min.

2.2.14 DNA sequencing

Cloned inserts or cDNA constructs in different plasmids were sequenced in order to rule out mutations and to verify the correct sequence. Therefore, plasmid samples and primers were sent to commercial sequencing companies (Seqlab, Göttingen or GATC, Konstanz). Obtained sequences were analyzed using the Lasergene software suite (Lasergene, DNAStar) or the 'align 2 sequences' function of the BLAST project:

http://www.ncbi.nlm.nih.gov/blast/bl2seq/wblast2.cgi

2.2.15 Short interfering RNAs in mammalian cells

Most eukaryotes possess a cellular defense system protecting their genomes against invading foreign genetic elements. Dicer RNase III rapidly processes dsRNA to small dsRNA fragments of distinct size and structure, the small interfering RNAs, which direct the sequence-specific degradation of the single-stranded mRNAs of the invading genes. In several organisms, introduction of double-stranded RNA has been proven to be a powerful tool to suppress gene expression.

For silencing genes specifically, siRNA target sites are typically chosen by scanning the mRNA sequence of interest for AA dinucleotides, recording the 19 nucleotides downstream of the AA, and then comparing the potential siRNA target sequences with an appropriate genome database to eliminate any sequences with significant homology to other genes. To facilitate this procedure a "siRNA Target Finder and Design Tool" provided by Ambion was used:

http://www.ambion.com/techlib/misc/siRNA_finder.html

Subsequently two complementary DNA oligonucleotides corresponding to the selected target sequence were synthesized (Thermo Electron).

The two oligonucleotides were mixed, heated at 90°C for 3 min and annealed at 37°C for 1 h. The annealed siRNA insert was used directly in a ligation reaction with a vector called pSilencer™ 1.0-U6 (Ambion) linearized with EcoR I and Apa I. pSilencer™ 1.0-U6 Expression Vector was designed for plasmid-based siRNA experiments.

To enable retroviral transduction the generated vector was digested with BamHI and the resulting insert was ligated into the retroviral vector pLNCD4 digested with the same enzyme. $HeLa_{mt}$ cells were transduced with this contruct as described in 2.3.4 by retroviral transduction of the generated retroviral vector. The vector pLNCD4 alone was used as a control. Successfully transduced target cells were sorted using cell surface localized CD4 as a marker.

Annealing buffer:	100 mM	Potassium acetate
	30 mM	HEPES-KOH pH 7.4
	2 mM	Magnesium acetate

2.3 Eukaryotic cell culture techniques

2.3.1 Maintaining cell lines

Adherent cell lines were grown on culture dishes in their respective culture medium at 37°C with 5% CO_2. The cells were splitted dependent on confluency every 3 to 5 days by washing with PBS and addition of 0.125% (w/v) Trypsin/EDTA in PBS. After 1 min incubation the trypsin solution was removed and the cells were resuspended in the appropriate volume of medium used for the culture dish. The cells were then seeded in the desired dilution on new culture dishes prepared with fresh medium.

PBS (Phosphate buffer saline):	140 mM	NaCl
	2.7 mM	KCl
	10 mM	Na_2HPO_4
	1.8 mM	KH_2PO_4
Trypsin/EDTA:	0.5 mM	EDTA
	0.125% (w/v)	Trypsin
		PBS

2.3.2 Freezing of eukaryotic cells

To prepare frozen stocks for long-term storage cells grown to about 100% confluency were washed once with PBS and trypsinized. Then the cells were resuspended in normal growth medium, transferred to a 15 ml tube and collected by centrifugation (200 g_{av}, 5 min, 4°C). The pellet was carefully resuspended in 2 ml freeze medium and transferred to 1.8 ml cryo-vials (Greiner). An alternative procedure is to resuspend the cells directly in freeze medium after trypsinization. The cryo-vials were frozen at -80°C in special cryo-boxes which ensure a temperature decrease of 1°C per minute. For long-term storage the frozen cryo-vials were transferred to liquid nitrogen cell storage tanks.

Freeze Medium:	20% (v/v)	FCS
	10% (v/v)	DMSO
	100 µg/ml	Streptomycin/Penicillin
		αMEM or DMEM

2.3.3 Thawing of eukaryotic cells

To unfreeze cells the cryo-vial was removed from liquid nitrogen and immediately thawed in a water bath at 37°C. The content was transferred to 20 ml fresh, prewarmed culture medium in a 50 ml tube and the cells were sedimented by centrifugation (200 g_{av}, 5 min, 4°C). To remove DMSO the medium was discarded and the cell pellet was resupended in fresh culture medium. The cells were then seeded on culture dishes of the same size they were taken from to prepare the frozen stocks and incubated at 37°C with 5% CO_2.

2.3.4 Viral transduction

To stably integrate reporter genes into the genome of target cells and finally generate genetically modified reporter cell lines, a MBS Mammalian Transfection Kit (Stratagene) was used according to the instructions of the manufacturer's manual. The procedure takes 5 days and consists of preparation of plasmids coding for virus components and the reporter gene, production of retroviral particles using HEK 293T as host cells, harvesting of the retroviral particles and infection of target cells.

The target cell lines were $CHO_{MCAT\text{-}TAM2}$ (Engling et al., 2002) and $HeLa_{MCAT\text{-}TAM2}$ (Seelenmeyer et al., 2003) expressing the murine cationic transporter MCAT-1 (Albritton et al., 1989; Davey et al., 1997) on the cell surface which is recognized by the virus and mediates docking and uptake. Additionally, the doxicycline-sensitive transactivator rtTA2-M2 (Urlinger et al., 2000) is constitutively expressed and allows production of reporter proteins in a doxicycline-dependent manner.

The reporter construct cDNAs were cloned either into the pRevTRE2, pLNCD4 or the pFB vector (2.2.13). pRevTRE2 is a expression vector which allows doxicycline-dependent protein synthesis due to a doxicycline transactivator responsive element mediating mRNA formation. The pLNCD4 and pFB vectors promote constitutive expression of the reporter construct. As a control GFP in the pFB vector was used which was constitutively expressed after successful transduction. The plasmid containing the reporter construct was mixed with two other

plasmids, pVPack-GP and pVPack-Eco, encoding the viral gag-pol elements (GP) and the viral envelope protein (Eco).

On Day 1 the corresponding DNA mixture was precipitated using 1 ml 100% (v/v) ethanol and 0.1 x volume 3 M sodium acetate. After incubation at -80°C for 30 minutes, the DNA pellet was collected by centrifugation at 12,000 g_{av} for 10 minutes. After discarding the supernatant 1 ml 70% (v/v) ethanol was added. After centrifugation (12,000 g_{av}, 4°C, 5 min) the supernatant was discarded and the wet pellet was stored at 4°C overnight. The virus producing HEK 293T cells were seeded on freshly prepared culture dishes to be used for transfection the next day. On day 2 HEK 293T cells were transfected with the three plasmids prepared the day before according to the manual of the MBS mammalian transfection kit and incubated for 72 h at 37°C to produce retroviral particles. On day 4 the $CHO_{MCAT\text{-}TAM2}$ or $HeLa_{MCAT\text{-}TAM2}$ cells were seeded on culture dishes in the desired dilution to be used for transduction 24 h later. On day 5 the virus particle containing medium was harvested from transfected HEK 293T cells and passed through a sterile filter. Subsequently, this medium was transferred to the target cells and transduction occurred by virus mediated gene transfer leading to stable integration of the reporter construct cDNA into genome of the target cell. Normal growth medium was added and the cells were incubated for two days with the retroviral particles. The cells were further analyzed using flow cytometry and transduction efficiency was measured by counting GFP positive cells transduced with pFB-hrGFP.

Vectors:	pVPack-GP	(Stratagene)
	pVPack-Eco	(Stratagene)
	pFB-hrGFP	(Clontech) derived from Moloney Murine Leukemia Virus (MMLV)
	pRevTRE2	(Clontech) derived from MMLV, contains tet-response element (TRE)

2.3.5 Addition of doxicycline

Doxicycline (Clontech) was added to the culture medium of different reporter cell lines, to induce protein expression by the tetracycline/doxicycline-responsive element for 48 h. A stock solution of 1 mg/ml in PBS was diluted 1:1,000 directly into the culture medium to reach a final concentration of 1 µg/ml.

2.4 Biochemical methods

2.4.1 Recombinant proteins

GST-Gal-1, GST-Gal-3 fusion constructs was cloned using the vector pGEX-2T (Amershan) and His_6-eGFP were cloned using pET-15b (Novagen). Appropriate PCR products were generated using the IMAGE clones 2666528 and 2419761 as a source for the ORFs of human Gal-1 and Gal-3. The plasmids were transformed into BL21 (DE3) cells (Invitrogen) (2.2.1) and the corresponding proteins were expressed in an ITPG inducible manner. Therefore a small amount of LB medium containing ampicillin was inoculated with transformed bacteria (Pre-culture; overnight; 37°C; constant shaking 300 rpm). The expression of the corresponding protein was induced by adding IPTG (0.5 mM) to the main-culture for 3 h at 37°C ($OD_{600} \approx 0.6$). Protein purification was achieved by affinity chromatography using GSH sepharose (Amershan) and Ni-NTA-agarose according to standard procedure.

A N-terminal fragment of CA125-C-TERM (defined by the NCBI clone AK024365) that corresponds to amino acids 1-356 (CA125-C-$Term_{1-356}$) was cloned into pIVEX 2.4b Nde (Roche) in order to express a His_6-tagged protein in vitro employing the Rapid Translation System RTS 100 (Rapid Translation System RTS 100 E.coli HY kit Cat. No. 3 186 148, Roche) according to manufacturer's manual.

Homogenous preparations of GST-Gal-1, His_6-eGFP and His_6-CA125-C-$TERM_{1-356}$, respectively, were used to generate polyclonal antisera in rabbits. Anti-Gal-1 antibodies were affinity-purified from the corresponding rabbit serum in two

steps: the serum was first incubated with GST-coupled beads to remove anti-GST-antibodies, followed by affinity purification of anti-Gal-1 antibodies on GST-Gal-1 coupled beads.

2.4.2 Preparation of cell lysates

Both wild-type and mutant forms of Gal-1-GFP and CGL-2-GFP fusion proteins were expressed in CHO cells by cultivating the cells in the presence of doxicycline (1 µg/ml) for 48 h at 37°C. Following detachment of cells from the culture dishes using PBS, 0.5 mM EDTA pH 8.0 (10 min, 37°C), cells were sedimented (200 g_{av}, 4°C, 5 min) and solubilized in PBS/TX-100 (1% (w/v)). Membranes were removed in two steps by centrifugation at 13,000 g_{av} (10 min, 4°C) and 100,000 g_{av} (1 h, 4°C). The supernatant was analyzed for the amounts of GFP fusion proteins based on GFP fluorescence as measured with a fluorescence plate reader (Molecular Devices SpectraMax Gemini XS).

2.4.3 Preparation of cell-free supernatants

CHO cells expressing GFP fusion proteins in a doxicycline-dependent manner were incubated in the presence of the antibiotic for 48 h at 37°C. The expressing cells were washed with PBS and detached by adding PBS, 0.5 mM EDTA. After incubation for 10 min at 37°C cells were harvested (200 g_{av}, 4°C, 5 min) and resuspended in PBS. Cell-free supernatants were prepared by homogenization combining freeze-thaw-cycles with sonication. Membranes were removed in two steps by centrifugation at 13,000 g_{av} (10 min, 4°C) and 100,000 g_{av} (1 h, 4°C). The resulting supernatant was analyzed for the amounts of GFP fusion proteins based on GFP fluorescence as measured with a fluorescence plate reader (Molecular Devices SpectraMax Gemini XS).

2.4.4 Determination of protein concentration based on GFP fluorescence

The concentration of a GFP fusion protein was determined employing a fluorescence plate reader (Molecular Devices SpectraMax Gemini XS).

30 µl of an unknown protein sample were transferred to a 96-well plate. The GFP fluorescence was determined by measuring fluorescence at 530 nm after excitation at 485 nm wavelength. Recombinant eGFP protein with a known protein concentration was used to calculate the protein amount in the unknown sample.

2.4.5 Sample preparation for SDS polyacrylamide gel electrophoresis

Samples were mixed with SDS sample buffer in a ratio of 3:1 followed by an incubation at 95°C for 5 min. Before loading the samples onto the gel a centrifugation step was performed (5,000 g_{av}, 4°C, 1 min) to collect all liquid at the bottom of the reaction tube or in case of cell lysates directly prepared in SDS sample buffer to sediment insoluble DNA aggregates (16,000 g_{av}, 4°C, 10 min). In the latter case only the supernatant was used.

SDS sample buffer (4x):	200 mM	Tris-HCl, pH 6.8
	25% (w/v)	Glycerol
	2% (w/v)	SDS
	0.2% (w/v)	Bromphenol Blue
	0.7 M	β-Mercaptoethanol

2.4.6 SDS polyacrylamide gel electrophoresis

To separate SDS denatured proteins according to their size SDS polyacrylamide gel electrophoresis was performed as described (Laemmli et al., 1970) using the Mini PROTEAN III Electrophoresis System (Bio-Rad).

Gels with dimensions of 80 x 73 mm and a thickness of 0.75 mm were casted between to glass plates of the respective size by first pouring the freshly prepared separating gel solution containing 13% acrylamide into the gel cassette fixed in a casting frame. Unpolymerized separating gel solution was overlayed with isopropanol to achieve an even surface. After polymerization the isopropanol was poured off and remains were removed with whatman filter paper. Then unpolymerized stacking gel solution was poured into the gel cassette and a plastic comb was inserted from the top, which forms the loading wells in the stacking gel. After polymerization the gels were stored at 4°C for up to 3 weeks or used directly.

To perform electrophoresis the gel was placed into the electrode assembly inside a clamping frame in the tank of the PROTEAN III system. Electrophoresis running buffer was added to the inner and outer chamber of the tank and the comb was carefully removed from the stacking gel. Samples were loaded by carefully pipetting into the wells of the stacking gel using extra-long loading pipet tips. Electrophoretic separation was performed at 200 V until the Bromphenol Blue front of the SDS sample buffer reached the end of the separating gel.

Separating Gel Solution:	13% Gel	
	1.68 ml	ddH_2O
	1.25 ml	1.5 M Tris-HCl, pH 8.8
	50 µl	10% (w/v) SDS
	2 ml	30% (w/v) Acrylamide/Bis
	25 µl	10% (w/v) APS
	2.5 µl	TEMED

Stacking Gel Solution:	4.8% Gel	
	1.53 ml	ddH_2O
	0.625 ml	0.5 M Tris-HCl, pH 6.8
	25 µl	10% (w/v) SDS
	335 µl	30% (w/v) Acrylamide/Bis
	12.5 µl	10 % (w/v) APS
	2.5 µl	TEMED

Electrophoresis running buffer:	25 mM	Tris-HCl, pH 8.3
	192 mM	Glycine
	0.1%	SDS

Alternatively Novex NuPAGE 10% Bis-Tris-HCl polyacrylamide-gels (pH 6.4) were employed using standard procedure. To separate proteins under reducing conditions 0.5 ml Antioxidant was added to the MES running buffer into the inner chamber of the XCEll II™ mini-cell apparatus. The run was performed at a 200 V for approximately 35 min.

MES running buffer:	1 M	MES
(20 x)	1 M	Tris Base
	69.3 mM	SDS
	20.5 mM	EDTA

2.4.7 SDS-PAGE protein molecular weight standards

As protein molecular weight standards either peqGOLD Protein-Marker I (Peqlab) or Odyssey Protein Molecular Weight Marker (LICOR) were used. The peqGold marker, ranging from 14 to 116 kDa, was used when analyzing the gel by Western blot using the ECL detection method. The Odyssey marker, ranging from 10 to 250 kDa, was applied when performing the analysis in an *Odyssey infrared imaging system* since the marker proteins were prestained with Coomassie and can

therefore be visualized by this system. Markers were applied by loading 1 to 5 µl of the premixed solutions onto the SDS-Gel.

2.4.8 Western blot analysis

To transfer proteins separated by SDS-PAGE to a polyvinylidene fluoride (PVDF) membrane for further analysis (Towbin et al., 1979), a wet blot transfer device was used (Mini Trans-Blot Cell, Bio-Rad). A PVDF membrane and two pieces of filter paper (Whatman 3MM, Whatman AG) were cut to the size of the separating gel. The PVDF membrane was activated by incubation in 100% methanol for 1 min. The membrane, filter paper, two sponges and a sandwich-blotting cassette were equilibrated in blotting buffer. The parts were assembled as depicted in the following figure avoiding air bubbles between the layers.

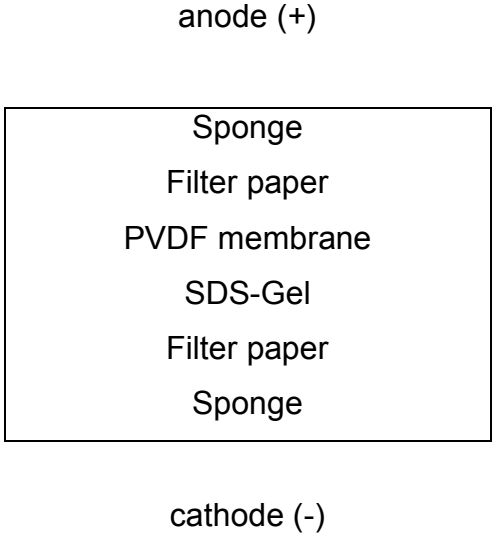

Fig. 4 Schematic overview: Assembly of a Western blot sandwich cassette.

The assembled blotting cassette was inserted into the transfer tank, an ice block for cooling was added and the tank was filled with blotting buffer. Protein transfer was performed at 100 V for 1 h under constant stirring.

Blotting buffer:	192 mM	Glycine
	25 mM	Tris, pH 8.4
	20% (v/v)	MetOH

2.4.9 Immunochemical protein detection using the ECL system

Western blotting was performed as described above using Immobilon-P PVDF membrane (Millipore Corporation). The membrane was incubated in blocking buffer for 1 h at room temperature or at 4°C overnight on a shaker. Following blocking the membrane was rinsed with PBS-T and incubated with primary antibodies directed against the protein of interest in the desired dilution for 1 h at room temperature on a shaker. Three washing steps for 5 min with PBS-T were applied and the membrane was incubated with secondary goat anti-rabbit IgG or goat anti-mouse IgG antibodies coupled to HRP in a 1:5,000 dilution. If samples derived from an immunoprecipitation experiment were analyzed monoclonal anti-rabbit IgG clone RG-16 HRP-coupled antibodies in a 1:3,000 dilution were used to detect only native antibodies excluding those derived from the IP procedure. After three times washing for 5 min with PBS-T on a shaker, visualization was performed using the enhanced chemiluminescence system (ECL, Amersham Pharmacia). The membrane was incubated with the ECL solution for 1 min at room temperature and chemiluminescence was detected using medical x-ray films (Super RX Medical X ray film, Fuji).

Blocking buffer:	5% (w/v)	Milk powder
		PBS-T
Primary antibody buffer:	3% (w/v)	BSA
	0.02% (w/v)	Sodium azide
		PBS-T
Secondary antibody buffer:	3% (w/v)	Milk powder
		PBS-T

2.4.10 Immunochemical protein detection using the LICOR system

Western blotting was performed as described above using Immobilon-FL PVDF membrane (Millipore Corporation) optimized for fluorescence detection. The membrane was incubated in blocking buffer for 1 h at room temperature on a shaker. Following blocking the membrane was rinsed two times for 5 min with PBS-T and incubated with primary antibodies directed against the protein of interest in the desired dilution for 1 h at room temperature on a shaker. Four washing steps for 5 min with PBS-T were applied followed by incubation with secondary goat anti-rabbit IgG or goat anti-mouse IgG antibodies coupled to the fluorophor Alexa 680 diluted 1:10,000 for 30 min at room temperature under constant shaking in the dark. Finally the membrane was washed four times for 5 min with PBS-T on a shaker and once with PBS without Tween 20. Visualization was performed using the *Odyssey infrared imaging system*.

Blocking buffer:	5% (w/v)	Milk powder
		PBS
Primary antibody buffer:	3% (w/v)	BSA
	0.02% (w/v)	Sodium azide
	0.1% (w/v)	Tween 20
		PBS
Secondary antibody buffer:	3% (w/v)	Milk powder
	0.01%(w/v)	SDS
	0.1% (w/v)	Tween 20
		PBS

2.4.11 Gal-1 affinity matrix and binding experiments employing subcellular fractions of S-HeLa cells

To perform affinity purification of Gal-1-interacting proteins, GST-Gal-1 and GST-Gal-3 fusion proteins, as well as GST as a control, were expressed in E.coli BL21 (DE3)) cells. Cells were resuspended in homogenization buffer, followed by cell breakage using an EmulsiFlex 5 (Avestin) cell disruptor. A 100,000 g_{av} supernatant was prepared and incubated with an appropriate amount of glutathione beads for 2 hours at 4°C on a rotating wheel. Following extensive washing using homogenization buffer, 250 µl of beads were used per binding experiment.

S-HeLa cells were cultured in spinner flasks according to standard procedure. Typically, cultures were grown to a density of about 6-7x10^5 cells per ml. Cells were collected by centrifugation (200 g_{av}, 4°C, 10 min) and resuspended in HeLa-homogenization buffer at 1 g cells per ml.

Following cell breakage using a Balch homogenizer, the homogenate was sequentially centrifuged twice at 1,000 g_{av} and twice at 3,500 g_{av}. The resulting supernatant was subjected to centrifugation at 100,000 g_{av}. Following separation of supernatant and sediment, the soluble fraction was diluted with PBS to achieve a final protein concentration of about 0.25 mg/ml. Typically, when starting with 5 g cells, the soluble fraction was adjusted to a final volume of 50 ml. The corresponding sediment was resuspended in 50 ml Resuspension buffer (membrane). Per experimental condition, 25 ml of the soluble or the membrane fraction were incubated with 250 µl of GSH beads coupled to GST-Gal-1, GST-Gal-3 or GST. Bound proteins were eluted sequentially with 100 mM lactose and 25 mM glutathione diluted in the corresponding buffers.

Homogenization buffer:	1 mM	DTT
	0.1% (w/v)	Triton X-100
	10% (w/v)	Glycerol
	5 mM	Pprotease inhibitor tabs
		PBS
HeLa-homogenization buffer:	25mM	Tris pH 7.5
	130 mM	KCl
	5 mM	Protease inhibitor tabs
Resuspension buffer (membrane):	1 mM	DTT
	1% (w/v)	NP-40
	5 mM	Protease inhibitor tabs
		PBS

2.4.12 Protein identification employing MALDI-Tof mass spectrometry

In order to identify proteins eluted from the Gal-1 affinity matrix, the eluates were separated on 10% Novex Bis-Tris gels (Invitrogen) followed by protein staining using the SilverQuest system (Invitrogen). After excision of gel pieces containing the individual proteins, in-gel trypsin digestion allowed extraction of tryptic peptides. Proteins were identified based on the masses of the peptides obtained in this way by employing MALDI-Tof mass spectrometry (Seelenmeyer et al., 2003).

2.4.13 Biotinylation of cell surface proteins

To analyze exported, cell surface bound material a biotinylation assay was performed as described (Seelenmeyer et al., 2005). A membrane impermeable biotinylation reagent that binds covalently to all free ε-amino groups of lysines present in surface associated proteins was added to the cells. Following lysis the biotinylated proteins were separated by incubation with streptavidin beads and the amounts of biotinylated and non-biotinylated proteins could be compared resembling the ratio of exported to non-exported reporter protein.

Galectin-GFP-fusion protein were expressed in the corresponding CHO cell lines by cultivation in the presence of doxicycline (1 µg/ml) for 48 h at 37°C (6-well plate; 70% confluency). The medium was removed and the cells were washed once with PBS. Medium and PBS wash were combined and subjected to immunoprecipitation using affinity-purified anti-GFP antibodies coupled to Protein A Sepharose (2.4.14).

After washing with cold PBS Ca^{2+}/Mg^{2+} cells were treated with a membrane-impermeable biotinylation reagent (EZ-Link Sulfo-NHS-SS-Biotin; Pierce; 0.5 mg/ml Biotin/Incubation buffer; 4°C, 30 min). To quench unbound biotinylation reagent cells were washed once with quenching buffer followed by an incubation with 500 µl quenching buffer for 20 min at 4°C. Then cells were washed two times with PBS and 200 µl lysis buffer were added per well. The cells were incubated 10 min at 37°C with lysis buffer and subsequently scraped off the cell culture plates using a rubber policeman. The cell solution was homogenized by pipetting and transfrerred to an eppendorf tube on ice. To complete lysis the samples were subjected to sonication in a water bath for 3 min and incubated for 15 min at room temperature being vortexed every 5 min. To remove insoluble material a centrifugation step (18,000 g_{av}, 10 min, 4°C) was performed and 10 µl of the supernatant were saved to function as an input sample for later analysis. The remaining lysate was added to 40 µl packed streptavidin beads equilibrated with lysis buffer and incubated for 1 h at room temperature under constant rotation to allow binding of biotinylated proteins to the streptavidin moiety. After the incubation the beads were washed two times with

washing buffer 1 and two times with washing buffer 2. Sedimentation of the beads was performed by centrifugation (3,000 g_{av}, 4°C, 1 min). After the last washing step the supernatant was carefully discarded and bound material was eluted by incubation with SDS sample buffer for 5 min at 95°C. Subsequently the samples were analyzed by SDS-PAGE and Western blotting.

PBS Ca^{2+}/Mg^{2+}:	1 mM	$MgCl_2$
	0.1 mM	$CaCl_2$
		PBS
Incubation buffer:	150 mM	$MgCl_2$
	10 mM	Triethanolamine, pH 9
	2 mM	$CaCl_2$
Quenching buffer :	100 mM	Glycine
		PBS Ca^{2+}/Mg^{2+}
Lysis buffer:	62.5 mM	EDTA
	50 mM	Tris-HCl, pH 7.5
	0.4% (w/v)	Deoxycholate
		Protease Inhibitor tablet (1/10 ml)
Washing buffer 1:	62.5 mM	EDTA
	50 mM	Tris-HCl, pH 7.5
	0.4% (w/v)	Deoxycholate
	1% (w/v)	NP-40
	0.5 M	NaCl

Washing buffer 2:	62.5 mM	EDTA
	50 mM	Tris-HCl, pH 7.5
	0.4% (w/v)	Deoxycholate
	0.1% (w/v)	NP-40
	0.5 M	NaCl

2.4.14 Immunoprecipitation of proteins

To immunoprecipitate GFP containing reporter molecules a mixture of Protein A-Sepahrose beads, CL-4B beads (Amersham Pharmacia) and 20% ethanol (1:1:2) was prepared and 40 µl slurry, corresponding to 20 µl pure beads, per sample were used. The beads were washed three times with IP-Buffer 1. Sedimentation was performed at 800 g_{av}, 3 min, 4°C. To couple affinity-purified anti-GFP antibodies to the beads, they were incubated with 20 µl anti-GFP antibodies (basic elution) in 180 µl Buffer 1 overnight at 4°C on a rotation wheel. Following the coupling procedure the beads were washed three times using IP-buffer 1. After sedimentation and removal of the buffer the sample consisting of 1 ml culture medium obtained from the respective reporter cell line grown on 6-well plates and 500 µl PBS obtained from washing the cells (see 2.4.13) were added to the beads followed by an 2 to 4 h incubation at 4°C. After the incubation with the medium sample the beads were washed three times with IP-buffer 1 and once with IP-buffer 2. Bound material was eluted by addition of SDS sample buffer and incubation at 95°C for 5 min.

IP-buffer 1:	25 mM	Tris-HCl, pH 7,4
	150 mM	NaCl
	1 mM	EDTA
	0.5% (w/v)	NP-40

IP-buffer 2:	25 mM	Tris-HCl, pH 7,4
	150 mM	NaCl
	1 mM	EDTA

2.4.15 Galectin binding to lactose-coupled beads

Detergent lysates of galectin-GFP expressing CHO cells were generated (2.4.2) and a sample was saved to function as input fraction. Following equilibration of lactose-coupled beads with PBS/TX-100 (1% (w/v) normalized amounts (50 GFP units corresponding to about 0.5 µg GFP) were incubated with 40 µl lactose-coupled beads (Sigma) for 1 h at 4°C to allow binding. After centrifugation (3000 g_{av}, 1 min, 4°C) a sample of the flow-through was saved for further analysis. After washing with PBS/TX-100 (1% (w/v)) bound proteins were eluted by adding SDS sample buffer. Comparable amounts of input (5%), flow-through (5%) and bound fraction (5%) were analyzed by Western blotting using affinity-purified anti-GFP antibodies (2.4.8).

2.4.16 Galectin binding to the cell surface of CHO cells

Cell-free supernatants of galectin-GFP expressing CHO cells (2.4.3) were analyzed for the amounts of GFP fusion protein (2.4.4). CHO cells not expressing the GFP reporter molecule were detached from cell culture dishes. Following washing with 250 mM lactose/PBS normalized amounts (150 GFP units corresponding to about 1.5 µg GFP) of the cell-free supernatants were incubated with CHO cells to allow binding to the cell surface (1 h, 4°C). Following treatment with affinity-purified anti-GFP antibodies and APC-conjugated secondary antibodies, cell surface binding was quantified by flow cytometry.

2.4.17 Stability analysis of Galectin-GFP fusion proteins in conditioned media derived from CHO cells

Cell-free supernatant of both wild–type and mutant forms of Gal-1-GFP and CGL-2-GFP fusion proteins, as well as GFP as a control, were prepared (2.4.3). Normalized amounts (50 GFP units corresponding to about 0.5 µg GFP, Molecular Devices SpectraMax Gemini XS) were diluted 1:10 in conditioned medium derived from CHO cells. Samples were then either directly subjected to immunoprecipitation employing anti-GFP antibodies, incubated for 48 h at 4°C followed by immunoprecipitation (2.4.14) or incubated for 48 h at 37°C followed by immunoprecipitation (2.4.14). In each case, bound material was eluted with SDS sample buffer. The samples were then analyzed by SDS Page and Western blotting using affinity-purified anti-GFP antibodies and anti-rabbit secondary antibodies (clone RG-16, see above) coupled to HRP (ECL detection).

2.5 Flow cytometry

2.5.1 Sample preparation for FACS analysis

To analyze GFP fluorescence and exported reporter proteins by specific antibody cell surface staining, cells were processed according to the following protocol and analyzed via FACS.

Cells were grown on 6-well plates to a confluency of about 70% in the absence or presence of doxicycline (1 µg/ml) to obtain samples from cells expressing reporter constructs and negative controls for direct comparison. After removal of the growth medium the cells were washed with 500 µl PBS and 500 µl *Cell Dissociation Buffer* (CDB, Invitrogen) or PBS/EDTA were added. The cells were incubated for 10 min at 37°C and detached by resuspension. After transfer to an Eppendorf tube on ice a centrifugation step was applied (200 g_{av}, 4°C, 5 min) and the supernatant was

discarded. The pellet was carefully resuspended in 300 µl αMEM containing the primary antibody in the desired dilution. After an incubation period of 1 h at 4°C under constant rotation, the cells were sedimented again and the pellet was washed once with αMEM without antibody. Then secondary antibodies coupled to the fluorophor Allophycocyanin were added in a 1:750 dilution in αMEM and cells were incubated for 30 min as described above. To remove secondary antibodies cells were washed once with αMEM and the pellet was resuspended in 500 µl sorting medium containing propidium iodide in a final concentration of 1 µg/ml to stain dead cells. The samples were subsequently measured using a FACSCalibur flow cytometer.

PBS/EDTA:	0.5 mM	EDTA
		PBS

Primary antibodies: αMEM/FCS (10% (v/v))

Affinity-purified anti-GFP anibodies (acidic elution) 1:200
Affinity-purified anti-Gal-1 antibodies (acidic elution) 1:200
Polyclonal anti-CA125 antibodies (1:50)
Monoclonal anti-CA125 (OC125) antibodies (1:200)

Secondary antibodies: αMEM/FCS (10% (v/v))

goat anti-rabbit IgG APC-coupled antibodies 1:750
goat anti-mouse IgG APC-coupled antibodies 1:750

Sorting Medium:	5% (v/v)	CDB
	0.2% (v/v)	FCS
		αMEM without FCS

2.5.2 Plate labelling technique

To prepare cells for FACS analysis using the plate labelling technique the cells were grown on 6-well plates to a confluency of about 70% in the absence or presence of doxicycline (1 µg/ml). Following washing with 500 µl PBS primary antibodies in the desired dilution were added in 600 µl αMEM and the plates were incubated for 1 h at 4°C under constant shaking. Cells were subsequently washed three times with 500 µl PBS and secondary antibodies were added in the desired dilution in 600 µl αMEM. The samples were incubated for 30 min at 4°C under constant shaking followed by three times washing with 500 µl PBS. The cells were detached by addition of 200 µl PBS/EDTA followed by an incubation period of 10 min at 37°C. The samples were resuspended and transferred to an Eppendorf tube containing 500 µl αMEM without FCS and propidium iodide in a dilution that results in final concentration of 1 µg/ml after addition of 200 µl cell suspension. GFP-derived and APC-derived fluorescence were measured simultaneously on a FACSCalibur two-laser system without the need of channel compensation.

Primary antibodies: αMEM/FCS (10% (v/v))

Affinity-purified rabbit anti-GFP anibodies (acidic elution) 1:200
Affinity-purified anti-Gal-1 antibodies (acidic elution) 1:200
Polyclonal anti CA125 antibodies (1:50)
Monoclonal anti-CA125 (OC125) antibodies (1:200)

Secondary antibodies: αMEM/FCS (10% (v/v))

Goat anti-rabbit IgG Allophycocyanin-coupled antibodies (1:750)
Goat anti-mouse IgG Allophycocyanin-coupled antibodies (1:750)

Sorting Medium:	5% (v/v)	CDB
	0.2% (v/v)	FCS
		αMEM without FCS

2.5.3 FACS sorting

FACS based sorting was performed in collaboration with Dr. Blanche Schwappach from the *Center of Molecular Biology Heidelberg* (ZMBH). Cells induced by addition of doxicycline for 48 h or grown after a sort in the absence of doxicycline for 7 days were detached from culture dishes using sterile CDB (Invitrogen) after washing once with PBS. The resulting suspension was added to 5 ml cell culture medium. After sedimention at 200 g_{av}, 4°C, 5 min the supernatant was removed and the pellet was carefully resuspended in sorting medium. The cells were filtered using cell strainer caps (Becton Dickinson) into 5 ml round bottom FACS tubes (Becton Dickinson) and propidium iodide in a final concentration of 1 µg/ml was added. Subsequently, cells were sorted using a FACSVantage or FACSAria sorting device for pools of 50.000 or 100.000 cells in 6-well plates or as single cells to generate clonal cell lines in 96-well plates.

2.6 Confocal microscopy

2.6.1 Sample preparation for confocal microscopy

For confocal microscopy cells were grown on glass coverslips to about 70% confluency in 24-well plates. Following two times washing with PBS on ice 200 µl PFA in PBS per well were added (3% (w/v)) and the cells were fixed without permeabilization for 20 min at 4°C. After removal of PFA the cells were washed four times with PBS. The coverslips were mounted on microscopic slides using Fluoromount G (Southern Biotechnology Associates). After hardening overnight at room temperature in the dark the specimens were sealed at the edge of the cover slip employing clear nail polish and analyzed using a Zeiss LSM 510 Meta confocal microscope.

PFA in PBS: 3% (w/v) PFA

For life cell imaging cells were grown to about 70% confluency in the presence of doxicycline in appropriate cell culture dishes and analyzed using a Zeiss LSM 510 Meta confocal microscope.

2.6.2 Immunostaining of cell surface proteins for confocal microscopy

Samples were prepared as described in 2.6.1. After fixation with PFA and two times washing with PBS, the samples were quenched by incubation with 250 µl quenching buffer for 10 min at 4°C followed by incubation with 250 µl blocking buffer (10 min, room temperature) to saturate unspecific antibody binding sites. Primary antibodies were added in the desired dilution in 250 µl blocking buffer per well for 1 h at room temperature. Following three times washing with PBS unspecific binding

sites were blocked again by incubation in 250 µl blocking buffer per well for 10 min at room temperature. Secondary antibodies were added in 250 µl blocking buffer per well and the specimens were incubated for 30 min at room temperature. After four times washing the samples were mounted as described in 2.6.1 and analyzed in a Zeiss LSM 510 Meta confocal microscope.

Quenching buffer:	50 mM	NH_4Cl
		PBS
Blocking buffer:	1% (w/v)	BSA
		PBS

Primary antibodies:	Blocking buffer:
	Affinity-purified anti-GFP antibodies (acidic elution) 1:50
	Affinity-purified anti gal-1 antibodies (acidic elution) 1:50
Secondary antibodies:	Blocking buffer:
	Goat anti-rabbit or goat anti-mouse IgG antibodies Alexa 546-coupled 1:750

3 Results

Some lectin-encoding genes are expressed constitutively (Stahl, 1992), whereas others are induced by gene activation under specific biological conditions (McEver, 1995; McEver et al., 1995). All membrane-bound and many soluble lectins are synthesized on ER-bound ribosomes and are delivered to their final destinations via the ER-Golgi pathway. Thus, the lectins themselves are often glycoproteins (Kjellen and Lindahl, 1991). However, a significant subset of soluble lectins such as galectins (Ahmed et al., 1996), heparin-binding growth factors and some cytokines are synthesized on free ribosomes and are delivered directly to the exterior of the cell by as yet poorly understood mechanisms involving translocation through the plasma membrane. By circumventing the conventional pathway of secretion, these molecules can avoid unwanted premature interactions with potential ligands that are synthesized within the same cell. In addition, some of these lectins, such as galectins (Barondes et al., 1994), are sensitive to the redox state of the environment and can remain active only in the reducing environment of the cytosol (Cho and Cummings, 1995a). Upon entering the oxidizing environment of the extracellular space, they must therefore immediately bind to ligands.

3.1 Identification of Gal-1 interacting proteins potentially involved in the export process of human Gal-1

Several crystal structures of animal lectins with their cognate ligands have been elucidated (Rini, 1995a; Rini, 1995b), allowing an understanding of these interactions at the level of atomic resolution. The principles that have emerged from these studies are as follows: First, the binding sites are of relatively low affinity and are found in shallow indentations on the surface of the proteins. Second, selectivity is mostly achieved via a combination of hydrogen bonds involving the hydroxyl groups of the sugars and by ‘van der Waals’ packing of the hydrophobic face of monosaccharide rings against aromatic amino acids side chains. Third, further selectivity can be

achieved by additional contacts between the saccharide and the protein, sometimes involving bridging water molecules or divalent cations. Finally, the actual region of contact between the saccharide and the polypeptide typically involves only one to three monosaccharide residues. As a consequence of all of the above, these lectins-binding sites tend to be of relatively low affinity, but of high specifity. The ability of such low-affinity sites to mediate biologically relevant interactions in the intact system thus appears to require multivalency (Weis and Drickamer, 1996).

The natural ligands for most lectins are typically complex glycoconjungates that carry clustered arrays of the cognate carbohydrate, thus cooperating with clustered lectins-binding sites to generate high-avidity binding (Drickamer and Taylor, 1993; Varki, 1994), which is further enhanced by mass transport effects (high local concentrations of ligands) (Sharon, 1993). In some instances (e.g. selectins) the nature of this clustering is not easily defined (Rosen and Bertozzi, 1994), and cooperation with other aspects of the underlying polypeptide may be necessary to generate optimal binding. However, it should be emphasized that unless it is correctly glycosylated and/or otherwise modified, the polypeptide is not itself the ligand. Typically, these polypeptides are simply carriers of the true ligands for lectins, which are made up of combinations of glycan units (Kjellen and Lindahl, 1991). In addition, recombinant lectins that are often used to identify potential biological ligands are usually multimeric in structure and/or are presented in multivalent clustered arrays in soluble complexes or on solid supports (Weis and Drickamer, 1996). Thus, although a variety of molecules may be found to bind to a given recombinant lectin in a glycosylation-dependent manner, only a few of these “ligands” may be actually involved in mediating biologically significant interactions (Varki, 1997). The challenge then is to tell the difference between what can bind to a recombinant lectin in an *in vitro* experiment, and what actually does bind *in vivo* to the native lectin in a biologically relevant manner. Indeed, the term ligand should probably be reserved for the latter type of biologically relevant structures.

3.1.1 Identification of CA125 as a Gal-1 counter receptor

To search for ligands of human Gal-1, a recombinant GST-Gal-1 fusion protein was attached to glutathione sepharose beads. As a source for proteinaceous Gal-1-binding partners S-HeLa cells were fractionated into a soluble and a membrane fraction. These fractions were incubated with the Gal-1 affinity matrix. Proteins bound to Gal-1 were eluted sequentially using lactose (Fig. 5, lanes 1-4) and glutathione (Fig. 5, lanes 5-8). This procedure allowed collecting proteins that interact with the Gal-1-matrix in a galactose-dependent manner, followed by elution of proteins bound to the matrix by a sugar-independent mechanism. As shown in Fig. 5, specifically bound proteins could be identified in lanes 2 (GST-Gal-1 matrix; soluble S-HeLa-fraction; eluted by lactose), lane 4 (GST-Gal-1 matrix, S-HeLa membrane fraction; eluted by lactose), lane 6 (GST-Gal-1 matrix, soluble S-HeLa fraction, eluted with glutathione) and lane 8 (GST-Gal-1 matrix, S-HeLa membrane fraction, eluted by glutathione) in comparison with the corresponding GST control matrices (lane 1, 3, 5 and 7).

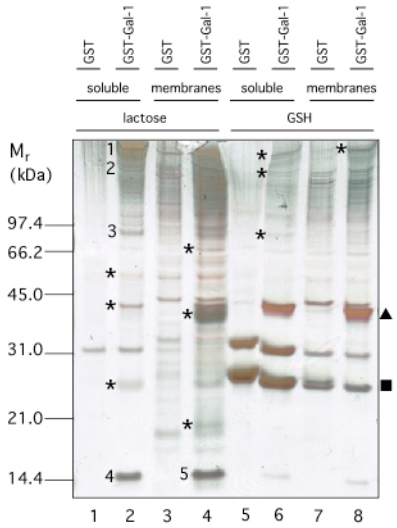

Fig. 5 Identification of CA125 as a counter receptor of Gal-1. Affinity purification of Gal-1-interacting proteins. Both soluble (lanes 1, 2, 5, 6) and membrane (lanes 3, 4, 7, 8) fractions of S-HeLa cells were incubated with either GST-Gal-1 beads (lanes 2, 4, 6, 8) or GST beads as a control (lanes 1, 3, 5, 7). Bound proteins were eluted sequentially with lactose (lanes 1-4) and glutathione (lanes 5-8), followed by separation on Novex NuPage 10% Bis-Tris gels. Protein bands were visualized using SilverQuest (Invitrogen).

Following mass spectrometry analyses, protein band # 2 was identified as a chondroitin sulfate proteoglycan, band # 3 was identified as the cell adhesion molecule L1-CAM, and band # 4 and # 5 were identified as Gal-1. Recombinant Gal-1 and S-HeLa-derived Gal-1 formed apparently a dimer that disassembled in the presence of lactose. Beside these known interactions, 16 tryptic peptides could be recovered from protein band # 1 whose masses were consistent with corresponding tryptic fragments of a potential ORF defined by cDNA clone AK024365 (NCBI database; Fig. 6, boxed sequences indicate peptides identified by mass spectrometry)

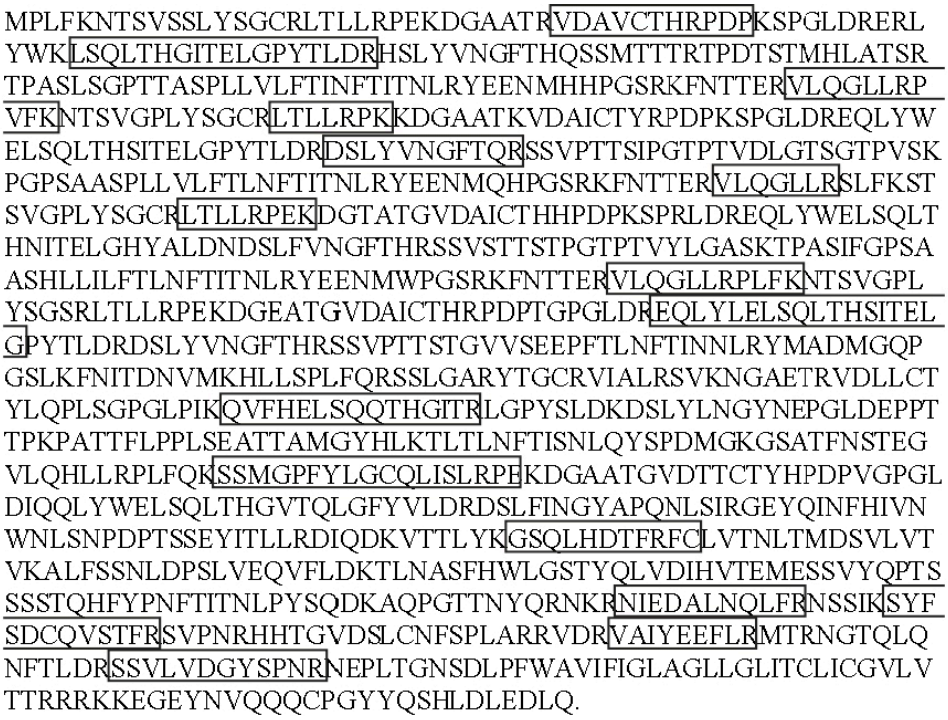

Fig. 6 Amino acid sequence of CA125-C-TERM. Boxed sequences indicate tryptic peptides derived from band 1 (Fig. 5 A, lane 2) as identified by mass spectrometry

In order to verify whether band # 1 is the gene product AK024365, a polyclonal antiserum against a recombinant protein corresponding to the N-terminal part (AA 1-356; M_r: ~ 39 kDa) of AK024365 was generated. As shown in Fig. 7, immunoreactive material with a broad high-molecular-weight migration behavior was detected in lane 2, 4, 6 and 8, which correspond to the various eluates of GST-Gal-1 matrix. No signal could be detected under control conditions. Binding of immunoreactive material to Gal-1 appeared to be mediated by a galactose-lectin interaction as more than 90% eluted upon treatment of the affinity matrix with lactose. About 80% of the total immunoreactive material was recovered from the soluble fraction, with the remaining population derived from the membrane fraction.

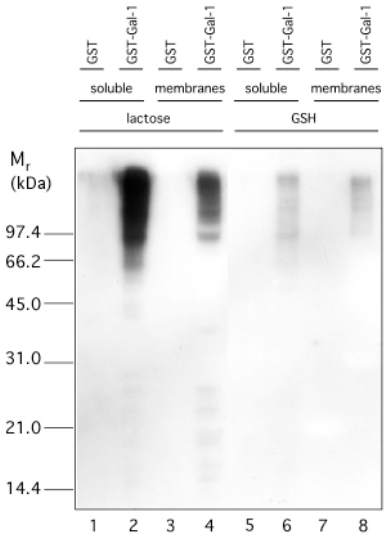

Fig. 7 Immunoblot analysis of the proteins eluted from the GST-Gal-1 and GST matrices, respectively. The fractions were loaded in the same order as shown in Fig. 5. The polyclonal antiserum against the N-terminal part of AK024365 was used as primary antibody followed by detection by ECL.

The AK024365 gene product was, found to represent a C-terminal fragment of 1148 amino acids in length of a giant mucin-like glycoprotein (O'Brien et al., 2001), (Yin and Lloyd, 2001). This mucin is identical to the ovarian cancer antigen CA125, an integral membrane protein present on the cell surface of tumor cells that has originally been defined by the mAb OC125 (Bast et al., 1981). Therefore, the eluates from the Gal-1 affinity matrix were analyzed for immunoreactivity based on OC125. As shown in Fig. 8, the pattern of immunoreactive bands detected with OC125 is strikingly similar to the pattern detected with the polyclonal anti-AK024365 antiserum. Since CA125 was reported to represent an integral membrane protein with a single transmembrane span that is cleaved in the extracellular domain in order to release soluble fragments, we conclude that the pattern of immunoreactive bands eluted from the galectin affinity matrix represents both soluble and membrane anchored fragments of CA125 (from now on, the 1148 amino acids, C-terminal fragment of CA125, defined by cDNA clone AK024365, will be termed CA125-C-TERM).

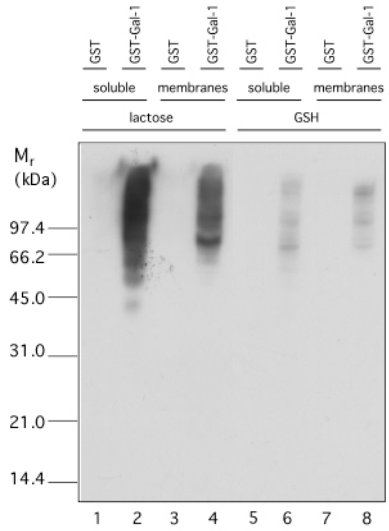

Fig. 8 **Immunoblot analysis** as shown in Fig. 7 employing the anti-CA125 antibody OC125 for the detection of CA125-derived fragments.

3.1.2 Specificity of CA125-mediated Galectin binding

All members of the galectin family tested so far bind to simple β-galactosides, but the affinity is relatively low, i.e. in the millimolar range. Surprisingly, the detailed glycan specificities for most galectins are not clear and each galectin may differ in its overall specificity (Lobsanov et al., 1993). All galectins appear to bind terminal β-galactosides, but some galectins differ significantly in their recognition of galactosyl residues within oligosaccharides (Zhou and Cummings, 1990). For example, both Gal-1 and Gal-3 bind simple lactosaminyl units as well as polylactosamine. However, Gal-3 binding to oligosaccharides is enhanced if the penultimate galactosyl residues are substituted with Galα1-3, GalNAcα1-3, or Fucα1-2 residues (Leffler and Barondes, 1986). In contrast, such substitution dramatically decreases binding by Gal-1. Several studies on Gal-1 have revealed that it displays much higher affinity for larger glycans containing repeating galactosyl residues. Interestingly, at least for Gal-1, its interaction with polylactosamine is not dependent on terminal galactose residues, but it does require at least two linear repeating disaccharide units. It is possible, that the interaction of Gal-1 with polylactosamine and other extended

glycans may be due to contributions of secondary binding sites on the protein. The potential endogenous glycoconjungate ligands have been investigated for only a few members of the galectin family. Potential ligands for Gal-1 and Gal-3 include basement membrane proteins, such as laminin and fibronectin, membrane receptors, such as integrin$\alpha_7\beta_1$, CD43, and CD45, lysosome-associated membrane proteins (LAMPs) and even certain gangliosides. However, the precise carbohydrate structures on these macromolecules that are recognized by galectins are not well defined. It is possible that each galectin differs somewhat in both oligosaccharide binding specificity and affinity for macromolecular ligands. The fact that Gal-1, for example, binds to a limited set of glycoconjungates suggests that the mere presence of galactose residues on glycoconjungates is not sufficient to promote their high-affinity binding to this lectin.

To analyze whether CA125 preferentially binds to certain β-galactoside specific lectins, we compared CA125 binding efficiency for Gal-1 with the efficiency for Gal-3, also a very well characterized member of the galectin family (Barondes et al., 1994; Hughes, 1999; Perillo et al., 1998; Rabinovich et al., 2002a). As shown in Fig. 9, S-HeLa-derived fragments of CA125 bind to Gal-1 twice as efficiently compared with Gal-3 (Fig. 9 A, B; compare lanes 1 and 2 as well as lane 3 and 4). This difference is significant because comparable amounts of Gal-1 and Gal-3 fusion proteins were used (Fig. 9 A, compare lane 9 and 10). In addition the total pattern (Fig. 9 C) of sugar-dependent interactions partners reveal proteins that specifically bind to Gal-1 and Gal-3, as well as proteins that bind equally efficient to Gal-1 and Gal-3, respectively. This shows that differential binding efficiency can be detected under the experimental conditions applied.

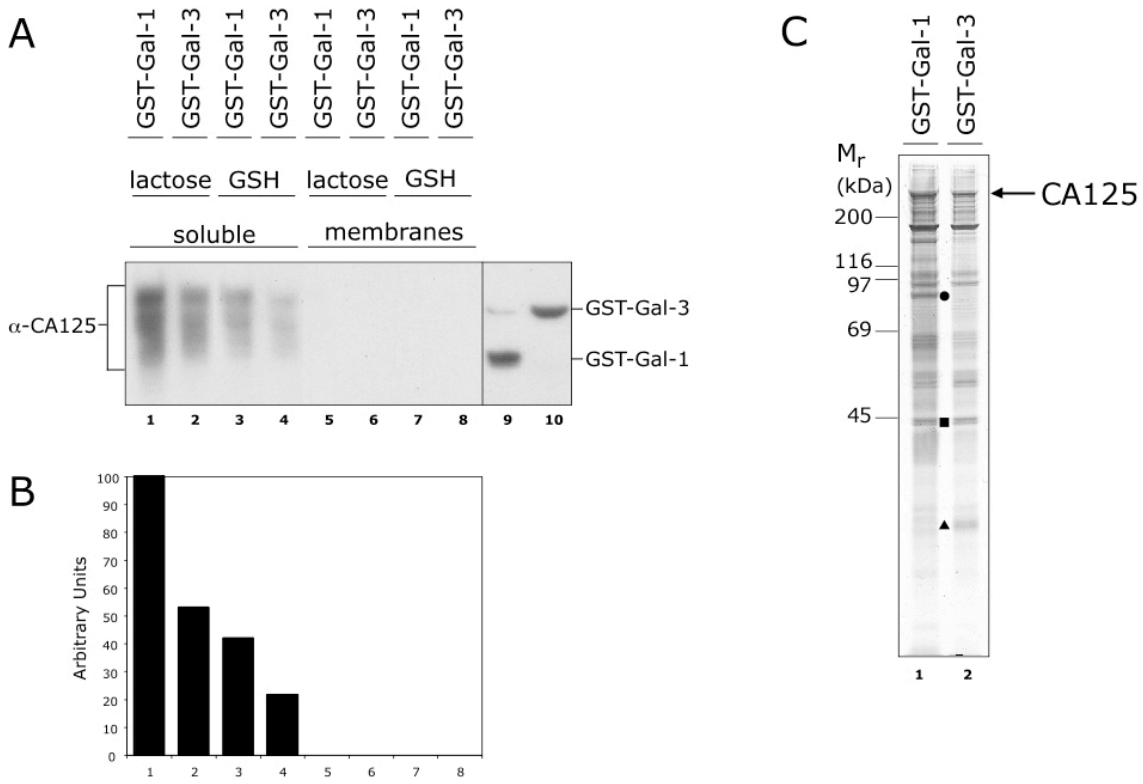

Fig. 9 CA125 displays differential binding efficiency towards Gal-1 when compared to Gal-3. A, Soluble (lanes 1 to 4) and membrane fractions (lanes 5 to 8) were prepared from S-HeLa cells followed by the incubation with either GST-Gal-1 (lanes 1, 3, 5 and 7) or GST-Gal-3 (lanes 2, 4, 6 and 8) beads. The amounts of GST-Gal-1 and GST-Gal-3 fusion proteins, respectively, used for affinity purification of CA125-derived fragments were shown to be comparable by western blotting employing affinity-purified anti-GST antibodies (lanes 9 and 10). Following extensive washing bound proteins were eluted sequentially with lactose (lanes 1, 2, 5 and 6) and glutathione (lanes 3, 4, 7 and 8). Eluted proteins were separated on 10% Novex NuPage Bis-Tris gels and transferred to a blotting membrane. ECL detection of CA125-derived fragments was performed employing the monoclonal antibody OC125. B, Quantitative analysis of CA125-derived fragments in the fractions shown in panel A employing Bio-Rad® QuantityOne® Software. C, Total protein pattern of lactose-eluted proteins derived from the Gal-1 matrix (lane 1) and the Gal-3 matrix (lane 2). Eluted proteins were separated on NuPage Bis-Tris gels (Invitrogen) followed by silver staining according to standard procedures. Lables indicate examples for proteins that preferentially bind to Gal-1 (●), Gal-3 (▲) or proteins that equally bind Gal-1 and Gal-3 (■).

To analyze further the binding efficiency of CA125 to galectins, CA125-C-TERM was expressed in adherent HeLa and CHO by retroviral transduction (3.2.1). A more defined protein band was observed (Fig. 10). CA125-C-TERM still has the ability of

full-length CA125 to bind to Gal-1. This observation is consistent with the fact that the CA125-C-TERM contains both the stalk domain of CA125 and almost three CA125 repeats structures that are O-glycosylated (O'Brien et al., 2001). CA125-C-TERM expressed in HeLa cells shows the same characteristics as endogenous full-length CA125 with regard to Gal-1 interactions as it binds Gal-1 about twice as efficient as Gal-3 (Fig. 10).

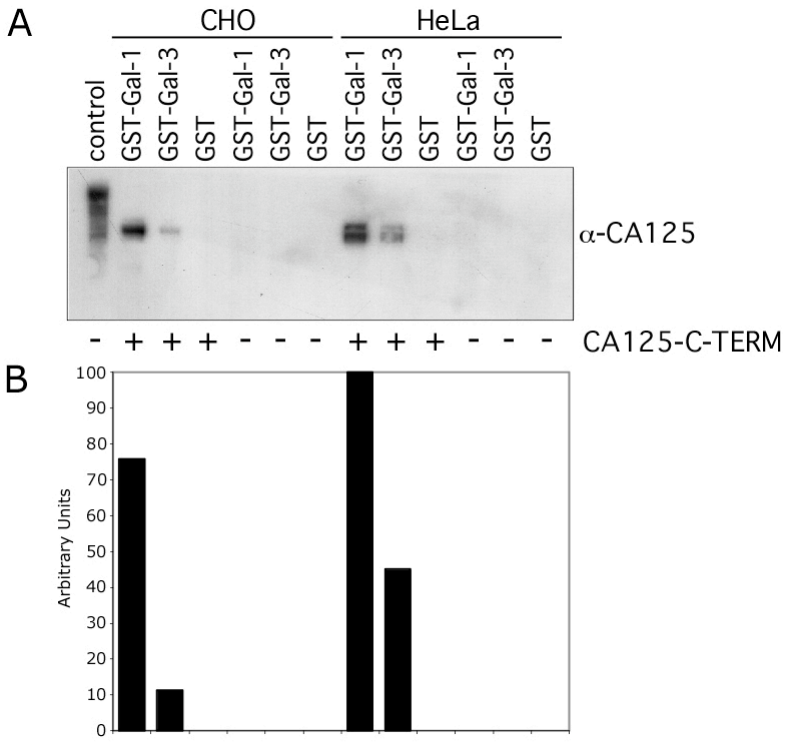

Fig. 10 An 1148 amino acids C-terminal fragment of CA125, CA125-C-TERM, retains the ability of CA125 to specifically bind Gal-1. CHO and HeLa cells were induced to express CA125-C-TERM by retroviral transduction. For comparison, CHO and HeLa cells were included that were treated with retroviral control particles. A detergent lysate of the cells was prepared and incubated with either GST-Gal-1-, GST-Gal-3 or GST beads. Following extensive washing the beads were treated with lactose. Eluted proteins were separated on 10% Novex NuPage Bis-Tris gels followed by transfer to a blotting membrane. CA125-C-TERM was then detected by OC125 staining employing ECL (panel A). For comparison, the pattern of CA125-derived fragments isolated from S-HeLa cells is shown in the leftmost lane (control). In panel B, the intensity of CA125-C-TERM-derived bands was quantified using Bio-Rad® QuantityOne® software.

By contrast, CA125-C-TERM expressed in CHO cells binds Gal-1 more than seven times as efficient as Gal-3 (Fig. 10). This demonstrates that, besides N- and/or O-linked sugar moieties of CA125, the proteinaceous core structure of CA125 contributes to the specificity of galectin recruitment. Moreover, a cell-type dependent galectin binding characteristics of CA125 was established.

In order to provide evidence for a direct interaction between CA125-C-TERM and Gal-1, crosslinking experiments were performed (Fig. 11). CA125-C-TERM bound to GST-Gal-1 beads was treated with the crosslinking reagent disuccinimidyl glutarate (DSG, Pierce). Crosslinking products with an apparent molecular mass of about 160-180 kDa can be detected using anti-Gal-1 antibody and anti-CA125 antibody. This size corresponds to the approximate molecular weight of CA125-C-TERM and Gal-1 in a 1:1 complex. The products have a smear-like appearance as expected for a glycoprotein-containing crosslinking product. This product is only observed in the presence of crosslinking reagent. Larger crosslinking products (> 180 kDa), which could indicate an indirect interaction of CA125 with Gal-1, cannot be detected.

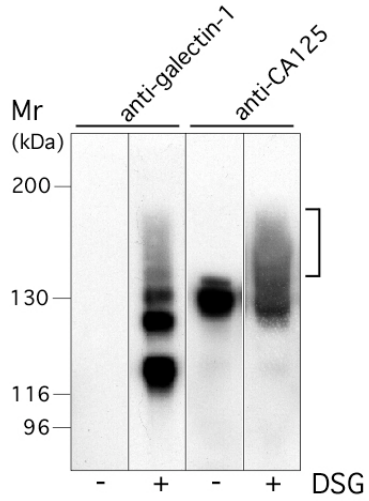

Fig. 11 A crosslinking experiment is shown employing disuccinimidyl glutarate (DSG; Pierce). CA125-C-TERM-expressing CHO cells were lysed with detergent followed by incubation of the cell-free supernatant with GST-Gal-1 beads. After extensive washing DSG was added at a final concentration of 0.5 mM. Crosslinking products were eluted with SDS sample buffer and analysed by SDS-PAGE and western blotting employing affinity-purified anti-Gal-1 and monoclonal anti-CA125 antibodies. The square bracket indicates crosslinking products with an apparent molecular mass of about 160 to 180 kDa positive for Gal-1 and CA125. In the range of 120 to 130 kDa other Gal-1-containing crosslinking products are observed.

3.1.3 CA125-C-TERM binding to Gal-1 depends on O-linked β-galactose-terminated oligosaccharide chains

To characterize further the molecular mechanism of Gal-1 binding to CA125, interaction studies were performed using cell lysates derived from CA125-C-TERM-expressing CHO cells grown in the presence of tunicamycin (Fig. 12). Under control conditions (Fig. 12 A, lanes 1-3), approximately 40% of CA125-C-Term could bind to GST-Gal-1 beads as calculated based on the input amount shown in lane 1 of Fig. 11. This value was set to 100% (Fig. 12 B) and the ratio of Gal-1 binding efficiency of CA125-C-TERM derived from tunicamycin-treated cells was calculated (Fig. 12 A, lanes 4-6). As shown in Fig. 12 B binding efficiency was reduced to 65% in comparison to control conditions. When CA125-C-TERM was expressed in $CHO_{clone13}$ cells that are incapable of translocating UDP-galactose into the lumen of

the Golgi and, therefore, neither form galactosylated glycoprotein nor glycolipids (Deutscher and Hirschberg, 1986), the binding capacity of CA125-C-TERM to GST-Gal-1 was almost completely abolished (Fig. 12 A, lanes 14-16). Under all experimental conditions, CA125-C-TERM binding to Gal-1 was specific (Fig. 12 B).

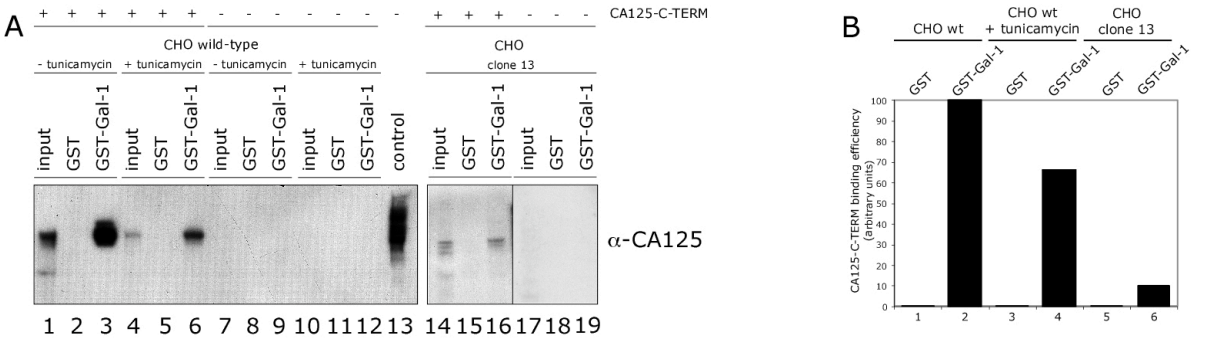

Fig. 12 Gal-1 binding to CA125-C-TERM largely depends on O-linked β-galactose-terminated oligosaccharide chains. $CHO_{MCAT-TAM2}$ (wild-type background with regard to galactosylation of both proteins and lipids) and $CHO_{clone13}$ cells (deficient with regard to galactosylation of both proteins and lipids; (Deutscher and Hirschberg, 1986)) stably expressing CA125-C-TERM were used to prepare cell-free detergent lysates followed by incubation with GST- and GST-Gal-1 beads, respectively. Where indicated $CHO_{MCAT-TAM2}$ were treated with 10 µg/ml tunicamycin for 18 hours at 37°C prior to cell lysis. In each experiment the CA125-C-TERM signal derived from 0.2% of the input was compared to 4% of the material bound to either GST- or GST-Gal-1 beads. Protein samples were separated on NuPage Bis-Tris gels (Novex) followed by CA125-C-TERM immunoblotting employing the monoclonal antibody OC125. A, Lysates derived from CA125-C-TERM-expressing $CHO_{MCAT-TAM2}$ cells (lanes 1-3), CA125-C-TERM-expressing $CHO_{MCAT-TAM2}$ cells treated with tunicamycin (lanes 4-6), CA125-C-TERM-deficient $CHO_{MCAT-TAM2}$ cells (lanes 7-9), CA125-C-TERM-deficient $CHO_{MCAT-TAM2}$ cells treated with tunicamycin (lanes 10-12), CA125-C-TERM-expressing $CHO_{clone13}$ cells (lanes 14-16) and CA125-C-TERM-deficient $CHO_{clone13}$ cells (lanes 17-19). In lane 13, HeLa-derived CA125 eluted from GST-Gal-1 beads is shown as a control. B, Quantitation of the results shown in panel A. Based on the input signal (0.2% of starting material; panel A, lane 1) about 40% of CA125-C-TERM present in the cell lysate is recovered on GST-Gal-1 beads under the conditions used (panel A, lane 3, 4% of eluate) as based on quantitation employing Bio-Rad® QuantityOne® software. This value was set to 100% binding efficiency and compared to CA125-C-TERM-Gal-1 binding efficiencies measured with lysates either derived from tunicamycin-treated $CHO_{MCAT-TAM2}$ cells or from $CHO_{clone13}$ cells. The results shown represent mean values of two independent experiments.

In order to investigate whether CA125-C-TERM binding to Gal-1 depends on *O*-linked galactose-terminated oligosaccharides chains in vivo, binding studies of exogenously added GST-Gal-1 to untreated CHO, tunicamycin treated CHO and $CHO_{clone13}$ cells were performed. As expected, untreated CHO cells show a high Gal-1 surface staining employing flow cytometry (Fig. 13, dark-blue curve). The binding activity was not saturated under these conditions. This binding activity was significantly reduced when cells were pre-treated with tunicamycin (Fig. 13, red curve). GST-Gal-1 binding to the cell surface was almost abolished in $CHO_{clone13}$ cells (Fig. 13, dark green curve), which allowed determining whether expression of CA125-C-TERM under these conditions is capable of binding Gal-1. As shown in Fig. 13, CA125-C-TERM cells surface expression does not alter cell-surface binding capacity for Gal-1 (Fig. 13 compare dark green and light green curves), demonstrating that Gal-1 binding to CA125-C-TERM requires its galactosylation. The combined data shown in Fig. 11, Fig. 12 and Fig. 13 suggest that the interaction between CA125-C-TERM and Gal-1 is direct.

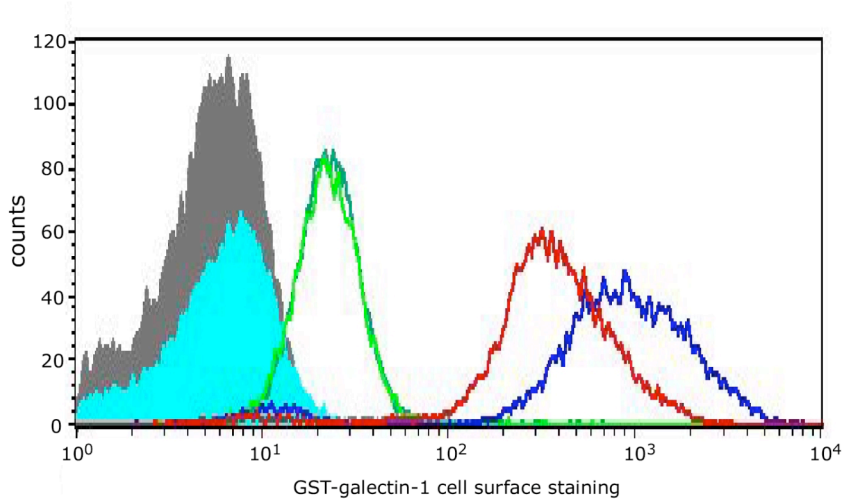

Fig. 13 CA125-C-TERM cell surface expression in $CHO_{clone13}$ cells does not result in increased binding capacity for exogenously added Gal-1. CA125-C-TERM-expressing- and CA125-C-TERM-deficient $CHO_{MCAT-TAM2}$- and $CHO_{clone13}$ cells were grown to 70% confluency. Where indicated, cells were treated with 10 µg/ml tunicamycin for 18 hours at 37°C. Cells were then dissociated from the culture plates followed by incubation with 40 µg/ml recombinant GST-Gal-1 for 30 min at room temperature. Following labeling with affinity-purified anti-Gal-1 antibodies under native conditions, the various samples were analyzed for cell surface-bound recombinant Gal-1 employing FACS. Autofluorescence (filled light-blue curve: $CHO_{MCAT-TAM2}$; filled grey curve: $CHO_{clone13}$) was determined based on cells not treated with antibodies). Untreated $CHO_{MCAT-TAM2}$ cells are shown in dark blue. Tunicamycin-treated $CHO_{MCAT-TAM2}$ cells are shown in red. $CHO_{clone13}$ cells are shown in dark-green (CA125-C-TERM-expressing) and light-green (CA125-C-TERM-deficient), respectively.

3.1.4 Despite lacking a N-terminal signal peptide, CA125-C-TERM is transported to the cell surface of CHO and HeLa cells

Endogenous CA125 is expressed on the cell surfaces of tumor cells (Bast et al., 1981). Based on structural analyses (O'Brien et al., 2001; Yin and Lloyd, 2001) no obvious N-terminal or internal signal peptide is present in the full-length CA125 and of the CA125-C-TERM. Like the N-terminal ER signal sequences, the internal signal sequence is recognized by an SRP, which brings the ribosome to the ER membrane and serve as a start-transfer signal for single-pass transmembrane protein that

initiates the translocation of the protein. In order to know more about the molecular mechanism of CA125 cell surface expression CA125-C-TERM transport to the cell surface was investigated. CA125-C-TERM was expressed in CHO and HeLa cells using retroviral transduction (Engling et al., 2002). Cell surface expression was analyzed by flow cytometry using the monoclonal anti-CA125 antibody OC125 (Fig. 14).

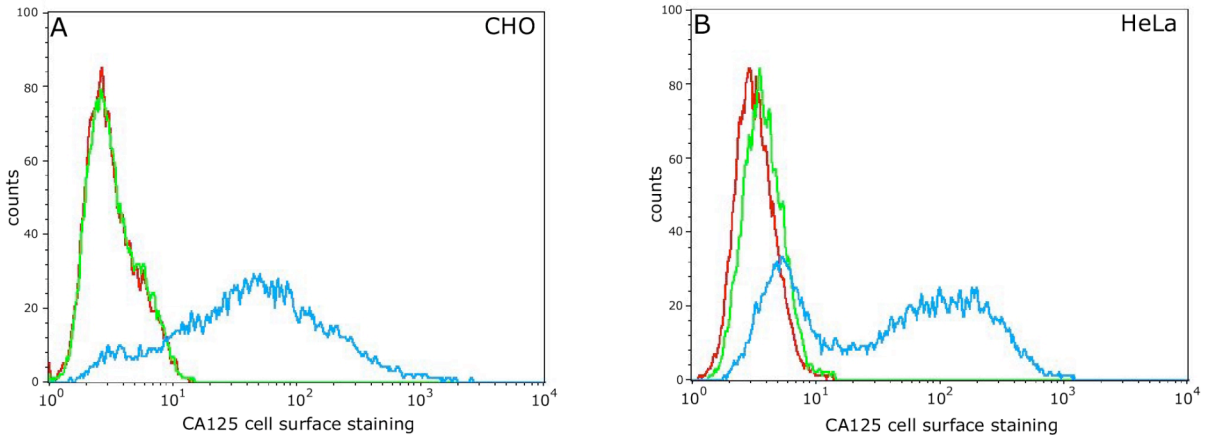

Fig. 14 CA125-C-TERM is transported to the cell surface of both CHO- and HeLa cells as determined by FACS. $CHO_{MCAT-TAM2}$ (panel A) and $HeLa_{MCAT-TAM2}$ (panel B) cells, respectively, were transduced with retroviral particles encoding CA125-C-TERM. Following 3 days of incubation at 37°C cells were dissociated from the culture plates using a protease-free buffer and processed with anti-CA125 antibodies (OC125). Primary antibodies were detected with anti-mouse antibodies coupled to Alexa488. CA125 cell surface localization was analyzed by FACS. Autofluorescence was determined with trypsin-treated cells (red curves). Non-transduced cells prepared in the absence of trypsin are indicated by green curves. CA125-C-TERM-transduced cells prepared in the absence of trypsin are indicated by blue curves.

Autofluorescence of CHO (Fig. 14 A) and HeLa (Fig. 14 B) was determined using trypsin-treated cells (red curves). Whereas CHO cells treated with retroviral control particles did not present endogenous CA125 on their cells surface. (Fig. 14 A, green curve), HeLa cells treated under identical conditions did contain small but significant amounts of endogenous CA125 on their surface (Fig. 14 B, green curve). After retroviral transduction of CA125-C-TERM, cell surface staining strongly increased for CHO and HeLa cells (Fig. 14 A, B; blue curves). The vast majority of

this signal disappeared when cells were treated with trypsin following flow cytometry analyses. Therefore, despite lacking a conventional signal peptide at the N-terminus, CA125-C-TERM is transported to the cell surface.

3.1.5 CA125-C-TERM is transported to the cell surface via the ER/Golgi-dependent secretory pathway

To analyze if CA125-C-TERM enters the classical secretory pathway or if it makes use of some kind of nonclassical mechanism of transport way the subcellular distribution in permeabilized and non-permeabilized CHO and HeLa cells was investigated employing confocal microscopy. In non-permeabilized cells (Fig. 15 A-D, CA125-C-TERM was detected on the cell surface of CHO and HeLa. CA125-C-TERM cell-surface staining was found not to be homogenous but rather appeared in subdomains with significant parts of the plasma membrane not stained at all.

Permeabilization of HeLa cells prior to anti-CA125 antibody treatment revealed that CA125-C-TERM expression results in its incorporation into membranes of the classical secretory pathway (Fig. 15 E-H), where it was colocalized with the Golgi marker p27 (Fullekrug et al., 1999; Jenne et al., 2002). This signal was specific, as it could not be observed when cells were treated with retroviral control particles (Fig. 15 E).

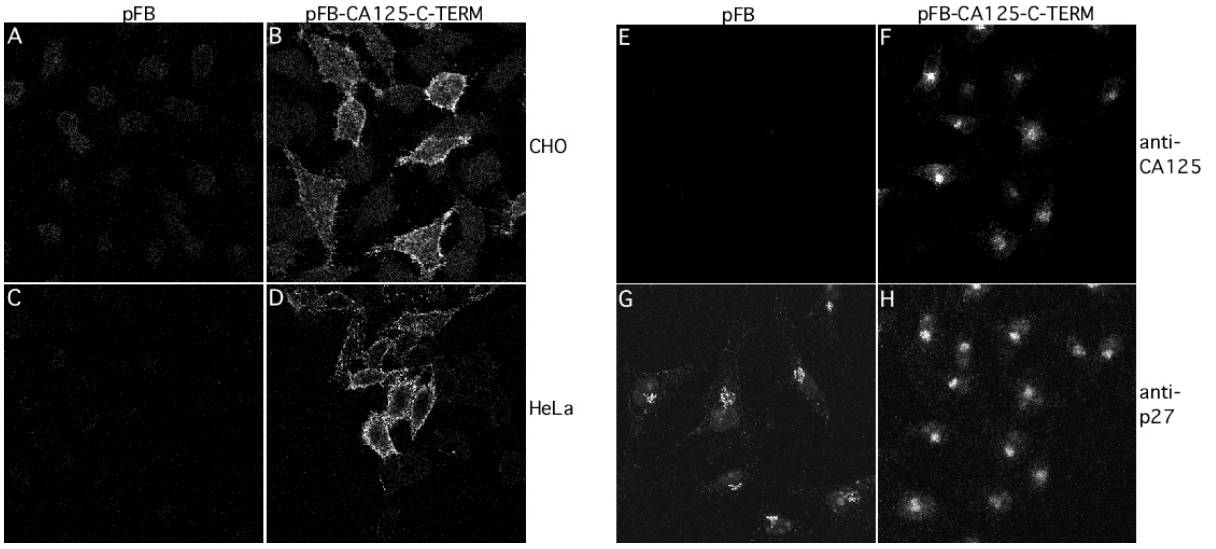

Fig. 15 CA125-C-TERM is transported to the cell surface of both CHO- and HeLa cells as determined by confocal microscopy. CHOMCAT-TAM2 and HeLaMCAT-TAM2 cells, respectively, were grown on glass cover slips followed by transduction with retroviral particles encoding CA125-C-TERM or with retroviral control particles that lack a cDNA insert in the viral genome. After 3 days of incubation at 37°C the cells were fixed with paraformaldehyde. Specimens shown in panels A-D represent CHOMCAT-TAM2 cells that were not permeabilized to visualize exclusively cell surface-localized CA125-C-TERM. Specimens shown in panels E-H represent TX-100-permeabilized HeLaMCAT-TAM2 cells in order to detect intracellular CA125-C-TERM. CA125-C-TERM was visualized with the monoclonal antibody OC125 (panels A, B, E-H). The Golgi marker p27 was detected with a polyclonal rabbit antiserum directed against a synthetic peptide that corresponds to the cytoplasmic tail of p27 (panels C and D) (Jenne et al., 2002). Double staining was performed using secondary antibodies coupled to Alexa488 and Alexa546, respectively. Specimens were analyzed with a Zeiss LSM510 confocal microscope.

Additionally, high-resolution confocal microscopy revealed CA125-C-TERM-positive staining of the nuclear envelope (Fig. 16 B, D), which is indicative for ER localization. This was confirmed by double labeling experiments using antibodies directed against the ER marker calreticulin (Fig. 16 A) (Sonnichsen et al., 1994). Whereas most of the calreticulin staining was found to be ER associated, only low amounts of CA125-C-TERM were found in the ER compared with the high amounts in the Golgi (Fig. 16, compare A and B). These results indicate that, after insertion into the ER membrane, CA125-C-TERM is efficiently transported in an anterograde direction from the ER to the Golgi. In order to investigate whether CA125-C-TERM-positive perinuclear structures represent endosomal compartments localized at the microtubal organizing center, CA125-C-TERM-expressing HeLa cells were treated with brefeldin A to disrupt the Golgi apparatus (Lippincott-Schwartz et al., 1989; Orci et al., 1991). As shown in Fig. 16 F, the compact perinuclear staining of CA125-C-TERM (Fig. 16 D) disappears after brefeldin A treatment. The resulting staining pattern matches brefeldin A-induced distribution of an established marker protein of the cis-Golgi, the KDEL receptor (Fig. 16 C, E) (Lewis and Pelham, 1990; Lewis and Pelham, 1992a; Lewis and Pelham, 1992b) (Fullekrug et al., 1997). These data established that CA125-C-TERM travels through the ER and the Golgi apparatus on its way to the cell surface.

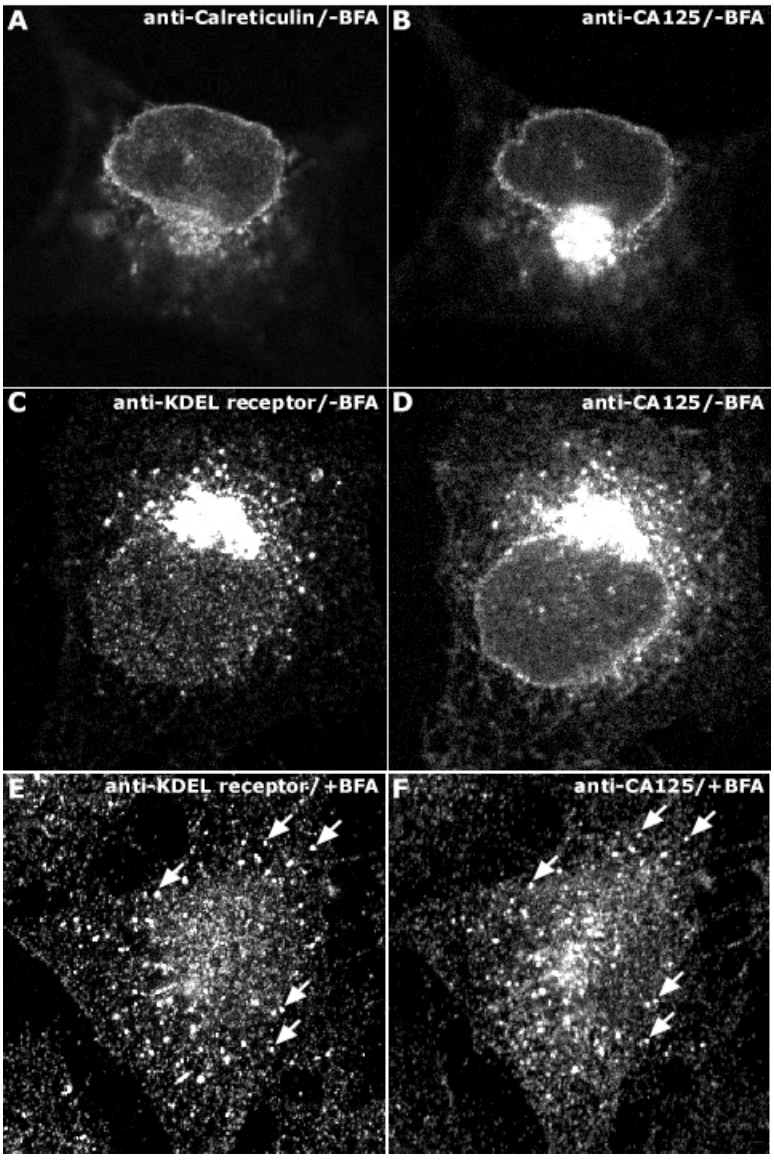

Fig. 16 Intracellular CA125-C-TERM is localized to organelles of the classical ER/Golgi-dependent secretory pathway. HeLa cells stably expressing CA125-C-TERM were grown on glass cover slips. At about 70% confluency cells were treated with brefeldin A (5 µg/ml) for 60 min or left untreated as a control. Following fixation with paraform aldehyde cells were treated with TX-100 to allow intracellular staining of antigens using antibodies directed against calreticulin, the KDEL receptor and CA125. Double staining was performed using secondary antibodies coupled to Alexa488 and Alexa546, respectively. Specimens were analyzed with a Zeiss LSM510 confocal microscope. A, anti-calreticulin, not treated with brefeldin A; B, anti-CA125, not treated with brefeldin A; C, anti-KDEL receptor, not treated with brefeldin A; D, anti-CA125, not treated with brefeldin A; E, anti-KDEL receptor, treated with brefeldin A; F, anti-CA125, treated with brefeldin A.

In order to functionally characterize the intracellular transport of CA125-C-TERM, an *in vivo* cell-surface expression experiment based on flow cytometry was performed in the presence and the absence of brefeldin A (Fig. 17). CA125-C-TERM-expressing HeLa cells were grown to about 70% confluency, followed by incubation for 90 minutes in the presence of brefeldin A. The cells were then trypsinized to remove pre-existing cell-surface CA125-C-TERM, spread onto new culture plates at the same cell density and were further incubated in the presence or absence of brefeldin A for 4 hours at 37°C, respectively. As a control, cells were applied to the same protocol without adding brefeldin A at any time point of the experiment. The amount of CA125-C-TERM transported to the cells surface within 4 hours in the absence of brefeldin A was set to 100% (Fig. 17 A, light green curve, Fig. 17 B, lane 2). Comparing the level of cell surface CA125-C-TERM under steady state conditions (Fig. 17 A, red curve; Fig. 17 B, lane 1), approximately 50% of the cell surface population recovers after trypsinization within 4 hours of incubation (Fig. 17 B, lane 2). When cells were treated with brefeldin A before trypsinization, followed by incubation for 4 hours in the absence of brefeldin A, the level of cell surface CA125-C-TERM was reduced by about 60% (Fig. 17 A, dark green curve, Fig. 17 B, lane 3). When cells were treated with brefeldin A at all time, cell surface transport of CA125-C-TERM was reduced up to 90% (Fig. 17 A, blue curve; Fig. 16 B, lane 4). These data combined with the confocal analysis of the subcellular distribution shown in Fig. 16 establish that CA125-C-TERM is transported to the cell surface via conventional secretory transport involving the ER and the Golgi apparatus.

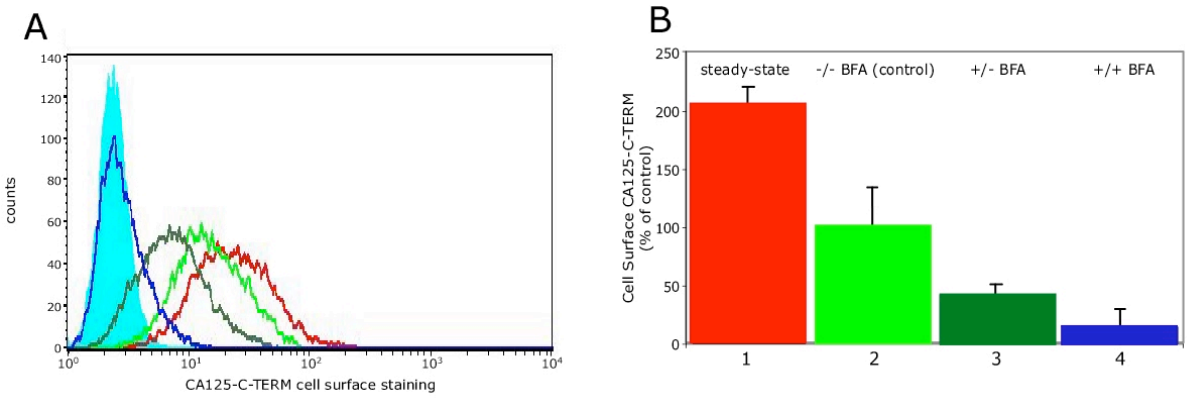

Fig. 17 CA125-C-TERM is transported to the cell surface via the classical ER/Golgi-dependent secretory pathway. HeLa cells stably expressing CA125-C-TERM were grown to 70% confluency. Where indicated brefeldin A was added to the medium at 5 µg/ml. Following incubation for 90 min at 37°C, cells were trypsinized to remove cell surface CA125-C-TERM and spreaded onto new culture plates at 70% confluency. The culture was then continued for 4 hours at 37°C in the presence or absence of brefeldin A as indicated. CA125-C-TERM transported to the cell surface within this time period was quantified by FACS employing the monoclonal antibody OC125. A, FACS histograms. Autofluorescence was determined by analyzing cells that were not treated with antibodies (light blue curve, filled). The red curve represents cells under steady-state-conditions. The light green curve represents cells that were not treated with brefeldin A. Cells that were grown for 90 min in the presence of brefeldin A followed by incubation for 4 hours in its absence are shown in dark green. Cells that were incubated with brefeldin A over the whole course of the experiment are shown in dark blue. B, Statistical analysis of 4 independent experiments. The colours of the bars correspond to the conditions detailed above.

3.1.6 Correlation of endogenous CA125 expression with increased cell surface expression of endogenous Gal-1 in CHO and HeLa cells

Our observation that CHO cells do not express detectable amounts of endogenous CA125 as opposed to HeLa cells (Fig. 14) is consistent with the fact that CHO cells are not derived from a tumor, whereas HeLa cells were isolated from cervix carcinoma (Gey et al., 1952). Therefore CA125-deficient CHO cells were compared with CA125-expressing HeLa cells for various parameters with regard to Gal-1.

Employing flow cytometry to analyze CHO and HeLa cells for the amount of cell surface expression of Gal-1, HeLa cells contain more than ten times as much Gal-1 on their surface compared with CHO cells (Fig. 18). For this purpose auto-fluorescence of CHO and HeLa cells was determined with trypsin treated cells and adjusted to the same value for both cell lines (Fig. 18 A, B; red curves). Using affinity-purified anti-Gal-1 antibodies, a relatively small but significant population of endogenous Gal-1 (A; green curve) could be detected on the surface of CHO cells when the cells were not treated with trypsin prior to the FACS analysis. This observation is consistent with various studies that demonstrate cells surface expression of endogenous Gal-1 (Cho and Cummings, 1995a; Cho and Cummings, 1995b; Lutomski et al., 1997). However, HeLa cells that express CA125 contain more than ten times the amount of endogenous Gal-1 on their cells surface (B; blue curve) compared with CA125-deficient CHO cells.

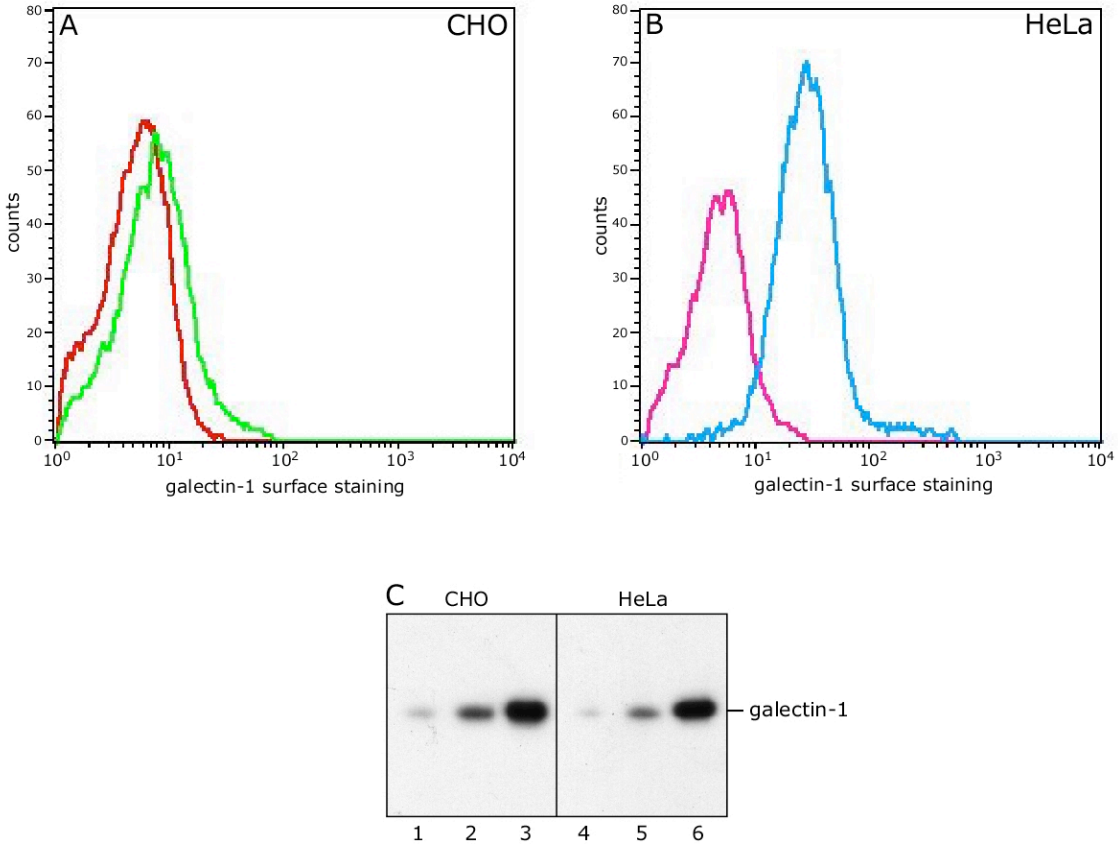

Fig. 18 Correlation of endogenous CA125 expression with cell surface expression of endogenous Gal-1 in CHO- and HeLa cells. CHO (panel A) and HeLa cells (panel B) were dissociated from culture plates employing a protease-free buffer. Native cells were labeled with affinity-purified anti-Gal-1 antibodies derived from a polyclonal rabbit antiserum. Cell surface staining was analyzed by FACS using anti-rabbit secondary antibodies coupled to allophycocyanine to detect primary antibodies. Autofluorescence levels (red curves in panel A and B) were determined with cells treated with trypsin prior to the FACS analysis. Gal-1 cell surface levels are indicated in green (CHO, panel A) and blue (HeLa, panel B), respectively. Total Gal-1 expression levels in CHO and HeLa cells, respectively, were analyzed by quantifying Gal-1 in total SDS cell lysates based on a western blot analysis (panel C). Lanes 1 and 4 represent the material of 20,000 cells, lanes 2 and 5 represent the material of 50,000 cells and lanes 3 and 6 represent the material of 150.000 cells. The results from CHO cells are shown in lanes 1 to 3, the results from HeLa cells are shown in lanes 4 to 6. Gal-1 was detected with an affinity-purified rabbit antiserum directed against recombinant full-length Gal-1.

We then investigate whether this effect is due to i) different total Gal-1 expression levels, ii) different cell surface binding capacities for Gal-1 or iii) different regulation of Gal-1 export in CHO and HeLa cells. As shown by Western blot analysis using affinity-purified anti-Gal-1 antibodies (Fig. 18 C), similar signals for Gal-1 were obtained from CHO and HeLa cells when the amount of SDS-lysed cells was titrated (20,000, 50,000 and 150,000 cells). Thus, CHO and HeLa cell do not differ to a significant extent in the total amount of Gal-1 expression.

Cell-surface binding capacity for Gal-1 was analyzed using FACS by titrating increasing amounts of a recombinant GST-Gal-1 fusion protein into cultures of CHO and HeLa cells, respectively. The total binding capacity for Gal-1 was found to exceed the amount of endogenous Gal-1 present on the cell surface of CHO and HeLa cells by a factor of more than 50-fold, with CHO cells being the cell type with an even higher Gal-1-binding capacity compare with HeLa cells. Therefore, the strikingly different amounts of endogenous cell-surface Gal-1 on CHO versus HeLa cells (Fig. 18 A, B) cannot be due to a lower Gal-1 binding capacity of CHO cells.

On the basis of these experiments one possible explanation of these results would be that CA125-expressing HeLa cells possess a more active Gal-1 export pathway than CA125-deficient CHO cells.

3.1.7 CA125 expression does not stimulate Gal-1 export

Nowadays, RNA interference has become as a common technique to study the functional consequence of reducing the expression of specific genes in mammalian cells (Tuschl, 2001; Tuschl and Borkhardt, 2002). RNAi is induced by transfecting cells with small interfering RNAs, comprising hairpin-forming 45-50mer RNA molecules (Caplen et al., 2001) that are complementary to the gene of interest resulting in mRNA degradation.

To further investigate the relation between Gal-1 export and binding to CA125 specific siRNAs directed against endogenous CA125 were generated to downregulate the expression of CA125 in adherent HeLa cells (termed HeLa RNAi CA125) (for sequence see material und method). A construct was generated in the retroviral expression vector pLNCD4 that upon transcription produces a siRNA directed against CA125 in HeLa cells (Brummelkamp et al., 2002; Sui et al., 2002). From this vector CD4 is constitutively expressed functioning as a cell surface marker. The vector pLNCD4 not containing an RNAi was introduced into HeLa cells as a control (termed HeLa RNAi CD4). A corresponding pool of CD4-positive HeLa cells was isolated by FACS sorting (3.2.1) using monoclonal anti-CD4 OC4 primary antibodies and APC-conjugated secondary antibodies.

The long-term goal of this RNAi approach was to analyze Gal-1 export from HeLa cells treated with RNAi against CA125 in comparison to HeLa cells expressing CA125 employing flow cytometry. To investigate downregulation of CA125 in transduced HeLa cells, recombinant GST-Gal-1 fusion protein was attached to glutathione-coupled sepharose beads. Detergent lysates of HeLa wild-type, HeLa RNAi CD4, HeLa RNAi CA125 and S-HeLa as a positive control for binding of CA125 to Gal-1 were generated and incubated with the GST-Gal-1-affinity matrix. Comparable amounts of proteins were incubated with the Gal-1 affinity matrix. Proteins bound to Gal-1 were eluted sequentially using lactose (Fig. 19, lane 1-4) and glutathione (Fig. 19, lane 5-8). Bound material was separated by SDS PAGE and

Western blot analysis using monoclonal anti-CA125 antibody and anti-mouse POD-conjugated secondary antibodies.

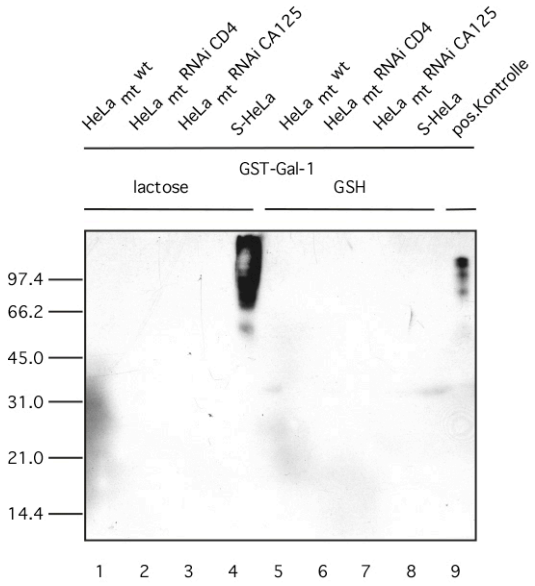

Fig. 19 Adherent HeLa cells do not express CA125 on their cell surface to a significant extent. Detergent lysates of HeLa cells (lane 1 and 5), HeLa transfected with a control RNAi (lane 2 and 6), HeLa cells stably transfected with RNAi directed against CA125 (lane 3 and 7) and S-HeLa (lane 4 and 8) were prepared and incubated with GST-Gal-1 beads (o/n, 4°C). Following extensive washing the beads were sequentially treated with lactose (lanes 1 to 4) and glutathione (lanes 5 to 8). Eluted proteins were separated on SDS-gels followed by transfer to a blotting membrane. CA125 was detected by OC125 staining (Zymed) employing ECL. As positive control CA125-derived fragments isolated in former experiments from S-HeLa cells were used (lane 9) (see 3.1).

The positive control for binding of CA125 to Gal-1 generated from S-HeLa cells showed the typical pattern for CA125 (Fig. 19, compare lane 4 and lane 9). CA125 bound to Gal-1 could not be detected in HeLa (Fig. 19, lane 1), HeLa RNAi CD4 (Fig. 19, lane 2) and HeLa RNAi CA125 (Fig. 19, lane 3) cells indicating that adherent HeLa cells do not express significant amounts of CA125 on their cell surface. As CA125 is not detectable in the control cell lines, these data suggest that the higher export efficiency observed for human Gal-1 in HeLa cells as shown in Fig. 18 is not related to CA125 expression.

3.2 Establishment of experimental systems to study unconventional secretion of Gal-1

Although galectins are secreted from cells, no galectin shows any evidence for a typical signal peptide, implying a non-classical export signal (Hirabayashi and Kasai, 1993; Hirabayashi et al., 1992; Marschal et al., 1992; Pfeifer et al., 1993). Non-classical secretion of Gal-1 has been first studied in skeletal muscle, where the protein moves from a diffuse intracellular to an extracellular location during *in vivo* development (Barondes et al., 1981; Cooper and Barondes, 1990; Harrison, 1991). In cultured myoblasts, Gal-1 remains in the cytosol until it is externalized during differentiation (Cooper and Barondes, 1990; Harrison and Wilson, 1992). There is also evidence for secretion of other galectins. A 14-kDa chicken galectin has been found in intestinal epithelial cells and directly shown to be secreted into the intestinal lumen (Beyer and Barondes, 1982). The reason why galectins are secreted by non-classical pathways is not known. One explanation is to segregate them from complementary glycoconjungate ligands that are externalized by the classical pathway to prevent interaction before externalization. Another possibility is that, in contrast to the unique classical secretion pathway, there may be multiple non-classical secretory mechanisms allowing selective secretion of different galectins in response to specific signals.

In order to investigate the mechanism of unconventional secretion in mammalian cells a novel assay was established that reconstitute secretion of unconventionally secreted protein such as Gal-1. By using stable cell lines and flow cytometry, Gal-1-GFP (termed Gal-1-GFP), GFP-Gal-1 (termed GFP-Gal-1) and GFP-CGL-2 can be determined on a quantitative basis. CGL-2 was identified as fungal galectin also unconventionally secreted by *Coprinopsis cinerea*. It is an orthologue to Gal-1 with 20% homologies. The homology to Gal-1 lies in the typical galectin fold of a CGL-2 monomer. The oligomeric state of this lectin is tetrameric and not dimeric like Gal-1. So far it was not known whether the mammalian export machinery recognizes this galectin as an export substrate (Walser et al., 2004; Walser et al., 2005).

3.2.1 Generation of cell lines

To generate CHO model cell lines expressing defined GFP fusion proteins in a doxicycline-dependent manner the following steps were performed. First, the murine orthologue of the cationic amino acid transporter MCAT-1 (Albritton et al., 1989; Davey et al., 1997) was stably transfected into $CHO_{wild\text{-}type}$ cells. Cell surface expression of MCAT-1 renders CHO cells permissive for retroviral transduction based on the ecotropic envelope protein of murine leukemia virus (Albritton et al., 1989; Davey et al., 1997). In a second step, $CHO_{MCAT\text{-}1}$ cells were transduced with an ecotropic retrovirus carrying a bicistronic construct encoding the doxicycline-sensitive transactivator rtTA2-M2 (Urlinger et al., 2000) and a truncated version of CD2 (Liu et al., 2000) that was used as a cell surface marker. A pool of CD2-positive cells was isolated by FACS sorting (from now on termed CHO_{mt}) and subjected to another round of retroviral transduction (Fig. 20).

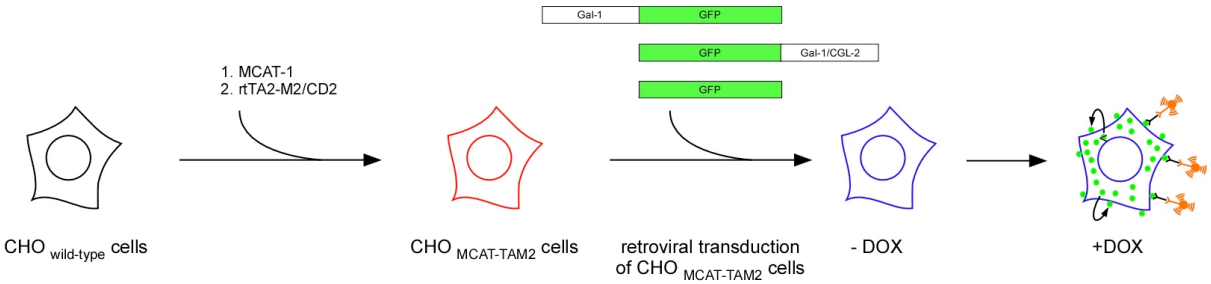

Fig. 20 Schematic overview: retroviral transduction to generate reporter cell lines

To analyze the export efficiency of human Gal-1 mutants stable CHO cell lines were generated. Due to the use of the viral vector pRevTRE2, a stable integration of the constructs into the genome of target cells (CHO_{mt}) was possible. Furthermore, a doxicycline/transactivator-responsive element in the vector pRevTRE2 allows doxicycline-dependent protein expression of Gal-1 and CGL-2 as GFP fusion proteins. A schematic overview of the GFP fusion proteins expressed in the corresponding CHO cell line is shown in Fig. 21. The calculated size of these GFP fusion proteins is about 40 kDa.

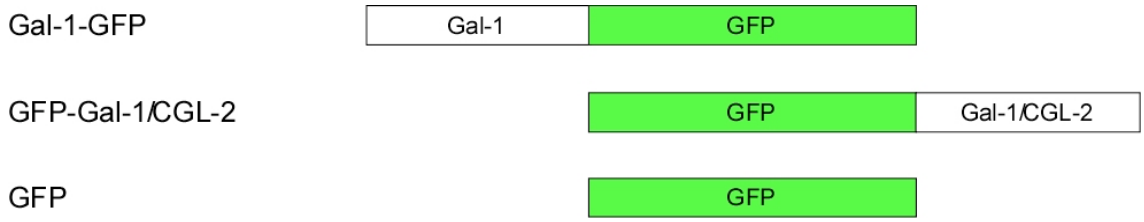

Fig. 21 Schematic overview: cDNA constructs

Retroviral particles carrying the reporter constructs (Fig. 21) were produced by HEK 293T cells and used for gene transfer. After viral transduction, reporter molecule expression was induced by adding doxicycline to the cell culture medium (standard condition: 1 µg/ml doxicycline, 48 h). The virally transduced cells were subjected to a FACS-based sorting procedure to generate clonal CHO_{mt} cell lines. Three days after retroviral transduction doxicycline was added to the cell culture medium for 24 h. Following this incubation period cells were detached from cell culture dishes using a protease-free buffer system and processed for FACS analysis. Dead cells were identified by staining with propidium iodide that intercalates into DNA of damaged and dead cells. 50,000 cells from each cell line were isolated by FACS sorting based on GFP fluorescence using a FACSVantage sorting device (Becton Dickinson, Heidelberg).

The obtained pools of cells were incubated for 7 days in the absence of doxicycline followed by the isolation of 50,000 cells from each population that did not display any GFP fluorescence.

Each of these cell pools was cultured for another period of 7 days including 24 h in the presence of doxicycline (1 µg/ml) at the end of the incubation. 50,000 cells were obtained by FACS sorting based on GFP fluorescence. Exemplarily, the results of the sorting procedure for all generated mutant cell lines of human Gal-1 are displayed for the cell line Gal-1-GFP, GFP-Gal-1, GFP-CGL-2 and GFP in Fig. 22 (panel A, Gal-1-GFP; panel B, GFP-Gal-1; panel C, GFP-CGL-2, panel D, GFP).

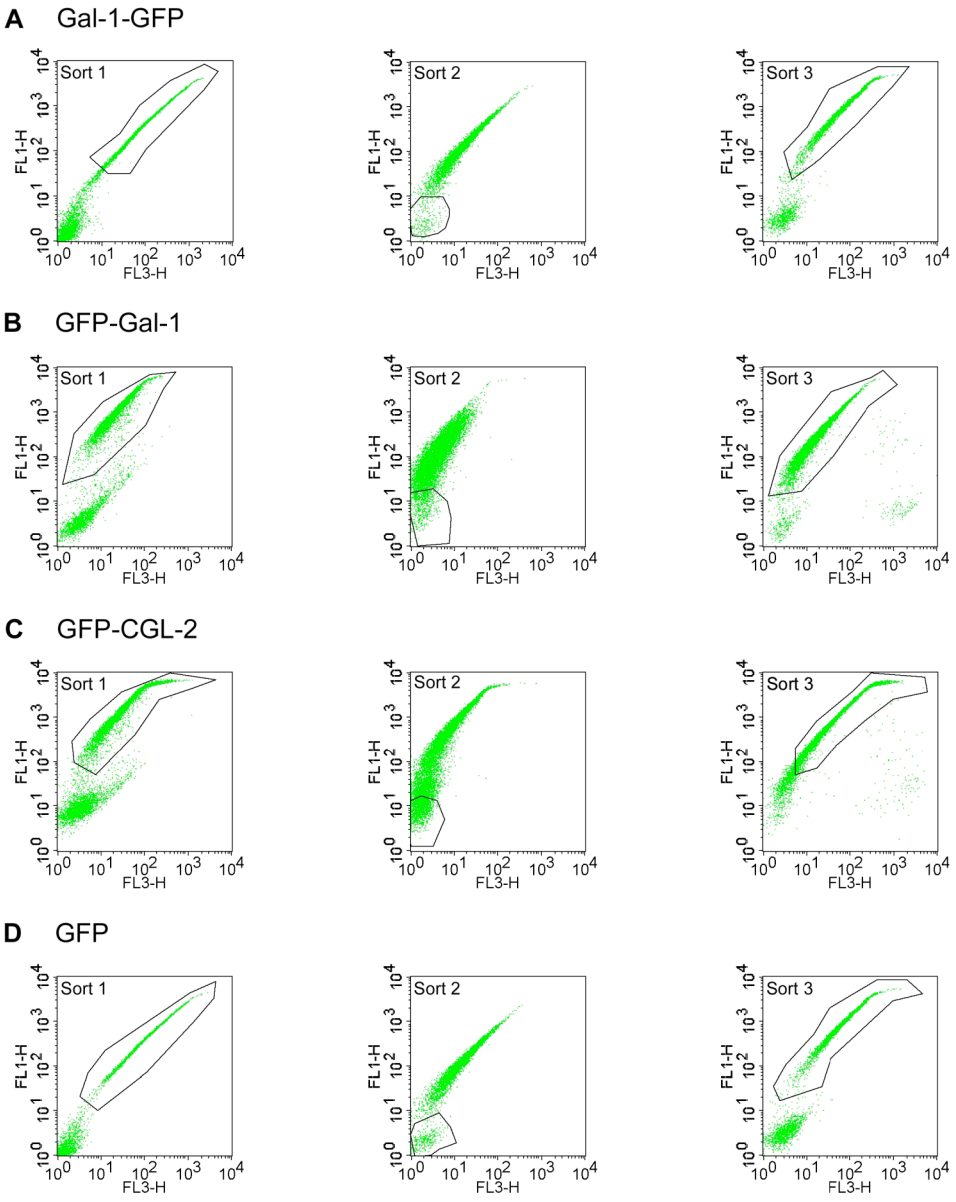

Fig. 22 FACS sorting based on GFP fluorescence to isolate reporter cell lines. Cells were detached from cell culture dishes using a protease-free buffer system and processed for FACS analysis to measure GFP fluorescence. Sort 1 displays cells 3 days after viral transduction incubated in the presence of 1 µg/ml doxicycline for 24 h. FL1-H represents the green channel measuring GFP fluorescence, FL3-H shows the red channel displaying propidium iodide staining (dead cells). 50,000 cells were sorted within the sorting window. Sort 2 shows cells grown for 7 days in the absence of doxicycline after sort 1. Again, 50,000 cells were sorted within the sorting window. Sort 3 shows cells 7 days after sort 2 incubated in the presence of 1µg/ml doxicycline for 24 h. In panel A the sorting procedure for Gal-1-GFP is shown, in panel B for GFP-Gal-1, in panel C for GFP-CGL-2 and in panel D for GFP.

3.2.2 Quantitative analysis of export of reporter constructs as analyzed by flow cytometry

The clonal CHO cell lines described above (see 3.2.1) were cultivated in the presence of doxicycline (1 µg/ml, 48 h) and prepared for FACS analysis using the plate labeling procedure described in material and methods. To detect the reporter molecules on the cell surface, exported material was labeled using affinity-purified anti-GFP primary antibodies and allophycocyanin-coupled secondary antibodies. Analysis was performed using a BD FACSCalibur system.

All cell lines expressed the corresponding GFP reporter construct in a doxicycline-dependent manner as shown by an increase of GFP fluorescence compared to CHO cells not transduced with the reporter construct (Fig. 23; GFP expression level, panel A, B, C, D, E,).

Concerning cell surface staining all galectin constructs showed a significant signal (Fig. 23; cell surface; panel B, C, D). However, the signal for the GFP-Gal-1 construct was lowered (Fig. 23, panel C) compared to the cell surface staining observed for Gal-1-GFP (Fig. 23, panel B).

The secretion of GFP-CGL-2 was analyzed in order to investigate whether the fungal galectin orthologue CGL-2 is a substrate for the Gal-1 export pathway in mammalian cells, although homologies between Gal-1 and CGL-2 are weak at the level of both the primary and the quaternary structure. Strikingly, GFP-CGL-2 fusion protein (Fig. 23, cell surface, panel D) was found to be exported with a similar efficiency as compared to Gal-1-GFP (Fig. 23, panel D).

As expected, probing for cell surface staining showed no signals for the control cell line CHO_{GFP} (Fig. 23, cell surface, panel E).

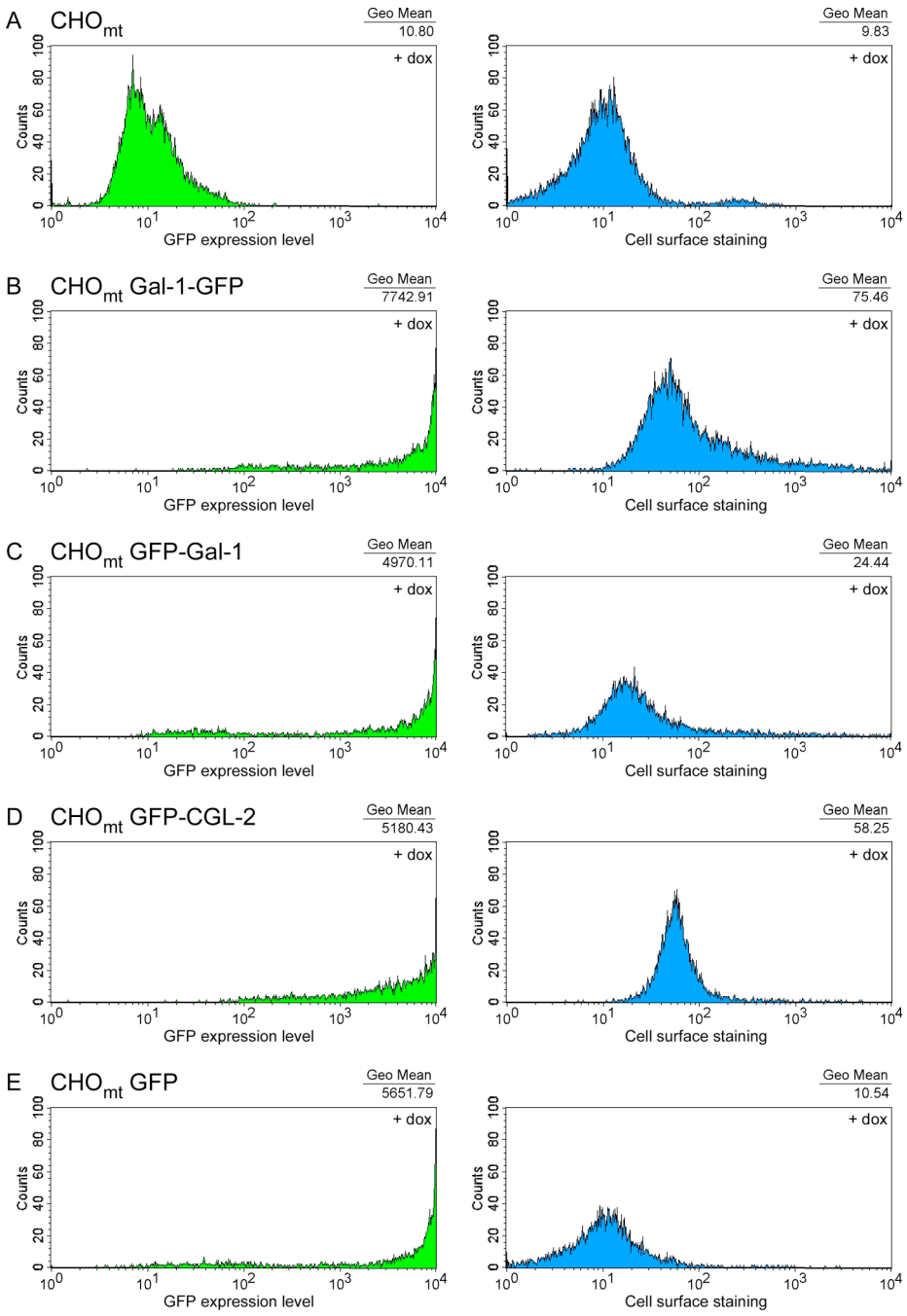

Fig. 23 Galectins are transported to the cell surface of CHO cells as determined by FACS. Following incubation with doxicycline (1 µg/ml) for 48 h, CHO cells expressed the corresponding fusion protein (Gal-1-GFP (panel B), GFP-Gal-1 (panel C), GFP-CGL-2 (panel D) and GFP (panel E). Cells were processed with affinity-purified anti-GFP antibodies. Primary antibodies were detected with APC-conjugated secondary antibodies. Cells were dissociated from cell culture plates using a protease-free buffer. GFP fusion protein localization was analyzed by FACS. Autofluorescence was determined employing CHO cells (panel A).

As shown in Fig. 23, employing flow cytometry, it was possible to quantitatively access unconventional secretion of Gal-1-GF, GFP-Gal-1 and GFP-CGL-2 fusion proteins *in vivo*.

3.2.3 Export of reporter constructs as analyzed by a cell surface biotinylation assay

To confirm the cell surface localization of the reporter molecules using an independent method, a biotinylation assay was used (Stegmayer et al., 2005). Therefore the CHO Gal-1-GFP, GFP-Gal-1, GFP-CGL-2 and GFP were cultivated in the presence of doxicycline for 48 h. Additionally, the cell culture medium of the cells was subjected to immunoprecipitation using affinity-purified anti-GFP antibodies coupled to protein A sepharose beads (Amershan). The cell surface biotinylation assay was combined with immunoprecipitation of the cell culture medium in order to detect galectin GFP fusion proteins bound to the cell surface as well as non-bound material present in the medium of cells.

The cells were incubated with a membrane-impermeable biotinylation reagent (EZ-link sulfo-NHS-SS-biotin, Pierce). The biotinylation reagent binds covalently to cell surface proteins via the ε-amino group of all accessible lysine residues. After detergent mediated cell lysis biotinylated and non-biotinylated proteins were separated using streptavidin-coupled beads. The biotinylated fraction (Fig. 24, lane 1), the non-biotinylated fraction (Fig. 24, lane 2), representing exported and not exported material, respectively, and the medium fraction (Fig. 24, lane 3) were analyzed by SDS-PAGE and Western blot analysis using affinity-purified anti-GFP antibodies and monoclonal anti-rabbit clone RG16 secondary antibodies.

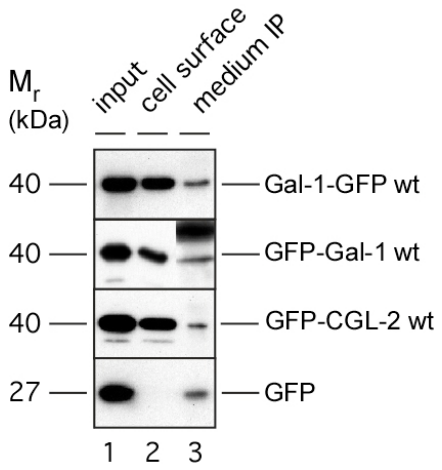

Fig. 24 Biochemical analysis of export of various galectin-GFP fusion proteins from CHO cells employing cell surface biotinylation and immunoprecipitation from cell culture supernatants. The fusion proteins indicated were expressed in CHO cells for 48 h at 37°C (6-well plates; 70% confluency; 1 µg/ml doxicycline) The medium was removed and subjected to immunoprecipitation using affinity-purified anti-GFP antibodies. Cells were treated with a membrane-impermeable biotinylation reagent. Following detergent-mediated cell lysis biotinylated and non-biotinylated proteins were separated employing streptavidin beads. Aliquots from the input material (lane 1; 1%), the biotinylated fraction (lane 2; 10%) and the immunoprecipitate from the cell culture medium fraction (lane 3; 50%) were analyzed by SDS PAGE and Western blotting using affinity-purified anti-GFP antibodies.

As shown in Fig. 24 all four reporter constructs were expressed at similar levels (Fig. 24, lane 1; 1%). The CHO cell lines expressing Gal-1-GFP, GFP-Gal-1 and GFP-CGL-2 secrete the corresponding reporter constructs efficiently as shown by the signals for biotinylated proteins in the eluate fractions and for non-bound proteins precipitated from the cell culture medium. Most of the extracellular Gal-1-GFP, GFP-Gal-1 and GFP-CGL-2 population was found to be associated with the cell surface of CHO cells (Fig. 24, lane 2, 10%) with only a minor portion being found in the medium (Fig. 24; lane 3, 50%). As expected and consistent with the flow cytometry data (Fig. 23, GFP, cell surface staining) GFP could not be detected on the cell surface (Fig. 24, lane 2). A small amount of GFP is detectable in the cell culture medium employing immunoprecipitation of the medium. This signal is likely to be derived from damaged cells.

The data obtained from the cell surface biotinylation assay are consistent with the observations made in the flow cytometry analysis (Fig. 23). Both assays are functional as exported protein is detectable on the cell surface.

3.2.4 Quantitative analysis of Galectin binding to cell surfaces using flow cytometry

Galectins are β-galactoside-specific lectins being associated with components of the extracellular matrix and counter receptors on the cell surface of mammalian cells (Barondes, 1984). One aim of this work was to identify the targeting motif mediating unconventional secretion of Gal-1. Therefore single amino acids were mutated. These mutations may influence the ability of Gal-1 to bind to natural ligands. In order to probe the binding ability of Gal-1 wild-type and mutant forms an *in vivo* binding assay was established.

Gal-1-GFP, GFP-Gal-1, GFP-CGL-2 and GFP proteins were expressed in CHO cells by incubating the corresponding cell lines in the presence of doxicycline (1 µg/ml) for 48 h at 37°C. Cell-free supernatants were prepared by homogenization combining freeze-thaw cycles with sonication. Membranes were removed in two steps by centrifugations at 13,000 g_{av} (10 min at 4°C) and 100,000 g_{av} (1 h at 4°C). The resulting supernatants were analyzed for the amounts of fusion protein based on GFP fluorescence as measured with a fluorescence plate reader (Molecular Devices SpectraMax Gemini XS). Normalized amounts of cell-free supernatants (150 GFP units corresponding to about 1.5 µg GFP) were incubated with CHO cells not expressing the various GFP fusion proteins for 1 h at 4°C to allow cell surface binding. Following treatment with affinity-purified anti-GFP antibodies and APC-conjugated secondary antibodies, cell surface binding was quantified by flow cytometry (Engling et al., 2002; Seelenmeyer et al., 2003).

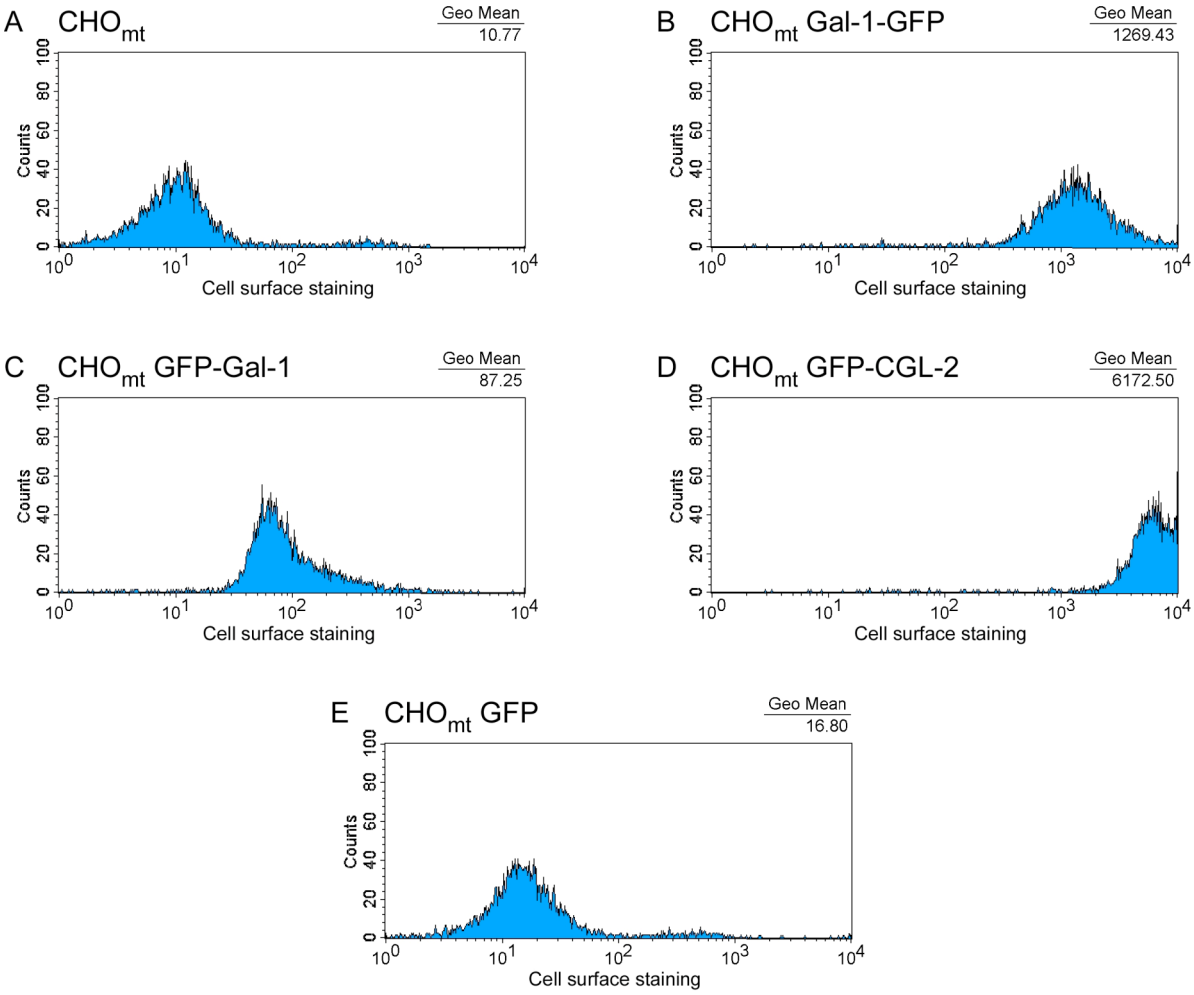

Fig. 25 Analysis of β-galactoside binding efficiency of various galectin-GFP fusion proteins based on binding to CHO cells. The various fusion proteins indicated were expressed in CHO cells. Cell-free supernatants were prepared and normalized by GFP fluorescence. The various supernatants were then incubated with CHO cells for 1 h at 4°C to allow cell surface binding. Following treatment with affinity-purified anti-GFP antibodies and APC-conjugated secondary antibodies, cell surface binding was quantified by flow cytometry.

The reporter molecules Gal-1-GFP and GFP-CGL-2 showed a strong cell surface signal demonstrating a highly efficient binding to CHO cells (Fig. 25, panel B and panel D). GFP-CGL-2 even bound with a higher efficiency to the outer leaflet of CHO cells than Gal-1-GFP, whereas GFP-Gal-1 exhibited a strongly reduced but significant cell surface signal (Fig. 25, compare panel A, B and C). As expected the signal observed for GFP was only slightly over background indicating that no cell surface binding occurred (Fig. 25, compare panel A and panel E).

Employing this experimental approach it is possible to determine the binding efficiencies of different galectin reporter constructs to β-galactoside-containg receptors *in vivo*.

3.2.5 Biochemical analysis of Galectin binding to counter receptors using lactose-coupled beads

To further analyze the β-galactoside binding ability of the reporter molecules with an independent biochemical method, an *in vitro* binding assay was established. Galectin GFP fusion proteins were expressed in CHO cells by incubation in the presence of doxicycline (1 µg/ml) for 48 h at 37°C. Following detachment of cells from the cell culture dishes using PBS/EDTA, cells were sedimented and lysed using PBS/TX-100. Insoluble material was removed by sequential centrifugation at 13,000 g_{av} (10 min at 4°C) and at 100,000 g_{av} (1 h at 4°C). The resulting supernatant was analyzed for the amounts of fusion proteins based on GFP fluorescence as measured with a fluorescence plate reader (Molecular Device SpectraMax Gemini XS). Normalized amounts of detergent lysates (50 GFP units corresponding to about 0.5 µg GFP) were then incubated with lactose-coupled beads (Sigma) for 1 h at 4°C. Following extensive washing in TX100-containing buffer bound material was eluted using SDS sample buffer. Input and flow-through fractions as well as the SDS eluates were analyzed by SDS PAGE and Western blotting using affinity-purified anti-GFP antibodies and POD-conjugated secondary antibodies.

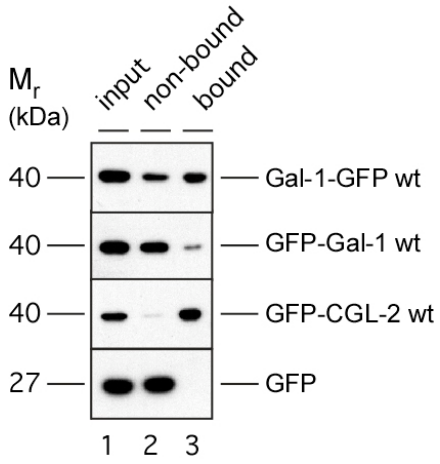

Fig. 26 Analysis of β-galactoside binding efficiency of various galectins expressed as GFP fusion proteins based on binding to lactose-coupled beads. Detergent lysates normalized by GFP fluorescence were incubated with lactose beads for 1 h at 4°C. The non-bound fraction was separated and, following extensive washing, bound material was eluted with SDS sample buffer. Input (lane 1, 5%), non-bound material (lane 2; 5%) and bound material (lane 3; 5%) were analyzed by SDS PAGE and Western blotting using affinity-purified anti-GFP antibodies.

When analyzing the binding efficiency of the fusion proteins Gal-1-GFP, GFP-Gal-1, GFP-CGL-2 and GFP in the *in vitro* binding assay, the data were consistent with the observations made in the *in vivo* analysis. Western blot analysis revealed that comparable amounts of all four reporter constructs were used for incubation with lactose-coupled beads (Fig. 26, lane 1, 5%). The reporter molecule Gal-1-GFP bound to the lactose affinity matrix indicated by a distinct band (Fig. 26, Gal-1-GFP, lane 3, 5%). Consistently with the observation made in the *in vivo* binding assay, binding efficiency of GFP-Gal-1 was reduced about 4-fold (Fig. 26, GFP-Gal-1, lane 3, 5%). The fungal galectin GFP-CGL-2 bound with a higher efficiency to the lactose affinity matrix since there was no detectable protein in the flow-through fraction and the intensity of the eluate was comparable with the signal obtained for Gal-1-GFP as the input signal is decreased. As expected GFP as a negative control for binding to lactose-coupled beads showed no signal in the bound fraction (Fig. 26; GFP, lane 3).

Taken together, both the *in vivo* and the *in vitro* binding assay are robust methods to investigate binding efficiencies of galectin fusion proteins to β-galactosides.

3.3 Mutational analysis of the export-targeting motif in human Gal-1

The canonical carbohydrate recognition domain (CRD) of galectins consists of approximately 130 amino acids, although only a small number of these residues directly contact carbohydrate ligands. A comparison of the sequences of approximately 30 galectins from many different organisms reveals that eight residues, which have been shown to be involved in the carbohydrate binding by X-ray crystallographic analysis, are invariant (in Gal-1: His 45, Asn 47, Arg 49, Val 60, Asn 62, Trp 69, Glu 72 and Arg 74 (Barondes et al., 1994). Although all galectins share a high degree of homology in their CRDs, two general subgroups of galectins can be distinguished, based on sequence homologies: the Gal-1 subfamily, which includes Gal-1 and -2, and the Gal-3 subfamily, which includes all others. Human Gal-1 and the fungal galectin CGL-2 from *Coprinopsis cinerea* show an overall identity about 20%.

3.3.1 Random mutagenesis of Gal-1

In order to investigate the export-targeting motif of Gal-1 a random mutagenesis of the human Gal-1 ORF employing low fidelity PCR was performed. As PCR template human Gal-1 ligated into the vector pGEM-T was used. The random mutations were generated using a concentration of 100 µM $MnCl_2$ in the PCR reaction mix. Under these conditions, during temperature cycling by *AmpliTaq* DNA polymerase, which has no proofreading activity like *PfuTurbo* polymerase, 8-12 mutations per 400 basepairs were inserted into the Gal-1 ORF (408 bp). Following digestion with BamHI and AgeI, the various mutated Gal-1 inserts were cloned into

the retroviral vector pRevTRE2/GFP. Employing this method 100 single retroviral DNA plasmids were generated having multiple distinct mutations. Following retroviral transduction of CHO cells (3.2.1), the export behavior of these Gal-1 mutants was analyzed by flow cytometry (3.2.2). Additionally, the β-galactoside binding ability of Gal-1 mutants was determined using the *in vivo* (3.2.4) and *in vitro* binding assay (3.2.5). Based on these experiments 14 export-deficient Gal-1 mutants were identified. The sequences of the corresponding DNA plasmids were determined and based on the observed mutations human Gal-1 was mutated by site-directed mutagenesis resulting in Gal-1-GFP mutants carrying individual mutations (3.3.2). In Table 3 the mutations identified in the random mutagenesis are shown.

Plasmid number (internal nomenclature)	Mutation
11	C3Y, N34S, D55G, N57Y, D135A
17	H45R, F51S, N57H, D103V
19	F46L, F80L, E87V, M121V
22	V60M, A95P, I118V, D126G
27	H53P, F92L, K118Q
64	N9F, H45N, E116D, K130T, D135Y
71	A52T, S84R, I90F
72	N34D, E75G, E106G
80	C3G, F109L, Y120C
82	N41I, G66S, M121L
86	E16K, N40D, Q84L, CV131W
89	A7T, V60M, A122S
92	N9G, C61S, F127I
97	E16K

Table 3 Mutated amino acids resulting in an export defect identified in the random mutagenesis screen employing low fidelity PCR

3.3.2 Site-directed mutagenesis

Site-directed mutagenesis was used to introduce point mutations, to switch amino acids and to delete multiple amino acids. The site-directed mutagenesis method was performed using *PfuTurbo* DNA polymerase, which has a 6-fold higher

fidelity in DNA synthesis than *Taq* DNA polymerase (Cline et al., 1996). The basic procedure utilizes a double-stranded DNA vector (pGEM-T) with the insert of interest (human Gal-1 and fungal CGL-2) and two synthetic oligonucleotide primers containing the desired mutation (see material and methods). The oligonucleotide primers, each complementary to opposite strands of the vector, were extented during temperature cycling by *PfuTurbo* DNA polymerase. Incorporation of the oligo-nucleotide primers generated mutated plasmids containing staggered nicks. Following temperature cycling, the product was treated with the endonuclease *DpnI*. *DpnI* is specific for methylated DNA and was used to digest the parental DNA template to select for newly synthesized DNA containing the desired mutation. This is possible since DNA isolated from almost all *E. coli* strands is methylated and therefore susceptible to *DpnI* digestion. The nicked vector DNA containing the desired mutation in Gal-1 was introduced into DH5α (Invitrogen) competent cells or XL-1 blue (2.2.1). Following digestion of isolated DNA with BamHI and AgeI the various mutated inserts were ligated into the retroviral vector pRevTRE2/GFP.

3.3.3 Characterization of Gal-1 mutants regarding export and binding to β-galactosides

In order to elucidate the export targeting motif 97 individual CHO cell lines expressing single mutants of Gal-1, 10 truncated versions of human Gal-1 and 3 truncated forms of CGL-2 were generated by stable integration of the corresponding DNA constructs using retroviral transduction (3.2.1) (Table 4). As control cell lines $CHO_{Gal\text{-}1\text{-}GFP}$, $CHO_{GFP\text{-}Gal\text{-}1}$, $CHO_{GFP\text{-}CGL\text{-}2}$ and CHO_{GFP} were used. The individual mutants were selected in three different ways: i) targeted mutagenesis based on the results obtained from the random mutagenesis approach ii) targeted mutagenesis of surface residues based on the crystal structure of Gal-1 iii) targeted mutagenesis of residues conserved between human Gal-1 and CGL-2 from *Coprinopsis cinerea* (3.3.2)

In Table 4 the individual Gal-1 mutants expressed in CHO cells as GFP fusion proteins in a doxicycline-dependent manner are listed. In addition to single amino acid mutations, N- and C-terminally truncated versions of human Gal-1 expressed as GFP fusion proteins were generated (Table 5).

Mutation (Gal-1-GFP)	Selection procedure
Gal-1-GFP	
C3A	Random mutagenesis
V6A	Conserved between Gal-1 and CGL-2
A7I	Random mutagenesis
N9A	Random mutagenesis
K13A	Conserved between Gal-1 and CGL-2
P14A	Conserved between Gal-1 and CGL-2
E16A	Random mutagenesis
V20A	Random mutagenesis
R21A	Conserved between Gal-1 and CGL-2
V32A	Conserved between Gal-1 and CGL-2
V32G	Conserved between Gal-1 and CGL-2
V32E	Conserved between Gal-1 and CGL-2
V32S	Conserved between Gal-1 and CGL-2
V32W	Conserved between Gal-1 and CGL-2
N34A	Random mutagenesis / conserved between Gal-1 and CGL-2
L35A	Random mutagenesis
K37E	Surface exposure
D38E	Surface exposure
D38K	Surface exposure
N40A	Random mutagenesis
N41A	Random mutagenesis / conserved between Gal-1 and CGL-2
L44A	Conserved between Gal-1 and CGL-2
L44D	Conserved between Gal-1 and CGL-2
L44F	Conserved between Gal-1 and CGL-2
L44S	Conserved between Gal-1 and CGL-2
H45A	Random mutagenesis / conserved between Gal-1 and CGL-2; Scott and Zhang, 2002
F46A	Random mutagenesis
R49A	Conserved between Gal-1 and CGL-2; Scott and Zhang, 2002; Ford et al., 2003
N51A	Random mutagenesis /
A52I	Random mutagenesis
H53A	Surface exposure / random mutagenesis / conserved between Gal-1 and CGL-2; López-Lucendo et al., 2004

H53E	Surface exposure / random mutagenesis / conserved between Gal-1 and CGL-2; López-Lucendo et al., 2004
H53G	Surface exposure / random mutagenesis / conserved between Gal-1 and CGL-2; López-Lucendo et al., 2004
G54A	Random mutagenesis and conserved between Gal-1 and CGL-2
D55A	Random mutagenesis
N57A	Random mutagenesis
V60A	Random mutagenesis
C61A	Random mutagenesis
D65A	Surface exposure
D65K	Surface exposure
G66A	Random mutagenesis
G67A	Conserved between Gal-1 and CGL-2
A68I	Conserved between Gal-1 and CGL-2
W69G	Conserved between Gal-1 and CGL-2; Hirabayashi et al., 1991
G70A	Conserved between Gal-1 and CGL-2
E72A	Conserved between Gal-1 and CGL-2; Hirabayashi et al., 1991
R74A	Conserved between Gal-1 and CGL-2
E75A	Random mutagenesis
F80A	Random mutagenesis and conserved between Gal-1 and CGL-2
F80K	Random mutagenesis and conserved between Gal-1 and CGL-2
F80S	Random mutagenesis and conserved between Gal-1 and CGL-2
P82A	Conserved between Gal-1 and CGL-2
S84A	Random mutagenesis
E87A	Random mutagenesis
I90A	Random mutagenesis and conserved between Gal-1 and CGL-2
F92A	Random mutagenesis
A95I	Random mutagenesis
D103A	Random mutagenesis
G104A	Conserved between Gal-1 and CGL-2
E106A	Random mutagenesis
F109A	Random mutagenesis
R112A	Conserved between Gal-1 and CGL-2;
R112H	Conserved between Gal-1 and CGL-2; lopez-Lucendo 2004
N114A	Conserved between Gal-1 and CGL-2
E116A	Random mutagenesis
A117I	Conserved between Gal-1 and CGL-2
I118A	Random mutagenesis and conserved between Gal-1 and CGL-2
N119E	Surface exposure
N119K	Surface exposure
N119W	Surface exposure
Y120A	Random mutagenesis and conserved between Gal-1 and CGL-2

Y120D	Random mutagenesis and conserved between Gal-1 and CGL-2
M121A	Random mutagenesis
A122I	Random mutagenesis and conserved between Gal-1 and CGL-2
D126A	Random mutagenesis
F127A	Random mutagenesis and conserved between Gal-1 and CGL-2
F127D	Random mutagenesis and conserved between Gal-1 and CGL-2
I129R	Surface exposure
K130A	Random mutagenesis
V132A	Surface exposure
V132E	Surface exposure
V132R	Surface exposure
F134E	Surface exposure
F134R	Surface exposure
GFP-CGL-2	
W72G	Conserved between Gal-1 and CGL-2

Table 4 Single amino acids changes in human Gal-1 and fungal CGL-2 based on the procedure and/or references shown in the right column.

Truncations
Gal-1-GFP
Gal-1-GFP ΔN5
Gal-1-GFP ΔN10
Gal-1-GFP ΔN20
Gal-1-GFP ΔN10-C129
GFP-Gal-1
GFP-Gal-1 ΔC4
GFP-Gal-1 ΔC9
GFP-Gal-1 ΔC20
GFP-Gal-1 ΔC30
GFP-Gal-1 ΔC40
GFP-Gal-1 ΔC50
GFP-CGL-2
GFP-CGL-2 ΔC11
GFP-CGL-2 ΔC111/S134E
GFP-CGL-2 ΔC16

Table 5 Truncated forms of human Gal-1 and fungal CGL-2

Using CHO cells expressing either the wild-type form of Gal-1, or the wild-type form of CGL-2 as positive controls as well as GFP as a negative control, the generated Gal-1 mutant cell lines were analyzed regarding export efficiency employing the FACS-based secretion assay and the biotinylation assay. Moreover, all mutant Gal-1 proteins were analyzed for their capability to interact with counter receptors based on binding to both CHO cells (Fig. 29; Fig. 33; Fig. 41) and lactose-coupled to beads (Fig. 30; Fig. 34; Fig. 42). These studies allowed to investigate whether a reduced surface signal of individual mutants results from a reduced binding efficiency to β-galactoside-containing glycolipids and glycoproteins on the cell surface. Based on these assays it was possible to identify 26 mutants, which showed the same phenotype as wild-type Gal-1 regarding export and binding ability (Table 6). 43 mutants were identified as being deficient in binding to β-galactoside-containing counter receptors by both the *in vivo* and the *in vitro* assay (Table 7). Some of these have been reported previously to be impaired in terms of binding to β-galactosides. 15 mutant forms of Gal-1 were characterized by controversial results regarding export and binding to their counter receptors (3.3.3.3) (Hirabayashi and Kasai, 1991). The phenotypes of truncated forms of Gal-1 are shown separately (3.3.3.4).

3.3.3.1 Gal-1 mutants without phenotype regarding export and binding to β-galactosides

To study the export of Gal-1 mutants the wild-type and the mutant forms of Gal-1 were expressed in a doxicycline-dependent manner and three independent experiments employing flow cytometry were performed. In order to be able to compare cell surface signals obtained from mutant cell lines expressing the reporter molecules at different levels, the expression of the wild-type form of Gal-1 was induced at different concentrations of doxicycline (1 µg/ml (1:1,000); 0.2 µg/ml (1:5,000); 0.1 µg/ml (1:10,000); 0.02 µg/ml (1:50,000); 0.01 µg/ml (1:100,000) doxicycline). The expression level and the cell surface staining of wild-type Gal-1-GFP under standard conditions (1 µg/ml doxicycline, 48 h, 37°C) were set to 100%. GFP-CGL-2 was used

as an additional positive control for unconventional secretion of galectins in CHO cells.

As shown in Fig. 27 (blue bar) the expression levels of the GFP fusion proteins varied for the various Gal-1 mutants. The single amino acid changes K13A, P14A, V32A, V32S, K37E, N40A, D65A, D65K, S84A and N118E of Gal-1-GFP showed approximately the same expression level under standard conditions (1 µg/ml doxicycline; 48 h, 37°C) as compared to the wild-type form of Gal-1-GFP. The mutations C3A, A7I, E16A, R21A, A52I, G66A, E75A, P82A, D103A, G104A, E106A, N114A, E116A, A117I, I118A and M121A in Gal-1-GFP resulted in a lower expression level indicated by decreased GFP fluorescence under standard conditions (1 µg/ml doxicycline, 48 h, 37°C). GFP used as a negative control for export from CHO cells and cell surface staining, showed an expression level comparable to Gal-1-GFP.

Related to different expression levels, all GFP fusion proteins of the mutated Gal-1 (Fig. 27; red bar) were detectable on the cell surface indicating that neither the export process nor the binding ability of these mutants are influenced by the individual single amino acid changes of each mutant form of Gal-1. The mutants P14A and M121A showed a reduced cell surface staining employing flow cytometry compared to the wild-type form of Gal-1. However, both mutants showed a significant signal for exported protein being associated with the plasma membrane as the signal is increased compared to the GFP negative control (Fig. 27).

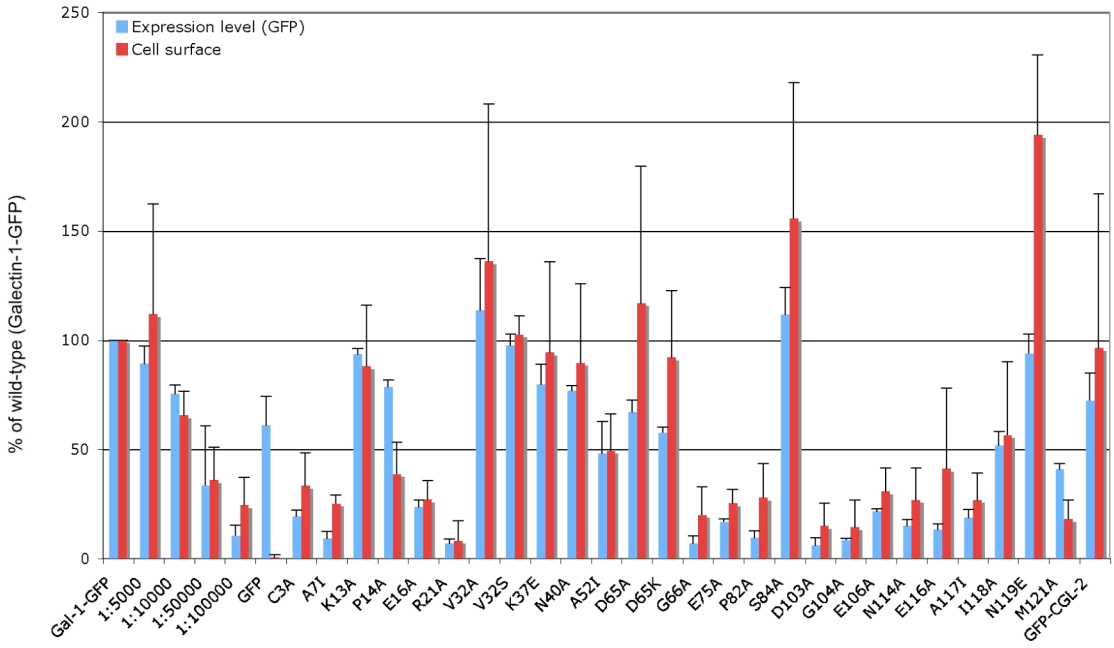

Fig. 27 Quantitative analysis of export of various galectin-GFP fusion proteins from CHO cells employing flow cytometry. CHO cells were grown on 6-well plates and induced with doxicycline for 48 h at 37°C to express the fusion proteins indicated. Following removal of medium, cells were labeled with affinity-purified anti-GFP antibodies followed by detachment of the cells using PBS/EDTA. GFP (expression level; blue) and APC-derived fluorescence (cell surface; red) were quantified by flow cytometry using Becton Dickinson FACSCalibur system (n=4)

In order to quantitatively study the export of Gal-1 mutants using an independent method, the cell surface biotinylation assay (Stegmayer et al., 2005) was combined with immunoprecipitation of Gal-1-GFP fusion proteins from the medium of expressing cells employing affinity-purified anti-GFP antibodies (3.2.3). Consistent with the data acquired by flow cytometry, the biochemical approach (Fig. 28) revealed that the wild-type and the mutant forms of Gal-1-GFP were expressed in a doxicycline-dependent manner. The input fraction (Fig. 28; lane 1; 1%) indicates the expression level of each fusion protein. The expression levels of the mutant A7I, E16A, K37E, E106A and V32S were low compared to the wild-type form of Gal-1-GFP. Western blot analysis revealed comparable amounts of all other mutants expressed in the corresponding CHO cell line. Most of the extracellular Gal-1-GFP wild-type population was associated with the cell surface of CHO cells (Fig. 28; lane

2; 10 %) with only a minor portion being found soluble in the medium (Fig. 28; lane 3; 50%). Strikingly, all mutant forms of Gal-1-GFP (Fig. 28; lane 2 and lane 3) identified in the FACS-based assay as being exported from CHO cell and detectable on the cell surface could also be detected bound to the cell surface of CHO cells employing the biotinylation assay. Although the signals for cell surface localized material of Gal-1 mutants A7I, E16A, K37E, E106A and M121A were weak (Fig. 28; lane 2), these mutant forms were not export deficient since the overall expression levels are reduced. These observations were consistent with the flow cytometry data. For all reporter molecules only a small fraction was found soluble in the medium of expressing cells as detected by immunoprecipitation employing affinity-purified anti-GFP antibodies.

CHO cells expressing Gal-1-GFP$_{S84A}$ (Fig. 28; Gal-1-GFP$_{S84A}$, lane 2 and 3) seemed to export the mutated GFP fusion protein to a higher extent compared to the wild-type form of Gal-1 (Fig. 28; Gal-1-GFP wt, lane 2 and 3) which is consistent with the observation made by flow cytometry (Fig. 27).

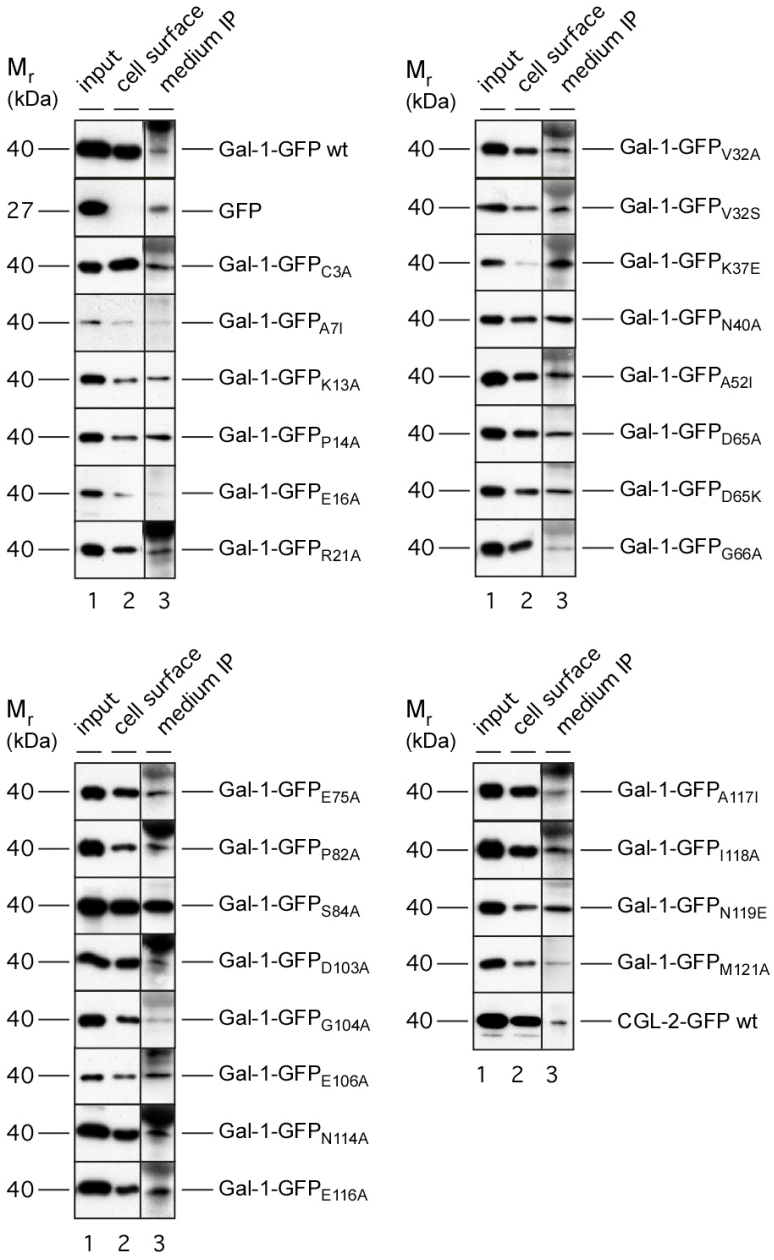

Fig. 28 Biochemical analysis of export of various galectin-GFP fusion proteins from CHO cells employing cell surface biotinylation and immunoprecipitation from cell culture supernatants. The fusion proteins indicated were expressed in CHO cells for 48 h at 37°C (6-well plates; 70% confluency; 1 µg/ml doxicycline) The medium was removed and subjected to immunoprecipitation using affinity-purified anti-GFP antibodies. Cells were treated with a membrane-impermeable biotinylation reagent. Following detergent-mediated cell lysis biotinylated and non-biotinylated proteins were separated employing streptavidin beads. Aliquots from the input material (lane 1; 1%), the biotinylated fraction (lane 2; 10%) and the immunoprecipitate from the cell culture medium fraction (lane 3; 50%) were analyzed by SDS PAGE and Western blotting using affinity-purified anti-GFP antibodies.

All mutant Gal-1 proteins were now analyzed for their capability to interact with counter receptors based on binding to both CHO cells (Fig. 29) and lactose-coupled beads (Fig. 30).

For the *in vivo* assay (Fig. 29) after detachment from cell culture plate CHO cells not expressing the GFP reporter molecule were incubated with cell-free supernatants prepared from CHO cells expressing the various Gal-1-GFP fusion proteins (3.2.4). Following treatment with affinity-purified anti-GFP antibodies and APC-conjugated secondary antibodies, binding of exogenously added GFP reporter molecules to the cell surface was analyzed by flow cytometry. The wild-type forms of Gal-1 and CGL-2 were used as positive controls for binding to the cell surface and the Gal-1 binding capacity was set to 100%, GFP served as a negative control. Some mutants such as A7I, V32A, V32S K37E, N40A, P82A, A117I, M121A and the wild-type form of CGL-2 bound even better to the cell surface of CHO cells (Fig. 29) when compared to Gal-1-GFP. The mutations C3A, P14A, A52I, E75A, D103A, G104A N114A and E116A showed approximately the same binding ability to the cell surface as Gal-1 wild-type. Amino acid changes K13A, E16A, R21A, D65A, D65K, G66A, I118A and N119E resulted in a reduced binding ability to β-galactosides on the cell surface.

The cell surface staining of mutant proteins S84A and E106A was reduced (S84A; 30%; E106A, 21%), but the signals differ significantly from the GFP negative control. These observations are consistent with the flow cytometry data. All mutants exported from CHO cells are also capable of binding to cell surface counter receptors *in vivo*.

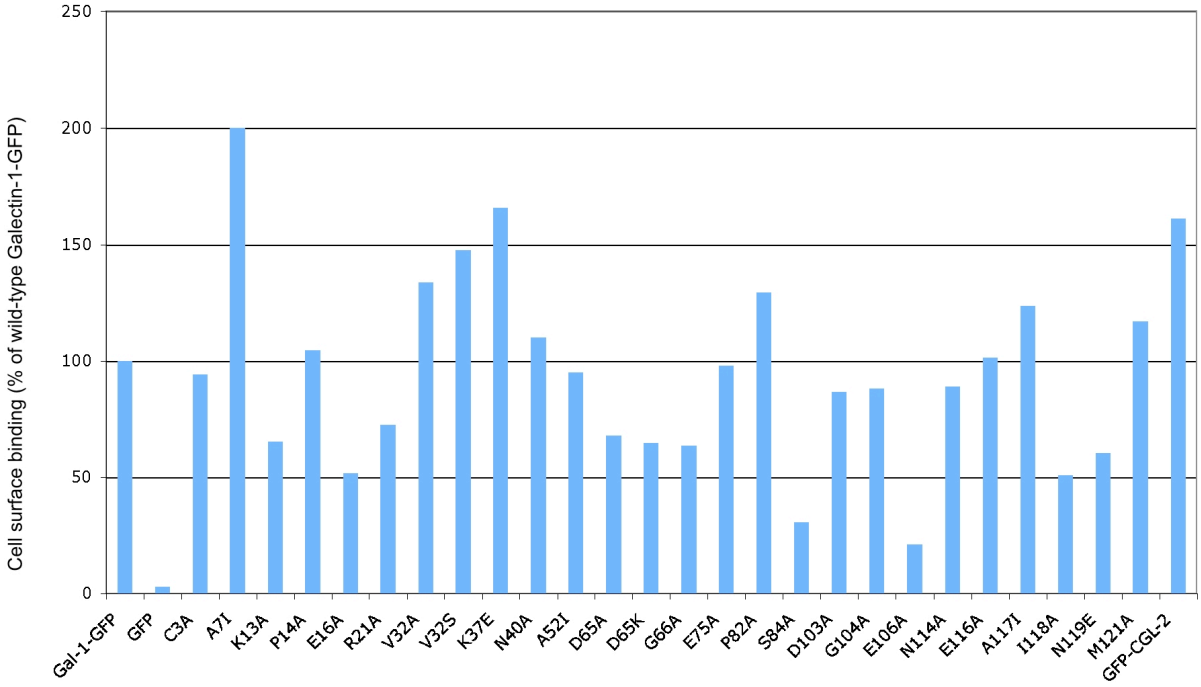

Fig. 29 Analysis of β-galactoside binding efficiency of various galectin-GFP fusion proteins based on binding to CHO cells. The various fusion proteins indicated were expressed in CHO cells. Cell-free supernatants were prepared and normalized by GFP fluorescence. The various supernatants were then incubated with CHO cells for 1 h at 4°C to allow cell surface binding. Following treatment with affinity-purified anti-GFP antibodies and APC-conjugated secondary antibodies, cell surface binding was quantified by flow cytometry.

To verify the data obtained by the *in vivo* assay the biochemical binding assay was performed. For this purpose detergent lysates of the various Gal-1 constructs were incubated with lactose-coupled beads (3.2.3). Input, flow-through and bound fractions were analyzed by SDS PAGE and Western blotting using affinity-purified anti-GFP antibodies.

As shown in Fig. 30 the amounts incubated with the lactose-coupled beads (Fig. 30, lane 1) varied between the various GFP fusion proteins although the input was normalized by measuring the GFP fluorescence of the fusion proteins employing a fluorescence plate reader. The input of Gal-1-GFP C3A, R21A, K37E, D65A, G104A and N119E was very low, but sufficient to detect bound material (Fig. 30; lane 3) on lactose-coupled beads. The only exception was R21A where no bound material is detectable. (Fig. 30, R21A, lane 3). The same observation could be made

regarding the mutants N40A and P82A, which seem to be impaired in binding to lactose-coupled beads. These observations are not consistent with the *in vivo* binding studies and with the secretion assays. In all three assays it was shown that these mutants were able to bind to their counter receptors.

All remaining mutants clearly bind to lactose-coupled beads as the various signals for bound materials were increased compared to the GFP negative control (Fig. 30; GFP, lane 3). Additionally they showed a similar binding ability compared to the positive controls Gal-1-GFP and GFP-CGL-2 (Fig. 30, Gal-1-GFP wt and GFP-CGL-2; lane 3). Consistently with the *in vivo* binding assay the mutants A7I and V32A and the wild-type form of CGL-2-GFP had an even higher β-galactoside binding efficiency *in vitro* (compare Fig. 29 and Fig. 30).

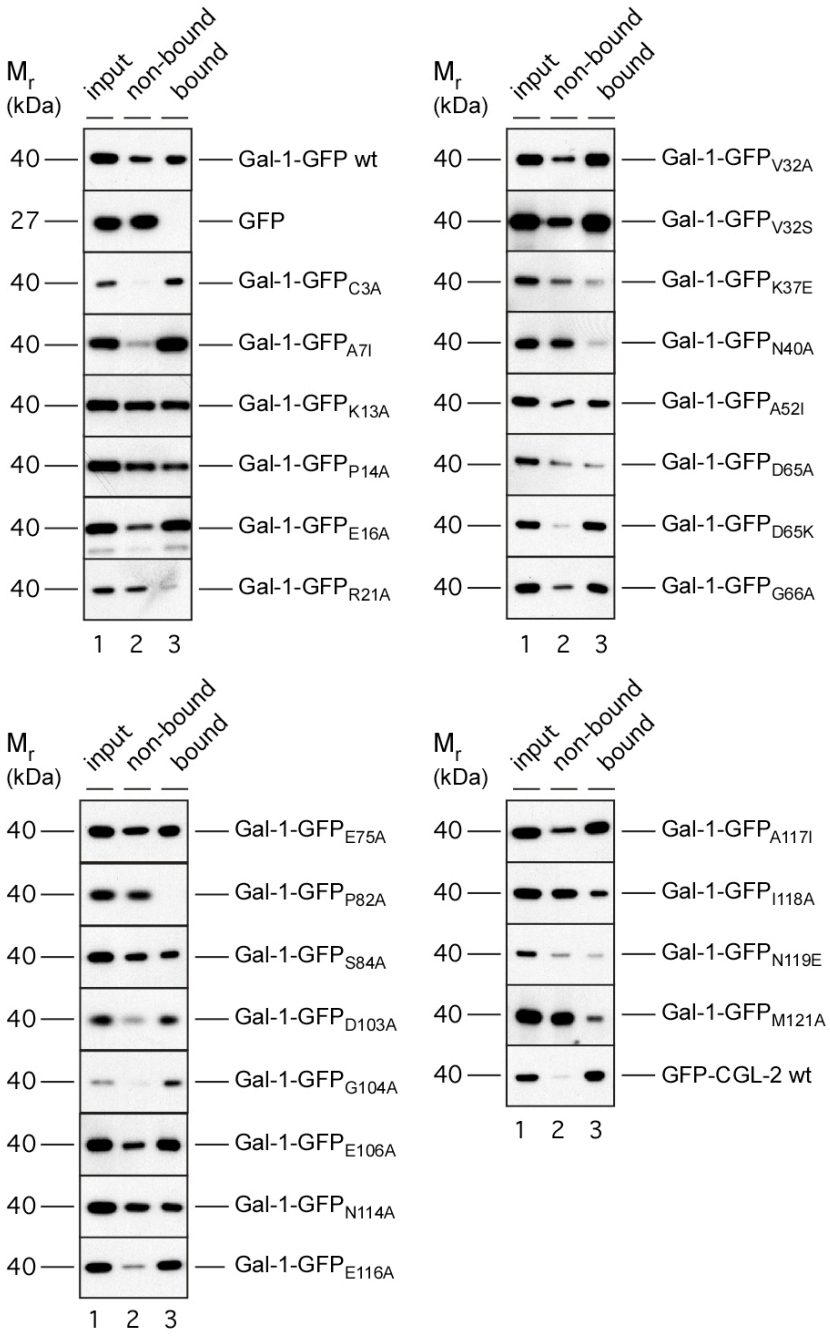

Fig. 30 Analysis of β-galactoside binding efficiency of various galectin-GFP fusion proteins based on binding to lactose-coupled beads. Detergent lysates normalized by GFP fluorescence were incubated with lactose beads for 1 h at 4°C. The non-bound fraction was removed and, following extensive washing, bound material was eluted with SDS sample buffer. Input (lane 1, 5%), non-bound material (lane 2; 5%) and bound material (lane 3; 5%) were analyzed by SDS PAGE and Western blotting using affinity-purified anti-GFP antibodies.

Taken together, all Gal-1 mutants listed in Table 6 result in a similar phenotype as the wild-type form of human Gal-1 concerning secretion and binding to β-galactosides.

Mutation	Phenotype
Gal-1-GFP	
C3A	Lower expression level in the FACS-based and biotinylation assay; cell surface signal, binding ability comparable to wild-type in both binding assays
A7I	Lower expression level in the FACS-based assay, highly reduced in the biotinylation assay; cell surface signal in both assays; binding capacity higher than wild-type in both binding assays
K13A	Approximately the same expression level and cell surface signal in both secretion assays than the wild-type; no binding defect
P14A	Approximately the same expression level and cell surface signal in both secretion assay than the wild-type; no binding defect
E16A	Lower expression level in the FACS-based and biotinylation assay; cell surface signal; binding capacity comparable to wild-type in both binding assays
R21A	Lower expression level in the FACS-based and biotinylation assay; cell surface signal in both assays; binding capacity comparable to wild-type in the in-vivo assay; reduced signal in the in-vitro binding assay
V32A	Approximately the same expression level and cell surface signal in both secretion assay than the wild-type; no binding defect
V32S	Approximately the same expression level and cell surface signal in both secretion assay than the wild-type; no binding defect
K37E	Approximately the same expression level and cell surface signal in the FACS-based assay than the wild-type; in the biotinylation assay reduced cell surface signal, increased signal in the cell culture medium; no binding defect
N40A	Approximately the same expression level and cell surface signal in the FACS-based assay and biotinylation assay than the wild-type; no binding defect
A52I	Approximately the same expression level and cell surface signal in the FACS-based secretion assay than the wild-type; reduced cells surface in the biotinylation assay; higher binding capacity in the in-vivo assay; reduced binding in the in vitro assay
D65A	Approximately the same expression level and cell surface signal in the FACS-based assay and biotinylation assay than the wild-type; no binding defect
D65K	Approximately the same expression level and cell surface signal in the FACS-based assay and biotinylation assay than the wild-type; no binding defect
G66A	Reduced expression in the FACS-based assay; good expression in the biotinylation assay; cell surface staining; no binding defect
E75A	Reduced expression in the FACS-based assay; good expression in the biotinylation assay; cell surface signal; no binding defect
P82A	Reduced expression in the FACS-based assay; good expression in the biotinylation assay; cell surface signal; no binding defect
S84A	Approximately the same expression level and cell surface signal in the FACS-based and biotinylation assay than the wild-type, even higher; no binding defect
D103A	Reduced expression in the FACS-based assay; good expression in the biotinylation assay; cell surface signal; no binding defect

G104A	Reduced expression in the FACS-based assay; good expression in the biotinylation assay; cell surface signal; no binding defect
E106A	Reduced expression in the FACS-based assay and in the biotinylation assay; cell surface signal; no binding defect
N114A	Reduced expression in the FACS-based assay; good expression in the biotinylation assay; cell surface signal; no binding defect
E116A	Reduced expression in the FACS-based assay; good expression in the biotinylation assay; cell surface signal; no binding defect
A117I	Reduced expression in the FACS-based assay; good expression in the biotinylation assay; cell surface signal; no binding defect
I118A	Reduced expression in the FACS-based assay; good expression in the biotinylation assay; cell surface signal; no binding defect
N119E	Approximately the same expression level and higher cell surface signal in the FACS-based assay than the wild-type, even higher; Expression and cell surface signal in the biotinylation assay comparable to the wild-type; no binding defect in vivo, reduced binding in vitro
M121A	Reduced expression in the FACS-based assay; good expression in the biotinylation assay; cell surface signal; no binding defect

Table 6 Summary of various human Gal-1 mutants without phenotype compared to the wild-type form of Gal-1-GFP

3.3.3.2 Identification of Gal-1 mutants deficient in binding to β-galactosides in glycoproteins and glycolipids

Based on findings that the glycolipid/glycoprotein composition of the cell surface may influence the export behavior of human Gal-1 (3.1.7) it was hypothesized that binding to counter receptors plays a role in non-classical export of human Gal-1. With this hypothesis in mind, mutants were analyzed whether they were defective in binding to β-galactosides in both assays (*in vivo* 3.2.4 and *in vitro* binding assay 3.2.5). Following FACS and biotinylation analysis the identified Gal-1 mutants deficient in cell surface localization in both secretion assays were carefully studied regarding the influence of the corresponding single amino acid mutations on ligand binding.

Using the wild-type forms of Gal-1-GFP and GFP-CGL-2 as positive controls for the unconventional secretion of galectins and GFP as a negative control, 43 Gal-1 mutants were identified not to be present on the outer leaflet of the plasma membrane employing flow cytometry (Fig. 31). As already described above the wild-

type and the mutant forms of Gal-1-GFP and GFP-CGL-2 fusion proteins were expressed in corresponding CHO cell lines by incubating the cells in the presence of doxicycline for 48 h at 37°C under standard conditions (3.2.2). The expression of the wild-type form of Gal-1 was induced at different concentrations of doxicycline (1 µg/ml (1:1,000); 0.2 µg/ml (1:5,000); 0.1 µg/ml (1:10,000); 0.02 µg/ml (1:5,0000); 0.01 µg/ml (1:100,000) doxicycline) in order to be able to compare cell surface signals obtained from mutant cell lines expressing the reporter molecules at different levels. The expression level and the cell surface staining of wild-type Gal-1-GFP under standard condition (1 µg/ml doxicycline, 48 h, 37°C) were set to 100%. Three independent experiments were performed to analyze export of the wild-type and the mutant forms of Gal-1-GFP.

As shown in Fig. 31 (blue bar) the expression level of the various GFP fusion proteins varied between the different generated CHO cell lines. Compared to Gal-1-GFP the mutant cell lines V6A, V20, D38E, L44F, H45A, R49A, H53A, H53E, H53G, W69A, E72A, R74A, F80A, F80S, R112A, N119K, N119W, Y120A, A122I, F127A V132A, F134E, F134R, the wild-type form of GFP-CGL-2 and GFP as a negative control for export showed approximately the same expression level as Gal-1-GFP. The GFP fusion proteins of Gal-1 mutants N34A, D38K, N41A, L44A, L44D, L44S, F46A, D55A, N57A, V60A, G67A, F80K, F109A, Y120D, F127D, I129R, V132E, V132R and the CGL-2 mutant W72G expressed the GFP reporter molecule to a lower extent (1 µg/ml doxicycline, 48 h, 37°C). The mutants N9A and G54A were expressed at very low levels. Strikingly, related to different expression levels almost all mutants showed clearly no cell surface staining as they did not differ from the GFP negative control to a significant extent. The mutations V20A, L44F, H53A, G67A, F109A, N119K, N119W, F127A, V132A, F134E and F134R showed a weak cell surface staining indicating that the fusion proteins were partially exported and bound to the cell surface (for further characterization see cell surface biotinylation assay; Fig. 32). The expression level and the cell surface staining of the mutant N9A, L44D, L44S and G54A were largely reduced. Independently of the low protein expression, reduced cell surface signals indicated that there was no exported GFP fusion protein bound to the cell surface (compare (1:100,000) doxicycline of the wild-type form of Gal-1).

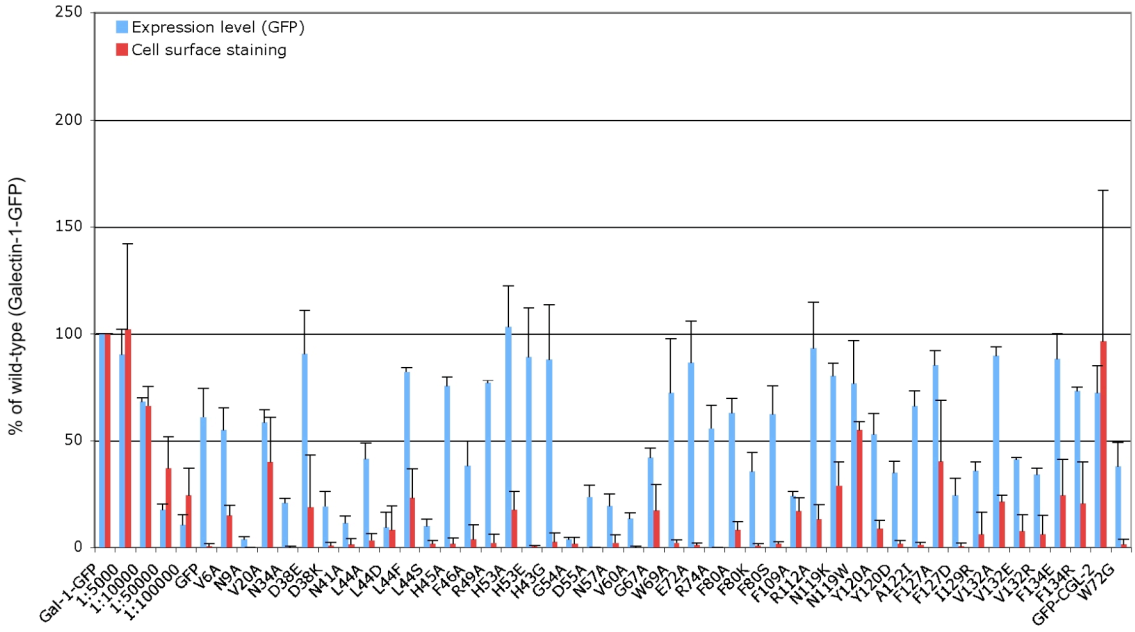

Fig. 31 Quantitative analysis of export of various galectin-GFP fusion proteins from CHO cells employing flow cytometry. CHO cells were grown on 6-well plates and induced with doxicycline for 48 h at 37°C to express the fusion protein indicated. Following removal of medium, cells were labeled with affinity-purified anti-GFP antibodies followed by detachment of the cells using PBS/EDTA. GFP (expression level; blue) and APC-derived fluorescence (cell surface; red) were quantified by flow cytometry using Becton Dickinson FACSCalibur system (n=4)

However, using the flow cytometry assay, only exported protein that is able to bind to the cell surface can be detected. Negative signals for cell surface staining can be explained by one of the following scenarios: i) because of the mutation the various proteins of Gal-1-GFP are not recognized any more as export substrates by the export machinery in CHO cells. ii) Export still occurs but the exported mutant proteins are not able to bind to counter receptors on the cell surface. Secreted GFP reporter molecules should then be detectable in the medium of expressing CHO cells. iii) The mutant forms showing the indicated phenotype in Fig. 31 are not secreted and are also not able to bind to β-galactosides so that the reporter molecules are neither detectable on the cell surface nor in the medium of expressing cells.

To distinguish between these three possibilities the following experiment was performed: conditioned medium from CHO cells expressing the various GFP reporter

molecules was removed and subjected to immunoprecipitation to detect soluble, secreted GFP fusion proteins. The cells were treated with a membrane-impermeable biotinylation reagent. After detergent-mediated cell lysis the biotinylated and the non-biotinylated fraction were separated employing streptavidin beads. The input (Fig. 32, lane 1, 1%) indicates the expression level of the various GFP fusion proteins. As shown in Fig. 32, most of the extracellular Gal-1-GFP was found to be associated with the cell surface of CHO cell (Fig. 32, Gal-1-GFP wt, lane 2; 10%). Only a minor portion could be precipitated from the medium (Fig. 32, Gal-1-GFP wt, lane 3; 50%). Regarding GFP-CGL-2 as a positive control, most of the secreted population was bound to the cell surface (Fig. 32, GFP-CGL-2 wt, lane 2; 10%) and only a minor portion was found soluble in the cell culture medium (Fig. 32, GFP-CGL-2 wt, lane 3; 50%). As expected GFP as a negative control was not associated with the cell surface (Fig. 32, GFP, lane 2, 10%). A weak signal could be detected in the medium of GFP-expressing CHO cells and, therefore, which is likely to be derived from damaged cells, was considered as background.

As depicted in Fig. 32 none of the mutants showed a significant signal of exported protein neither bound the cell surface nor soluble in the medium compared to the GFP negative control (Fig. 32, lane 2 and lane 3). Some mutants (N41A, L44D, R49A, H53E, G54A, R74A, F80K, F80S, R112A, Y120D, F127D, V132R and GFP-CGL-2 W72G) showed a weak population bound to the cell surface (Fig. 32, lane 2; 10%). This exported surface-bound fraction might be caused by unspecific release and was considered as background.

The mutants N34A, D38K, L44S, H45A, F46A, H53A, H53G, N57A, V60A, W69G, E72A and V132E were clearly defective in both export and binding as they neither show GFP reporter molecules bound to the cell surface nor exported protein soluble in the cell culture medium. One possible explanation might be that degradation of mutated Gal-1-GFP fusion protein causes the absence of such signals on the cell surface and the medium. As mutated proteins were expressed the specific mutation may cause a stability problem. Therefore mutants, which are not able any more to bind to ligands, needed to be investigated for stability (3.3.3.2.1).

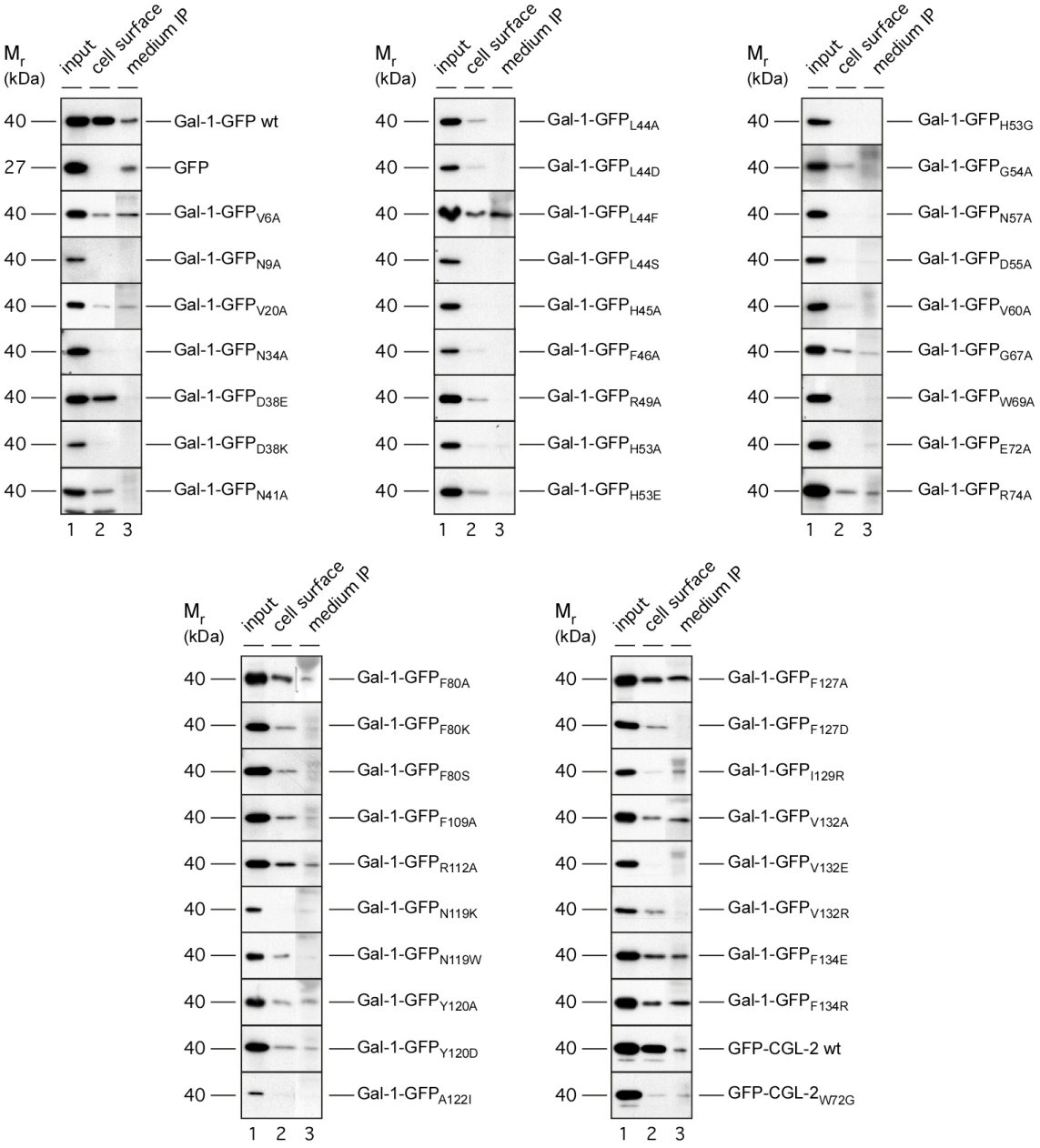

Fig. 32 Biochemical analysis of export of various galectins as GFP fusion proteins from CHO cells employing cell surface biotinylation and immunoprecipitation from cell culture supernatants. The fusion proteins indicated were expressed in CHO cells for 48 h at 37°C (6-well plates; 70% confluency; 1 µg/ml doxicycline) The medium was removed and subjected to immunoprecipitation using affinity-purified anti-GFP antibodies. Cells were treated with a membrane-impermeable biotinylation reagent. Following detergent-mediated cell lysis biotinylated and non-biotinylated proteins were separated employing streptavidin beads. Aliquots from the input material (lane 1; 1%), the biotinylated fraction (lane 2; 10%) and the immunoprecipitate from the cell culture medium fraction (lane 3; 50%) were analyzed by SDS PAGE and Western blotting using affinity-purified anti-GFP antibodies.

Some of the mutant forms of Gal-1 shown in Fig. 32 (H45A, R49A (Scott and Zhang, 2002); H53A/E/G, (Lopez-Lucendo et al., 2004); W69G, E72A, R74A (Hirabayashi and Kasai, 1991) have been reported previously to be impaired in terms of binding to β-galactoside-containing counter receptors (Table 3). Therefore all mutants were analyzed regarding their binding ability to β-galactosides employing CHO cells and lactose-coupled beads.

As already shown before the wild-type form of Gal-1-GFP and GFP-CGL-2 bind to β-galactosides (Fig. 33) and were detectable on the cell surface of CHO employing flow cytometry (3.2.4) The cell surface signal of bound Gal-1-GFP was set to 100%. Almost all mutants were clearly defective in binding to β-galactosides on CHO cells as the cell surface signal of bound protein is comparable to the GFP negative control.

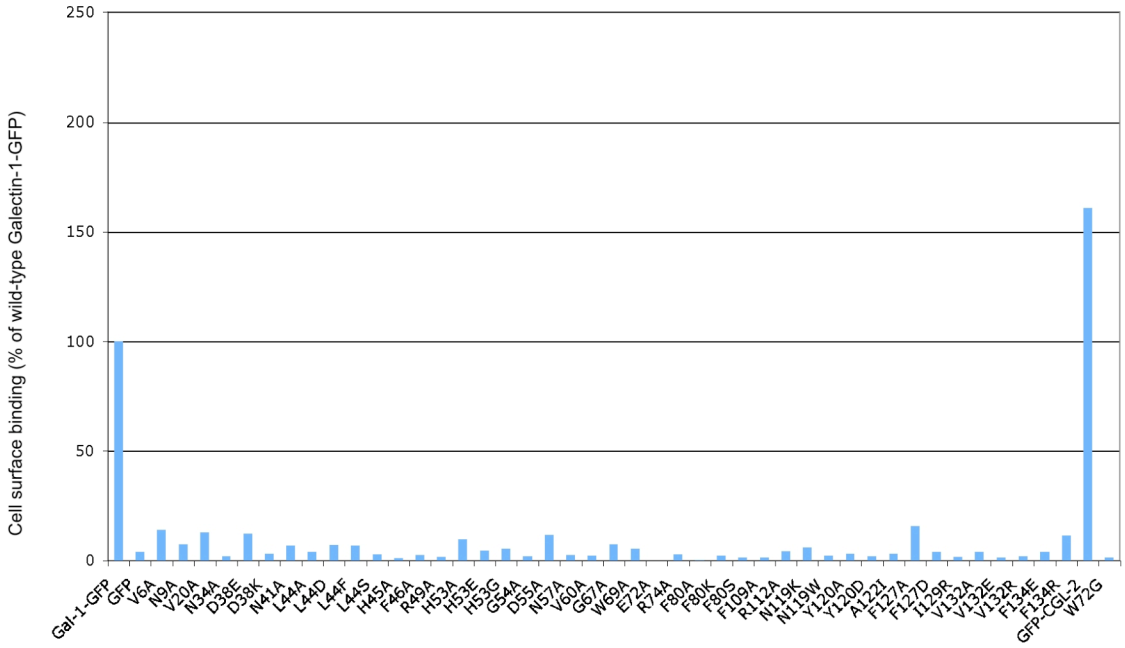

Fig. 33 Analysis of β-galactoside binding efficiency of various galectin-GFP fusion proteins based on binding to CHO cells. The various fusion proteins indicated were expressed in CHO cells. Cell-free supernatants were prepared and normalized by GFP fluorescence. The various supernatants were then incubated with CHO cells for 1 h at 4°C to allow cell surface binding. Following treatment with affinity-purified anti-GFP antibodies and APC-conjugated secondary antibodies, cell surface binding was quantified by flow cytometry.

Additionally, the identified mutants deficient in binding to CHO cell surface were analyzed using the *in vitro* binding assay employing lactose-coupled beads (3.2.5). Input (Fig. 34, lane 1, 5%), flow-through (Fig. 34, lane 2, 5%) and bound material (Fig. 34, lane 3, 5%) were analyzed by SDS PAGE and Western blotting using affinity-purified anti-GFP antibodies.

As shown in Fig. 34, the Western blot analysis revealed that similar amounts of Gal-1-GFP, GFP-CGL-2 as positive controls (Fig. 34, lane 1) and of the mutants N34A, D38K, N41A, L44A, L44D, L44S, H45A, R49A, H53A, H53E, H53G, G54A, N57A, V60A, W69G, E72A, R74A, F80a, F80S, R112A, Y120D, F127D, I129R, V132E, V132R and CGL-2-GFP W72G were applied to lactose-coupled beads, whereas the amount of Gal-1-GFP F46A was much lower. As shown in Fig. 34, the wild-type form of Gal-1-GFP and CGL-2-GFP clearly bound to the lactose-coupled beads, as there was a reduced signal for the non-bound fraction (Fig. 34; lane 2, 5%) and a clear signal for lactose-bound material (Fig. 34; lane 3, 5%). All mutants were clearly defective in binding to lactose, since they did not differ from the GFP negative control (Fig. 34, lane 3). These data are consistent with the observation made in the corresponding *in vivo* binding studies (Fig. 33).

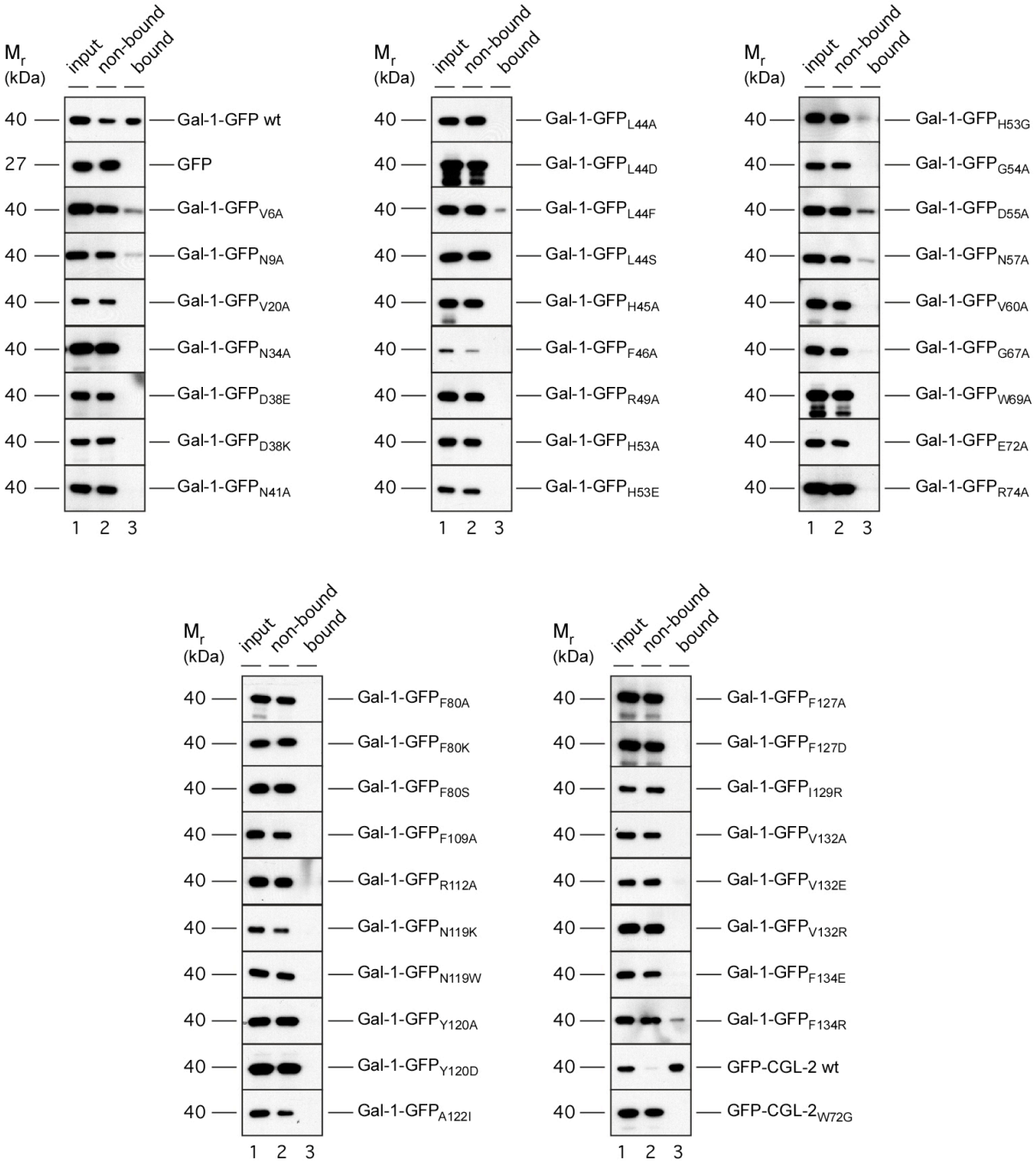

Fig. 34 Analysis of β-galactoside binding efficiency of various galectin-GFP fusion proteins based on binding to lactose-coupled beads. Detergent lysates normalized by GFP fluorescence were incubated with lactose beads for 1 h at 4°C. The non-bound fraction was separated and, following extensive washing, bound material was eluted with SDS sample buffer. Input (lane 1, 5%), non-bound material (lane 2; 5%) and bound material (lane 3; 5%) were analyzed by SDS PAGE and Western blotting using affinity-purified anti-GFP antibodies

Taken together, all mutants listed in Table 7 were found to be deficient both in β-galactoside binding and export as they were neither detectable on the cell surface nor in the medium of the corresponding cell lines. These observations indicate that the interaction of Gal-1 with β-galactoside-containing cell surface receptors is a prerequisite for its unconventional secretion.

However, an alternative explanation for the absence of mutant forms of Gal-1-GFP from the medium would be that the GFP reporter molecule is degraded under non-reducing conditions present outside cells. To investigate the stability of a mutated protein a degradation assay was established (3.3.3.2.1).

Mutation	**Phenotype**
Gal-1-GFP	
V6A	Expression level comparable with the wild-type in the FACS-based assay; good expression employing the biotinylation assay; no exported protein employing flow cytometry and biotinylation assay; binding defect in both assays
N9A	Very low expression level comparable with the wild-type in the FACS-based assay; low expression level in the biotinylation assay; no exported protein employing flow cytometry and biotinylation assay; binding defect in both assays
V20A	Expression level comparable with the wild-type in the FACS-based assay; good expression employing the biotinylation assay; no exported protein employing flow cytometry and biotinylation assay; binding defect in both assays
N34A	Lower expression level than with the wild-type in the FACS-based assay; good expression employing the biotinylation assay; no exported protein employing flow cytometry and biotinylation assay; binding defect in both assays
D38E	Expression level comparable with the wild-type in the FACS-based assay; good expression employing the biotinylation assay; reduced signal of exported protein employing flow cytometry and biotinylation assay; binding defect in both assays
D38K	Lower expression level than with the wild-type in the FACS-based assay; good expression employing the biotinylation assay; no exported protein employing flow cytometry and biotinylation assay; binding defect in both assays
N41A	Lower expression level than with the wild-type in the FACS-based assay; good expression employing the biotinylation assay; no exported protein employing flow cytometry and biotinylation assay; binding defect in both assays
L44A	Lower expression level than with the wild-type in the FACS-based assay; good expression employing the biotinylation assay; no exported protein employing flow cytometry and biotinylation assay; binding defect in both assays
L44D	Lower expression level than with the wild-type in the FACS-based assay; good expression employing the biotinylation assay; no exported protein employing flow cytometry and biotinylation assay; binding defect in both assays
L44F	Expression level comparable with the wild-type in the FACS-based assay; good expression employing the biotinylation assay; reduced signal of exported protein employing flow cytometry and biotinylation assay; binding defect in both assays

L44S	Lower expression level than with the wild-type in the FACS-based assay; good expression employing the biotinylation assay; no exported protein employing flow cytometry and biotinylation assay; binding defect in both assays
H45A	Expression level comparable with the wild-type in the FACS-based assay; good expression employing the biotinylation assay; no exported protein employing flow cytometry and biotinylation assay; binding defect in both assays
F46A	Lower expression level than with the wild-type in the FACS-based assay; good expression employing the biotinylation assay; no exported protein employing flow cytometry and biotinylation assay; binding defect in both assays
R49A	Expression level comparable with the wild-type in the FACS-based assay; good expression employing the biotinylation assay; no exported protein employing flow cytometry and biotinylation assay; binding defect in both assays
H53A	Expression level comparable with the wild-type in the FACS-based assay; good expression employing the biotinylation assay; no exported protein employing flow cytometry and biotinylation assay; binding defect in both assays
H53E	Expression level comparable with the wild-type in the FACS-based assay; good expression employing the biotinylation assay; no exported protein employing flow cytometry and biotinylation assay; binding defect in both assays
H53G	Expression level comparable with the wild-type in the FACS-based assay; good expression employing the biotinylation assay; no exported protein employing flow cytometry and biotinylation assay; binding defect in both assays
G54A	Very low expression level comparable with the wild-type in the FACS-based assay; good expression employing the biotinylation assay; no exported protein employing flow cytometry and biotinylation assay; binding defect in both assays
D55A	Lower expression level than with the wild-type in the FACS-based assay; good expression employing the biotinylation assay; no exported protein employing flow cytometry and biotinylation assay; binding defect in both assays
N57A	Lower expression level than with the wild-type in the FACS-based assay; good expression employing the biotinylation assay; no exported protein employing flow cytometry and biotinylation assay; binding defect in both assays
V60A	Lower expression level than with the wild-type in the FACS-based assay; good expression employing the biotinylation assay; no exported protein employing flow cytometry and biotinylation assay; binding defect in both assays
G67A	Lower expression level than with the wild-type in the FACS-based assay; good expression employing the biotinylation assay; no exported protein employing flow cytometry and biotinylation assay; binding defect in both assays
W69G	Expression level comparable with the wild-type in the FACS-based assay; good expression employing the biotinylation assay; no exported protein employing flow cytometry and biotinylation assay; binding defect in both assays
E72A	Expression level comparable with the wild-type in the FACS-based assay; good expression employing the biotinylation assay; no exported protein employing flow cytometry and biotinylation assay; binding defect in both assays
R74A	Expression level comparable with the wild-type in the FACS-based assay; good expression employing the biotinylation assay; no exported protein employing flow cytometry and biotinylation assay; binding defect in both assays
F80A	Expression level comparable with the wild-type in the FACS-based assay; good expression employing the biotinylation assay; no exported protein employing flow cytometry and biotinylation assay; binding defect in both assays

F80K	Lower expression level than with the wild-type in the FACS-based assay; good expression employing the biotinylation assay; no exported protein employing flow cytometry and biotinylation assay; binding defect in both assays
F80S	Expression level comparable with the wild-type in the FACS-based assay; good expression employing the biotinylation assay; no exported protein employing flow cytometry and biotinylation assay; binding defect in both assays
F109A	Lower expression level than with the wild-type in the FACS-based assay; good expression employing the biotinylation assay; no exported protein employing flow cytometry and biotinylation assay; binding defect in both assays
R112A	Expression level comparable with the wild-type in the FACS-based assay; good expression employing the biotinylation assay; no exported protein employing flow cytometry and biotinylation assay; binding defect in both assays
N119K	Expression level comparable with the wild-type in the FACS-based assay; low expression level in the biotinylation assay; no exported protein employing flow cytometry and biotinylation assay; binding defect in both assays
N119W	Expression level comparable with the wild-type in the FACS-based assay; good expression employing the biotinylation assay; no exported protein employing flow cytometry and biotinylation assay; binding defect in both assays
Y120A	Expression level comparable with the wild-type in the FACS-based assay; good expression employing the biotinylation assay; no exported protein employing flow cytometry and biotinylation assay; binding defect in both assays
Y120D	Lower expression level than with the wild-type in the FACS-based assay; good expression employing the biotinylation assay; no exported protein employing flow cytometry and biotinylation assay; binding defect in both assays
A122I	Expression level comparable with the wild-type in the FACS-based assay; low expression level in the biotinylation assay; no exported protein employing flow cytometry and biotinylation assay; binding defect in both assays
F127A	Expression level comparable with the wild-type in the FACS-based assay; good expression employing the biotinylation assay; reduced signal of exported protein employing flow cytometry and biotinylation assay; binding defect in both assays
F127D	Lower expression level than with the wild-type in the FACS-based assay; good expression employing the biotinylation assay; no exported protein employing flow cytometry and biotinylation assay; binding defect in both assays
I129R	Lower expression level than with the wild-type in the FACS-based assay; good expression employing the biotinylation assay; no exported protein employing flow cytometry and biotinylation assay; binding defect in both assays
V132A	Expression level comparable with the wild-type in the FACS-based assay; good expression employing the biotinylation assay; no exported protein employing flow cytometry and biotinylation assay; binding defect in both assays
V132E	Lower expression level than with the wild-type in the FACS-based assay; good expression employing the biotinylation assay; no exported protein employing flow cytometry and biotinylation assay; binding defect in both assays
V132R	Lower expression level than with the wild-type in the FACS-based assay; good expression employing the biotinylation assay; no exported protein employing flow cytometry and biotinylation assay; binding defect in both assays
F134E	Expression level comparable with the wild-type in the FACS-based assay; good expression employing the biotinylation assay; no exported protein employing flow cytometry and biotinylation assay; binding defect in both assays

F134R	Expression level comparable with the wild-type in the FACS-based assay; good expression employing the biotinylation assay; no exported protein employing flow cytometry and biotinylation assay; binding defect in both assays
GFP-CGL-2	
GFP-CGL-2 W72G	Lower expression level than with the wild-type in the FACS-based assay; good expression employing the biotinylation assay; no exported protein employing flow cytometry and biotinylation assay; binding defect in both assays

Table 7 Summary of various human Gal-1 mutants being deficient in both binding to β-galactosides and export from CHO cells.

3.3.3.2.1 Gal-1 mutants deficient for binding to β-galactosides are not degraded in conditioned medium derived from CHO cells

In the case of galectins binding to β-galactoside is of great importance. Galectins are highly sensitive to the redox state of the environment and can remain active only in the reducing environment of the cytosol. Following export galectins must immediately bind to their counter receptors on the cell surface in order to fulfill their function.

Based on the known secretion (Fig. 31 and Fig. 32) and binding assays (Fig. 33 and Fig. 34) 43 mutants were identified to be deficient regarding export from CHO cells and binding to β-galactosides. Stable mutant proteins, which lost their ability to bind to the cell surface, should be detectable in the cell culture medium of expressing CHO cells if export occurs. An alternative explanation for the absence of mutated proteins from the cell culture medium is that these proteins are subjected to degradation since they cannot bind to their counter receptors.

Therefore these Gal-1 mutants deficient in β-galactoside binding were analyzed with regard to their stability in conditioned medium derived from CHO cells in order to test whether protein degradation causes their absence from the supernatants of expressing cells. Cell-free supernatants of the various proteins deficient in binding to β-galactosides were prepared (Table 7). Normalized amounts (150 GFP units corresponding to about 1.5 µg GFP) measured with a fluorescence plate reader were

added to conditioned medium. The corresponding Gal-1-GFP mutant protein diluted in conditioned medium was either subjected immediately to immunoprecipitation using affinity-purified anti-GFP antibodies or incubated for 48 h at 37°C (the experimental condition of a secretion assay employing the cell surface biotinylation assay and the FACS-based secretion assay) followed by immunoprecipitation. Following SDS PAGE degradation of the various Gal-1-GFP mutants were analyzed by Western blotting using affinity-purified anti-GFP antibodies.

As shown in Fig. 35, the wild-type forms of Gal-1-GFP, GFP-CGL-2 and GFP were used as negative controls for degradation. 33 mutant forms of Gal-1 and one mutant of CGL-2 deficient in binding were analyzed for degradation. The wild-type form of Gal-1 and CGL-2, GFP and the β-galactoside-binding mutants were not degraded when incubated with condition CHO medium at 37°C for 48 hours (Fig. 35, compare lane 1, 10%, and lane 2, 10%) since Western blot analysis revealed the same amounts for non-incubated and incubated fractions. Human Gal-1 and fungal CGL-2 are highly stable under the experimental conditions applied. Additionally, mutations of single amino acid in Gal-1 and CGL-2 causing in a defect in binding to counter receptors did not result in their degradation. Regarding the mutants N41A, L44A and V60A there was a slightly reduced signal indicating that these proteins are partially degraded (Fig. 35, lane 1 and 2).

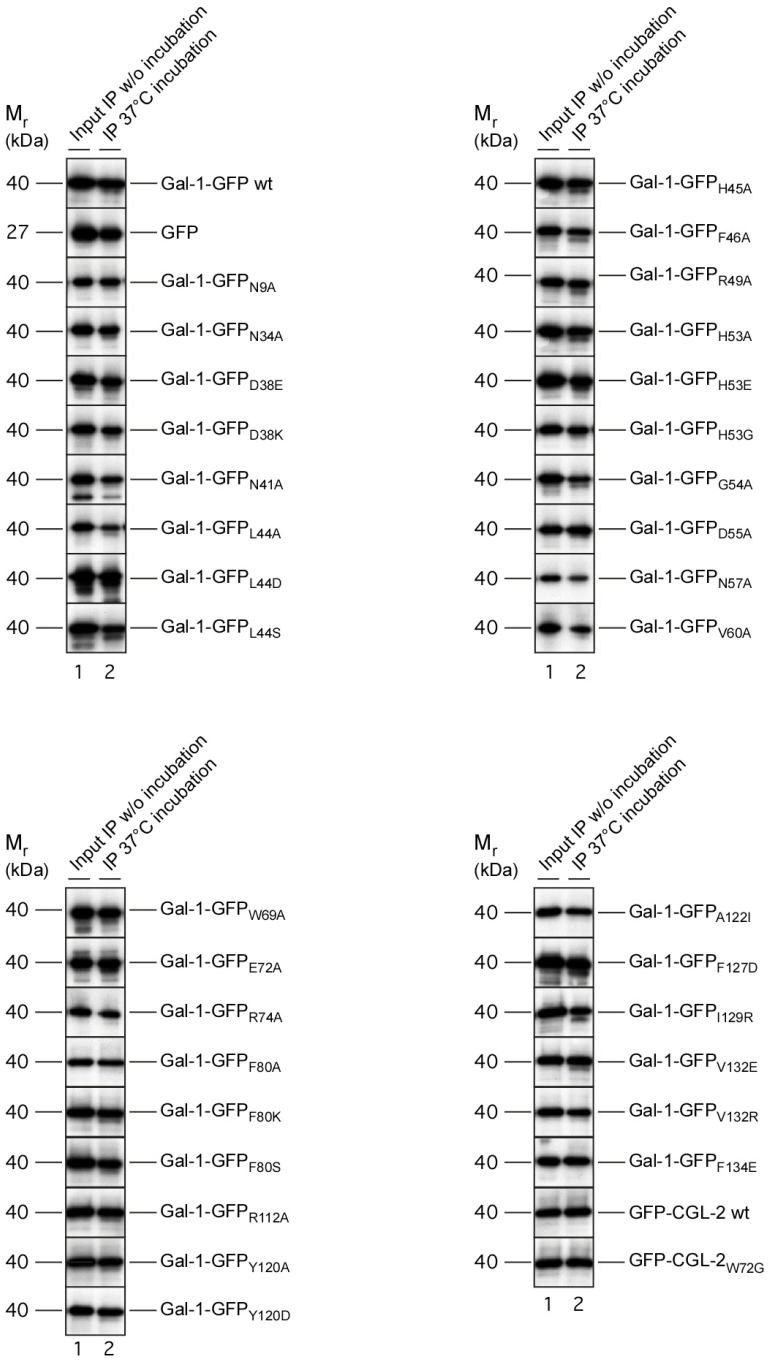

Fig. 35 Stability of galectin-GFP fusion proteins in conditioned media derived from CHO cells. The fusion protein indicated were expressed in CHO cells for 48 h at 37°C (6-well paltes; 70% confluency). From each cell line, a cell-free supernatant was prepared. Normalized amounts (GFP fluorescence) were incubated in conditioned medium derived from CHO cells for the times indicated followed by immunoprecipitation (lanes 1 and 2) using affinity-purified anti-GFP antibodies. The samples were analyzed by SDS PAGE and Western blotting using antibodies directed against GFP. Lane 1: no incubation (IP, 10%); lane 2: incubation for 48 h at 37°C (IP, 10%).

3.3.3.2.2 Wild-type forms of both Gal-1 and CGL-2 fail to be exported from CHO cells lacking functional counter receptors for Galectins

To address the question whether counter receptors play a direct role in the export mechanism of galectins, another experimental approach was taken. For this purpose, cell lines expressing various forms of Gal-1 (Gal-1-GFP, Gal-1-GFP_{W69G}, Gal-1-GFP_{E72A}) and CGL-2 (GFP-CGL-2, GFP-CGL-2_{W72G}) as GFP fusion proteins were generated based on a CHO mutant cell line termed clone 13 (3.1.3; Fig. 12). In this mutant cell line, the Golgi-resident transporter for UDP-galactose is defective and, therefore, these cells cannot produce galectin counter receptors since galactosyltransferases in the Golgi lumen do not receive activated galactose residues as substrates (Deutscher and Hirschberg, 1986). As a result, both glycoproteins and glycolipids derived from clone 13 cells do not contain β-galactosides in their sugar moieties and, therefore, do not bind galectins on their cell surface (Fig. 13). If β-galactosides localized to the cell surface are necessary for Gal-1 export into the extracellular space, the wild-type form of Gal-1 and CGL-2 expressed as GFP fusion proteins should not be secreted from $CHO_{clone13}$ cells.

Following retroviral transduction of $CHO_{clone13}$ cells all proteins were stably expressed as GFP fusion proteins using the doxicycline-dependent transactivator system (3.2.1). CHO cells expressing the corresponding reporter molecules were used as positive controls.

The cell surface biotinylation assay combined with immunoprecipitation of the various GFP fusion proteins from the medium of expressing CHO and $CHO_{clone13}$ cells was performed under standard conditions (1 µg/ml doxicycline, 48 h, 37°C).

As shown in the cell surface biotinylation experiments (Fig. 36) both Gal-1-GFP (panel A; lanes 2 and 3) and CGL-2-GFP (panel D; lanes 11 and 12) were efficiently exported from $CHO_{wild\text{-}type}$ cells as inducated the combined signals for cell surface and medium fractions.

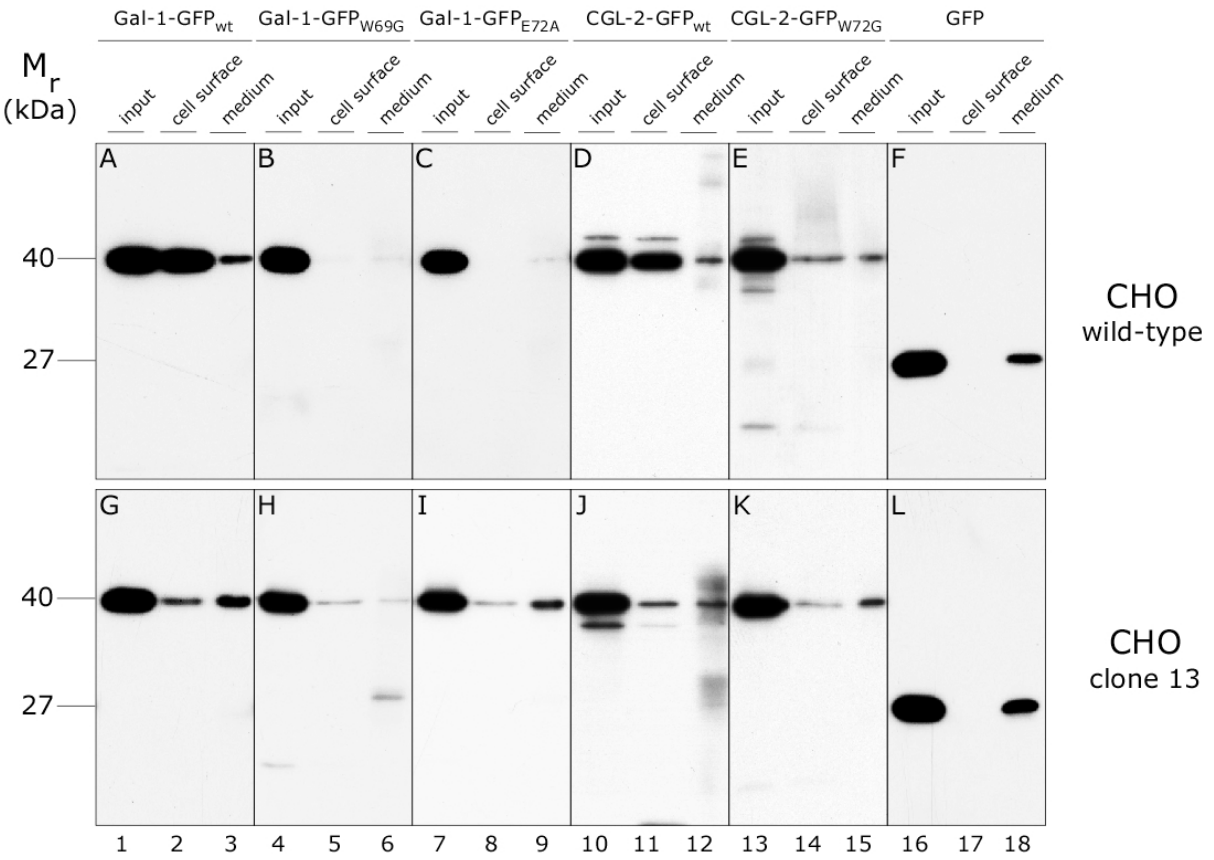

Fig. 36 Comparative analysis of export of galectin-GFP fusion proteins from $CHO_{wild\text{-}type}$ and $CHO_{clone\ 13}$ cells employing cell surface biotinylation and immunoprecipitation from cell culture supernatants. The fusion proteins indicated were expressed in both $CHO_{wild\text{-}type}$ (panels A-F) and $CHO_{clone\ 13}$ cells (panels G-L9) for 48 h at 37°C (6-well plates; 70% confluency; 1 µg/ml doxicycline). The medium was removed and subjected to immuno-precipitation using affinity-purified anti-GFP antibodies. Cell surfaces were treated with a membrane-impermeable biotinylation reagent. Following detergent-mediated cell lysis, biotinylated and non-biotinylated proteins were separated employing streptavidin beads. Aliquots from the input material (lane 1; 0.25%), the biotinylated fraction (lane 2; 25%) and the immunoprecipitate from the cell culture medium fraction (lane 3; 25%) were analyzed by SDS PAGE and Western blotting using affinity-purified anti GFP antibodies.

By contrast, when expressed in $CHO_{clone13}$ cells, the wild-type forms of Gal-1 and CGL-2 GFP fusion proteins failed to get access to the extracellular space as the combined signals for cell surface and medium fractions (Fig. 36, panels G; lanes 2 and 3; and J; lanes 11 and 12) did not differ significantly from the GFP negative control (Fig. 36; panel F and L; lanes 17 and 18) and were largely reduced as

compared to those observed in $CHO_{wild\text{-}type}$ cells (panels A and D). As expected, export of β-galactoside binding deficient mutants (Fig. 36; Gal-1-GFP_{W69G}, Gal-1-GFP_{E72A} and CGL-2-GFP_{W72G}) were not only blocked in $CHO_{wild\text{-}type}$ cells (Fig. 36, panels B, C and E; Fig. 36, panels B, C and E) but also in $CHO_{clone13}$ cells (Fig. 36, panels H, I and K).

In Fig. 37 export from both $CHO_{wild\text{-}type}$ and $CHO_{clone13}$ cells of the various Galectin-GFP fusion proteins (calculating the signals resulting from cells surface biotinylation and immunoprecipitation from the cell culture supernatants) was quantified using fluorescent secondary antibodies employing a LI-COR Odyssey imaging system. For each fusion protein, the combined signals derived from cell surface biotinylation and material from the cell culture supernatant were expressed as percentage of the overall expression level of a given fusion protein. To compare export of the various fusion proteins, secretion of Gal-1-GFP from $CHO_{wild\text{-}type}$ cells was set to 100%. The wild-type forms of both Gal-1-GFP and CGL-2-GFP are secreted from $CHO_{wild\text{-}type}$ cells; however, export is largely reduced when Gal-1-GFP and CGL-2-GFP are expressed in $CHO_{clone13}$ cells. The various mutant forms of Gal-1 and CGL-2 are neither exported from $CHO_{wild\text{-}type}$ nor from $CHO_{clone13}$ cells to a significant extent.

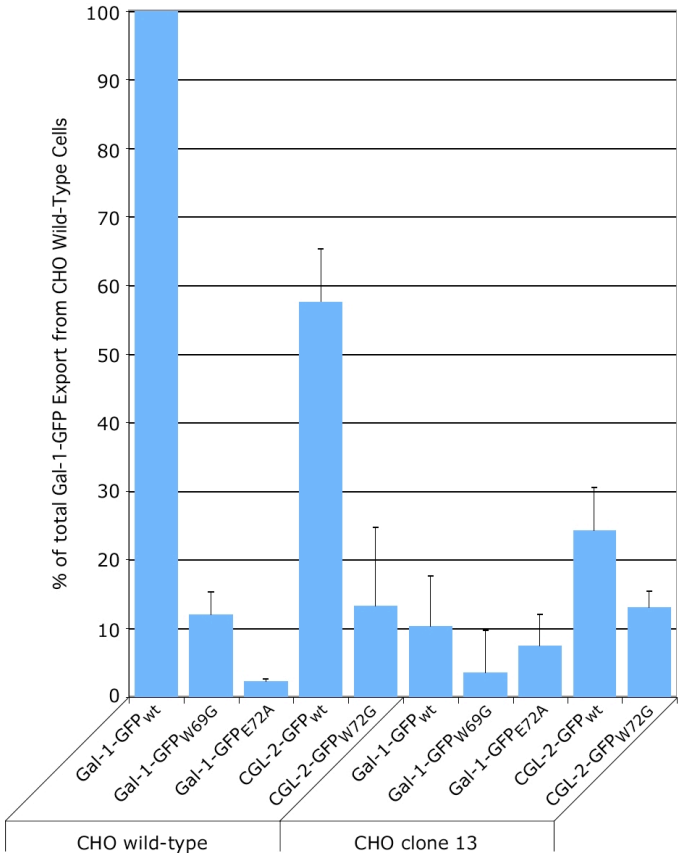

Fig. 37 Quantification of export of galectin-GFP fusion proteins from $CHO_{wild\text{-}type}$ and $CHO_{clone13}$ cells employing cell surface biotinylation and immunoprecipitation from cell culture supernatants. The fusion proteins indicated were expressed in both $CHO_{wild\text{-}type}$ and $CHO_{clone13}$ cells for 48 h at 37°C (6-well plates; 70% confluency). The medium was removed and subjected to immunoprecipitation using affinity-purified anti-GFP antibodies. Cell surfaces were treated with a membrane-impermeable biotinylation reagent. Following detergent-mediated cell lysis, biotinylated and non-biotinylated proteins were separated employing streptavidin beads. Aliquots from the input material (0.25%), the biotinylated fraction (25%) and the immunoprecipitate from the cell culture medium fraction (25%) were analyzed by SDS PAGE and Western blotting using affinity purified anti-GFP antibodies. Primary antibodies were detected with alexa 680-coupled anti-rabbit secondary antibodies. Signal for Gal-1-GFP fusion proteins and GFP were quantified using a Li-COR Odyssey imaging system. The combined signals for the cell medium and the material associate with the cell surface were calculated as a percentage of total amounts of galectin-GFP fusion protein expressed in each case. These data were corrected for unspecific release as monitored by GFP present in the medium of the cells. The extracellular population of Gal-1-GFP secreted from $CHO_{wild\text{-}type}$ cells was set to 100%.

3.3.3.2.3 Subcellular distribution of Gal-1-GFP and CGL-2-GFP reporter molecules in $CHO_{wild\text{-}type}$ and $CHO_{clone13}$ cells

Galectins are synthesized on free ribosomes in the cytosol and delivered to the outer leaflet of the plasma membrane. Mutations of single amino acids in human Gal-1 and fungal CGL-2 may result in a change of cytosolic distribution leading to an export defect. To compare the subcellular distribution of Gal-1 and CGL-2 mutant forms with the corresponding wild-type proteins, the cell lines described above (3.3.3.2.2) were analyzed by confocal microscopy (Fig. 38).

In Fig. 38 a typical subset of Gal-1- and CGL-2-GFP reporter molecules deficient in export and binding to β-galactosides was analyzed employing confocal microscopy. CHO cells and $CHO_{clone13}$ cells were grown on glass cover slips for 48 h at 37°C in the presence of doxicycline. In contrast to the live-imaging cells, fixed CHO cells and $CHO_{clone13}$ cells were incubated with affinity-purified anti-GFP antibodies and anti-rabbit alexa 546 antibodies to detect GFP fusion protein bound to the cell surface.

When living $CHO_{wild\text{-}type}$ cells were visualized, all reporters were found in the cytoplasm as well as to some extent to the nucleus (Fig. 38, first column). In general, a similar picture was observed following fixation both for $CHO_{wild\text{-}type}$ and $CHO_{clone13}$ cells (Fig. 38, second and fourth column); however, in some cases aggregates or particulate structures were observed that apparently represent fixation artifacts. Consistent with the FACS experiments shown in Fig. 27, cell surface staining of all cell lines employing affinity-purified anti-GFP antibodies revealed an extracellular population in $CHO_{wild\text{-}type}$ cells only for the wild-type forms of Gal-1-GFP and CGL-2-GFP (Fig. 38, third column). In $CHO_{clone13}$ cells, cell surface staining could not be detected for any of the reporter molecules including the wild-type forms of Gal-1 and CGL-2 (Fig. 38, fifth column).

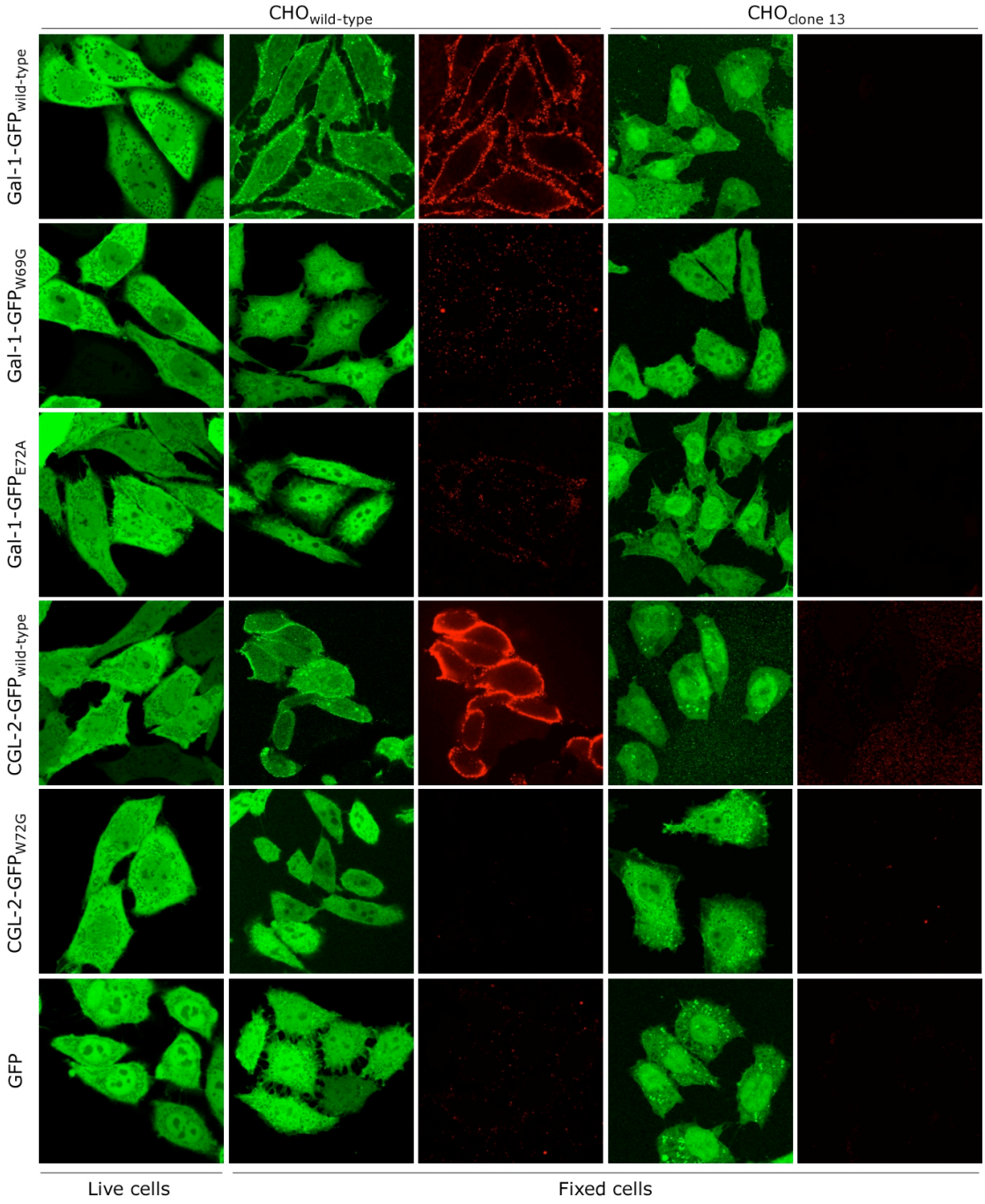

Fig. 38 Subcellular distribution of Gal-1-GFP and CGL-2-GFP reporter molecule in $CHO_{wild\text{-}type}$ and $CHO_{clone13}$ as revealed by confocal microscopy. 1st row, Gal-1-GFP; 2nd row, Gal-1-GFP_{W69G}; 3rd row, Gal-1-GFP_{E72A}; 4th row, CGL-2-GFP; 5th row, CGL-2-GFP_{W72G}; 6th row, GFP. 1st column, GFP live imaging; 2nd column, GFP imaging of fixed $CHO_{wild\text{-}type}$ cells; 3rd column, cell surface staining of fixed $CHO_{wild\text{-}type}$ cells employing affinity-purified anti-GFP antibodies; 4th column, GFP imaging of fixed $CHO_{clone13}$ cells; 5th column, cell surface staining of fixed $CHO_{clone13}$ cells employing affinity-purified anti-GFP antibodies.

3.3.3.3 Characterization of Gal-1 mutants showing inconsistent phenotypes regarding export and binding to β-galactosides

Data obtained for some Gal-1 mutants were not consistent employing the known assays (3.2.2, 3.2.3, 3.2.4, 3.2.5) and therefore it was not possible to classify the various mutants. They do not have the same characteristics as the wild-type form of Gal-1 regarding export and binding ability employing the secretion and binding assays. However, they do also not behave like the identified mutants deficient in binding and export.

Fig. 39 shows the average of three independent experiments of the FACS-based secretion assay. The expression level and the cell surface staining of wild-type Gal-1-GFP as positive control for secretion (standard condition: 1 µg/ml doxicycline, 48 h), detected by affinity-purified anti-GFP antibodies followed by treatment with APC-conjugated secondary antibodies, was set to 100%. Several doxicycline concentrations ranging from 1 µg/ml to 0.02 µg/ml were applied to be able to compare cell surface signals obtained from mutant cell lines expressing the reporter molecules at different levels. GFP was used as a negative control for secretion (3.2.2).

To confirm independently the export behavior of the various mutant proteins the cell surface biotinylation assay in combination with immunoprecipitation from the cell culture medium was performed (Fig. 40). It is of great importance to combine these secretion assays with the analysis of β-galactoside binding ability to characterize each mutant. Therefore the binding ability was investigated using the CHO cell-based *in vivo* assay (Fig. 41) and the *in vitro* assay employing lactose-coupled beads (Fig. 42).

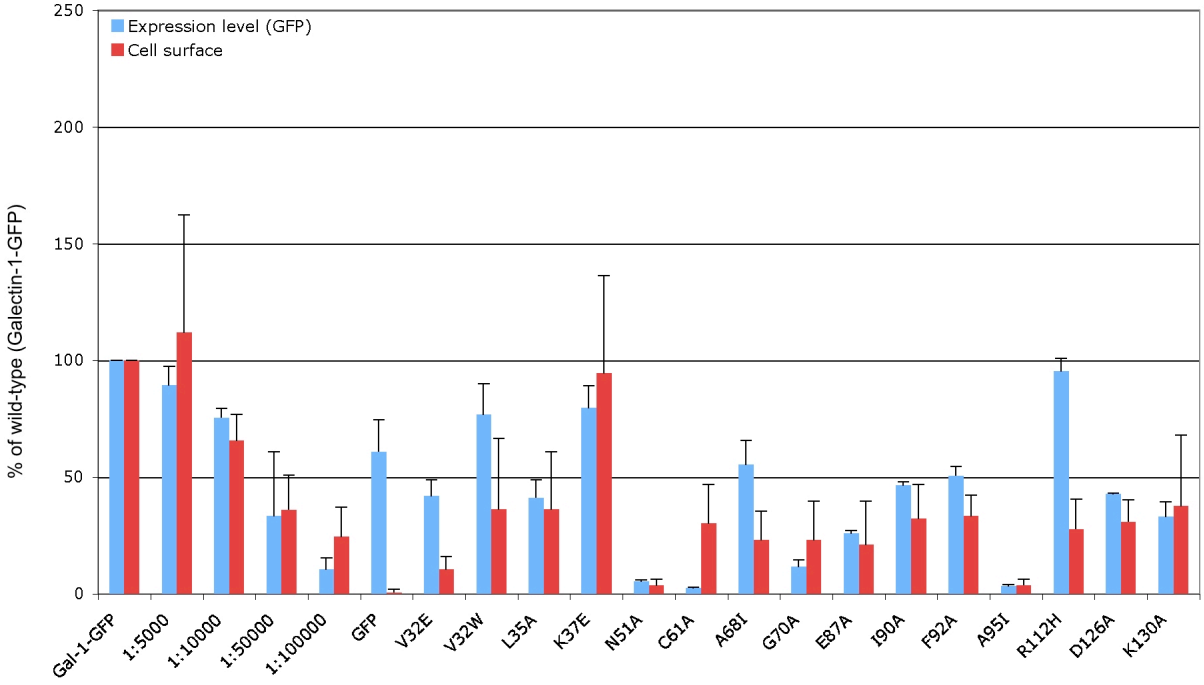

Fig. 39 Quantitative analysis of export of various galectin-GFP fusion proteins from CHO cells employing flow cytometry. CHO cells were grown on 6-well plates and induced with doxicycline for 48 h at 37°C to express the fusion protein indicated. Following removal of medium, cells were labeled with affinity-purified anti-GFP antibodies followed by detachment of the cells using PBS/EDTA. GFP (expression level; blue) and APC-derived fluorescence (cell surface; red) were quantified by flow cytometry using Becton Dickinson FACSCalibur system (n=4)

The cell lines CHO Gal-1-GFP$_{N51A}$, CHO Gal-1-GFP$_{C61A}$, CHO Gal-1-GFP$_{G70A}$, CHO Gal-1-GFP$_{E87A}$ and CHO Gal-1-GFP$_{A95I}$ showed inconsistent results concerning export and binding to β-galactoside-containing counter receptors. This is probably due to a reduced stability of the mutated proteins as indicated by low expression levels determined by the GFP fluorescence measured in the FACS-based assay.

Regarding the results of the secretion assays (Fig. 39 and Fig. 40) the mutants I90A, F92A, D126A and K130A were expressed and exported at levels comparable to the wild-type form of Gal-1. These observations are not consistent with the fact that these mutants were deficient in binding to β-galactosides employing lactose-coupled beads (Fig. 42). Employing the *in vivo* binding assay all mutant showed a

reduced binging ability to β-galactoside-containing counter receptors on the cell surface of CHO cells (Fig. 41).

Gal-1-GFP$_{V32E}$:

The expression of the mutant protein V32E was slightly reduced (Fig. 39). However, the amount of expressed protein was sufficient to investigate the secretion from CHO cells employing flow cytometry and the cell surface biotinylation assay. The cell surface staining employing both secretion assays was reduced (Fig. 39, 10% cell surface staining; Fig. 40, lane 2 and 3). This mutant was able to bind to counter receptors analyzed by binding to CHO cells (Fig. 41, 52%) and to lactose-coupled beads (Fig. 42, lane 3). According to the ability to bind to its counter receptors, the mutation seems to cause a partial export defect independent of the ability to bind to β-galactosides.

Gal-1-GFP$_{V32W}$:

Changing the amino acid valin on position 32 into tryptophane (V32W) did not result in a reduced binding capacity to counter receptors (Fig. 41, 67%; Fig. 42, lane 3). However, the cell surface signal employing flow cytometry (Fig. 39, 36%) and the biotinylation assay (Fig. 40, lane 2 and 3) was slightly reduced indicating that this mutant is also partially defective in export mutant without being impaired in binding to β-galactosides.

Gal-1-GFP$_{L35A}$:

The FACS-based secretion assay (Fig. 39) and the cell surface biotinylation assay (Fig. 40) of the Gal-1 mutant L35A indicated no export and binding defect. In both assays there was protein bound to the cell surface comparable to the wild-type form of Gal-1. Investigating the binding properties of this mutant the binding ability was highly reduced (Fig. 41, 26%). Strikingly, no binding to lactose-coupled beads was detectable (Fig. 42, lane 3). According to both assays (Fig. 41 and Fig. 42) no exported protein should be able to bind to the cell surface. The cell surface signal may result from unspecific binding of this mutated protein. However, regarding the secretion assays this mutant seems to be exported.

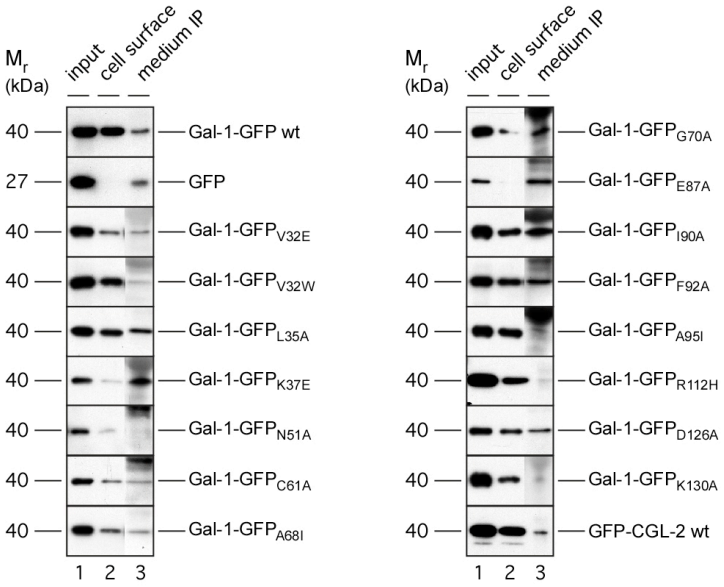

Fig. 40 Biochemical analysis of export of various galectin-GPF fusion proteins from CHO cells employing cell surface biotinylation and immunoprecipitation from cell culture supernatants. The fusion proteins indicated were expressed in CHO cells for 48 h at 37°C (6-well plates; 70% confluency; 1 µg/ml doxicycline) The medium was removed and subjected to immunoprecipitation using affinity-purified anti-GFP antibodies. Cells were treated with a membrane-impermeable biotinylation reagent. Following detergent-mediated cell lysis biotinylated and non-biotinylated proteins were separated employing streptavidin beads. Aliquots from the input material (lane 1; 1%), the biotinylated fraction (lane 2; 10%) and the immunoprecipitate from the cell culture medium fraction (lane 3; 50%) were analyzed by SDS PAGE and Western blotting using affinity-purified anti-GFP antibodies.

Gal-1-GFP$_{K37E}$:

The data obtained for the mutant Gal-1 K37E were highly inconsistent. Employing flow cytometry (Fig. 39) the expression level was comparable to the wild-type form of Gal-1. The cell surface staining detecting exported protein bound to the cell surface was reduced indicating that there is reduced export efficiency (Fig. 39, 26%). These results were confirmed by the cell surface biotinylation assay in combination with immunoprecipitation from cell culture medium (Fig. 40, lane 2, cell surface and lane 3, immunoprecipitation of the medium of expressing cell). Employing the *in vivo* binding assay the mutant was able to bind to the cell surface even better than the wild-type indicating that this mutation results in an export defect. Regarding the *in vitro* binding assay, which was not consistent with the *in vivo* assay, the binding ability was reduced, indicating that this mutant is impaired in binding and export. Taken together this mutant protein seems to be exported to a lower extent compared to the wild-type form of Gal-1.

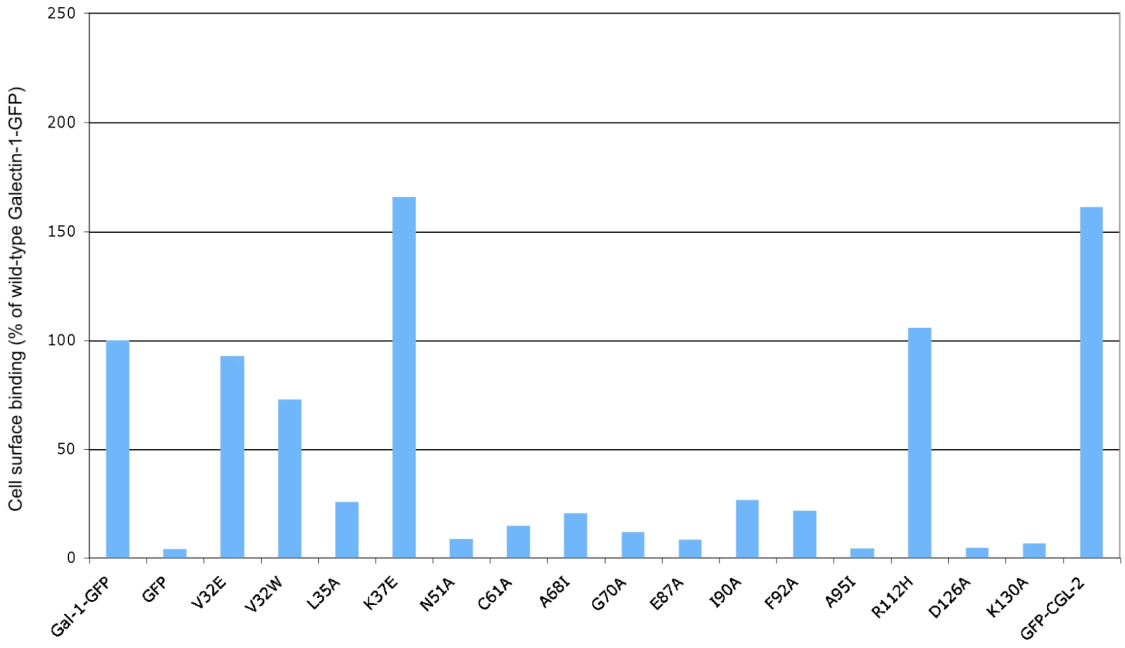

Fig. 41 Analysis of β-galactoside binding efficiency of various galectin-GFP fusion proteins based on binding to CHO cells. The various fusion proteins indicated were expressed in CHO cells. Cell-free supernatant were prepared and normalized by GFP fluorescence. The various supernatants were then incubated with CHO cells for 1 h at 4°C to allow cell surface binding. Following treatment with affinity-purified anti-GFP antibodies and APC-conjugated secondary antibodies, cell surface binding was quantified by flow cytometry.

Gal-1-GFP$_{A68I}$:

The mutant A68I seemed to be impaired in binding and export. Both secretion assays (Fig. 39 and Fig. 40) indicated a reduced cell surface signal, which is consistent with hypothesis that binding to β-galactosides is required for Gal-1 export. The binding efficiency in the *in vivo* assay was reduced (Fig. 41, 20%), however, as analyzed by the *in vitro* assay, the ability to bind to lactose-coupled beads is comparable to the wild-type form of Gal-1.

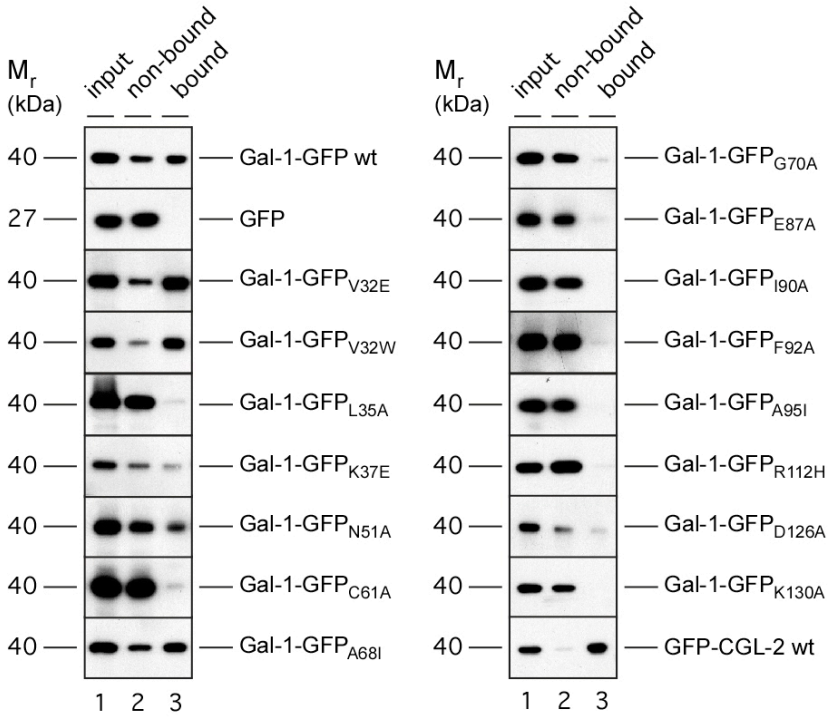

Fig. 42 Analysis of β-galactoside binding efficiency of various galectin-GFP fusion proteins based on binding to lactose-coupled beads. Detergent lysates normalized by GFP fluorescence were incubated with lactose beads for 1 h at 4°C. The non-bound fraction was separated and, following extensive washing, bound material was eluted with SDS sample buffer. Input (lane 1, 5%), non-bound material (lane 2, 5%) and bound material (lane 3, 5%) were analyzed by SDS PAGE and Western blotting using affinity-purified anti-GFP antibodies.

Gal-1-GFP$_{R112H}$:

The expression level of the mutant R112H based on the GFP fluorescence measured by the FACS was comparable to the wild-type form of Gal-1-GFP (Fig. 39, 95%), whereas the exported fraction indicated by cell surface staining is largely reduced (Fig. 40, 27.5%). This is consistent with the data obtained from the cell surface biotinylation assay. There was an exported population bound to the cell surface, but the signal was clearly reduced compared to the wild-type form of Gal-1-GFP. It is known from literature that this mutant does not result in a binding defect to β-galactosides (Lopez-Lucendo et al., 2004). Analyzing the binding ability employing the *in vivo* assay this observation could be confirmed (Fig. 41, 105%). However, the results obtained from the *in vitro* binding assay (Fig. 42) are not consistent with these

data. These observations suggest that mutant R112H is export-deficient without losing the ability to bind to its counter receptors.

Mutation	Phenotype
Gal-1-GFP	
V32E	Reduced expression in both secretion assays; reduced cell surface staining in both assays; no binding defect
V32W	Comparable expression in both secretion assays; reduced cell surface staining in both assays; no binding defect
L35A	No export and binding defect indicated by both secretion assays; binding ability is reduced in both binding assays
K37E	Employing flow cytometry, no binding and no export defect; employing biotinylation assay reduced cell surface staining; no binding defect in the in-vivo binding assay; reduced binding ability employing the in-vitro binding assay
N51A	Very low expression level in both secretion assays; no cell surface staining; reduced binding ability in both binding assays
C61A	Low expression level in the FACS-based assay and biotinylation assay; binding defect
A68I	Impaired in binding and export employing flow cytometry, biotinylation assays and the in vivo binding assay; inconsistent data employing the in-vitro binding assay
G70A	Cell surface staining in both secretion assay; impaired in binding to β-galactosides in both binding assays
E87A	Cell surface staining employing the biotinylation assay; no cell surface staining employing flow cytometry; impaired in binding to β-galactosides in both binding assays
I90A	Cell surface staining in both secretion assay; impaired in binding to β-galactosides in both binding assays
F92A	Cell surface staining in both secretion assay; impaired in binding to β-galactosides in both binding assays
A95I	No detectable population on the cell surface employing flow cytometry; cell surface staining in the biotinylation assay; impaired in binding to β-galactosides in both binding assays
R112H	Reduced cell surface staining in both secretion assays; no binding defect employing both binding assays.
D126A	Cell surface staining in both secretion assay; impaired in binding to β-galactosides in both binding assays
K130A	Cell surface staining in both secretion assay; impaired in binding to β-galactosides in both binding assays

Table 8 Summary of various human Gal-1 mutants

3.3.3.4 Characterization of truncated human Gal-1

The molecular structure of human Gal-1 involves a β-sandwich consisting of two antiparallel β-sheets of five (Fi-F5) and six (S1-S6a/b) strands, respectively. The N- and C-terminus of each monomer are positioned at the dimer interface and the carbohydrate recognition domains are located at the far ends of the same face of the surface, which presents a long negatively charged cleft in the cavity (Fig. 3). Dimer formation of galectins is important for their biological roles, based on bivalency, Gal-1 has cross-linking properties. So far it is not known if Gal-1 is secreted as monomer or as homodimer. In order to investigate the influence of the dimer formation on the unconventional secretion of Gal-1, CHO cells expressing truncated versions of human Gal-1 as GFP fusion proteins were generated by retroviral transduction. Therefore either the N-terminus (Gal-1-GFP ΔN5, ΔN10 and ΔN20) or the C-terminus of Gal-1 (GFP-Gal-1 ΔC4, ΔC9, ΔC20, ΔC30, ΔC40, ΔC50) was deleted. Additionally, a clonal CHO cell line was generated expressing Gal-1 truncated at the N-terminus and the C-terminus (Gal-1-GFP ΔN10-C129). The orthologue CGL-2 was again used as additional positive control. Accordingly, CHO cells were generated to express truncated forms of CGL-2. The truncated galectins were investigated regarding export from CHO cells and β-galactoside binding ability employing the secretion and binding assays described in the previous sections.

Fig. 43 shows the FACS-based secretion assay of the truncated Gal-1 fusion proteins. The expression level and the cell surface staining of Gal-1-GFP were set to 100%.

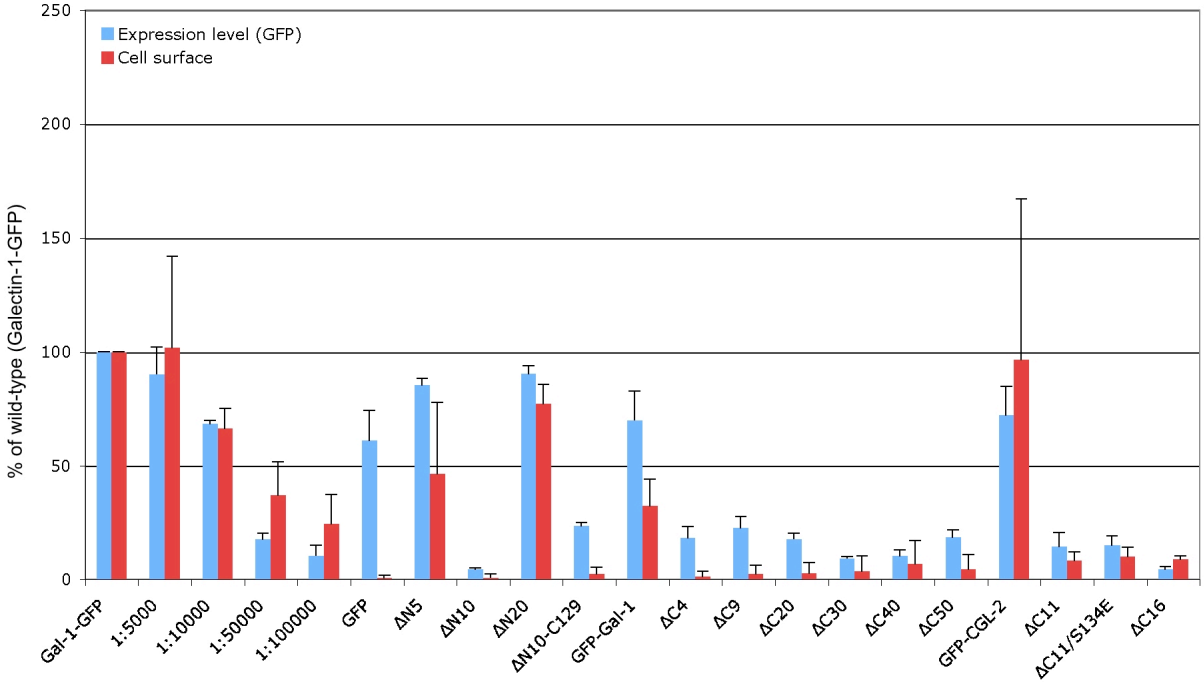

Fig. 43 Quantitative analysis of export of various galectin-GFP fusion proteins from CHO cells employing flow cytometry. CHO cells were grown on 6-well plates and induced with doxicycline for 48 h at 37°C to express the fusion protein indicated. Following removal of medium, cells were labeled with affinity-purified anti-GFP antibodies followed by detachment of the cells using PBS/EDTA. GFP (expression level; blue) and APC-derived fluorescence (cell surface; red) were quantified by flow cytometry using Becton Dickinson FACSCalibur system (n=4).

The CHO cell lines Gal-1-GFP$_{\Delta N10}$, CHO Gal-1-GFP$_{\Delta N10\text{-}C129}$, CHO Gal-1-GFP$_{\Delta C4}$, CHO Gal-1-GFP$_{\Delta C9}$, CHO Gal-1-GFP$_{\Delta C20}$, CHO Gal-1-GFP$_{\Delta C30}$, CHO Gal-1-GFP$_{\Delta C40}$, CHO Gal-1-GFP$_{\Delta C50}$, CHO CGL-2-GFP$_{\Delta C11}$, CHO CGL-2-GFP$_{\Delta C11/S134E}$ and CHO CGL-2-GFP$_{\Delta C16}$ express the various GFP fusion protein at very low levels measured by the GFP fluorescence employing flow cytometry. This is most likely caused by reduced stability of these truncated proteins. Due to the low expression level it was difficult to analyze these mutants for their export behavior in CHO cells (Fig. 43).

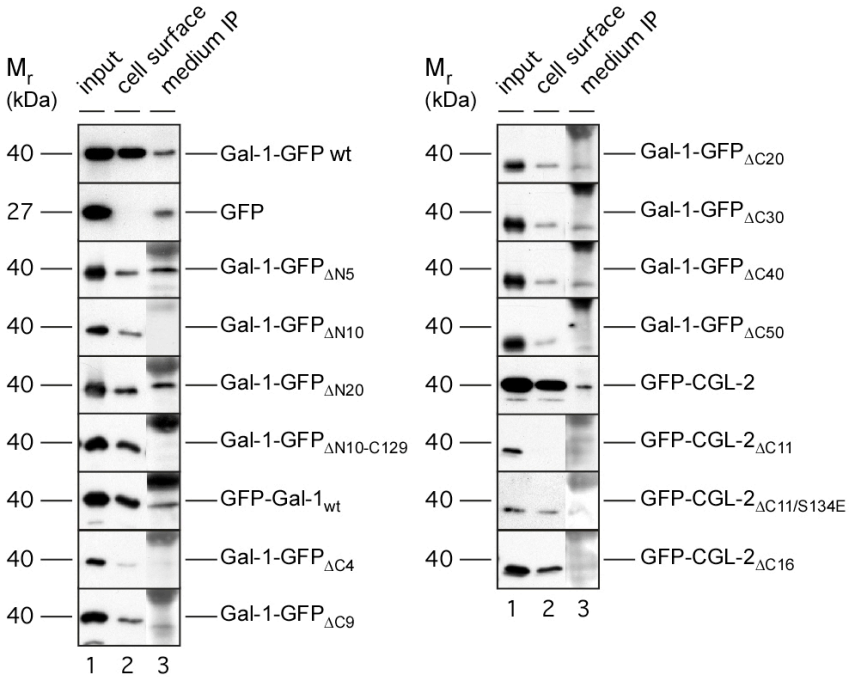

Fig. 44 Biochemical analysis of export of various galectin-GPF fusion proteins from CHO cells employing cell surface biotinylation and immunoprecipitation from cell culture supernatants. The fusion proteins indicated were expressed in CHO cells for 48 h at 37°C (6-well plates; 70% confluence; 1 µg/ml doxicycline) The medium was removed and subjected to immunoprecipitation using affinity-purified anti GFP antibodies. Cells were treated with a membrane-impermeable biotinylation reagent. Following detergent-mediated cell lysis biotinylated and non-biotinylated proteins were separated employing streptavidin beads. Aliquots from the input material (lane 1; 1%), the biotinylated fraction (lane 2; 10%) and the immunoprecipitate from the cell culture medium fraction (lane 3; 50%) were analyzed by SDS PAGE and Western blotting using affinity-purified anti-GFP antibodies.

To confirm the observations made by the FACS-based secretion assay, CHO cells expressing the truncated Gal-1 and CGL-2 GFP fusion proteins in a doxicycline-dependent manner, were subjected to cell surface biotinylation assay in combination with immunoprecipitation of the cell culture medium to detect soluble exported protein. Since there was no cell surface signal and no precipitated material observed, it can be concluded that all these mutated proteins failed to get externalized by the mammalian export machinery (Fig. 44, lane 2).

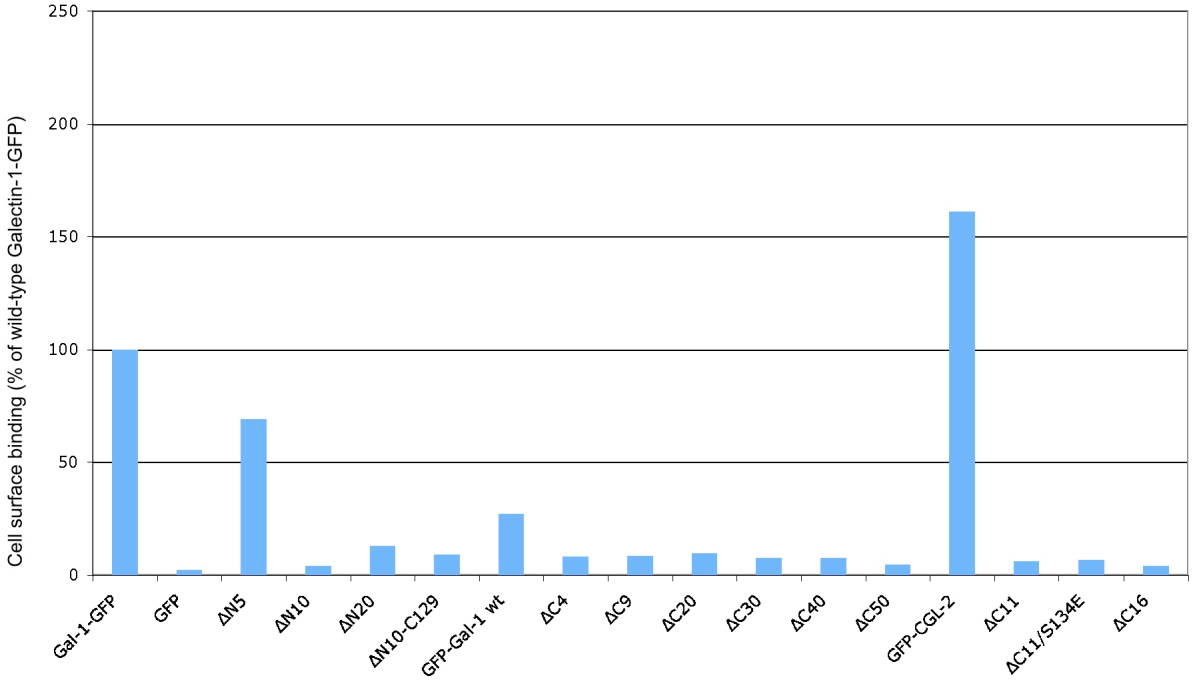

Fig. 45 Analysis of β-galactoside binding efficiency of various galectin-GFP fusion proteins based on binding to CHO cells. The various fusion proteins indicated were expressed in CHO cells. Cell-free supernatant were prepared and normalized by GFP fluorescence. The various supernatants were then incubated with CHO cells for 1 h at 4°C to allow cell surface binding. Following treatment with affinity-purified anti-GFP antibodies and APC-conjugated secondary antibodies, cell surface binding was quantified by flow cytometry.

Investigating the binding ability of these mutant proteins to β-galactoside-containing counter receptors, cell-free supernatant of the various GFP reporter molecules was incubated with CHO cells in order to allow binding of the truncated GFP fusion proteins to the cell surface. Following incubation with affinity-purified anti-GFP antibodies and secondary APC-conjugated antibodies, binding to cell surface was measured by flow cytometry (Fig. 45). Binding of Gal-1-GFP to CHO cell was set to 100% and GFP was used as negative control. For the *in vitro* assay detergent lysates of the various GFP fusion proteins were incubated with lactose-coupled beads. The binding ability was analyzed by SDS-PAGE and Western blotting using affinity-purified anti-GFP antibodies. None of the GFP fusion protein was able to bind to its ligand employing the *in vivo* and the *in vitro* binding assay (Fig. 45 and Fig. 46).

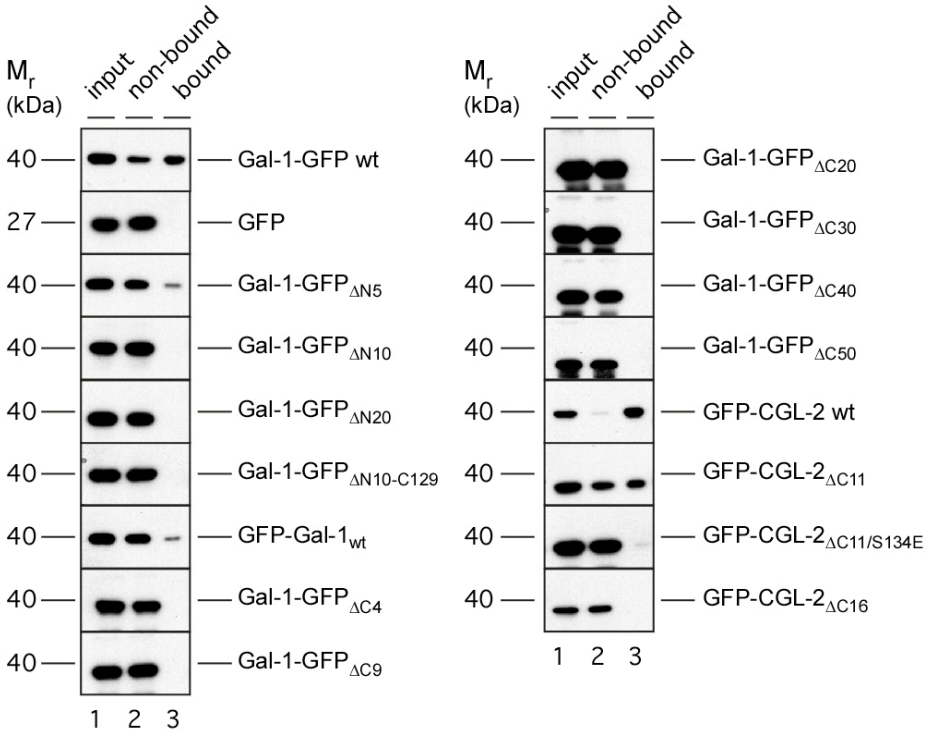

Fig. 46 Analysis of β-galactoside binding efficiency of various galectin-GFP fusion proteins based on binding to lactose-coupled beads. Detergent lysates normalized by GFP fluorescence were incubated with lactose beads for 1 h at 4°C. The non-bound fraction was separated and, following extensive washing, bound material was eluted with SDS sample buffer. Input (lane 1, 5%), non-bound material (lane 2, 5%) and bound material (lane 3, 5%) were analyzed by SDS PAGE and Western blotting using affinity purified anti-GFP antibodies.

As shown in Fig. 43 the expression of the N-terminal truncations ΔN5 and ΔN20 was induced in the presence of doxicycline. The cell surface signal of Gal-1-GFP$_{\Delta N5}$ was slightly reduced as compared to Gal-1-GFP. The export efficiency of Gal-1-GFP$_{\Delta N20}$ was similar to the wild-type form of Gal-1-GFP as indicated by the cell surface signal employing flow cytometry. The data obtained in the biotinylation assay were consistent with the observations made in the FACS-based secretion assay (Fig. 44). Investigating binding to the cell surface and to lactose-coupled beads Gal-1-GFP$_{\Delta N5}$ was able to interact with β-galactosides in both assays (Fig. 45 and Fig. 46). The truncation ΔN20 resulted in a loss of binding ability to counter receptors in the *in vivo* and in the *in vitro* assay. However, these observations are not consistent with the fact that ΔN20 was detectable bound to the cell surface employing both secretion assays (Fig. 45 and Fig. 46). Further studies are needed to clarify this contradiction.

Taken these observations together it is difficult to conclude whether dimer formation is required for export. However, if the deletion of the N- or C-termini results in a defect in binding to counter receptors on the cell surface, an export defect was observed, consistent with the hypothesis that binding to β-galactosides is required for the unconventional secretion of Gal-1.

4 Discussion

The majority of extracellular proteins is exported from mammalian cells by the ER/Golgi-dependent secretory pathway, which is well characterized at the molecular level. All eukaryotic cells from yeast to man are characterized by this secretory machinery that recognizes signal peptide-containing proteins resulting in their translocation across the membrane of the endoplasmic reticulum (ER) (Schatz and Dobberstein, 1996). Once localized to the lumen of the ER, secretory proteins are packaged into transport vesicles provided they pass ER quality control measures, a process that results in cargo delivery to the Golgi apparatus (Lee et al., 2004). Upon fusion of post-Golgi transport carriers with the plasma membrane, classical secretory proteins get released into the extracellular space (Keller and Simons, 1997; Palade, 1975).

In addition to signal peptide-containing secretory proteins, a heterogeneous group of extracellular proteins has been discovered that does not make use of signal peptide-dependent secretory transport. Both the release mechanisms and the molecular identity of the secretory machineries involved have remained elusive while these secretory proteins have defined extracellular functions, they do not contain functional signal peptides and, consistently, are rejected by the ER membrane translocation machinery (Cleves, 1997; Hughes, 1999; Nickel, 2003; Nickel, 2005; Prudovsky et al., 2003). Furthermore, the extracellular appearance of such molecules is not compromised in the presence of brefeldin A (BFA), a drug that blocks ER/Golgi-dependent secretory transport. These observations led to the postulation of alternative secretory mechanisms in eukaryotic cells that are fully functional in the absence of an intact ER/Golgi system. Interestingly, unconventional secretory proteins comprise a group of molecules of high biomedical relevance such as the proangiogenic growth factor FGF-2. FGF-2 is a tumor-produced, direct-acting stimulator of angiogenesis, a process that is essential for tumor growth and metastasis (Nugent and Iozzo, 2000). Other examples include inflammatory cytokines such as interleukin 1β (Braddock and Quinn, 2004) and migration inhibitory factor (MIF) (Lue et al., 2002) as well as a family of stage-regulated surface

molecules from Leishmania parasites termed hydrophilic acylated surface proteins (HASP) implicated in host cell infection (Denny et al., 2000; Stegmayer et al., 2005).

Gal-1 is another remarkable member of unconventionally secreted proteins. This lectin of the extracellular matrix is involved in many cellular processes like differentiation, proliferation, cell adhesion and tumor-mediated immune suppression (Perillo et al., 1995) and binds to β-galactosides on glycoproteins and glycolipids of the plasma membrane. By elucidating the molecular machinery, it would be possible to develop or to find inhibitors, which specifically block secretion of Gal-1. Therefore one aim of the present thesis was to establish an experimental system based on genetically modified CHO cell lines to investigate the export of Gal-1 *in vivo*. Additionally, interacting proteins with Gal-1 were isolated and analyzed for a potential function in the molecular export mechanism of Gal-1 employing the established cell system. Furthermore, based on this system single amino acid mutants of Gal-1 were generated to identify the export targeting motif by investigating their export behavior and their binding ability to β-galactosides.

4.1 Identification and characterization of CA125 as a Gal-1 counter receptor

Protein-protein and protein-carbohydrate interaction studies were performed in order to affinity-purify proteins that interact with human Gal-1. Employing mass spectrometry one of the obtained Gal-1 interacting partners was identified as CA125. This conclusion was drawn from the fact that 16 tryptic peptides could be identified as parts of the translation product of the cDNA clone AK024365 (NCBI) that, based on sequence information reported by laboratories of Lloyd and O'Brien, encodes the 1148 C-terminal amino acids of CA125 (CA125-C-TERM) (O'Brien et al., 2001; Yin and Lloyd, 2001). These results were confirmed by immunological identification of CA125-derived antigens by both the original anti-CA125 antibody OC125 (Bast et al., 1981) and a rabbit antiserum directed against the N-terminal 356 amino acids of CA125-C-TERM. Since the majority of the material bound to the Gal-1 affinity matrix

was eluted with lactose, it was concluded that the interaction is galactose dependent. These data were confirmed by experiments demonstrating that the interaction between CA125-C-TERM and Gal-1 both *in vitro* and *in vivo* is almost completely abolished when CA125-C-TERM is expressed in a CHO mutant that is deficient for galactosylation of glycoproteins and glycolipids (Deutscher and Hirschberg, 1986). Interestingly, CA125-C-TERM binding to Gal-1 is only partially inhibited when cells were grown in the presence of tunicamycin, a drug that inhibits *N*-glycosylation. These data demonstrated that the interaction of CA125-C-TERM with Gal-1 largely depends on O-linked β-galactose-terminated oligosaccharide chains.

CA125 was originally discovered by Bast and colleagues using the ovarian cell line OVCA433 as an immunogen for the generation of monoclonal antibodies (Bast et al., 1981). However, ever since, the molecular identity and biological function of the CA125 cancer antigen has remained elusive. From immunological studies, CA125 is known to be present on the cell surface of ovarian cancer cells; however, it has also been found in other carcinomas and, to a limited extent, in normal secretory tissues (Hardardottir et al., 1990; O'Brien et al., 2001; Zurawski et al., 1988). The results may provide the first insight into a potential biological function of CA125, as there exists a link to a family of β-galactoside-specific lectins of the ECM, the galectins (Barondes et al., 1994; Hughes, 1999; Perillo et al., 1998; Rabinovich et al., 2002a). This observation might be of significant biomedical importance, since galectins themselves are tumor markers involved in the regulation of cell proliferation and tumor progression (Perillo et al., 1998). In this context, CA125 cell surface expression by tumor tissues might effect cell attachment to the ECM in a Gal-1-dependent manner (Seelenmeyer et al., 2003).

Two research groups independently succeeded in cloning the gene that encodes CA125 (O'Brien et al., 2001; Yin and Lloyd, 2001), showing that CA125 is a giant mucin-like glycoprotein that consists of more than 11,000 amino acids. Full-length CA125 has been suggested to represent a type I transmembrane protein with a single membrane-spanning domain close to the C-terminus. The extracellular domain contains repeat structures that are likely to be heavily O-glycosylated (O'Brien et al., 2001). Besides its nature as an integral membrane protein, soluble

fragments of CA125 have been observed (Fendrick et al., 1997; Lloyd and Yin, 2001). Apparently, phosphorylation of the cytoplasmic domain causes extracellular cleavage of the N-terminal domain, which results in the release of soluble fragments into the extracellular space (Fendrick et al., 1997; Lloyd and Yin, 2001).

4.2 Specificity of CA125 binding to Galectins

Gal-1 is the primary ligand for CA125 in comparison to Gal-3 (Seelenmeyer et al., 2003), the second most-abundant member of the galectin family. The observed interaction does not appear to represent a simple carbohydrate-lectin-interaction but rather depends on additional aspects of specificity based on the proteinaceous environment. Moreover, as CA125-C-TERM expressed in CHO cells showed an even higher preference towards binding to Gal-1, it seems that the cellular background in which CA125 is expressed also has a significant influence on its binding efficiency for members of the galectin family. Therefore, on the basis of these experiments, CA125 represents a specific galectin counter receptor with Gal-1 as the primary ligand. Since CA125 expression appears to be largely restricted to tumor cells, it seems likely that tumor cell attachment to the ECM can be modulated in a Gal-1 dependent manner (Seelenmeyer et al., 2003).

CA125-C-TERM encodes about three O-glycosylated repeat structures and the N-and O-glycosylated stalk structure of the extracellular domain, the transmembrane span and the cytoplasmic domain of full-length CA125. These structural features are consistent with the finding that CA125-C-TERM retains binding activity towards Gal-1. Intriguingly, expression of this construct in both CHO and HeLa cells results in CA125-C-TERM cell surface expression. In spite of the lack of an N-terminal signal peptide in both full-length CA125 and CA125-C-TERM, CA125-C-TERM cell-surface localization is mediated by ER/Golgi dependent secretory transport. Thus, CA125 represents a classical secretory cargo protein whose molecular mechanism of insertion into the membrane of the ER might be interesting to investigate. As signal-peptide-independent mechanisms of protein insertion into the ER have been described (Kutay et al., 1995), it will also be of interest to analyze how CA125 ER

insertion compares with these known processes. In the case of CA125 its signal sequence might to be internal. An internal signal sequence leads the ribosome to the ER membrane. Like the N-terminal ER signal sequence, the internal signal sequence is recognized by an SRP, which brings the ribosome to the ER membrane and serves as a start-transfer signal that initiates the translocation of the protein. After release from the translocator, the internal start transfer sequence remains in the lipid bilayer as a single membrane-spanning α-helix. Internal start-transfer sequences can bind to the translocation apparatus in two orientations. The orientation of the inserted start-transfer sequence determines, which protein segment is moved across the membrane into the ER lumen. In one case, the resulting membrane protein has its C-terminus on the luminal side, while in other, it has its N-terminus on the luminal side. The orientation of the start-transfer sequence depends on the distribution of nearby charged amino acids. Moreover, given its huge size of more than 11.000 amino acids additionally the mucin-like levels of glycosylation, questions arise about the mode of intracellular transport on its way to the cell surface.

In order to investigate the relevance of the reported interaction regarding the origin of the cell lines used, non-tumor derived CHO cells (Puck et al., 1958) and the Cervix carcinoma cell line S-HeLa (Gey et al., 1952; Scherer et al., 1953) were compared for CA125 expression. While fragments of endogenous CA125 from the S-HeLa cell line could be isolated, no CA125 fragments bound to the Gal-1 affinity matrix could be detected when CHO cells were used as source for Gal-1 interacting proteins. This observation is consistent with the detection of endogenous cell surface CA125 in HeLa cells and the lack of surface localized CA125 in CHO cells based on flow cytometry. Moreover, these data are consistent with studies that suggest that CA125 is expressed primarily in tumor tissues. Employing the FACS based *in vivo* assay, developed in this thesis, HeLa cells were characterized by more than tenfold higher levels of cell-surface Gal-1 when compared with CHO cells. It was shown that CHO and HeLa cells do not differ with regard to total expression levels of Gal-1 as well as cell surface binding capacity for Gal-1. Therefore, HeLa cells seem to be significantly more efficient in the unconventional secretion of Gal-1 compared to CHO cells (Seelenmeyer et al., 2003).

4.3 CA125 expression does not stimulate Gal-1 export

On the basis of the experimental observations mentioned above, it was postulated that CA125-expressing HeLa cells possess a more efficient export pathway for Gal-1 than CA125-deficient CHO cells. However, CA125 expression does not stimulate Gal-1 export as HeLa cells express CA125 on their cell surface only in small amounts. The reason for the more efficient Gal-1 export from HeLa cells compared to CHO cells is likely to be the altered glycosylation pattern on the cell surface of tumor-derived cells rather than a single counter receptor present on the cell surface. Changes in glycan composition are a universal feature of cancer cells (Hakomori, 1986; Wickus and Robbins, 1973), and certain types of glycan structures are well-known markers for tumor progression (Feizi, 1985; Hakomori, 1986). Like normal cells during embryogenesis, tumor cells undergo activation and rapid growth, adhere to a variety of other cell types and cell matrices, and invade tissues. Embryonic development and cellular activation in vertebrates are typically accompanied by changes in cellular glycosylation profiles. Thus, it is not surprising that glycosylation changes are also a universal feature of malignant transformation and tumor progression (Bhaumik et al., 1998; Kang et al., 1996).

The classic reports of increased size of tumor cell glycopeptides have been convincingly explained (Yoshimura et al., 1995) by an increase in β1-6 branching of N-glycans, which results from an enhanced expression of GlcNAc transferase V (Demetriou et al., 1995; Hakomori, 1986). GlcNAc transferase V plays a very important role in cancer biology (Demetriou et al., 1995). The increased expression of GlcNAc transferase V may cause an increase of polylactosamine chains, which are recognized by galectins. The higher amount of Gal-1 counter receptors seems to be responsible for the more efficient export of Gal-1.

4.4 Analysis of Gal-1 and CGL-2 regarding export to the cell surface and binding to β-galactosides

The phenomenon of non-classical protein secretion has been known for more than 15 years (Cooper and Barondes, 1990; Rubartelli et al., 1990); however, the molecular machinery mediating this process remains elusive. It is even unclear whether the various proteins known to be secreted by non-conventional means make use of a common molecular mechanism (Hughes, 1999). In fact, distinct machineries seem to mediate different export processes. For example, the mechanism of IL-1β secretion seems to involve intracellular vesicles (Andrei et al., 1999) whereas Gal-1 is likely to be externalized by plasma membrane blebbing (Mehul and Hughes, 1997). Another example are the distinct characteristics of FGF-1 versus FGF-2 secretion since FGF-1 export is sensitive to heat shock (Jackson et al., 1992), whereas FGF-2 export is not (Mignatti et al., 1992). The relatively poor knowledge about the molecular components involved in these processes emphasizes the need for establishing novel experimental systems in order to reveal the molecular mechanisms of unconventional secretory processes.

A key aspect of this study was to reconstitute Gal-1 secretion in living cells based on read-out methods that provide a precise and quantitative analysis of its export process. Therefore, genetically modified CHO cell lines stably expressing N- and C-terminally GFP-tagged Gal-1 in a doxicycline-dependent manner were generated as follows: CHO cells were transfected with the mouse orthologue of the cationic amino acid transporter (MCAT-1), thereby making them permissive to ecotropic retroviruses (Albritton et al., 1989; Davey et al., 1997). After virus-mediated introduction of a doxicycline-sensitive transactivator (Urlinger et al., 2000) the various galectin-GFP cDNA constructs were integrated into the genomic DNA of the host cells by retroviral transduction (Engling et al., 2002). Following several rounds of FACS sorting cell pools were isolated and functionally characterized with regard to non-conventional secretion of the galectin reporter molecules. Two independent approaches were established to analyze the export of Gal-1-GFP fusion proteins.

i) FACS-based secretion assays. Based on this assay, it was possible to quantitatively assess the amount of Gal-1 released to the extracellular space in living cells. Following its unconventional secretion Gal-1-GFP binds to β-galactosides of glycolipids and glycoproteins on the outer leaflet of the plasma membrane. This allows specific detection of secreted Gal-1-GFP with affinity-purified anti-GFP antibodies under native conditions. Following antibody processing the cells could be analyzed with regard to GFP fluorescence and cell surface signal by flow cytometry. GFP-derived fluorescence was used to normalize the overall expression of the reporter molecule under various experimental conditions.

ii) Biochemical secretion assay employing cell surface biotinylation. In order to demonstrate an external population of Gal-1-GFP fusion proteins associated with cell surface using an independent approach, a biochemical method was established employing a membrane-impermeable biotinylation reagent. After detergent-mediated cell lysis exported biotinylated proteins bound to the plasma membrane were isolated by streptavidin-coupled beads. This assay was combined with immunoprecipitation analysis of the cell culture medium using affinity-purified anti-GFP antibodies. Based on this approach, it was possible to investigate exported Gal-1 bound to counter receptors on the cell surface (Stegmayer et al., 2005) as well as soluble material potentially present in the cell culture supernatant (Seelenmeyer et al., 2005).

One aim of this thesis was to identify an export targeting motif in Gal-1 which directs the protein to its export machinery. Therefore single site mutations were generated in Gal-1. Since mutations in Gal-1 potentially result in an altered binding ability to β-galactosides, binding properties of N- and C-terminal GFP-tagged Gal-1 to β-galactosides were investigated as well. Therefore, two independent assays were established.

iii) *In vivo* binding of Gal-1-GFP to β-galactoside-containing counter receptors on the cell surface of CHO cells. For the *in vivo* binding assay cell-free supernatants of CHO cells expressing the various Gal-1 reporter molecules were incubated with CHO cells not expressing the GFP fusion protein to allow binding to the cell surface. This assay allows analyzing Gal-1 binding under native conditions employing flow cytometry using affinity-purified anti-GFP antibodies.

iv) *In vitro* binding of Gal-1 to lactose. This *in vitro* assay was developed to assess the lactose binding capacity of Gal-1. For this purpose detergent lysates of CHO cells expressing various Gal-1-GFP reporter molecules were generated. After incubation with lactose-coupled beads, binding was analyzed by Western blotting using affinity-purified anti-GFP antibodies. However, binding to lactose-coupled beads does not reflect the conditions present in the extracellular space *in vivo*, as the proteinaceous environment can also influence binding of Gal-1 to its natural ligands (Seelenmeyer et al., 2003).

These four mentioned assays were used to characterize Gal-1 mutants obtained by random mutagenesis, site-directed mutagenesis and N-and C-terminal truncations.

4.5 Mutational analysis of the export targeting motif of Gal-1 and CGL-2

In order to identify a putative export targeting motif in Gal-1, the experimental systems described above were used to systematically analyze Gal-1 mutant proteins. 97 individual CHO cell lines expressing single mutants and truncated versions of Gal-1-GFP and CGL-2-GFP fusion proteins were generated by stable integration of the corresponding DNA constructs into the genome of CHO cells using retroviral transduction. As control cell lines $CHO_{Gal\text{-}1\text{-}GFP}$, $CHO_{GFP\text{-}Gal\text{-}1}$, $CHO_{GFP\text{-}CGL\text{-}2}$ and CHO_{GFP} were used.

The individual mutants were selected in three different ways:

i) Targeted mutagenesis based on results obtained from a random mutagenesis approach. A low fidelity PCR was performed in the presence of 100 µM $MnCl_2$ using the ORF of Gal-1 as template, thereby multiple mutants were randomly inserted into Gal-1. After retroviral transduction of CHO cells with the corresponding plasmids Gal-1-GFP mutants characterized by an altered secretion and binding efficiency as compared to Gal-1-GFP were identified. All amino acid changes were individually introduced into Gal-1 by site-directed mutagenesis in order to investigate the effect of every single amino acid exchange regarding export and binding of mutated Gal-1-GFP proteins.

ii) Targeted mutagenesis of surface residues based on the crystal structure of Gal-1 (Liao et al., 1994). The crystal structure of human Gal-1 was analyzed for amino acids exposed on the protein surface as potential sites for interactions with other proteins responsible for the translocation process.

iii) Targeted mutagenesis of residues conserved between human Gal-1 and CGL-2 from *Coprinopsis cinerea*. The primary structures of human Gal-1 and the fungal galectin CGL-2 were analyzed for conserved amino acids although the homology between these two lectins is very weak at the level of both the primary and the quaternary structure (Lobsanov et al., 1993) (Walser et al., 2004). However, the tertiary structure of CGL-2 shows the typical galectin fold and, additionally, CGL-2 specifically binds to β-galactosides.

iv) Dimerization. It has been shown for FGF-1 to be released as a homodimer in an unconventional manner in response to temperature stress (Tarantini et al., 1995). One feature of Gal-1 that has particular biological relevance is the quaternary structure that is important with regard to ligand cross-linking and Gal-1-mediated signal transduction (Lopez-Lucendo et al., 2004). Kinetic studies of wild-type and mutant CGL-2 proteins demonstrate that the tetrameric organization is essential for functionality (Walser et al., 2004). Therefore the N-terminus and the C-terminus, which form the dimer interface in Gal-1, were truncated in order to investigate whether dimer formation influences the translocation process.

Generally, the original amino acids were replaced by alanine residues, which represents a small, uncharged hydrophobic amino acid that is considered as neutral. The various mutations were generated by site-directed mutagenesis and the corresponding constructs were stably integrated into the genome of CHO cells by retroviral transduction. Cell pools expressing the corresponding mutated Gal-1-GFP fusion protein in the presence of doxicycline were generated by FACS sorting (Fig. 22). These pools were characterized regarding unconventional secretion and binding efficiency to β-galactoside-containing counter receptors. About 31% of the analyzed CHO mutants showed the same phenotype as the wild-type form of Gal-1-GFP. 51% of the mutants were found to be impaired in export and binding to β-galactosides. 6% of the generated mutant cell lines resulted in low expression levels as measured by the GFP fluorescence indicating that the mutation causes overall protein instability.

The analysis of about 12% of the generated mutant proteins did not provide consistent results regarding quantitation of unconventional secretion and binding to β-galactosides.

4.5.1 Galectin mutants deficient in binding to β-galactosides are also deficient in export from CHO cells

Various mutated Gal-1-GFP reporter molecules were stably integrated into the genome of CHO cells (4.4). After FACS sorting based on GFP fluorescence the generated cell pools expressed the corresponding GFP reporter molecules in a doxicycline-dependent manner. With these inducible cell lines it was possible to investigate the binding and export behavior of mutated Gal-1-GFP fusion proteins. As already mentioned it was suggested that counter receptors might influence the export efficiency of unconventionally secreted proteins (Seelenmeyer et al., 2003). Therefore, a focus of the mutational analysis was to identify Gal-1 mutants that are deficient in binding to β-galactosides. Employing the described binding assays (4.4) 43 single site mutations in Gal-1 were identified which result in a binding defect to β-galactoside-containing ligands. To analyze whether these binding mutants are also defective in export, secretion of the mutated Gal-1-GFP fusion proteins was analyzed employing flow cytometry and the biotinylation assay. Since only proteins bound to the cell surface are detectable by these methods, no signals were observed when analyzing β-galactoside binding deficient mutants. To investigate whether exported Gal-1-GFP mutant proteins can be found in the cell culture medium of expressing cells, immunoprecipitation was performed using affinity-purified anti-GFP antibodies. Strikingly, not a single Gal-1 mutant deficient in binding to β-galactosides could be detected in the extracellular space (3.3.3.2). A similar observation was made concerning the unconventionally secreted protein FGF-2, which binds to heparan sulfate proteoglycans (HSPG) on the cell surface of CHO cells (Schäfer et al., 2004). To analyze the influence of HSPGs on the export process sodium chlorate was added to CHO cells. This substance competes with sulfate ions for binding to the ATP-sulfyrulase and inhibits thereby the generation of heparan sulfates (Klaassen

and Boles, 1997; Safaiyan et al., 1999). Subsequently, plasma membrane derived inside-out vesicles were generated from these cells and applied to an *in vitro* secretion assay that allows to analyze the translocation process of exogenously added FGF-2 by protease protection experiments (Schäfer et al., 2004). Interestingly, FGF-2 failed to traverse the membrane of inside-out vesicles derived from sodium chlorate treated CHO cells (Tobias Schäfer, personal communication). In addition, it was shown that CHOpgsA-745 cells, a CHO mutant cell line which lack glycosyl-aminoglycans on their cell surface, do not secrete FGF-2 employing flow cytometry and the cell surface biotinylation assay (Christoph Zehe, personal communication).

It was shown previously that single site mutations can influence the stability of Gal-1 (Cho and Cummings, 1995a; Hirabayashi and Kasai, 1991; Lopez-Lucendo et al., 2004) and galectins are generally sensitive to the redox state of the environment. Upon entering the oxidizing milieu of the extracellular space, stabilization of galectins is achieved through binding to their ligands (Cho and Cummings, 1995a). Therefore, when a mutation results in a binding defect to β-galactosides, it is of great importance to investigate whether the absence of Gal-1 reporter molecules in the medium is due to an export defect or a result of protein degradation. Therefore, cell-free supernatants of the various Gal-1-GFP fusion proteins were diluted in conditioned medium derived from CHO cells. The proteins were either immediately subjected to immunoprecitation using affinity-purified anti-GFP antibodies or first incubated under the experimental conditions applied in the secretion assays, as they were found to be stable up to 48 hours of incubation at 37°C.

Employing this assay it was possible to exclude that the absence of Gal-1-GFP in the cell culture medium of expressing cells results from degradation of the various mutated proteins.

To further verify that a functional interaction between Gal-1 and its counter receptors is essential for its translocation process, secretion was analyzed in a somatic CHO mutant cell line ($CHO_{clone13}$) defective in a Golgi-resident transporter that is required for translocation of activated galactose from the cytoplasm into the lumen of the Golgi, a process essential for the generation of β-galactoside-containing

glycolipids and glycoproteins (Deutscher and Hirschberg, 1986). Intriguingly, wild-type Gal-1 fails to get exported from this mutant cell line demonstrating that indeed secretion of Gal-1 from mammalian cells strictly depends on a functional interaction between Gal-1 and its counter receptors. Interestingly, Gal-1 from $CHO_{clone13}$ cells export can be reconstituted when the cells co-cultivated with $CHO_{wild\text{-}type}$ cells that do not express the fusion protein (Julia Ritzerfeld, personal communication). In this case $CHO_{wild\text{-}type}$ cells provide the β-galactoside-containing counter receptors on the cell surface required for the unconventional secretion of Gal-1-GFP.

Additionally, these data are supported by findings on CGL-2, a distant relative of Gal-1 from the multicellular fungus *Coprinopsis cinerea*. Even though similarities between CGL-2 and Gal-1 are very weak at the level of the primary structure (Lobsanov et al., 1993; Walser et al., 2004), CGL-2 is recognized by mammalian cells as an export substrate. Strikingly, a single-site mutation (W72G) that is known to cause CGL-2 binding deficiency to β-galactosides (Walser et al., 2004) results in a block of export of CGL-2 from CHO cells, consistent with our findings that functional interactions with counter receptors are essential for the overall export process.

4.5.2 Characterization of N- and C-terminal truncated forms of Gal-1

As already mentioned Gal-1 is able to form homodimers consisting of 14 kDa subunits each containing a single carbohydrate-binding site. The lectin is synthesized in the cytosol of mammalian cells where it accumulates in a monomeric form and is actively, but slowly secreted ($t_{1/2} \approx$ 20 h). The exported form requires glycoconjugate ligands to fold properly and acquire stability. The functional lectin exists in a monomer-dimer equilibrium with a K_d of ~ 7 µM and a slow equilibrium rate ($t_{1/2} \approx$ 10 h) (Cho and Cummings, 1995b). To explore functional differences between monomeric and dimeric forms regarding the unconventional secretion of human Gal-1, mutants truncated at the extreme N- and C-terminus, which are involved in subunit interactions, were generated. After retroviral transduction of the truncated reporter molecules, the corresponding CHO cells expressed the GFP fusion proteins in a

doxicycline-dependent manner. These CHO cells were characterized with regard to secretion and binding efficiency to β-galactosides employing the four read-out systems described above (4.4). All truncated versions of Gal-1-GFP resulted in decreased protein stability as indicated by lowered protein amounts per cell except Gal-1-GFP$_{\Delta N5}$ and Gal-1-GFP$_{\Delta N20}$, which were characterized by normal expression levels and export efficiency as compared to the wild-type form of Gal-1-GFP. Additionally, all of these truncated forms of Gal-1-GFP including Gal-1-GFP$_{\Delta N20}$ were impaired in binding to their counter receptors, whereas Gal-1-GFP$_{\Delta N5}$ showed wild-type characteristics. Based on the stability problems of these truncated versions it was difficult to analyze their export behavior.

Hydrophobic interactions between amino acid side chains seem to occur mainly between amino acids on the first β-strands (residues 5-8) at the N-terminus and amino acids on the last β-strand (residues 127-133) at the C-terminus. Precisely, dimer formation appears to result mainly from interactions between Val 6 of monomer A and Ala 7 on monomer B, Ile 129 on monomer A and Phe 134 of monomer B, and Phe 134 on monomer A and Ile 129 of monomer B. Mutating these amino acid residues to hydrophilic amino acids results in impaired dimer formation (Cho and Cummings, 1996). Therefore, in addition to the N- and C-terminal truncations described above, the mutant cell lines CHO Gal-1-GFP$_{V6A}$, CHO Gal-1-GFP$_{I129R}$, CHO and CHO Gal-1-GFP$_{F134E}$ were generated and analyzed regarding export and binding to β-galactosides.

Cho and colleagues investigated the mutant Gal-1$_{V6D}$ for binding to lactosyl-sepharose and observed that this mutation drastically affects carbohydrate-binding activity (Liao et al., 1994). Results of native gel electrophoresis, density gradient sedimentation, and size-exclusion HPLC demonstrate that Gal-1$_{V6D}$ exists as monomeric species. It was reasoned that the apparent reduced affinity of Gal-1$_{V6D}$ to lactosyl-sepaharose could result from its inability to dimerize. Further experiments are needed to analyze the influence of dimer formation on the unconventional secretion of Gal-1-GFP and on the binding ability. Analysis of GFP$_{V6A}$, Gal-1-GFP$_{I129R}$, Gal-1-GFP$_{F134E}$ and Gal-1-GFP$_{F134E}$ by native gel electrophoresis, density gradient sedimentation and size-exclusion HPLC of Gal-1- may give new insights in the translocating process of Gal-1 in mammalian cells.

4.6 Detailed analysis of Gal-1-GFP$_{R112H}$

Reflecting the strict conservation of a set of crucial amino acid residues as galectin sequence signature, the general architecture of the carbohydrate-binding site in human Gal-1 is very similar to that observed in other members of the galectin family, encompassing the antiparallel β-strands S4-S6a/S6b on the concave face of one β-sheet. The highly conserved amino acid residues involved in interactions with the bound disaccharide lactose are His 45, Asn 47, Arg 49, Val 60, Asn 62, Trp 69, Glu 72 and Arg 74 and they are invariably found in these β-strands (Lopez-Lucendo et al., 2004). In particular, Trp 69 participates in stacking interactions with carbons C3, C4 and C5 on the b-face of the galactose ring. This moiety is crucial to distinguish galactose from glucose through its preference for the axial hydroxyl-group on C4. With respect to the R112H mutant the substitution introduced accounts for a notable alteration of the architecture of the carbohydrate-binding site. As a consequence of this mutation the highly conserved amino acids His 53 and Trp 69 are shifted from their original position. This shift did not result in loosing the ability to bind to β-galactosides as demonstrated by thermodynamic binding studies (Lopez-Lucendo et al., 2004). Although this observation was confirmed by the *in vivo* binding assay (Fig. 41) the recognition of β-galactosides may be influenced as binding to lactose-coupled beads did not longer occur (Fig. 42). This observation provides evidence that beside sugar moieties a carbohydrate-lectin interaction depends on additional aspects of specificity based on the proteinaceous environment (Seelenmeyer et al., 2003). Similar results regarding export and binding to β-galactosides were obtained for Gal-1-GFP$_{V32E}$.

A possible explanation for the potential export deficiency of Gal-1-GFP$_{R112H}$ and Gal-1-GFP$_{V32E}$ is that a specific transporter exists, which is not able to recognize these mutated proteins independent of sugar binding ability. An alternative explanation might be that the described mutants are impaired in dimer formation. Further studies are required to characterize the decreased export efficiency.

4.7 Potential models for the unconventional secretion of Gal-1

Regarding the molecular mechanism of Gal-1 export from mammalian cells, there are three possible scenarios that would be consistent with the presented data. On the one hand, galectin counter receptors on the cell surface might be part of a molecular trap through which secreted Gal-1 molecules would be removed from equilibrium between an intracellular and an extracellular pool of Gal-1 (Fig. 47 panel A). In principle, the extracellular galectin trap could be necessary for sustained Gal-1 export of the cytoplasmic pool. However, in the absence of functional interactions between Gal-1 and its counter receptors, secretion is apparently fully blocked. Therefore, the trapping mechanism does not satisfactorily explain our observation, as Gal-1 transport should be observed at least to a certain extent until equilibrium between intra- and extracellular pools is reached.

In a second model, β-galactoside-containing cell surface molecules might be tightly coupled to the translocation machinery (Fig. 47 panel B) and function by exerting a pulling force at the extracellular side of a putative translocation pore required for directional transport of Gal-1 across the plasma membrane.

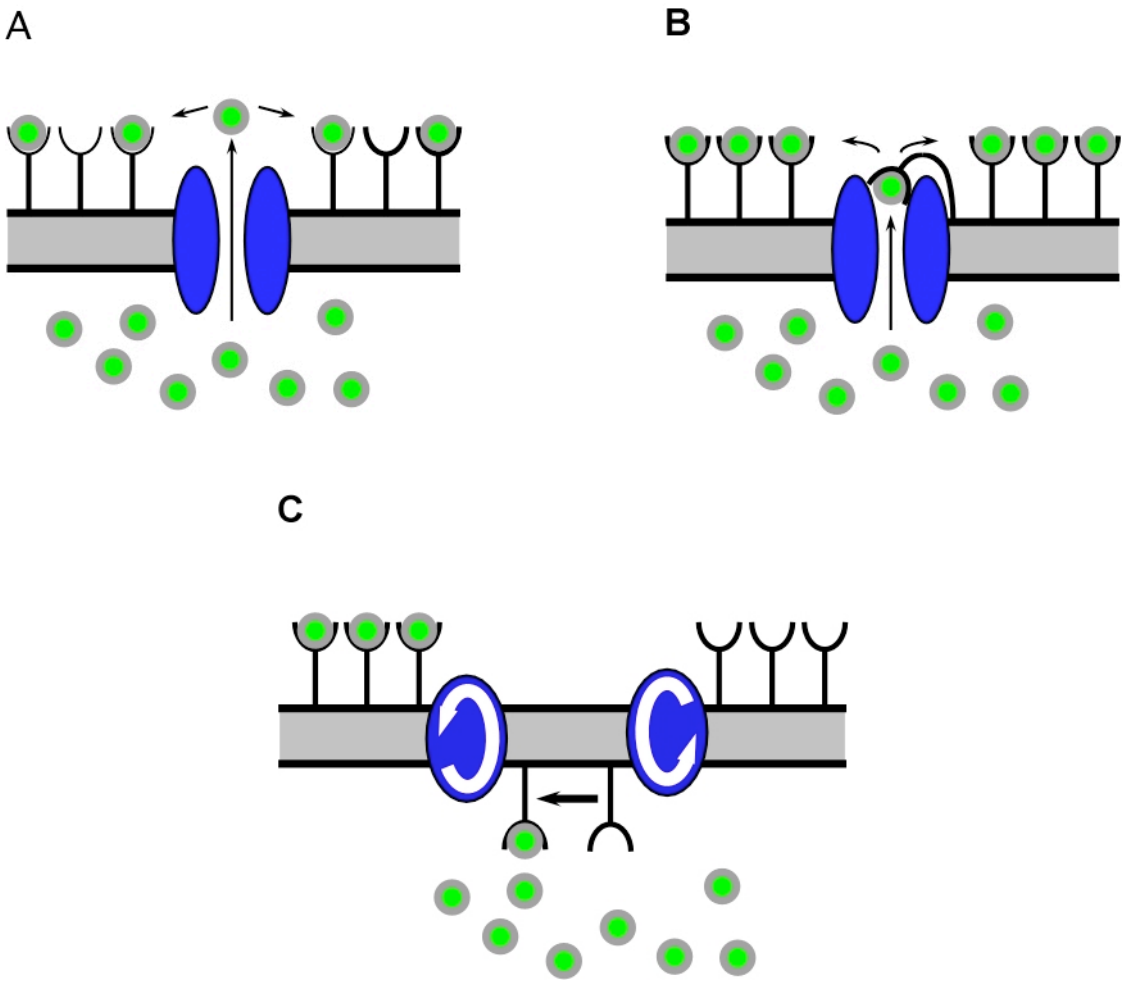

Fig. 47 Schematic overview of potential mechanisms mediating Gal-1 membrane translocation. A. Gal-1 is removed from an equilibrium (sink mechanism). B. Counter receptors exert a pulling force on Gal-1. C. Counter receptors act as export receptors. For details see text.

An alternative explanation of the presented results would be that β-galactoside-containing counter receptors act as export receptors for Gal-1 (Fig. 47, panel C). It might be speculated that Gal-1 interactions with counter receptors are not restricted to the extracellular space but rather already occur on the cytoplasmic side of the plasma membrane. This assumption is not consistent with the established view that for instant glycolipids are exclusively localized to the extracellular leaflet of the plasma membrane with glycan moieties being exposed to the extracellular space. However, it appears possible that a subpopulation of β-galactoside-containing glycolipids which probably would not be detectable under steady-state conditions gets

translocated to the inner leaflet of the plasma membrane. This translocation might be catalyzed by a plasma membrane resident flippase. In this model, re-translocation of counter receptors occupied by Gal-1 would mediate export to the extracellular space.

All described models (Fig. 47) indicate a direct translocation of Gal-1 across the plasma membrane. Mehul and colleagues reported that Gal-3 is transported directly to the plasma membrane prior to secretion and released into the extracellular space by vesicular budding from cos-7 and J774.2 cells because they were able to isolate extracellular vesicles containing Gal-3 by isopycnic centrifugation (Mehul and Hughes, 1997). Additionally, vesicular structures budding of cos-7 cell surface were detected employing confocal microscopy using polyclonal anti-Gal-3 antibodies. Membrane blebbing is a common feature at the periphery of many cell types, including fibroblasts (Lee et al., 1993), neutrophils (Stein and Luzio, 1991) and chondrocytes (Hale and Wuthier, 1987), that is regulated by intracellular calcium in some cases (Shukla et al., 1978). Although the results of pulse-chase analyses suggest an intermediate role of extracellular vesicles in the export of Gal-3 from macrophage J774.2 cells, the possibility that at least a part of the lectin may be translocated directly from plasma membrane domains into the extracellular space could not be excluded since a small but significant amount of the lectin was detected in the soluble fraction of conditioned medium obtained from cos-7 and J774.2 cells. As the isolated vesicles were not analyzed for apoptotic markers like Annexin V it might be that they result from apoptotic cells (Miller, 2004).

Independently, Cooper et al. demonstrated that Gal-1 expressed in myoblasts is externalized upon differentiation, whereas creatine kinase and lactate dehydrogenase - markers for unspecific release - remain intracellularly (Cooper and Barondes, 1990). Therefore, extracellular Gal-1 cannot be due to cell death or transient membrane disruption of a small fraction of the cultured cell population. As myoblasts differentiate, Gal-1 also appears to be concentrated directly underneath the plasma membrane as visualized by confocal microscopy. Concentrated patches of ectoplasmic Gal-1 are then evaginated from the plasma membrane and form extracellular vesicles enriched in the lectin. The final step in externalization of Gal-1 is presumed to occur when evaginated vesicles are disrupted (Cooper and Barondes,

1990). However, employing confocal microscopy of CHO cells expressing Gal-1-GFP in a doxicycline dependent manner, no membrane blebs were detectable neither in living nor in fixed cells indicating that Gal-1 is externalized by a mechanism independent of vesicular structures (Seelenmeyer et al., 2005).

While the proposed export models are certainly speculative at this point, they are consistent with several observations that have been made previously. First, galectin membrane translocation has been reported to occur at the level of the plasma membrane (Cooper and Barondes, 1990; Hughes, 1999; Mehul and Hughes, 1997; Nickel, 2003; Schäfer et al., 2004). Second, Huet and colleagues recently reported pharmacological evidence that Gal-4 secretion is impaired in epithelial cells following treatment with 1-benzyl-2-acetamido-2-deoxy-α-D-galactopyranoside, an inhibitor of glycosylation (Delacour et al., 2005). Third, evidence has been reported that membrane translocation of both FGF-2 and Gal-1 occurs in a folded state (Backhaus et al., 2004).

In the context of the current study, this finding is of particular interest since the models described above can only be true if the β-galactoside binding site of Gal-1 remains functional during membrane translocation. In this regard, the putative translocation machinery might be functionally related to the bacterial twin arginine translocation system mediating protein secretion in a fully folded state (Oates et al., 2005; Robinson and Bolhuis, 2004).

The findings presented in this work also provide a potential explanation for the apparent non-existence of a linear targeting motif in Gal-1. The presented data conclusively point to a direct role of counter receptors as export adaptors and the β-galactoside binding motif of Gal-1 as the primary targeting element. In this context, it is interesting to note that secretion from *Saccharomyces cerevisiae* of both rat Gal-1 and *Coprinospsis cinerea* CGL-2 has been reported (Cleves et al., 1996) (Boulianne et al., 2000). This organism does not contain endogenous galectins and the existence of glycolipids and glycoproteins containing β-galactosides has not yet been clarified. Therefore, it remains to be investigated whether secretion of galectins from

Saccharomyces cerevisiae occurs by a molecular mechanism similar to that of mammalian cells.

Finally, it is of note that the secretory mechanism being postulated in this thesis provides a functional basis for quality control in the overall process of Gal-1 secretion. As the β-galactosides binding motif of Gal-1 is shown to be the primary targeting element for secretion, quality control is in place since only properly folded Gal-1 will be recognized by the export machinery (Nickel, 2005).

4.8 Future perspectives

The established Gal-1 secretion assays employing flow cytometry and cell surface biotinylation analysis were shown to be robust methods to investigate non-classical export processes in molecular detail. To clarify if β-galactoside-containing glycoproteins or glycolipids are involved in the export mechanism, the mutagenized subclone GM95 of the murine melanoma cell line B16 (Ito and Komori, 1996; Komori et al., 1999; Smith et al., 2003) will be analyzed for secretion of Gal-1-GFP expressed in a doxicycline-dependent manner. This cell line lacks the ceramide-glucosyl transferase gene and does not present glycolipids on the cell surface. MEB4 cells represent the parental cell line of GM95 cells containing a functional ceramide-glucosyl transferase gene (Spilsberg et al., 2003) and, unlike GM95, produce functional glycolipids and glycoproteins. Based on these cell lines it will be possible to distinguish between the postulated models (Fig. 47). If the export machinery in GM95 cells is functional and exported Gal-1-GFP is detectable on the cell surface bound to β-galactoside-containing glycoproteins, it can be excluded that the translocation of Gal-1-GFP is mediated by a membrane-resident flippase.

The FACS based Gal-1 secretion assay will form the basis for a number of future applications such as the systematic screening for specific inhibitors from complex compound libraries. Additionally, systematic screening using RNAi libraries will be conducted in future experiments. For example, both an RNAi library directed against all ABC transporters known in the human genome and a complex library covering all genes (≈ 22.000 genes) in the human genome will be tested regarding

export efficiency of Gal-1-GFP under knock-down conditions in HeLa cells. Based on this it might be possible to isolate a single counter receptor for Gal-1, which mediates specifically the translocation process across the plasma membrane.

References

Adams, L., Scott, G. K., and Weinberg, C. S. (1996). Biphasic modulation of cell growth by recombinant human galectin-1. Biochim Biophys Acta *1312*, 137-144.

Ahmed, H., Pohl, J., Fink, N. E., Strobel, F., and Vasta, G. R. (1996). The primary structure and carbohydrate specificity of a beta-galactosyl-binding lectin from toad (Bufo arenarum Hensel) ovary reveal closer similarities to the mammalian galectin-1 than to the galectin from the clawed frog Xenopus laevis. J Biol Chem *271*, 33083-33094.

Albritton, L. M., Tseng, L., Scadden, D., and Cunningham, J. M. (1989). A putative murine ecotropic retrovirus receptor gene encodes a multiple membrane-spanning protein and confers susceptibility to virus infection. Cell *57*, 659-666.

Alce, T. M., Gokool, S., McGhie, D., Stager, S., and Smith, D. F. (1999). Expression of hydrophilic surface proteins in infective stages of Leishmania donovani. Mol Biochem Parasitol *102*, 191-196.

Amara, J. F., Cheng, S. H., and Smith, A. E. (1992). Intracellular protein trafficking defects in human disease. Trends Cell Biol *2*, 145-149.

Andrei, C., Dazzi, C., Lotti, L., Torrisi, M. R., Chimini, G., and Rubartelli, A. (1999). The secretory route of the leaderless protein interleukin 1beta involves exocytosis of endolysosome-related vesicles. Mol Biol Cell *10*, 1463-1475.

Andrei, C., Margiocco, P., Poggi, A., Lotti, L. V., Torrisi, M. R., and Rubartelli, A. (2004). Phospholipases C and A2 control lysosome-mediated IL-1 beta secretion: Implications for inflammatory processes. Proc Natl Acad Sci U S A *101*, 9745-9750.

Auron, P. E., Webb, A. C., Rosenwasser, L. J., Mucci, S. F., Rich, A., Wolff, S. M., and Dinarello, C. A. (1984). Nucleotide sequence of human monocyte interleukin 1 precursor cDNA. Proc Natl Acad Sci U S A *81*, 7907-7911.

Backhaus, R., Zehe, C., Wegehingel, S., Kehlenbach, A., Schwappach, B., and Nickel, W. (2004). Unconventional protein secretion: membrane translocation of FGF-2 does not require protein unfolding. J Cell Sci *117*, 1727-1736.

Barlowe, C. (1998). COPII and selective export from the endoplasmic reticulum. Biochim Biophys Acta *1404*, 67-76.

Barondes, S. H. (1984). Soluble lectins: a new class of extracellular proteins. Science *223*, 1259-1264.

Barondes, S. H., Beyer, E. C., Springer, W. R., and Cooper, D. N. (1981). Endogenous lectins in chickens and slime molds: transfer from intracellular to extracellular sites. J Supramol Struct Cell Biochem *16*, 233-242.

Barondes, S. H., Cooper, D. N., Gitt, M. A., and Leffler, H. (1994). Galectins. Structure and function of a large family of animal lectins. J Biol Chem *269*, 20807-20810.

Bast, R. C., Jr., Feeney, M., Lazarus, H., Nadler, L. M., Colvin, R. B., and Knapp, R. C. (1981). Reactivity of a monoclonal antibody with human ovarian carcinoma. J Clin Invest *68*, 1331-1337.

Baum, L. G., Pang, M., Perillo, N. L., Wu, T., Delegeane, A., Uittenbogaart, C. H., Fukuda, M., and Seilhamer, J. J. (1995a). Human thymic epithelial cells express an endogenous lectin, galectin-1, which binds to core 2 O-glycans on thymocytes and T lymphoblastoid cells. J Exp Med *181*, 877-887.

Baum, L. G., Seilhamer, J. J., Pang, M., Levine, W. B., Beynon, D., and Berliner, J. A. (1995b). Synthesis of an endogeneous lectin, galectin-1, by human endothelial cells is up-regulated by endothelial cell activation. Glycoconj J *12*, 63-68.

Beyer, E. C., and Barondes, S. H. (1982). Secretion of endogenous lectin by chicken intestinal goblet cells. J Cell Biol *92*, 28-33.

Bhaumik, M., Harris, T., Sundaram, S., Johnson, L., Guttenplan, J., Rogler, C., and Stanley, P. (1998). Progression of hepatic neoplasms is severely retarded in mice lacking the bisecting N-acetylglucosamine on N-glycans: evidence for a glycoprotein factor that facilitates hepatic tumor progression. Cancer Res *58*, 2881-2887.

Black, R. A., Kronheim, S. R., Cantrell, M., Deeley, M. C., March, C. J., Prickett, K. S., Wignall, J., Conlon, P. J., Cosman, D., Hopp, T. P., and et al. (1988). Generation of biologically active interleukin-1 beta by proteolytic cleavage of the inactive precursor. J Biol Chem *263*, 9437-9442.

Blobel, G., and Dobberstein, B. (1975a). Transfer of proteins across membranes. I. Presence of proteolytically processed and unprocessed nascent immunoglobulin light chains on membrane-bound ribosomes of murine myeloma. J Cell Biol *67*, 835-851.

Blobel, G., and Dobberstein, B. (1975b). Transfer to proteins across membranes. II. Reconstitution of functional rough microsomes from heterologous components. J Cell Biol *67*, 852-862.

Bonaldi, T., Talamo, F., Scaffidi, P., Ferrera, D., Porto, A., Bachi, A., Rubartelli, A., Agresti, A., and Bianchi, M. E. (2003). Monocytic cells hyperacetylate chromatin protein HMGB1 to redirect it towards secretion. Embo J *22*, 5551-5560.

Bonifacino, J. S., and Glick, B. S. (2004). The mechanisms of vesicle budding and fusion. Cell *116*, 153-166.

Boulianne, R. P., Liu, Y., Aebi, M., Lu, B. C., and Kues, U. (2000). Fruiting body development in Coprinus cinereus: regulated expression of two galectins secreted by a non-classical pathway. Microbiology *146 (Pt 8)*, 1841-1853.

Braddock, M., and Quinn, A. (2004). Targeting IL-1 in inflammatory disease: new opportunities for therapeutic intervention. Nat Rev Drug Discov *3*, 330-339.

Brummelkamp, T. R., Bernards, R., and Agami, R. (2002). A system for stable expression of short interfering RNAs in mammalian cells. Science *296*, 550-553.

Burgess, W. H., and Maciag, T. (1989). The heparin-binding (fibroblast) growth factor family of proteins. Annu Rev Biochem *58*, 575-606.

Caplen, N. J., Parrish, S., Imani, F., Fire, A., and Morgan, R. A. (2001). Specific inhibition of gene expression by small double-stranded RNAs in invertebrate and vertebrate systems. Proc Natl Acad Sci U S A *98*, 9742-9747.

Carey, D. J., and Hirschberg, C. B. (1981). Topography of sialoglycoproteins and sialyltransferases in mouse and rat liver Golgi. J Biol Chem *256*, 989-993.

Cerra, R. F., Haywood-Reid, P. L., and Barondes, S. H. (1984). Endogenous mammalian lectin localized extracellularly in lung elastic fibers. J Cell Biol *98*, 1580-1589.

Chen, Y. A., and Scheller, R. H. (2001). SNARE-mediated membrane fusion. Nat Rev Mol Cell Biol *2*, 98-106.

Chiariotti, L., Salvatore, P., Frunzio, R., and Bruni, C. B. (2004). Galectin genes: regulation of expression. Glycoconj J *19*, 441-449.

Cho, M., and Cummings, R. D. (1995a). Galectin-1, a beta-galactoside-binding lectin in Chinese hamster ovary cells. I. Physical and chemical characterization. J Biol Chem *270*, 5198-5206.

Cho, M., and Cummings, R. D. (1995b). Galectin-1, a beta-galactoside-binding lectin in Chinese hamster ovary cells. II. Localization and biosynthesis. J Biol Chem *270*, 5207-5212.

Cho, M., and Cummings, R. D. (1996). Characterization of monomeric forms of galectin-1 generated by site-directed mutagenesis. Biochemistry *35*, 13081-13088.

Clark, R., and Griffiths, G. M. (2003). Lytic granules, secretory lysosomes and disease. Curr Opin Immunol *15*, 516-521.

Cleves, A. E. (1997). Protein transports: the nonclassical ins and outs. Curr Biol *7*, R318-320.

Cleves, A. E., Cooper, D. N., Barondes, S. H., and Kelly, R. B. (1996). A new pathway for protein export in Saccharomyces cerevisiae. J Cell Biol *133*, 1017-1026.

Cleves, A. E., and Kelly, R. B. (1996). Rehearsing the ABCs. Protein translocation. Curr Biol *6*, 276-278.

Cline, J., Braman, J. C., and Hogrefe, H. H. (1996). PCR fidelity of pfu DNA polymerase and other thermostable DNA polymerases. Nucleic Acids Res *24*, 3546-3551.

Cooper, D. N., and Barondes, S. H. (1990). Evidence for export of a muscle lectin from cytosol to extracellular matrix and for a novel secretory mechanism. J Cell Biol *110*, 1681-1691.

Cooper, D. N., Massa, S. M., and Barondes, S. H. (1991). Endogenous muscle lectin inhibits myoblast adhesion to laminin. J Cell Biol *115*, 1437-1448.

Cosson, P., and Letourneur, F. (1994). Coatomer interaction with di-lysine endoplasmic reticulum retention motifs. Science *263*, 1629-1631.

Couraud, P. O., Casentini-Borocz, D., Bringman, T. S., Griffith, J., McGrogan, M., and Nedwin, G. E. (1989). Molecular cloning, characterization, and expression of a human 14-kDa lectin. J Biol Chem *264*, 1310-1316.

Creek, K. E., and Morre, D. J. (1981). Translocation of cytidine 5'-monophosphosialic acid across Golgi apparatus membranes. Biochim Biophys Acta *643*, 292-305.

Crocker, P. R. (2002). Siglecs: sialic-acid-binding immunoglobulin-like lectins in cell-cell interactions and signalling. Curr Opin Struct Biol *12*, 609-615.

Crocker, P. R., and Feizi, T. (1996). Carbohydrate recognition systems: functional triads in cell-cell interactions. Curr Opin Struct Biol *6*, 679-691.

Dalbey, R. E., and Von Heijne, G. (1992). Signal peptidases in prokaryotes and eukaryotes--a new protease family. Trends Biochem Sci *17*, 474-478.

Danguy, A., Camby, I., and Kiss, R. (2002). Galectins and cancer. Biochim Biophys Acta *1572*, 285-293.

Davey, R. A., Hamson, C. A., Healey, J. J., and Cunningham, J. M. (1997). In vitro binding of purified murine ecotropic retrovirus envelope surface protein to its receptor, MCAT-1. J Virol *71*, 8096-8102.

de Waard, A., Hickman, S., and Kornfeld, S. (1976). Isolation and properties of beta-galactoside binding lectins of calf heart and lung. J Biol Chem *251*, 7581-7587.

Delacour, D., Gouyer, V., Zanetta, J. P., Drobecq, H., Leteurtre, E., Grard, G., Moreau-Hannedouche, O., Maes, E., Pons, A., Andre, S.*, et al.* (2005). Galectin-4 and sulfatides in apical membrane trafficking in enterocyte-like cells. J Cell Biol *169*, 491-501.

Demetriou, M., Nabi, I. R., Coppolino, M., Dedhar, S., and Dennis, J. W. (1995). Reduced contact-inhibition and substratum adhesion in epithelial cells expressing GlcNAc-transferase V. J Cell Biol *130*, 383-392.

Denny, P. W., Gokool, S., Russell, D. G., Field, M. C., and Smith, D. F. (2000). Acylation-dependent protein export in Leishmania. J Biol Chem *275*, 11017-11025.

Deutscher, S. L., Creek, K. E., Merion, M., and Hirschberg, C. B. (1983). Subfractionation of rat liver Golgi apparatus: separation of enzyme activities involved in the biosynthesis of the phosphomannosyl recognition marker in lysosomal enzymes. Proc Natl Acad Sci U S A *80*, 3938-3942.

Deutscher, S. L., and Hirschberg, C. B. (1986). Mechanism of galactosylation in the Golgi apparatus. A Chinese hamster ovary cell mutant deficient in translocation of UDP-galactose across Golgi vesicle membranes. J Biol Chem *261*, 96-100.

Dinarello, C. A. (1991). Inflammatory cytokines: interleukin-1 and tumor necrosis factor as effector molecules in autoimmune diseases. Curr Opin Immunol *3*, 941-948.

Dinarello, C. A. (1997). Interleukin-1. Cytokine Growth Factor Rev *8*, 253-265.

Drickamer, K., and Taylor, M. E. (1993). Biology of animal lectins. Annu Rev Cell Biol *9*, 237-264.

Dunphy, W. G., Fries, E., Urbani, L. J., and Rothman, J. E. (1981). Early and late functions associated with the Golgi apparatus reside in distinct compartments. Proc Natl Acad Sci U S A *78*, 7453-7457.

Elliott, G., and O'Hare, P. (1997). Intercellular trafficking and protein delivery by a herpesvirus structural protein. Cell *88*, 223-233.

Engling, A., Backhaus, R., Stegmayer, C., Zehe, C., Seelenmeyer, C., Kehlenbach, A., Schwappach, B., Wegehingel, S., and Nickel, W. (2002). Biosynthetic FGF-2 is targeted to non-lipid raft microdomains following translocation to the extracellular surface of CHO cells. J Cell Sci *115*, 3619-3631.

Fajka-Boja, R., Szemes, M., Ion, G., Legradi, A., Caron, M., and Monostori, E. (2002). Receptor tyrosine phosphatase, CD45 binds galectin-1 but does not mediate its apoptotic signal in T cell lines. Immunol Lett *82*, 149-154.

Farquhar, M. G. (1981). Membrane recycling in secretory cells: implications for traffic of products and specialized membranes within the Golgi complex. Methods Cell Biol *23*, 399-427.

Feizi, T. (1985). Demonstration by monoclonal antibodies that carbohydrate structures of glycoproteins and glycolipids are onco-developmental antigens. Nature *314*, 53-57.

Fendrick, J. L., Konishi, I., Geary, S. M., Parmley, T. H., Quirk, J. G., Jr., and O'Brien, T. J. (1997). CA125 phosphorylation is associated with its secretion from the WISH human amnion cell line. Tumour Biol *18*, 278-289.

Fleischer, B. (1981). Orientation of glycoprotein galactosyltransferase and sialyltransferase enzymes in vesicles derived from rat liver Golgi apparatus. J Cell Biol *89*, 246-255.

Fleischer, B., Fleischer, S., and Ozawa, H. (1969). Isolation and characterization of Golgi membranes from bovine liver. J Cell Biol *43*, 59-79.

Flieger, O., Engling, A., Bucala, R., Lue, H., Nickel, W., and Bernhagen, J. (2003). Regulated secretion of macrophage migration inhibitory factor is mediated by a non-classical pathway involving an ABC transporter. FEBS Lett *551*, 78-86.

Flinn, H. M., Rangarajan, D., and Smith, D. F. (1994). Expression of a hydrophilic surface protein in infective stages of Leishmania major. Mol Biochem Parasitol *65*, 259-270.

Florkiewicz, R. Z., Majack, R. A., Buechler, R. D., and Florkiewicz, E. (1995). Quantitative export of FGF-2 occurs through an alternative, energy- dependent, non-ER/Golgi pathway. J Cell Physiol *162*, 388-399.

Freyssinet, J. M. (2003). Cellular microparticles: what are they bad or good for? J Thromb Haemost *1*, 1655-1662.

Fullekrug, J., Sonnichsen, B., Schafer, U., Nguyen Van, P., Soling, H. D., and Mieskes, G. (1997). Characterization of brefeldin A induced vesicular structures containing cycling proteins of the intermediate compartment/cis-Golgi network. FEBS Lett *404*, 75-81.

Fullekrug, J., Suganuma, T., Tang, B. L., Hong, W., Storrie, B., and Nilsson, T. (1999). Localization and recycling of gp27 (hp24gamma3): complex formation with other p24 family members. Mol Biol Cell *10*, 1939-1955.

Furst, J., Sutton, R. B., Chen, J., Brunger, A. T., and Grigorieff, N. (2003). Electron cryomicroscopy structure of N-ethyl maleimide sensitive factor at 11 A resolution. Embo J *22*, 4365-4374.

Gahl, W. A. (1997). Carbohydrate-deficient glycoprotein syndrome: hidden treasures. J Lab Clin Med *129*, 394-395.

Gardella, S., Andrei, C., Ferrera, D., Lotti, L. V., Torrisi, M. R., Bianchi, M. E., and Rubartelli, A. (2002). The nuclear protein HMGB1 is secreted by monocytes via a non-classical, vesicle-mediated secretory pathway. EMBO Rep *3*, 995-1001.

Gey, G. O., Coffman, W. D., and Kubicek, M. T. (1952). Tissue culture studies of the prolieferative capacity of cervical carcinoma and normal epithelium. Cancer Res *12*, 264-265.

Giudicelli, V., Lutomski, D., Levi-Strauss, M., Bladier, D., Joubert-Caron, R., and Caron, M. (1997). Is human galectin-1 activity modulated by monomer/dimer equilibrium? Glycobiology *7*, viii-x.

Goldberg, J. (2000). Decoding of sorting signals by coatomer through a GTPase switch in the COPI coat complex. Cell *100*, 671-679.

Goldberg, R. L., and Toole, B. P. (1983). Monensin inhibition of hyaluronate synthesis in rat fibrosarcoma cells. J Biol Chem *258*, 7041-7046.

Goud, B. (1992). Small GTP-binding proteins as compartmental markers. Semin Cell Biol *3*, 301-307.

Graham, T. R., and Emr, S. D. (1991). Compartmental organization of Golgi-specific protein modification and vacuolar protein sorting events defined in a yeast sec18 (NSF) mutant. J Cell Biol *114*, 207-218.

Gray, C. A., Adelson, D. L., Bazer, F. W., Burghardt, R. C., Meeusen, E. N., and Spencer, T. E. (2004). Discovery and characterization of an epithelial-specific galectin in the endometrium that forms crystals in the trophectoderm. Proc Natl Acad Sci U S A *101*, 7982-7987.

Gray, C. A., Dunlap, K. A., Burghardt, R. C., and Spencer, T. E. (2005). Galectin-15 in ovine uteroplacental tissues. Reproduction *130*, 231-240.

Hajihosseini, M. K., and Heath, J. K. (2002). Expression patterns of fibroblast growth factors-18 and -20 in mouse embryos is suggestive of novel roles in calvarial and limb development. Mech Dev *113*, 79-83.

Hakomori, S. (1986). Tumor-associated glycolipid antigens, their metabolism and organization. Chem Phys Lipids *42*, 209-233.

Hale, J. E., and Wuthier, R. E. (1987). The mechanism of matrix vesicle formation. Studies on the composition of chondrocyte microvilli and on the effects of microfilament-perturbing agents on cellular vesiculation. J Biol Chem *262*, 1916-1925.

Hamon, Y., Luciani, M. F., Becq, F., Verrier, B., Rubartelli, A., and Chimini, G. (1997). Interleukin-1beta secretion is impaired by inhibitors of the Atp binding cassette transporter, ABC1. Blood *90*, 2911-2915.

Hardardottir, H., Parmley, T. H., 2nd, Quirk, J. G., Jr., Sanders, M. M., Miller, F. C., and O'Brien, T. J. (1990). Distribution of CA 125 in embryonic tissues and adult derivatives of the fetal periderm. Am J Obstet Gynecol *163*, 1925-1931.

Harrison, F. L. (1991). Soluble vertebrate lectins: ubiquitous but inscrutable proteins. J Cell Sci *100 (Pt 1)*, 9-14.

Harrison, F. L., and Wilson, T. J. (1992). The 14 kDa beta-galactoside binding lectin in myoblast and myotube cultures: localization by confocal microscopy. J Cell Sci *101 (Pt 3)*, 635-646.

Hebert, D. N., Garman, S. C., and Molinari, M. (2005). The glycan code of the endoplasmic reticulum: asparagine-linked carbohydrates as protein maturation and quality-control tags. Trends Cell Biol *15*, 364-370.

Hennet, T. (2002). The galactosyltransferase family. Cell Mol Life Sci *59*, 1081-1095.

Hernandez, J. D., and Baum, L. G. (2002). Ah, sweet mystery of death! Galectins and control of cell fate. Glycobiology *12*, 127R-136R.

High, S., Andersen, S. S., Gorlich, D., Hartmann, E., Prehn, S., Rapoport, T. A., and Dobberstein, B. (1993). Sec61p is adjacent to nascent type I and type II signal-anchor proteins during their membrane insertion. J Cell Biol *121*, 743-750.

High, S., Gorlich, D., Wiedmann, M., Rapoport, T. A., and Dobberstein, B. (1991). The identification of proteins in the proximity of signal-anchor sequences during their targeting to and insertion into the membrane of the ER. J Cell Biol *113*, 35-44.

Hirabayashi, J., and Kasai, K. (1991). Effect of amino acid substitution by sited-directed mutagenesis on the carbohydrate recognition and stability of human 14-kDa beta-galactoside-binding lectin. J Biol Chem *266*, 23648-23653.

Hirabayashi, J., and Kasai, K. (1993). The family of metazoan metal-independent beta-galactoside-binding lectins: structure, function and molecular evolution. Glycobiology *3*, 297-304.

Hirabayashi, J., Satoh, M., and Kasai, K. (1992). Evidence that Caenorhabditis elegans 32-kDa beta-galactoside-binding protein is homologous to vertebrate beta-galactoside-binding lectins. cDNA cloning and deduced amino acid sequence. J Biol Chem *267*, 15485-15490.

Hirschberg, C. B., and Snider, M. D. (1987). Topography of glycosylation in the rough endoplasmic reticulum and Golgi apparatus. Annu Rev Biochem *56*, 63-87.

Hohl, T. M., Parlati, F., Wimmer, C., Rothman, J. E., Sollner, T. H., and Engelhardt, H. (1998). Arrangement of subunits in 20 S particles consisting of NSF, SNAPs, and SNARE complexes. Mol Cell *2*, 539-548.

Holmgren, A. (1989). Thioredoxin and glutaredoxin systems. J Biol Chem *264*, 13963-13966.

Holton, J. B. (1996). Galactosaemia: pathogenesis and treatment. J Inherit Metab Dis *19*, 3-7.

Hugel, B., Martinez, M. C., Kunzelmann, C., and Freyssinet, J. M. (2005). Membrane microparticles: two sides of the coin. Physiology (Bethesda) *20*, 22-27.

Hughes, R. C. (1999). Secretion of the galectin family of mammalian carbohydrate-binding proteins. Biochim Biophys Acta *1473*, 172-185.

Ito, M., and Komori, H. (1996). Homeostasis of cell-surface glycosphingolipid content in B16 melanoma cells. Evidence revealed by an endoglycoceramidase. J Biol Chem *271*, 12655-12660.

Jackson, A., Friedman, S., Zhan, X., Engleka, K. A., Forough, R., and Maciag, T. (1992). Heat shock induces the release of fibroblast growth factor 1 from NIH 3T3 cells. Proc Natl Acad Sci U S A *89*, 10691-10695.

Jahn, R., and Grubmuller, H. (2002). Membrane fusion. Curr Opin Cell Biol *14*, 488-495.

Jahn, R., and Sudhof, T. C. (1999). Membrane fusion and exocytosis. Annu Rev Biochem *68*, 863-911.

Jeffers, M., Shimkets, R., Prayaga, S., Boldog, F., Yang, M., Burgess, C., Fernandes, E., Rittman, B., Shimkets, J., LaRochelle, W. J., and Lichenstein, H. S. (2001). Identification of a novel human fibroblast growth factor and characterization of its role in oncogenesis. Cancer Res *61*, 3131-3138.

Jenne, N., Frey, K., Brugger, B., and Wieland, F. T. (2002). Oligomeric state and stoichiometry of p24 proteins in the early secretory pathway. J Biol Chem *277*, 46504-46511.

Kang, R., Saito, H., Ihara, Y., Miyoshi, E., Koyama, N., Sheng, Y., and Taniguchi, N. (1996). Transcriptional regulation of the N-acetylglucosaminyltransferase V gene in human bile duct carcinoma cells (HuCC-T1) is mediated by Ets-1. J Biol Chem *271*, 26706-26712.

Keller, P., and Simons, K. (1997). Post-Golgi biosynthetic trafficking. J Cell Sci *110 (Pt 24)*, 3001-3009.

Kirchhausen, T. (2000). Three ways to make a vesicle. Nat Rev Mol Cell Biol *1*, 187-198.

Kirchhausen, T., Bonifacino, J. S., and Riezman, H. (1997). Linking cargo to vesicle formation: receptor tail interactions with coat proteins. Curr Opin Cell Biol *9*, 488-495.

Kirikoshi, H., Sagara, N., Saitoh, T., Tanaka, K., Sekihara, H., Shiokawa, K., and Katoh, M. (2000). Molecular cloning and characterization of human FGF-20 on chromosome 8p21.3-p22. Biochem Biophys Res Commun *274*, 337-343.

Kjellen, L., and Lindahl, U. (1991). Proteoglycans: structures and interactions. Annu Rev Biochem *60*, 443-475.

Klaassen, C. D., and Boles, J. W. (1997). Sulfation and sulfotransferases 5: the importance of 3'-phosphoadenosine 5'-phosphosulfate (PAPS) in the regulation of sulfation. Faseb J *11*, 404-418.

Kobayashi, Y., Yamamoto, K., Saido, T., Kawasaki, H., Oppenheim, J. J., and Matsushima, K. (1990). Identification of calcium-activated neutral protease as a

processing enzyme of human interleukin 1 alpha. Proc Natl Acad Sci U S A *87*, 5548-5552.

Komori, H., Ichikawa, S., Hirabayashi, Y., and Ito, M. (1999). Regulation of intracellular ceramide content in B16 melanoma cells. Biological implications of ceramide glycosylation. J Biol Chem *274*, 8981-8987.

Kopitz, J., von Reitzenstein, C., Burchert, M., Cantz, M., and Gabius, H. J. (1998). Galectin-1 is a major receptor for ganglioside GM1, a product of the growth-controlling activity of a cell surface ganglioside sialidase, on human neuroblastoma cells in culture. J Biol Chem *273*, 11205-11211.

Kornfeld, R., and Kornfeld, S. (1985). Assembly of asparagine-linked oligosaccharides. Annu Rev Biochem *54*, 631-664.

Kutay, U., Ahnert-Hilger, G., Hartmann, E., Wiedenmann, B., and Rapoport, T. A. (1995). Transport route for synaptobrevin via a novel pathway of insertion into the endoplasmic reticulum membrane. Embo J *14*, 217-223.

Kuwabara, I., Sano, H., and Liu, F. T. (2003). Functions of galectins in cell adhesion and chemotaxis. Methods Enzymol *363*, 532-552.

Laemmli, U. K., Beguin, F., and Gujer-Kellenberger, G. (1970). A factor preventing the major head protein of bacteriophage T4 from random aggregation. J Mol Biol *47*, 69-85.

Lahm, H., Andre, S., Hoeflich, A., Kaltner, H., Siebert, H. C., Sordat, B., von der Lieth, C. W., Wolf, E., and Gabius, H. J. (2004). Tumor galectinology: insights into the complex network of a family of endogenous lectins. Glycoconj J *20*, 227-238.

Lanteri, M., Giordanengo, V., Hiraoka, N., Fuzibet, J. G., Auberger, P., Fukuda, M., Baum, L. G., and Lefebvre, J. C. (2003). Altered T cell surface glycosylation in HIV-1 infection results in increased susceptibility to galectin-1-induced cell death. Glycobiology *13*, 909-918.

Lawyer, F. C., Stoffel, S., Saiki, R. K., Myambo, K., Drummond, R., and Gelfand, D. H. (1989). Isolation, characterization, and expression in Escherichia coli of the DNA polymerase gene from Thermus aquaticus. J Biol Chem *264*, 6427-6437.

Lee, M. C., Miller, E. A., Goldberg, J., Orci, L., and Schekman, R. (2004). Bi-directional protein transport between the ER and Golgi. Annu Rev Cell Dev Biol *20*, 87-123.

Lee, T. L., Lin, Y. C., Mochitate, K., and Grinnell, F. (1993). Stress-relaxation of fibroblasts in collagen matrices triggers ectocytosis of plasma membrane vesicles containing actin, annexins II and VI, and beta 1 integrin receptors. J Cell Sci *105 (Pt 1)*, 167-177.

Leffler, H., and Barondes, S. H. (1986). Specificity of binding of three soluble rat lung lectins to substituted and unsubstituted mammalian beta-galactosides. J Biol Chem *261*, 10119-10126.

Letourneur, F., Gaynor, E. C., Hennecke, S., Demolliere, C., Duden, R., Emr, S. D., Riezman, H., and Cosson, P. (1994). Coatomer is essential for retrieval of dilysine-tagged proteins to the endoplasmic reticulum. Cell *79*, 1199-1207.

Lewis, M. J., and Pelham, H. R. (1990). A human homologue of the yeast HDEL receptor. Nature *348*, 162-163.

Lewis, M. J., and Pelham, H. R. (1992a). Ligand-induced redistribution of a human KDEL receptor from the Golgi complex to the endoplasmic reticulum. Cell *68*, 353-364.

Lewis, M. J., and Pelham, H. R. (1992b). Sequence of a second human KDEL receptor. J Mol Biol *226*, 913-916.

Liao, D. I., Kapadia, G., Ahmed, H., Vasta, G. R., and Herzberg, O. (1994). Structure of S-lectin, a developmentally regulated vertebrate beta-galactoside-binding protein. Proc Natl Acad Sci U S A *91*, 1428-1432.

Lindstedt, R., Apodaca, G., Barondes, S. H., Mostov, K. E., and Leffler, H. (1993). Apical secretion of a cytosolic protein by Madin-Darby canine kidney cells. Evidence for polarized release of an endogenous lectin by a nonclassical secretory pathway. J Biol Chem *268*, 11750-11757.

Lippincott-Schwartz, J., Yuan, L. C., Bonifacino, J. S., and Klausner, R. D. (1989). Rapid redistribution of Golgi proteins into the ER in cells treated with brefeldin A: evidence for membrane cycling from Golgi to ER. Cell *56*, 801-813.

Liu, F. T., Patterson, R. J., and Wang, J. L. (2002). Intracellular functions of galectins. Biochim Biophys Acta *1572*, 263-273.

Liu, F. T., and Rabinovich, G. A. (2005). Galectins as modulators of tumour progression. Nat Rev Cancer *5*, 29-41.

Liu, X., Constantinescu, S. N., Sun, Y., Bogan, J. S., Hirsch, D., Weinberg, R. A., and Lodish, H. F. (2000). Generation of mammalian cells stably expressing multiple genes at predetermined levels. Anal Biochem *280*, 20-28.

Lloyd, K. O., and Yin, B. W. (2001). Synthesis and secretion of the ovarian cancer antigen CA 125 by the human cancer cell line NIH:OVCAR-3. Tumour Biol *22*, 77-82.

Lobsanov, Y. D., Gitt, M. A., Leffler, H., Barondes, S. H., and Rini, J. M. (1993). X-ray crystal structure of the human dimeric S-Lac lectin, L-14-II, in complex with lactose at 2.9-A resolution. J Biol Chem *268*, 27034-27038.

Lopez-Lucendo, M. F., Solis, D., Andre, S., Hirabayashi, J., Kasai, K., Kaltner, H., Gabius, H. J., and Romero, A. (2004). Growth-regulatory human galectin-1:

crystallographic characterisation of the structural changes induced by single-site mutations and their impact on the thermodynamics of ligand binding. J Mol Biol *343*, 957-970.

Lue, H., Kleemann, R., Calandra, T., Roger, T., and Bernhagen, J. (2002). Macrophage migration inhibitory factor (MIF): mechanisms of action and role in disease. Microbes Infect *4*, 449-460.

Lupashin, V., and Sztul, E. (2005). Golgi tethering factors. Biochim Biophys Acta *1744*, 325-339.

Lutomski, D., Fouillit, M., Bourin, P., Mellottee, D., Denize, N., Pontet, M., Bladier, D., Caron, M., and Joubert-Caron, R. (1997). Externalization and binding of galectin-1 on cell surface of K562 cells upon erythroid differentiation. Glycobiology *7*, 1193-1199.

Marschal, P., Herrmann, J., Leffler, H., Barondes, S. H., and Cooper, D. N. (1992). Sequence and specificity of a soluble lactose-binding lectin from Xenopus laevis skin. J Biol Chem *267*, 12942-12949.

Martinez, M. C., Tesse, A., Zobairi, F., and Andriantsitohaina, R. (2005). Shed membrane microparticles from circulating and vascular cells in regulating vascular function. Am J Physiol Heart Circ Physiol *288*, H1004-1009.

McEver, R. P. (1995). Regulation of function and expression of P-selectin. Agents Actions Suppl *47*, 117-119.

McEver, R. P., Moore, K. L., and Cummings, R. D. (1995). Leukocyte trafficking mediated by selectin-carbohydrate interactions. J Biol Chem *270*, 11025-11028.

McKean, P. G., Denny, P. W., Knuepfer, E., Keen, J. K., and Smith, D. F. (2001). Phenotypic changes associated with deletion and overexpression of a stage-regulated gene family in Leishmania. Cell Microbiol *3*, 511-523.

McNeil, P. L., Muthukrishnan, L., Warder, E., and D'Amore, P. A. (1989). Growth factors are released by mechanically wounded endothelial cells. J Cell Biol *109*, 811-822.

Mehul, B., and Hughes, R. C. (1997). Plasma membrane targetting, vesicular budding and release of galectin 3 from the cytoplasm of mammalian cells during secretion. J Cell Sci *110 (Pt 10)*, 1169-1178.

Mellman, I., and Simons, K. (1992). The Golgi complex: in vitro veritas? Cell *68*, 829-840.

Mellman, I., and Warren, G. (2000). The road taken: past and future foundations of membrane traffic. Cell *100*, 99-112.

Meyer, D. I., Krause, E., and Dobberstein, B. (1982). Secretory protein translocation across membranes-the role of the "docking protein'. Nature *297*, 647-650.

Meyer, T., and Rustin, G. J. (2000). Role of tumour markers in monitoring epithelial ovarian cancer. Br J Cancer *82*, 1535-1538.

Mignatti, P., Morimoto, T., and Rifkin, D. B. (1992). Basic fibroblast growth factor, a protein devoid of secretory signal sequence, is released by cells via a pathway independent of the endoplasmic reticulum-Golgi complex. J Cell Physiol *151*, 81-93.

Mignatti, P., and Rifkin, D. B. (1991). Release of basic fibroblast growth factor, an angiogenic factor devoid of secretory signal sequence: a trivial phenomenon or a novel secretion mechanism? J Cell Biochem *47*, 201-207.

Miller, E. (2004). Apoptosis measurement by annexin v staining. Methods Mol Med *88*, 191-202.

Mironov, A. A., Beznoussenko, G. V., Polishchuk, R. S., and Trucco, A. (2005). Intra-Golgi transport: a way to a new paradigm? Biochim Biophys Acta *1744*, 340-350.

Misumi, Y., Misumi, Y., Miki, K., Takatsuki, A., Tamura, G., and Ikehara, Y. (1986). Novel blockade by brefeldin A of intracellular transport of secretory proteins in cultured rat hepatocytes. J Biol Chem *261*, 11398-11403.

Moiseeva, E. P., Javed, Q., Spring, E. L., and de Bono, D. P. (2000). Galectin 1 is involved in vascular smooth muscle cell proliferation. Cardiovasc Res *45*, 493-502.

Moiseeva, E. P., Williams, B., and Samani, N. J. (2003). Galectin 1 inhibits incorporation of vitronectin and chondroitin sulfate B into the extracellular matrix of human vascular smooth muscle cells. Biochim Biophys Acta *1619*, 125-132.

Morre, J., Merlin, L. M., and Keenan, T. W. (1969). Localization of glycosyl transferase activities in a Golgi apparatus-rich fraction isolated from rat liver. Biochem Biophys Res Commun *37*, 813-819.

Mossessova, E., Bickford, L. C., and Goldberg, J. (2003). SNARE selectivity of the COPII coat. Cell *114*, 483-495.

Nagy, Z. (2005). The last neuronal division: a unifying hypothesis for the pathogenesis of Alzheimer's disease. J Cell Mol Med *9*, 531-541.

Nguyen, J. T., Evans, D. P., Galvan, M., Pace, K. E., Leitenberg, D., Bui, T. N., and Baum, L. G. (2001). CD45 modulates galectin-1-induced T cell death: regulation by expression of core 2 O-glycans. J Immunol *167*, 5697-5707.

Nickel, W. (2003). The mystery of nonclassical protein secretion. Eur J Biochem *270*, 2109-2119.

Nickel, W. (2005). Unconventional secretory routes: direct protein export across the plasma membrane of Mammalian cells. Traffic *6*, 607-614.

Nickel, W., Brugger, B., and Wieland, F. T. (2002). Vesicular transport: the core machinery of COPI recruitment and budding. J Cell Sci *115*, 3235-3240.

Nie, Z., Hirsch, D. S., and Randazzo, P. A. (2003). Arf and its many interactors. Curr Opin Cell Biol *15*, 396-404.

Nugent, M. A., and Iozzo, R. V. (2000). Fibroblast growth factor-2. Int J Biochem Cell Biol *32*, 115-120.

O'Brien, T. J., Beard, J. B., Underwood, L. J., Dennis, R. A., Santin, A. D., and York, L. (2001). The CA 125 gene: an extracellular superstructure dominated by repeat sequences. Tumour Biol *22*, 348-366.

Oates, J., Barrett, C. M., Barnett, J. P., Byrne, K. G., Bolhuis, A., and Robinson, C. (2005). The Escherichia coli twin-arginine translocation apparatus incorporates a distinct form of TatABC complex, spectrum of modular TatA complexes and minor TatAB complex. J Mol Biol *346*, 295-305.

Orci, L., Palmer, D. J., Ravazzola, M., Perrelet, A., Amherdt, M., and Rothman, J. E. (1993). Budding from Golgi membranes requires the coatomer complex of non-clathrin coat proteins. Nature *362*, 648-652.

Orci, L., Stamnes, M., Ravazzola, M., Amherdt, M., Perrelet, A., Sollner, T. H., and Rothman, J. E. (1997). Bidirectional transport by distinct populations of COPI-coated vesicles. Cell *90*, 335-349.

Orci, L., Tagaya, M., Amherdt, M., Perrelet, A., Donaldson, J. G., Lippincott-Schwartz, J., Klausner, R. D., and Rothman, J. E. (1991). Brefeldin A, a drug that blocks secretion, prevents the assembly of non-clathrin-coated buds on Golgi cisternae. Cell *64*, 1183-1195.

Ornitz, D. M., and Itoh, N. (2001). Fibroblast growth factors. Genome Biol *2*, REVIEWS3005.

Ozeki, Y., Matsui, T., Yamamoto, Y., Funahashi, M., Hamako, J., and Titani, K. (1995). Tissue fibronectin is an endogenous ligand for galectin-1. Glycobiology *5*, 255-261.

Pace, K. E., Hahn, H. P., Pang, M., Nguyen, J. T., and Baum, L. G. (2000). CD7 delivers a pro-apoptotic signal during galectin-1-induced T cell death. J Immunol *165*, 2331-2334.

Pace, K. E., Lee, C., Stewart, P. L., and Baum, L. G. (1999). Restricted receptor segregation into membrane microdomains occurs on human T cells during apoptosis induced by galectin-1. J Immunol *163*, 3801-3811.

Palade, G. (1975). Intracellular aspects of the process of protein synthesis. Science *189*, 347-358.

Pekkari, K., Avila-Carino, J., Bengtsson, A., Gurunath, R., Scheynius, A., and Holmgren, A. (2001). Truncated thioredoxin (Trx80) induces production of interleukin-12 and enhances CD14 expression in human monocytes. Blood *97*, 3184-3190.

Pekkari, K., Gurunath, R., Arner, E. S., and Holmgren, A. (2000). Truncated thioredoxin is a mitogenic cytokine for resting human peripheral blood mononuclear cells and is present in human plasma. J Biol Chem *275*, 37474-37480.

Perillo, N. L., Marcus, M. E., and Baum, L. G. (1998). Galectins: versatile modulators of cell adhesion, cell proliferation, and cell death. J Mol Med *76*, 402-412.

Perillo, N. L., Pace, K. E., Seilhamer, J. J., and Baum, L. G. (1995). Apoptosis of T cells mediated by galectin-1. Nature *378*, 736-739.

Perillo, N. L., Uittenbogaart, C. H., Nguyen, J. T., and Baum, L. G. (1997). Galectin-1, an endogenous lectin produced by thymic epithelial cells, induces apoptosis of human thymocytes. J Exp Med *185*, 1851-1858.

Pfeffer, S. (2001a). Vesicle tethering factors united. Mol Cell *8*, 729-730.

Pfeffer, S. R. (2001b). Rab GTPases: specifying and deciphering organelle identity and function. Trends Cell Biol *11*, 487-491.

Pfeifer, K., Haasemann, M., Gamulin, V., Bretting, H., Fahrenholz, F., and Muller, W. E. (1993). S-type lectins occur also in invertebrates: high conservation of the carbohydrate recognition domain in the lectin genes from the marine sponge Geodia cydonium. Glycobiology *3*, 179-184.

Pimenta, P. F., Pinto da Silva, P., Rangarajan, D., Smith, D. F., and Sacks, D. L. (1994). Leishmania major: association of the differentially expressed gene B protein and the surface lipophosphoglycan as revealed by membrane capping. Exp Parasitol *79*, 468-479.

Powers, T., and Walter, P. (1996). The nascent polypeptide-associated complex modulates interactions between the signal recognition particle and the ribosome. Curr Biol *6*, 331-338.

Prudovsky, I., Mandinova, A., Soldi, R., Bagala, C., Graziani, I., Landriscina, M., Tarantini, F., Duarte, M., Bellum, S., Doherty, H., and Maciag, T. (2003). The non-classical export routes: FGF1 and IL-1alpha point the way. J Cell Sci *116*, 4871-4881.

Puck, T. T., Cieciura, S. J., and Robinson, A. (1958). Genetics of somatic mammalian cells. III. Long-term cultivation of euploid cells from human and animal subjects. J Exp Med *108*, 945-956.

Rabinovich, G. A., Alonso, C. R., Sotomayor, C. E., Durand, S., Bocco, J. L., and Riera, C. M. (2000). Molecular mechanisms implicated in galectin-1-induced apoptosis: activation of the AP-1 transcription factor and downregulation of Bcl-2. Cell Death Differ *7*, 747-753.

Rabinovich, G. A., Baum, L. G., Tinari, N., Paganelli, R., Natoli, C., Liu, F. T., and Iacobelli, S. (2002a). Galectins and their ligands: amplifiers, silencers or tuners of the inflammatory response? Trends Immunol *23*, 313-320.

Rabinovich, G. A., Rubinstein, N., and Toscano, M. A. (2002b). Role of galectins in inflammatory and immunomodulatory processes. Biochim Biophys Acta *1572*, 274-284.

Raman, R., Venkataraman, G., Ernst, S., Sasisekharan, V., and Sasisekharan, R. (2003). Structural specificity of heparin binding in the fibroblast growth factor family of proteins. Proc Natl Acad Sci U S A *100*, 2357-2362.

Rapoport, T. A. (1991). Protein transport across the endoplasmic reticulum membrane: facts, models, mysteries. Faseb J *5*, 2792-2798.

Rapoport, T. A. (1992). Transport of proteins across the endoplasmic reticulum membrane. Science *258*, 931-936.

Rapoport, T. A., Gorlich, D., Musch, A., Hartmann, E., Prehn, S., Wiedmann, M., Otto, A., Kostka, S., and Kraft, R. (1992). Components and mechanism of protein translocation across the ER membrane. Antonie Van Leeuwenhoek *61*, 119-122.

Rapoport, T. A., Rolls, M. M., and Jungnickel, B. (1996). Approaching the mechanism of protein transport across the ER membrane. Curr Opin Cell Biol *8*, 499-504.

Resh, M. D. (2004). Membrane targeting of lipid modified signal transduction proteins. Subcell Biochem *37*, 217-232.

Revest, J. M., DeMoerlooze, L., and Dickson, C. (2000). Fibroblast Growth Factor 9 Secretion Is Mediated by a Non-cleaved Amino- terminal Signal Sequence. J Biol Chem *275*, 8083-8090.

Rini, J. M. (1995a). Lectin structure. Annu Rev Biophys Biomol Struct *24*, 551-577.

Rini, J. M. (1995b). X-ray crystal structures of animal lectins. Curr Opin Struct Biol *5*, 617-621.

Robinson, C., and Bolhuis, A. (2004). Tat-dependent protein targeting in prokaryotes and chloroplasts. Biochim Biophys Acta *1694*, 135-147.

Robinson, M. S. (1987). 100-kD coated vesicle proteins: molecular heterogeneity and intracellular distribution studied with monoclonal antibodies. J Cell Biol *104*, 887-895.

Rosen, S. D., and Bertozzi, C. R. (1994). The selectins and their ligands. Curr Opin Cell Biol *6*, 663-673.

Rothman, J. E. (2002). Lasker Basic Medical Research Award. The machinery and principles of vesicle transport in the cell. Nat Med *8*, 1059-1062.

Rothman, J. E., and Orci, L. (1990). Movement of proteins through the Golgi stack: a molecular dissection of vesicular transport. Faseb J *4*, 1460-1468.

Rothman, J. E., and Wieland, F. T. (1996). Protein sorting by transport vesicles. Science *272*, 227-234.

Rubartelli, A., Bajetto, A., Allavena, G., Wollman, E., and Sitia, R. (1992). Secretion of thioredoxin by normal and neoplastic cells through a leaderless secretory pathway. J Biol Chem *267*, 24161-24164.

Rubartelli, A., Bonifaci, N., and Sitia, R. (1995). High rates of thioredoxin secretion correlate with growth arrest in hepatoma cells. Cancer Res *55*, 675-680.

Rubartelli, A., Cozzolino, F., Talio, M., and Sitia, R. (1990). A novel secretory pathway for interleukin-1 beta, a protein lacking a signal sequence. EMBO J *9*, 1503-1510.

Rubartelli, A., and Sitia, R. (1991). Interleukin 1 beta and thioredoxin are secreted through a novel pathway of secretion. Biochem Soc Trans *19*, 255-259.

Sacchettini, J. C., Baum, L. G., and Brewer, C. F. (2001). Multivalent protein-carbohydrate interactions. A new paradigm for supermolecular assembly and signal transduction. Biochemistry *40*, 3009-3015.

Safaiyan, F., Kolset, S. O., Prydz, K., Gottfridsson, E., Lindahl, U., and Salmivirta, M. (1999). Selective effects of sodium chlorate treatment on the sulfation of heparan sulfate. J Biol Chem *274*, 36267-36273.

Sahaf, B., and Rosen, A. (2000). Secretion of 10-kDa and 12-kDa thioredoxin species from blood monocytes and transformed leukocytes. Antioxid Redox Signal *2*, 717-726.

Saiki, R. K., Gelfand, D. H., Stoffel, S., Scharf, S. J., Higuchi, R., Horn, G. T., Mullis, K. B., and Erlich, H. A. (1988). Primer-directed enzymatic amplification of DNA with a thermostable DNA polymerase. Science *239*, 487-491.

Sanford, G. L., and Harris-Hooker, S. (1990). Stimulation of vascular cell proliferation by beta-galactoside specific lectins. Faseb J *4*, 2912-2918.

Sato, S., Burdett, I., and Hughes, R. C. (1993a). Secretion of the baby hamster kidney 30-kDa galactose-binding lectin from polarized and nonpolarized cells: a pathway independent of the endoplasmic reticulum-Golgi complex. Exp Cell Res *207*, 8-18.

Sato, T., Furukawa, K., Autero, M., Gahmberg, C. G., and Kobata, A. (1993b). Structural study of the sugar chains of human leukocyte common antigen CD45. Biochemistry *32*, 12694-12704.

Sayeed, A., and Ng, D. T. (2005). Search and destroy: ER quality control and ER-associated protein degradation. Crit Rev Biochem Mol Biol *40*, 75-91.

Schachter, H., Jabbal, I., Hudgin, R. L., Pinteric, L., McGuire, E. J., and Roseman, S. (1970). Intracellular localization of liver sugar nucleotide glycoprotein glycosyltransferases in a Golgi-rich fraction. J Biol Chem *245*, 1090-1100.

Schäfer, T., Zentgraf, H., Zehe, C., Brügger, B., Bernhagen, J., and Nickel, W. (2004). Unconventional secretion of fibroblast growth factor 2 is mediated by direct translocation across the plasma membrane of mammalian cells. J Biol Chem *279*, 6244-6251.

Schatz, G., and Dobberstein, B. (1996). Common principles of protein translocation across membranes. Science *271*, 1519-1526.

Schekman, R., and Orci, L. (1996). Coat proteins and vesicle budding. Science *271*, 1526-1533.

Scherer, W. F., Syverton, J. T., and Gey, G. O. (1953). Studies on the propagation in vitro of poliomyelitis viruses. IV. Viral multiplication in a stable strain of human malignant epithelial cells (strain HeLa) derived from an epidermoid carcinoma of the cervix. J Exp Med *97*, 695-710.

Schmid, S. L. (1997). Clathrin-coated vesicle formation and protein sorting: an integrated process. Annu Rev Biochem *66*, 511-548.

Schweigerer, L., Neufeld, G., Friedman, J., Abraham, J. A., Fiddes, J. C., and Gospodarowicz, D. (1987). Capillary endothelial cells express basic fibroblast growth factor, a mitogen that promotes their own growth. Nature *325*, 257-259.

Scott, K., and Zhang, J. (2002). Partial identification by site-directed mutagenesis of a cell growth inhibitory site on the human galectin-1 molecule. BMC Cell Biol *3*, 3.

Seelenmeyer, C., Wegehingel, S., Lechner, J., and Nickel, W. (2003). The cancer antigen CA125 represents a novel counter receptor for galectin-1. J Cell Sci *116*, 1305-1318.

Seelenmeyer, C., Wegehingel, S., Tews, I., Kunzler, M., Aebi, M., and Nickel, W. (2005). Cell surface counter receptors are essential components of the unconventional export machinery of galectin-1. J Cell Biol *171*, 373-381.

Serafini, T., Orci, L., Amherdt, M., Brunner, M., Kahn, R. A., and Rothman, J. E. (1991). ADP-ribosylation factor is a subunit of the coat of Golgi-derived COP-coated vesicles: a novel role for a GTP-binding protein. Cell *67*, 239-253.

Sharon, N. (1993). Lectin-carbohydrate complexes of plants and animals: an atomic view. Trends Biochem Sci *18*, 221-226.

Shin, J. T., Opalenik, S. R., Wehby, J. N., Mahesh, V. K., Jackson, A., Tarantini, F., Maciag, T., and Thompson, J. A. (1996). Serum-starvation induces the extracellular appearance of FGF-1. Biochim Biophys Acta *1312*, 27-38.

Shukla, S. D., Berriman, J., Coleman, R., Finean, J. B., and Michell, R. H. (1978). Membrane protein segregation during release of microvesicles from human erythrocytes. FEBS Lett *90*, 289-292.

Siebert, H. C., Andre, S., Lu, S. Y., Frank, M., Kaltner, H., van Kuik, J. A., Korchagina, E. Y., Bovin, N., Tajkhorshid, E., Kaptein, R.*, et al.* (2003). Unique conformer selection of human growth-regulatory lectin galectin-1 for ganglioside GM1 versus bacterial toxins. Biochemistry *42*, 14762-14773.

Sitia, R., and Braakman, I. (2003). Quality control in the endoplasmic reticulum protein factory. Nature *426*, 891-894.

Smith, A. E., Lilie, H., and Helenius, A. (2003). Ganglioside-dependent cell attachment and endocytosis of murine polyomavirus-like particles. FEBS Lett *555*, 199-203.

Song, W. K., Wang, W., Sato, H., Bielser, D. A., and Kaufman, S. J. (1993). Expression of alpha 7 integrin cytoplasmic domains during skeletal muscle development: alternate forms, conformational change, and homologies with serine/threonine kinases and tyrosine phosphatases. J Cell Sci *106 (Pt 4)*, 1139-1152.

Sonnichsen, B., Fullekrug, J., Nguyen Van, P., Diekmann, W., Robinson, D. G., and Mieskes, G. (1994). Retention and retrieval: both mechanisms cooperate to maintain calreticulin in the endoplasmic reticulum. J Cell Sci *107 (Pt 10)*, 2705-2717.

Sonnichsen, B., Watson, R., Clausen, H., Misteli, T., and Warren, G. (1996). Sorting by COP I-coated vesicles under interphase and mitotic conditions. J Cell Biol *134*, 1411-1425.

Spilsberg, B., Van Meer, G., and Sandvig, K. (2003). Role of lipids in the retrograde pathway of ricin intoxication. Traffic *4*, 544-552.

Stahl, P. D. (1992). The mannose receptor and other macrophage lectins. Curr Opin Immunol *4*, 49-52.

Stahl, P. D., and Barbieri, M. A. (2002). Multivesicular bodies and multivesicular endosomes: the "ins and outs" of endosomal traffic. Sci STKE *2002*, PE32.

Stegmayer, C., Kehlenbach, A., Tournaviti, S., Wegehingel, S., Zehe, C., Denny, P., Smith, D. F., Schwappach, B., and Nickel, W. (2005). Direct transport across the plasma membrane of mammalian cells of Leishmania HASPB as revealed by a CHO export mutant. J Cell Sci *118*, 517-527.

Stein, J. M., and Luzio, J. P. (1991). Ectocytosis caused by sublytic autologous complement attack on human neutrophils. The sorting of endogenous plasma-membrane proteins and lipids into shed vesicles. Biochem J *274 (Pt 2)*, 381-386.

Stinchcombe, J., Bossi, G., and Griffiths, G. M. (2004). Linking albinism and immunity: the secrets of secretory lysosomes. Science *305*, 55-59.

Stoorvogel, W., Kleijmeer, M. J., Geuze, H. J., and Raposo, G. (2002). The biogenesis and functions of exosomes. Traffic *3*, 321-330.

Streuli, M., Hall, L. R., Saga, Y., Schlossman, S. F., and Saito, H. (1987). Differential usage of three exons generates at least five different mRNAs encoding human leukocyte common antigens. J Exp Med *166*, 1548-1566.

Sudhof, T. C. (2004). The synaptic vesicle cycle. Annu Rev Neurosci *27*, 509-547.

Sui, G., Soohoo, C., Affar el, B., Gay, F., Shi, Y., Forrester, W. C., and Shi, Y. (2002). A DNA vector-based RNAi technology to suppress gene expression in mammalian cells. Proc Natl Acad Sci U S A *99*, 5515-5520.

Tajima, S., Lauffer, L., Rath, V. L., and Walter, P. (1986). The signal recognition particle receptor is a complex that contains two distinct polypeptide chains. J Cell Biol *103*, 1167-1178.

Tarantini, F., Gamble, S., Jackson, A., and Maciag, T. (1995). The cysteine residue responsible for the release of fibroblast growth factor-1 resides in a domain independent of the domain for phosphatidylserine binding. J Biol Chem *270*, 29039-29042.

Thompson, C. B. (1995). Apoptosis in the pathogenesis and treatment of disease. Science *267*, 1456-1462.

Towbin, H., Staehelin, T., and Gordon, J. (1979). Electrophoretic transfer of proteins from polyacrylamide gels to nitrocellulose sheets: procedure and some applications. Proc Natl Acad Sci U S A *76*, 4350-4354.

Trombetta, E. S., and Parodi, A. J. (2003). Quality control and protein folding in the secretory pathway. Annu Rev Cell Dev Biol *19*, 649-676.

Trudel, C., Faure-Desire, V., Florkiewicz, R. Z., and Baird, A. (2000). Translocation of FGF2 to the cell surface without release into conditioned media [In Process Citation]. J Cell Physiol *185*, 260-268.

Tuschl, T. (2001). RNA interference and small interfering RNAs. Chembiochem *2*, 239-245.

Tuschl, T., and Borkhardt, A. (2002). Small interfering RNAs: a revolutionary tool for the analysis of gene function and gene therapy. Mol Interv *2*, 158-167.

Ungar, D., and Hughson, F. M. (2003). SNARE protein structure and function. Annu Rev Cell Dev Biol *19*, 493-517.

Urlinger, S., Baron, U., Thellmann, M., Hasan, M. T., Bujard, H., and Hillen, W. (2000). Exploring the sequence space for tetracycline-dependent transcriptional activators: novel mutations yield expanded range and sensitivity. Proc Natl Acad Sci U S A *97*, 7963-7968.

van den Brule, F., Califice, S., Garnier, F., Fernandez, P. L., Berchuck, A., and Castronovo, V. (2003). Galectin-1 accumulation in the ovary carcinoma peritumoral

stroma is induced by ovary carcinoma cells and affects both cancer cell proliferation and adhesion to laminin-1 and fibronectin. Lab Invest *83*, 377-386.

van den Brule, F. A., Buicu, C., Baldet, M., Sobel, M. E., Cooper, D. N., Marschal, P., and Castronovo, V. (1995). Galectin-1 modulates human melanoma cell adhesion to laminin. Biochem Biophys Res Commun *209*, 760-767.

Varki, A. (1992). Selectins and other mammalian sialic acid-binding lectins. Curr Opin Cell Biol *4*, 257-266.

Varki, A. (1994). Selectin ligands. Proc Natl Acad Sci U S A *91*, 7390-7397.

Varki, A. (1997). Selectin ligands: will the real ones please stand up? J Clin Invest *99*, 158-162.

Wakisaka, N., Murono, S., Yoshizaki, T., Furukawa, M., and Pagano, J. S. (2002). Epstein-barr virus latent membrane protein 1 induces and causes release of fibroblast growth factor-2. Cancer Res *62*, 6337-6344.

Walser, P. J., Haebel, P. W., Kunzler, M., Sargent, D., Kues, U., Aebi, M., and Ban, N. (2004). Structure and functional analysis of the fungal galectin CGL2. Structure (Camb) *12*, 689-702.

Walser, P. J., Kues, U., Aebi, M., and Kunzler, M. (2005). Ligand interactions of the Coprinopsis cinerea galectins. Fungal Genet Biol *42*, 293-305.

Walter, P. (1992). Protein translocation. Travelling by TRAM. Nature *357*, 22-23.

Walter, P., Gilmore, R., and Blobel, G. (1984). Protein translocation across the endoplasmic reticulum. Cell *38*, 5-8.

Walzel, H., Schulz, U., Neels, P., and Brock, J. (1999). Galectin-1, a natural ligand for the receptor-type protein tyrosine phosphatase CD45. Immunol Lett *67*, 193-202.

Warren, G., and Malhotra, V. (1998). The organisation of the Golgi apparatus. Curr Opin Cell Biol *10*, 493-498.

Watanabe, N., and Kobayashi, Y. (1994). Selective release of a processed form of interleukin 1 alpha. Cytokine *6*, 597-601.

Weber, T., Zemelman, B. V., McNew, J. A., Westermann, B., Gmachl, M., Parlati, F., Sollner, T. H., and Rothman, J. E. (1998). SNAREpins: minimal machinery for membrane fusion. Cell *92*, 759-772.

Weis, W. I., and Drickamer, K. (1996). Structural basis of lectin-carbohydrate recognition. Annu Rev Biochem *65*, 441-473.

Wickus, G. G., and Robbins, P. W. (1973). Plasma membrane proteins of normal and Rous sarcoma virus-transformed chick-embryo fibroblasts. Nat New Biol *245*, 65-67.

Wilson, K. P., Black, J. A., Thomson, J. A., Kim, E. E., Griffith, J. P., Navia, M. A., Murcko, M. A., Chambers, S. P., Aldape, R. A., Raybuck, S. A., and et al. (1994). Structure and mechanism of interleukin-1 beta converting enzyme. Nature *370*, 270-275.

Wimmer, C., Hohl, T. M., Hughes, C. A., Muller, S. A., Sollner, T. H., Engel, A., and Rothman, J. E. (2001). Molecular mass, stoichiometry, and assembly of 20 S particles. J Biol Chem *276*, 29091-29097.

Yang, R. Y., Hsu, D. K., and Liu, F. T. (1996). Expression of galectin-3 modulates T-cell growth and apoptosis. Proc Natl Acad Sci U S A *93*, 6737-6742.

Yang, R. Y., Hsu, D. K., Yu, L., Ni, J., and Liu, F. T. (2001). Cell cycle regulation by galectin-12, a new member of the galectin superfamily. J Biol Chem *276*, 20252-20260.

Yin, B. W., and Lloyd, K. O. (2001). Molecular cloning of the CA125 ovarian cancer antigen: identification as a new mucin, MUC16. J Biol Chem *276*, 27371-27375.

Yoshimura, M., Ihara, Y., and Taniguchi, N. (1995). Changes of beta-1,4-N-acetylglucosaminyltransferase III (GnT-III) in patients with leukaemia. Glycoconj J *12*, 234-240.

Zerial, M., and Stenmark, H. (1993). Rab GTPases in vesicular transport. Curr Opin Cell Biol *5*, 613-620.

Zhou, Q., and Cummings, R. D. (1990). The S-type lectin from calf heart tissue binds selectively to the carbohydrate chains of laminin. Arch Biochem Biophys *281*, 27-35.

Zhou, Q., and Cummings, R. D. (1993). L-14 lectin recognition of laminin and its promotion of in vitro cell adhesion. Arch Biochem Biophys *300*, 6-17.

Zhou, X., Engel, T., Goepfert, C., Erren, M., Assmann, G., and von Eckardstein, A. (2002). The ATP binding cassette transporter A1 contributes to the secretion of interleukin 1beta from macrophages but not from monocytes. Biochem Biophys Res Commun *291*, 598-604.

Zimmermann, K. C., Bonzon, C., and Green, D. R. (2001). The machinery of programmed cell death. Pharmacol Ther *92*, 57-70.

Zurawski, V. R., Jr., Knapp, R. C., Einhorn, N., Kenemans, P., Mortel, R., Ohmi, K., Bast, R. C., Jr., Ritts, R. E., Jr., and Malkasian, G. (1988). An initial analysis of preoperative serum CA 125 levels in patients with early stage ovarian carcinoma. Gynecol Oncol *30*, 7-14.

Herewith I declare that this thesis is my own work and that I cited all references and help used. I consent to this thesis being deposited in and distributed by the Library of the Ruperto Carola University, Heidelberg.

November 2005

Acknowledgement

I want to express my gratitude to Prof. Dr. rer. nat. Walter Nickel for giving me the opportunity to work in his laboratory on this interesting project as well as for his outstanding supervision, scientific advice, dedicated support and help during all the time.

My sincere gratitude and appreciation goes to Sabine Wegehingel for her expertise and skilful work throughout our project and for a cordial atmosphere in the lab.

I want to thank Prof. Dr. rer. nat. Michael Brunner for being my second appraiser.

I would like to thank Dr. rer. nat. Ivo Tews for his support on the structural analysis of Gal-1 and Christoph Rutz for his helpful introduction into confocal microscopy.

I am grateful to Angelika Kehlenbach and Julia Lenz for their generous help with FACS sorting.

I am deeply indebted to Christoph Zehe for his critical comments on the manuscript, for very fruitful discussions, his time spending with proofreading and for “just being there”.

A huge “Thank you” goes to Carolin Stegmayer not only for sitting next to me.

A special thank goes to my writing fellow Rafael Backhaus for mental support, food sharing and helpful discussions during our long nightly typing sessions in the lab.

I thank all past and present members of the ‘Nickellab’, who provided a pleasant, friendly and productive atmosphere in the lab. Without Rafael Backhaus, Lucía Cespón Torrado, Antje Ebert, André Engling, Julia Ritzerfeld, Carolin Stegmayer, Koen Temmerman, Stella Tournaviti, Sabine Wegehingel, Jaz Woo and Christoph Zehe this work would have been less successful.

Additionally, I am grateful to all past and present members of the “3rd floor”, especially Julien Béthune, Dr. Britta Brügger, Boyan Jeynov, Ingrid Meißner, Dr. Dorothee Lay, Barbara Schröter, Dr. Dominik Wegmann and Sandra Zitzler.

I would like to thank all my friends - especially Ute Baumann, Rebecca Frey and Roland Olbrich - for their support, understanding, encouragement, for good conversations, listening and finally sharing good and bad times with me.

Abschließend möchte ich mich besonders bei meinen Eltern Gisela und Dieter Seelenmeyer, sowie bei meiner Schwester Sabine Seelenmeyer für ihre engagierte Unterstützung, ihre stetigen Ermutigungen, ihr grosses Verständnis und Ihre uneingeschränkte Zuneigung bedanken.

Ernst zu nehmende Forschung erkennt man daran,
daß plötzlich zwei Probleme existieren,
wo es vorher nur eines gegeben hat.

Thorstein Bunde Veblen (1857-1929)